



UNIVERSITY OF
BIRMINGHAM

**SELF-STRUCTURING FOODS BASED ON
ACID-SENSITIVE GELLAN GUM SYSTEMS
TO IMPACT ON SATIETY**

By

JENNIFER FRANCES BRADBEER

A thesis submitted to

The University of Birmingham

for the degree of

DOCTOR OF PHILOSOPHY

School of Chemical Engineering

College of Engineering and Physical Sciences

The University of Birmingham

September 2013

UNIVERSITY OF
BIRMINGHAM

University of Birmingham Research Archive

e-theses repository

This unpublished thesis/dissertation is copyright of the author and/or third parties. The intellectual property rights of the author or third parties in respect of this work are as defined by The Copyright Designs and Patents Act 1988 or as modified by any successor legislation.

Any use made of information contained in this thesis/dissertation must be in accordance with that legislation and must be properly acknowledged. Further distribution or reproduction in any format is prohibited without the permission of the copyright holder.

Abstract

A novel approach that may impact on satiety, whilst meeting the demands of consumers, is the use of hydrocolloids that respond to the environment (acidic) conditions inside the human stomach by self-structuring. This thesis seeks to investigate the *in vitro* acid-induced gelation (“structuring”) of the mixed biopolymer systems; low-acyl and high-acyl gellan gum, and low-acyl gellan fluid gels.

To explore this concept, a variety of acid structures were obtained, which were characterised by texture analysis, rheology and dynamic scanning calorimetry. The gel structures were found to rely on the pH, hydrocolloid concentration, percentage weight of each hydrocolloid used and the processing conditions used during their production.

It is suggested that the use of gel alone is more than capable of providing prolonged satiety but leads to unpleasant sensations for the consumer if there is no delivery of energy to the body to compliment the sensation of satiety. Materials should be included that will modulate the energy delivery and slowly release calories over time. This research shows that the addition of co-solutes such as sugar and the measurement of their subsequent release from hydrocolloid gels could provide a first step to tackling these issues.

Acknowledgements

I would like to thank my supervisors Professor Ian Norton and Dr Fotios Spyropoulos for their help and encouragement throughout this project. Their support has been invaluable. I would also like to thank my post-doc supervisor Dr Robin Hancocks for his guidance and patience.

Credit is also due to the administrative and technical staff within the department, in particular Lynn Draper and Elaine Mitchell for their assistance and training, and the dynamic duo Bob and Bill who never failed to support and entertain.

My time in the department has been enriched by the many friends and colleagues, past and present, that I have been fortunate enough to meet and work with and I have many happy memories.

I would also like to acknowledge the BBSRC for funding which has enabled this work to be completed.

Finally, I would like to thank my family, especially my mum Wendy and my sister Ally, for their love, support, tolerance and patience. Special thanks should also go to my dad Bill, who got me started on this road, but sadly couldn't be with me at the end. Dad, this is for you.

Table of Contents

Abstract	I
Acknowledgements	II
Table of Contents	III
List of Figures	VIII
List of Tables	XVI
Nomenclature	XVII
Chapter 1 Introduction	2
1.1. Background	3
1.2. Objectives	9
Chapter 2 Literature Review	11
2.1. Hydrocolloids	12
2.1.1. Gellan gum	15
2.1.1.1. Origin and production	15
2.1.1.2. Molecular structure	16
2.1.1.3. Gelation	18
2.1.1.4. Conformation	22
2.2. Texture of gellan gum: Factors affecting gel texture	29
2.2.1. Effects of cations	29
2.2.2. Effect of excess salt and acids	34
2.2.3. Effect of sugars	35
2.2.4. Effect of acyl substituents	40
2.3. Rheology of solutions and gels	43
2.4. “Weak gels” (fluid gels)	46
2.5. Future developments: Gellan gum	49
2.6. Food processing in the human digestive system	49
Chapter 3 Experimental	55
3.1. Materials	56
3.1.1. Biopolymer solutions	56
3.1.1.1. Low Acyl and High Acyl Gellan Gum	56
3.1.1.2. Hydrochloric Acid	56
3.1.1.3. Gelatin	56
3.1.1.4. Sugars	56
3.1.1.5. Sodium Azide	57
3.1.1.6. Starch Assay Kit	57
3.1.1.7. Sucrose Assay Kit	58
3.1.1.8. Fructose Assay Kit	59

3.2.	Methodology	60
3.2.1.	Study of low acyl and high acyl mixed and mixed acid gellan gum quiescent gels	60
3.2.1.1.	Preparation of mixed gels	60
3.2.1.2.	Texture analysis	60
3.2.1.2.1.	Post-production exposure to an acidic environment	63
3.2.1.3.	Rheological analysis	63
3.2.1.4.	Differential scanning calorimetry	64
3.2.1.5.	Polarimetry	64
3.2.2.	Kinetic studies of low acyl gellan gum fluid gels produced using a scraped surface heat exchanger and a jacketed pin-stirrer	65
3.2.2.1.	The scraped surface heat exchanger	65
3.2.2.2.	The pin-stirrer	68
3.2.2.3.	Set-up	69
3.2.2.4.	Viscosity measurements post fluid gel production	71
3.2.2.5.	Examination of the fluid gel physical properties	71
3.2.3.	Kinetic studies of low acyl gellan gum fluid gels produced using a jacketed pin-stirrer	72
3.2.3.1.	Set-up	72
3.2.3.2.	Viscosity measurements post fluid gel production	74
3.2.3.3.	Study of the microstructure recovery	74
3.2.3.3.1.	Structure development	74
3.2.3.3.2.	Strain-recovery test	74
3.2.3.4.	Examination of the fluid gel properties	75
3.2.3.5.	Differential scanning calorimetry	75
3.2.4.	Effect of processing conditions on low acyl gellan gum fluid gels	76
3.2.4.1.	Set-up	76
3.2.4.2.	Viscosity measurements post fluid gel production	77
3.2.4.3.	Strain-recovery test	77
3.2.4.4.	Differential scanning calorimetry	80
3.2.4.5.	Particle size determination	80
3.2.5.	Kinetic studies of low acyl gellan gum fluid gels produced using a rheometer	81
3.2.5.1.	Rheometer configuration and set-up	81
3.2.5.2.	Viscosity measurements during fluid gel production	81
3.2.5.3.	Viscosity measurements post fluid gel production	83
3.2.5.4.	Particle size determination	83
3.2.5.5.	Study of the microstructure recovery	83
3.2.5.5.1.	Microstructure ripening	84
3.2.5.5.2.	Strain-recovery test	85
3.2.5.6.	Study of the gel de-structuring and restructuring	85
3.2.6.	Acid exposure of low acyl gellan gum fluid gels	86
3.2.6.1.	Direct acid addition	86

	3.2.6.1.1. Viscosity measurements post fluid gel production	87
	3.2.6.1.2. Study of the gel de-structuring	87
	3.2.6.2. Post-production acid exposure	88
3.2.7.	Study of % co-solute (sugar) release from low acyl gellan gum and co-solute mixed quiescent gels	89
	3.2.7.1. Preparation of the low acyl gellan gum and co-solute mixed quiescent gels	89
	3.2.7.2. Gel Texture	90
	3.2.7.3. Kinetic study of the low acyl gellan gum and co-solute mixed quiescent gels	90
	3.2.7.4. Measuring the % co-solute release using spectrophotometry	90
	3.2.7.4.1. Measuring the % co-solute release over time	95
3.2.8.	Study of % co-solute (sugar) release from low acyl gellan gum and co-solute mixed fluid gels	96
	3.2.8.1. Preparation of the low acyl gellan gum and co-solute mixed fluid gels	96
	3.2.8.2. Study of the low acyl gellan gum and co-solute mixed fluid gel de-structuring	97
	3.2.8.3. Measuring the % co-solute release using spectrophotometry	97
Chapter 4	Acid-sensitive Low and High Acyl Mixed Gellan Gum Systems	100
4.1.	Introduction	101
4.2.	Results & Discussion	101
	4.2.1. Characterisation of mixed gellan gels	101
	4.2.1.1. Gel structure	101
	4.2.1.2. Viscometric material response	104
	4.2.1.3. Viscoelastic material response	107
	4.2.1.4. Identification of enthalpic conformational transitions using DSC	109
	4.2.2. Post-production exposure of gels to an acidic environment	113
	4.2.3. Acid exposure during gelation	117
	4.2.3.1. Viscometric material response	117
	4.2.3.2. Viscoelastic material response	119
	4.2.3.3. Identification of enthalpic conformational transitions using DSC with decreasing pH	121
	4.2.4. Effect of biopolymer concentration	129
	4.2.4.1. Gel structure	129
	4.2.4.2. Enthalpic ordering of gellan gum	134
4.3.	Conclusions	139
Chapter 5	Low Acyl Gellan Gum Fluid Gels	140
5.1.	Introduction	141
5.2.	Results & Discussion	141

5.2.1.	Kinetic studies of low acyl gellan gum fluid gels produced using a jacketed pin-stirrer	141
5.2.1.1.	Viscometric material response post fluid gel production	141
5.2.1.2.	Structure development	143
5.2.1.3.	Structure recovery	146
5.2.1.4.	The coil-helix transition	149
5.2.1.5.	Identification of enthalpic conformational transitions using DSC	155
5.2.2.	Kinetic studies of low acyl gellan gum fluid gels produced using a scraped surface heat exchanger and jacketed pin-stirrer	158
5.2.3.	Effect of processing conditions on low acyl gellan gum fluid gels	160
5.2.3.1.	Viscometric material response post fluid gel production	160
5.2.3.2.	Structure recovery	165
5.2.3.3.	Identification of enthalpic conformational transitions using DSC	170
5.2.3.4.	Particle size determination	180
5.2.4.	Kinetic studies of low acyl gellan gum fluid gels produced using a rheometer	183
5.2.4.1.	Effect of shear rate during fluid gel production	183
5.2.4.2.	The coil-helix transition	186
5.2.4.3.	Viscometric material response post fluid gel production	192
5.2.4.4.	Effect of cooling rate during fluid gel production	194
5.2.4.5.	Particle size determination	198
5.2.4.6.	Microstructure ripening	201
5.2.4.7.	Structure recovery	203
5.2.5.	Acid exposure of low acyl gellan gum fluid gels	208
5.2.5.1.	Direct acid addition	208
5.2.5.1.1.	Viscometric material response post acid fluid gel production	208
5.2.5.1.2.	Viscoelastic material response	211
5.2.5.2.	Post-production acid exposure	213
5.2.5.2.1.	Effect of biopolymer concentration	214
5.2.5.2.2.	Effect of processing conditions	219
5.2.5.2.3.	Effect of pH	228
5.3.	Conclusions	230
Chapter 6	Low Acyl Gellan Gum and Co-solute Mixed Gels	232
6.1.	Introduction	233
6.2.	Results & Discussion	233
6.2.1.	Characterisation of low acyl gellan gum and co-solute mixed quiescent gels, and a subsequent measure of their % co-solute release	233
6.2.1.1.	Gel structure	233
6.2.1.1.1.	Glucose	233
6.2.1.1.2.	Sucrose and Fructose	239

6.2.1.2.	Viscoelastic material response: Identification of the coil-helix transition	251
6.2.1.2.1.	Glucose	251
6.2.1.2.2.	Sucrose and Fructose	259
6.2.1.3.	Measuring the % co-solute release using spectrophotometry	266
6.2.1.3.1.	Glucose	266
6.2.1.3.2.	Sucrose and Fructose	267
6.2.1.4.	Measuring the % co-solute release over time	271
6.2.1.4.1.	Glucose and Sucrose	271
6.2.2.	Characterisation of low acyl gellan gum and co-solute mixed fluid gels, and a subsequent measure of their % co-solute release	275
6.2.2.1.	Viscoelastic material response: Identification of the helix-coil transition	275
6.2.2.1.1.	Glucose and Sucrose	275
6.2.2.2.	Measuring the % co-solute release using spectrophotometry	281
6.2.2.2.1.	Glucose and Sucrose	281
6.3.	Conclusions	283
Chapter 7	Conclusions and Future Recommendations	285
7.1.	Conclusions	286
7.1.1.	Acid-sensitive low and high acyl mixed gellan gum systems	286
7.1.2.	Low acyl gellan gum fluid gels	288
7.1.3.	Low acyl gellan gum and co-solute mixed gels	289
7.2.	Future Recommendations	293
Chapter 8	References	294
Chapter 9	Appendices	312
9.1.	Conferences and Publications	313

List of Figures

- 2.1 Molecular structures of gellan gum in its native (a) and deacylated (b) forms.
- 2.2 Schematic models for the gelation of gellan adapted from those proposed by (a) Robinson et al. (1991) and (b) Gunning & Morris (1990) and presented in Morris et al. (2012). Filled circles in each model denote cations that encourage the aggregation of double helices.
- 2.3 Typical mechanical spectra (taken directly from Morris et al. (2012)) of (a) a true gel, (b) a semi-dilute solution of entangled polymer coils, and (c) a dilute polymer solution.
- 3.1 A typical true strain/true stress curve obtained during uniaxial compression of gellan gum acid gels adapted from Figure 1, Norton et al. (2011). Also shown is how the data in the plot is interpreted to give the total work to failure, bulk modulus and Young's modulus for the acid gel structures
- 3.2 Rheometer peltier plate and cone and plate geometry with the fixed humidity trap to reduce evaporation.
- 3.3 Schematic diagram of the scraped surface heat exchanger (a-unit). Units are expressed in mm.
- 3.4 Schematic diagram of the pin-stirrer (c-unit). Units are expressed in mm.
- 3.5 Schematic diagram of the scraped surface heat exchanger and pin-stirrer experimental set-up employed for fluid gel production.
- 3.6 Schematic diagram of the pin-stirrer heat exchanger experimental set-up employed for fluid gel production. ' T ' denotes the thermocouples measuring the temperatures of the fluid entering (T_{in}) and exiting (T_{exit}) the pin-stirrer.
- 4.1 Bulk modulus (a) and work up to fracture (b) for 3 wt.% low acyl gellan gels as a function of increasing high acyl gellan percentage (0 – 100 % of the total biopolymer added). All measurements were carried out in triplicate with a compression rate of 1 mm/s. The error bars were determined from the standard deviations of these measurements collectively. Where error bars cannot be observed, they are smaller than the data points.
- 4.2 Viscosity measurements of 0.5 wt.%, pH 5 mixed gellan aqueous solutions during a temperature cooling ramp (90 – 5 °C) at 2 °C/min, using a constant shear rate of 0.5 s⁻¹. Each of the viscosity readings are based on a single sample measurement.
- 4.3 Elastic modulus (a) and viscous modulus (b) measurements at 1.06 Hz versus temperature for 0.5 wt.%, pH 5, low acyl gellan aqueous solutions as a function of increasing high acyl gellan proportion (0, 30, 50, 70, and 100 %) during a temperature cooling ramp (90 – 10 °C), whilst performing frequency tables from 0.1 – 10 Hz at 10 °C intervals. Each of the modulus readings are based on a single sample measurement.

- 4.4 μ -DSC exothermic (a) and endothermic (b) peaks (baseline subtracted) for 0.5 wt.% low acyl gellan gum solutions with 0, 50, and 100 % high acyl gellan, at their natural pH. A cooling and heating rate of 0.2 °C/min was implemented. Note that heat flow y-values have been added and subtracted to separate the curves from each other for clarity. Each curve is based on a single sample measurement, due to the lengthy experimental procedure of 15 hours, 40 minutes.
- 4.5 The bulk modulus (a) and work up to fracture (b) data for mixed gellan gels after production, and after exposure to acid. All measurements were carried out in triplicate with a compression rate of 1 mm/s. The error bars were determined from the standard deviations of these measurements collectively. Where error bars cannot be observed, they are smaller than the data points.
- 4.6 Viscosity measurements of 0.5 wt.%, 70 % high acyl mixed gellan aqueous solutions at varying pH values during a temperature cooling ramp (90 – 5 °C) at 2 °C/min, using a constant shear rate of 0.5 s⁻¹. Each of the viscosity readings are based on a single sample measurement.
- 4.7 Elastic modulus (a) and viscous (b) measurements at 1.06 Hz versus temperature for 0.5 wt.%, 70 % high acyl mixed gellan aqueous solutions as a function of pH (natural – 2) during a temperature cooling ramp (90 – 10 °C), whilst performing frequency tables from 0.1 – 10 Hz at 10 °C intervals. Each of the modulus readings are based on a single sample measurement.
- 4.8 μ -DSC exothermic (a, c, e) and endothermic (b, d, f) peaks (baseline subtracted) for 0.5 wt.% low acyl gellan gum solutions with 0, 50, and 100 % high acyl gellan, as a function of pH (4 – 2). A cooling and heating rate of 0.2 °C/min was implemented. Note that heat flow y-values have been added and subtracted to separate the curves from each other for clarity. Further, the 100:0 (LA:HA), pH 3 cooling curve in Figure 4.8a is representative of a 2 wt.% concentrated sample. Each curve is based on a single sample measurement, due to the lengthy experimental procedure of 15 hours, 40 minutes.
- 4.9 True stress/true strain curves for the 50 % high acyl mixed gellan gels at pH 4, as a function of increasing gellan concentration (1 to 2 wt.%). All measurements were carried out in triplicate with a compression rate of 1 mm/s. The error bars were determined from the standard deviations of these measurements collectively. Where error bars cannot be observed, they are smaller than the data points.
- 4.10 Bulk modulus (a – b) and work up to fracture (c – d) for the mixed gellan gels, as a function of pH at gellan concentrations 1 wt.% and 2 wt.% respectively, each stored at 5 °C. Note, where data plots are missing, the gels formed were not strong enough to be tested. All measurements were carried out in triplicate with a compression rate of 1 mm/s. The error bars were determined from the standard deviations of these measurements collectively. Where error bars cannot be observed, they are smaller than the data points.
- 4.11 Variation of optical rotation (365 nm) with temperature for 0.025 wt.% low acyl gellan gum solutions with 0 (a), and 100 (b) % high acyl gellan on cooling (two runs) and heating in double distilled water, using a scan rate of 2 °C/min.

- 4.12 Variation of optical rotation (365 nm) with temperature for double distilled water on cooling (two runs) and heating. Each reading is based on a single sample measurement.
- 4.13 Variation of optical rotation (578 nm) with temperature for 5 wt.% gelatin (from porcine skin) aqueous solution on cooling and heating in double distilled water. Each reading is based on a single sample measurement.
- 5.1 Viscosity flow curves for 1 and 2 wt.% low acyl gellan gum fluid gels produced using a jacketed pin-stirrer (1500 rpm shaft speed, 100 ml/min pump rate, 20 °C water bath, ~ 30 °C/min cooling rate), as a function of increasing shear exposure time. 1 cycle is equal to one full pass through the pin-stirrer unit. The continuous cycle is when the inlet and outlet solution tubes are fed from the final sample container to create a linked system. Samples were collected from each after equilibrium had been achieved. Each of the viscosity readings are based on a single sample measurement.
- 5.2 Storage (G') and loss (G'') moduli as a function of time for 1 and 2 wt.% low acyl gellan gum fluid gels produced using a jacketed pin-stirrer, during a table of frequencies test (0.1 – 100 rad/s at 20 °C). Each of the modulus readings are based on a single sample measurement.
- 5.3 Storage (G') and loss (G'') moduli from stress-sweep measurements for 1 and 2 wt.% low acyl gellan gum fluid gels produced using a jacketed pin-stirrer (1st cycle samples only), performed at 1 Hz. The 1st sweep was carried out 24 hours after the production of the fluid gels and, after a “resting” stage of 10 min, it was followed by a 2nd sweep. Each of the stress-sweep moduli values are based on a single sample measurement.
- 5.4 Storage (G') and loss (G'') moduli for 1 and 2 wt.% low acyl gellan gum fluid gels produced using a jacketed pin-stirrer, during a low-amplitude oscillation temperature cooling ramp (a) (90 – 20 °C) and heating ramp (b) (20 – 95 °C) at 1 °C/min (10 rad/s at 1 % strain). Each of the modulus readings are based on a single sample measurement. Note that the data enclosed in the boxed region in each of the figures ((a) and (b)) is representative of the respective inserts shown.
- 5.5 μ -DSC endothermic (heating) (a) and exothermic (cooling) (b) peaks (baseline subtracted) for 1 and 2 wt.% low acyl gellan gum fluid gels produced using a jacketed pin-stirrer (1st cycle samples only). A cooling and heating rate of 0.5 °C/min was implemented. The first heating scan shows melting of a fluid gel; the second, a quiescent gel. Note that heat flow y-values have been added and subtracted to separate the curves from each other for clarity. Each curve is based on a single sample measurement, due to the lengthy experimental procedure of 11 hours, 40 minutes.
- 5.6 Viscosity flow curves for 0.25 (a, b) and 1 wt.% (c, d) low acyl gellan gum fluid gels produced using a jacketed pin-stirrer (average cooling rate, °C/min (per pump rate): 15 (50), 40 (100), 60 (150), 75 (200)) with shaft speeds of 1500 and 1000 rpm (a, c) and 500 and 275 rpm (b, d) and varying pump rate speeds (50 – 200 ml/min). Each of the viscosity readings are based on a single sample measurement.

- 5.7 Storage (G') and loss (G'') moduli from stress-sweep measurements (1 Hz) for 0.25 and 1 wt.% low acyl gellan gum fluid gels produced using a jacketed pin-stirrer (~ 60 °C/min cooling rate) with a pump rate of 150 ml/min and shaft speeds of 1500 (a), 1000 (b), 500 (c) and 275 rpm (d). The 1st sweep was carried out 24 hours after the production of the fluid gels and, after a “resting” stage of 10 min, it was followed by a 2nd sweep. Each of the stress-sweep moduli values are based on a single sample measurement.
- 5.8 μ -DSC endothermic (heating) (a, b) and exothermic (cooling) (c, d) peaks (baseline subtracted) for 0.25 wt.% low acyl gellan gum fluid gels produced using a jacketed pin-stirrer (average cooling rate, °C/min (per pump rate): 15 (50), 40 (100), 60 (150), 75 (200)) with a shaft speed of 1500 rpm and pump rates of 50 and 100 ml/min (a, c) and 150 and 200 ml/min (b, d). A cooling and heating rate of 0.5 °C/min was implemented. The first heating scan shows melting of a fluid gel; the second, a quiescent gel. Each curve is based on a single sample measurement, due to the lengthy experimental procedure of 11 hours, 40 minutes. Note that the curves have been separated (on the heat flow axis) for clarity.
- 5.9 μ -DSC endothermic (heating) (a, b) and exothermic (cooling) (c, d) peaks (baseline subtracted) for 0.25 wt.% low acyl gellan gum fluid gels produced using a jacketed pin-stirrer (average cooling rate, °C/min (per pump rate): 15 (50), 40 (100), 60 (150), 75 (200)) with a pump rate of 50 ml/min and shaft speeds of 1500 and 1000 rpm (a, c) and 500 rpm (b, d). A cooling and heating rate of 0.5 °C/min was implemented. The first heating scan shows melting of a fluid gel; the second, a quiescent gel. Each curve is based on a single sample measurement, due to the lengthy experimental procedure of 11 hours, 40 minutes. Note that the curves have been separated (on the heat flow axis) for clarity.
- 5.10 Micrographs for 0.25 wt.% low acyl gellan gum fluid gels produced using a jacketed pin-stirrer (average cooling rate, °C/min (per pump rate): 15 (50), 40 (100), 60 (150), 75 (200)) with a shaft speed of 1000 rpm and pump rates of 50 (a), 100 (b), 150 (c) and 200 ml/min (d). Scale = 20 μ m.
- 5.11 Viscosity profiles of 2 wt.% low acyl gellan gum fluid gels, during their production process, as a function of the applied shear rate (0.5 – 1000 s^{-1}). All systems were subjected to a constant cooling rate of 3 °C/min from 90 – 5 °C. Each of the viscosity readings at each shear rate are based on a single sample measurement.
- 5.12 Storage (G') and loss (G'') moduli at 1.585 Hz for 2 wt.% low acyl gellan gum fluid gels produced within a rheometer (50 s^{-1} applied shear rate, 3 °C/min cooling rate) following frequency tables from 0.1 – 10 Hz every 10 °C during temperature heating (a) and cooling ramps (b) between 20 – 90 °C. Each of the modulus readings are based on a single sample measurement.
- 5.13 Shear thinning behaviour of 2 wt.% low acyl gellan gum fluid gels (produced within a rheometer using a range of applied shear rates (0.5 – 1000 s^{-1})), measured immediately after their formation process. All systems were subjected to a constant cooling rate of 3 °C/min between 90 – 5 °C during formation. Each viscosity value is based on a single sample measurement.

- 5.14 Viscosity profiles of 2 wt.% low acyl gellan gum fluid gels, during their production process, as a function of the applied cooling rate (0.5 – 4 °C/min). All systems were subjected to a constant shear rate of (a) 5 s⁻¹, (b) 50 s⁻¹, (c) 200 s⁻¹ and (d) 1000 s⁻¹ between 90 – 5 °C. Each viscosity value is based on a single sample measurement.
- 5.15 Micrographs of 2 wt.% low acyl gellan gum fluid gels produced using a rheometer with an applied cooling rate of 1 °C/min and shear rates of (a) 1, (b) 5, (c) 50, and 100 s⁻¹ (d). Scale = 20 μm.
- 5.16 Storage (G') modulus for 2 wt.% low acyl gellan fluid gels produced within a rheometer using different shear rates (0.5 – 1000 s⁻¹) and a cooling rate of 3 °C/min between 90 – 5 °C, immediately after production. Each modulus value is based on a single sample measurement.
- 5.17 Storage (G') and loss (G'') moduli from stress-sweep measurements (1 Hz) for 2 wt.% low acyl gellan gum fluid gels produced within a rheometer using the shear and cooling rates (a) 5 s⁻¹, 1 °C/min, (b) 100 s⁻¹, 4 °C/min and (c) 100 s⁻¹, 6 °C/min. The 1st sweep was carried out 24 hours after the production of the fluid gels and, after a “resting” stage of 10 min, it was followed by a 2nd sweep. Each of the stress-sweep moduli values are based on a single sample measurement.
- 5.18 Viscometric data as a function of pH for 1 wt.% low acyl gellan gum fluid gels produced within a jacketed pin-stirrer (1500 rpm shaft speed, 100 ml/min pump rate, 15 °C water bath, ~ 30 °C/min cooling rate) (a), and 1 wt.% low acyl gellan quiescent gels (b) for comparison. Each viscosity value is based on a single sample measurement.
- 5.19 Storage (G') moduli at 1.00 Hz as a function of pH, for 1 wt.% low acyl gellan gum fluid gels produced within a jacketed pin-stirrer (1500 rpm shaft speed, 100 ml/min pump rate, 15 °C water bath, ~ 30 °C/min cooling rate), following frequency tables from 0.1 – 10 Hz every 10 °C during a temperature heating ramp. Each modulus value is based on a single sample measurement.
- 5.20 True stress/true strain curves for 1 and 2 wt.% low acyl gellan gum fluid gels produced using a jacketed pin-stirrer (1500 rpm shaft speed, 100 ml/min pump rate, 20 °C water bath, ~ 30 °C/min cooling rate), following exposure to a 0.5 % HCl acid bath soak overnight. All measurements were carried out in triplicate with a compression rate of 1 mm/s. Where error bars cannot be observed, they are smaller than the data points.
- 5.21 Bulk modulus and total work up to fracture data for 1 and 2 wt.% low acyl gellan gum fluid gels produced using a jacketed pin-stirrer (1500 rpm shaft speed, 100 ml/min pump rate, 20 °C water bath, ~ 30 °C/min cooling rate), following exposure to a 0.5 % HCl acid bath soak overnight.
- 5.22 True stress/true strain curves for 1 and 2 wt.% low acyl gellan gum quiescent gels, following exposure to a 0.5 % HCl acid bath soak overnight. All measurements were carried out in triplicate with a compression rate of 1 mm/s. Where error bars cannot be observed, they are smaller than the data points.
- 5.23 Bulk modulus and total work up to fracture data for 1 and 2 wt.% low acyl gellan gum quiescent, following exposure to a 0.5 % HCl acid bath soak overnight.

- 5.24 True stress/true strain curves for 0.25 and 1 wt.% low acyl gellan gum fluid gels produced within a jacketed pin-stirrer (average cooling rate, °C/min (per pump rate): 15 (50), 40 (100), 60 (150), 75 (200)) using varying shaft speeds (1500 – 275 rpm) and pump rates (a) 50, (b) 100, (c), 150, and 200 (d) ml/min, following exposure to a 0.5 % HCl acid bath soak overnight. All measurements were carried out in triplicate with a compression rate of 1 mm/s. Where error bars cannot be observed, they are smaller than the data points.
- 5.25 Bulk modulus and total work up to fracture data for 0.25 and 1 wt.% low acyl gellan gum fluid gels produced within a jacketed pin-stirrer (average cooling rate, °C/min (per pump rate): 15 (50), 40 (100), 60 (150), 75 (200)) using varying pump rates (50 – 200 ml/min) and shaft speeds (a) 275, (b) 500, (c), 1000, and 1500 (d) rpm, following exposure to a 0.5 % HCl acid bath soak overnight.
- 5.26 True stress/true strain curves as a function of pH for 1 wt.% low acyl gellan gum fluid gels produced within a jacketed pin-stirrer (1500 rpm shaft speed, 100 ml/min pump rate, 15 °C water bath, ~ 30 °C/min cooling rate), and 1 wt.% low acyl gellan gum quiescent gels, following exposure to a 0.5 % HCl acid bath soak overnight. All measurements were carried out in triplicate with a compression rate of 1 mm/s. Where error bars cannot be observed, they are smaller than the data points.
- 5.27 Bulk modulus and total work of failure data as a function of pH for 1 wt.% low acyl gellan gum fluid gels produced within a jacketed pin-stirrer (1500 rpm shaft speed, 100 ml/min pump rate, 15 °C water bath, ~ 30 °C/min cooling rate), and 1 wt.% low acyl gellan gum quiescent gels, following exposure to a 0.5 % HCl acid bath soak overnight.
- 6.1 True stress/true strain curves for 2 wt.% (a), 3 wt.% (b) and 4 wt.% (c) low acyl gellan gum quiescent gels, as a function of increasing % glucose substitution (0 – 50 %). All measurements were carried out in triplicate with a compression rate of 1 mm/s. Where error bars cannot be observed, they are smaller than the data points.
- 6.2 Bulk modulus (a) and work up to fracture (b) data for the low acyl gellan gum quiescent gels substituted with 0 – 50 % glucose, as a function of increasing polymer concentration (2 – 4 wt.%).
- 6.3 True stress/true strain curves for 2 wt.% (a), 3 wt.% (b) and 4 wt.% (c) low acyl gellan gum quiescent gels, as a function of increasing % sucrose substitution (0 – 50 %). All measurements were carried out in triplicate with a compression rate of 1 mm/s. Where error bars cannot be observed, they are smaller than the data points.
- 6.4 True stress/true strain curves for 2 wt.% (a), 3 wt.% (b) and 4 wt.% (c) low acyl gellan gum quiescent gels, as a function of increasing % fructose substitution (0 – 50 %). All measurements were carried out in triplicate with a compression rate of 1 mm/s. Where error bars cannot be observed, they are smaller than the data points.
- 6.5 Bulk modulus (a) and work up to fracture (b) data for the low acyl gellan gum quiescent gels substituted with 0 – 50 % sucrose, as a function of increasing polymer concentration (2 – 4 wt.%).

- 6.6 Bulk modulus (a) and work up to fracture (b) data for the low acyl gellan gum quiescent gels substituted with 0 – 50 % fructose, as a function of increasing polymer concentration (2 – 4 wt.%).
- 6.7 Elastic (a) and viscous (b) modulus measurements at 1 Hz versus temperature for 2 wt.% low acyl gellan gum quiescent gels, as a function of increasing % glucose substitution (0 – 50 %) during a temperature cooling ramp (90 – 10 °C), whilst performing frequency tables from 0.1 – 10 Hz at 10 °C intervals. Each of the modulus readings are based on a single sample measurement.
- 6.8 Elastic (a) and viscous (b) modulus measurements at 1 Hz versus temperature for 2 wt.% low acyl gellan gum quiescent gels, as a function of increasing % sucrose substitution (0 – 50 %) during a temperature cooling ramp (90 – 10 °C), whilst performing frequency tables from 0.1 – 10 Hz at 10 °C intervals. Each of the modulus readings are based on a single sample measurement.
- 6.9 Elastic (a) and viscous (b) modulus measurements at 1 Hz versus temperature for 2 wt.% low acyl gellan gum quiescent gels, as a function of increasing % fructose substitution (0 – 50 %) during a temperature cooling ramp (90 – 10 °C), whilst performing frequency tables from 0.1 – 10 Hz at 10 °C intervals. Each of the modulus readings are based on a single sample measurement.
- 6.10 Measurement of % sugar (glucose (G), sucrose (S) and fructose (F)) released from low acyl gellan gum quiescent gels substituted with 10 – 50 % sugar following an 18 hour diffusion period, as a function of increasing polymer concentration (2 – 4 wt.%). All measurements were carried out in triplicate. Where error bars cannot be observed, they are smaller than the data points.
- 6.11 Measurement of % glucose released over time (hours) from 2 wt.% low acyl gellan gum quiescent gels substituted with 10 – 50 % glucose, as a function of increasing diffusion time (a) and increasing % glucose substitution (b). All measurements were carried out in triplicate. Where error bars cannot be observed, they are smaller than the data points.
- 6.12 Measurement of % sucrose released over time (hours) from 2 wt.% low acyl gellan gum quiescent gels substituted with 10 – 50 % sucrose, as a function of increasing diffusion time (a) and increasing % sucrose substitution (b). All measurements were carried out in triplicate. Where error bars cannot be observed, they are smaller than the data points.
- 6.13 Elastic (a) and viscous (b) modulus measurements at 1 Hz versus temperature for 0.5 wt.% low acyl gellan gum fluid gels, as a function of increasing % glucose substitution (0 – 50 %) during a temperature heating ramp (10 – 90 °C), whilst performing frequency tables from 0.1 – 10 Hz at 10 °C intervals. Each of the modulus readings are based on a single sample measurement.
- 6.14 Elastic (a) and viscous (b) modulus measurements at 1 Hz versus temperature for 0.5 wt.% low acyl gellan gum fluid gels, as a function of increasing % sucrose substitution (0 – 50 %) during a temperature heating ramp (10 – 90 °C), whilst performing frequency tables from 0.1 – 10 Hz at 10 °C intervals. Each of the modulus readings are based on a single sample measurement.

- 6.15 Measurement of % glucose released from low acyl gellan gum fluid gels substituted with 10 – 50 % glucose following an 18 hour diffusion period, as a function of increasing polymer concentration (0.5 – 2 wt.%). All measurements were carried out in triplicate. Where error bars cannot be observed, they are smaller than the data points.
- 6.16 Measurement of % sucrose released from low acyl gellan gum fluid gels substituted with 10 – 50 % sucrose following an 18 hour diffusion period, as a function of increasing polymer concentration (0.5 – 2 wt.%). All measurements were carried out in triplicate. Where error bars cannot be observed, they are smaller than the data points.

List of Tables

- 3.1 Set up parameters for the *LA* gellan gum fluid gel solutions formulated using scraped surface heat exchanger and the pin-stirrer unit under consistent flow rate and shaft speed conditions.
- 3.2 Set up parameters for the *LA* gellan gum fluid gel solutions formulated using the pin-stirrer unit under consistent flow rate and shaft speed conditions. Each of the T_{in} and T_{exit} values are based on a single sample measurement.
- 3.3 Set up parameters for the 0.25 wt.% *LA* gellan gum fluid gel solutions formulated using the pin-stirrer unit under varying flow rate and shaft speed conditions. Each of the T_{in} and T_{exit} values are based on a single sample measurement.
- 3.4 Set up parameters for the 1 wt.% *LA* gellan gum fluid gel solutions formulated using the pin-stirrer unit under varying flow rate and shaft speed conditions. Each of the T_{in} and T_{exit} values are based on a single sample measurement.
- 3.5 Set up parameters for the 1 wt.% *LA* gellan gum acid fluid gel solutions formulated using the pin-stirrer unit using varying recirculating water bath temperatures. Each of the T_{in} and T_{exit} values are based on a single sample measurement.
- 3.6 Set up parameters for the 0.5 – 2 wt.% *LA* gellan gum – glucose fluid gel solutions formulated using the pin-stirrer unit under consistent flow rate and shaft speed conditions. Each of the T_{in} and T_{exit} values are based on a single sample measurement.
- 3.7 Set up parameters for the 0.5 – 2 wt.% *LA* gellan gum – sucrose fluid gel solutions formulated using the pin-stirrer unit under consistent flow rate and shaft speed conditions. Each of the T_{in} and T_{exit} values are based on a single sample measurement.
- 4.1 Table of differential scanning calorimetry measurements (to 3 s.f.) for 0.5 wt.% low acyl gellan aqueous solutions with 0, 50, and 100 % high acyl gellan, for a variety of pH values, where ΔH is the amount of heat energy gained or lost by the solutions. The asterisks (*) in the table indicate where no clear peak detection was observed for the corresponding material components. Each of the ΔH and T_{max} values are based on a single sample measurement.
- 5.1 Table of differential scanning calorimetry measurements (to 3 s.f.) for 1 and 2 wt.% low acyl gellan gum fluid gels produced using a jacketed pin-stirrer (1st cycle samples only), where ΔH is the amount of heat energy gained or lost by the solutions. Each of the ΔH and T_{max} values are based on a single sample measurement.
- 5.2 Table of DSC measurements (to 3 s.f.) for a selection of 0.25 wt.% low acyl gellan gum fluid gel samples produced using a jacketed pin-stirrer (average cooling rate, °C/min (per pump rate): 15 (50), 40 (100), 60 (150), 75 (200)) with varying pump rates (50 – 200 ml/min) and shaft speeds (1500 – 500 rpm), where ΔH is the amount of heat energy gained or lost by the solutions. Each of the ΔH and T_{max} values are based on a single sample measurement.

Nomenclature

Rheology

G'	Storage (elastic) modulus
G''	Loss (viscous) modulus
$[\eta]$	Intrinsic viscosity
δ	Phase angle ($\tan^{-1} G''/G'$)
E'	Storage modulus for longitudinal oscillation
$ G^* $	Complex modulus
ω	Frequency of oscillation
$ \eta^* $	Complex dynamic viscosity
η	Steady-shear viscosity
$\tan \delta$	Loss tangent (G''/G')
G_e	Storage modulus (G') at equilibrium
τ	Resistance (stress)
T_{melt}	Melting temperature

Other

C^*	Critical overlap concentration
C_s	Added salt concentration
ΔS	Entropy
T	Temperature
T_{ch}	Coil-helix transition temperature
T_{sg}	Sol-gel transition temperature
T_m	Midpoint temperature
T_{in}	Inlet temperature
T_{exit}	Exit temperature
T_{max}	Maximum heat flow temperature
T_{hc}	Helix-coil transition temperature
$[\gamma]$	Activity coefficient
ϕ	Osmotic coefficient
f	Transport coefficient
C_T	Total cation concentration
C_p	Concentration of charged groups on the polymer
α_T	Total cation activity
γ	Fraction of thermodynamically-free counterions
ϕ_c	Osmotic coefficient when the polymer is in the coil form
ϕ_h	Osmotic coefficient when the polymer is in the ordered helix form
C_T^*	Critical total cation concentration
C^2	Concentration squared
C_o	Minimum concentration
C	Concentration
E	Young's modulus (σ/ϵ)
σ_b	Break stress
ϵ_b	Strain at break
σ_b/ϵ_b	Modulus at break
f_a	Residual acetyl substituent
f_g	Residual glycerol substituent
σ	Stress

ε	Strain
μm	Micro-metre
\mathcal{E}_H	True strain
σ_T	True stress
\mathcal{E}_E	Engineering strain
\mathcal{E}_H	True (Hencky) strain
σ_E	Engineering stress
σ_T	True stress
H_o	Initial sample height
A_o	Cross-sectional area of sample
F	Applied compression force
h	Sample height
$\dot{\gamma}$	Rotating velocity
Q	Amount of heat energy gained or lost

Abbreviations

WHO	World Health Organisation
NMR	Nuclear Magnetic Resonance
GDL	Glucono-Delta-Lactone
CSLM	Confocal Scanning Laser Microscopy
HCl	Hydrochloric Acid
UV-Vis	Ultraviolet-Visible
EFSA	European Food Safety Authority
HA	High Acyl
LA	Low Acyl
DSC	Dynamic (differential) Scanning Calorimetry
OR	Optical Rotation
CD	Circular Dichroism
AFM	Atomic Force Microscopy
GG	Gellan Gum
1H NMR	Proton Nuclear Magnetic Resonance
LBG	Locust Bean Gum
GO/P	Glucose Oxidase/Peroxidase
ATP	Adenosine Triphosphate
G6P	Glucose-6-Phosphate
NAD	Nicotinamide Adenine Dinucleotide
G6PDH	Glucose-6-Phosphate Dehydrogenase
ADP	Adenosine Diphosphate
NADH	Nicotinamide Adenine Dinucleotide (reduced form)
PGI	Phosphoglucose Isomerase
SSHE	Scraped Surface Heat Exchanger
FDA	Food and Drug Administration
RPM	Rotations Per Minute
CFD	Computational Fluid Dynamic
CP	Cone and Plate
LVR	Linear Viscoelastic Region
GI	Gastrointestinal Tract
SEM	Scanning Electron Microscopy

Chapter 1

INTRODUCTION

1.1. Background

Before the 20th century, obesity was rare (Haslam, 2007). In 1997 however, the World Health Organisation (*WHO*) formally recognized obesity as a global epidemic (Caballero, 2007). As of 2008 the *WHO* estimated that globally at least 500 million adults are obese, with higher rates among women than men. Once considered a problem only of high-income countries, obesity rates are rising worldwide and affecting both the developed and developing world (Tsigosa, 2008).

The common approach adopted by the food industry to tackle this increasing global obesity problem is to reduce the amounts of calories consumed by reducing fat, sugar and salt contents' in foods. It is well known that morbid obesity can be addressed by lowering an individual's food intake. Today, food tastes good, is enjoyable, is softer, but does not satisfy hunger for significant time periods. Thus individuals feel hungry more quickly and subsequently want to eat again, often between meals. Clearly, there is a market for a foodstuff, which satiates hunger through a slow digestive process and retains its appeal to the consumer.

A new approach which forms the basis of this thesis, that may well impact on people's appetite without an adverse effect on consumer response, is the use of hydrocolloids that respond to the low pH conditions inside the stomach by self-structuring. The overall concept is, to formulate foods that are structured with a pH-sensitive hydrocolloid, and designed to structure the contents of the stomach; subsequently controlling the desire to overeat. Previous studies have investigated the ability of alginate to structure the stomach contents (Hoad et al., 2004; Norton et al., 2006a), and demonstrated via NMR imaging that structuring did occur within the stomach, which satisfied hunger. However, the alginate proved sensitive to calcium ions,

and produced acid gels too quickly, prior to consumption, which rendered it difficult to be added to foods.

An alternative hydrocolloid that forms acid gels is gellan gum (Yamamoto & Cunha, 2007). This has received little attention and has only been investigated under slow acid release from D-glucono- δ -lactone (GDL), with just a few exceptions that have studied acid gelation by direct addition of acid (Norton et al., 2011), a process more relevant to digestion. Gellan gum was thus chosen as the model hydrocolloid in this work. It is a gel-forming, carboxylated extracellular polysaccharide secreted by the organism *Sphingomonas elodea* during aerobic fermentation (Kang & Veeder, 1982). The gellan polymer consists of the monosaccharides β -D-glucose, β -D-glucuronic acid and α -L-rhamnose in molar ratios of 2:1:1 (Sanderson, 1990) linked together to form a primary linear structure. The biopolymer is produced with two acyl substituents present on the 3-linked glucose, L-glycerol positioned at O(2) and acetyl at O(6). Direct recovery of the polysaccharide from the fermentation broth yields the high acyl form whereas deacylation by alkali treatment results in the low acyl variant. Gellan gum is currently commercially available in both the high acyl and the low acyl form. Structurally the two polymers are very similar albeit the acyl groups, but each gives rise to very different gel structures with different material properties. When hot solutions of gellan gum are cooled in the presence of gel-promoting cations gels ranging in texture from brittle to elastic are formed, principally through cation-mediated helix-helix aggregation (Gibson & Sanderson, 1997). Intermediate mechanical properties between those of the individual components are seen when combining low acyl gellan with high acyl gellan to form mixed gels (Sanderson et al., 1988a); these retain high setting temperatures normally associated with high acyl products and ion sensitivity of low acyl products (Sworn, 1999).

Further, it is an advantage for food manufacturers to add a mixed biopolymer system that is formed from variants of one polymer to existing food products, in that just one polymer (e.g. gellan) can be listed in the ingredients list, rather than multiple polymers (often listed as E-numbers), which generally lead to consumer concern.

The acid gelation of acid-sensitive mixed biopolymer systems has not previously been investigated. Thus a clear opportunity exists in investigating the acid gelation of a mixture of low acyl and high acyl gellan to gain an insight into the acid gel structures that can be produced by the direct addition of acid. Additionally, the conditions found in the stomach after ingestion of food products incorporating such systems can be simulated, by assessing the mixed gel structures in an acid environment over a prolonged time period.

Acid-sensitive mixed biopolymer systems are a solution to single biopolymer acid gels structuring too quickly. For example, by introducing high acyl gellan as a disrupter polymer to a low acyl gellan system prior to gelation, rapid structuring of the latter can be prevented by carefully manipulating the gel properties by varying their proportions both at natural pH and following exposure to acid. It is this solution, which forms the basis of the first results chapter, “Acid-sensitive Low and High Acyl Mixed Gellan Gum Systems”.

Polysaccharides are widely used as replacements for undesirable ingredients, particularly in low fat and reduced calorie formulated foods or within enhanced satiety products (Tang et al., 1994; Brown et al., 1996; Garrec et al., 2012; Norton et al., 2006a). It has become increasingly evident, however that the use of hydrocolloids only as simple gelling and thickening agents does not offer the industry and consumer driven attributes of a healthy, convenient but still high in quality formulated product (Gabriele et al., 2009). This has led to the development of fluid (or sheared) gels, which can be

formulated to satisfy a wide range of structural requirements (Cassin et al., 2000; Norton et al., 2000).

Fluid gels are formed by applying an appropriate shear field to a biopolymer solution undergoing gelation; as a result a highly concentrated (high volume fraction) suspension of gelled particles is formed (Brown et al., 1996). There has been much discussion of the applications of fluid gels within foods; most of which exploit the polysaccharides' ability to form firm, brittle gels under quiescent cooling. Gellan gum (Sworn et al., 1995; Sworn, 2000; Sworn, 2009; Valli et al., 2001; Caggioni et al., 2007) is a multifunctional hydrocolloid with potential for use in a wide variety of food products as a gelling, texturising, stabilising, film forming, suspending and structuring agent (Kelco Division of Merck and Co., 1993; Sanderson, 1990; Gibson, 1992). This work (presented in Chapter 5: "Low Acyl Gellan Gum Fluid Gels") has focused on results obtained with low acyl gellan gum since it is prone to form clear gels, while high acyl gellan yields opaque gels with less thermal stability; the gel phase transition temperatures of the *LA* gellan gum (30 – 50 °C) are lower than those of the native gellan gum (70 – 80 °C), which makes the formation of fluid gels easier and cheaper.

The ordering of helices in gellan gum fluid gels is restricted to small volumes controlled by shear forces applied during the mechanical treatment during the cooling step (Valli et al., 2001). Fluid gels are heterogeneous materials at the microstructural level since polymer-rich microgels coexist with polymer-poor or even polymer-depleted regions. On the other hand, the consistency of fluid gels has also been achieved allowing gelation to occur in quiescent conditions provided specific gellan and gel-promoting ion concentrations are used (Sworn et al., 1995; Rodríguez-Hernández et al., 2003). The latter study demonstrated the heterogeneous microstructure of Na-low acyl gellan gum weak gels by confocal scanning laser microscopy (CSLM).

It is well known that the gelling ability of traditional gelling agents such as agarose and carrageenan is diminished at low pH (Moritaka et al., 1995). Research and development into ingredients that could form gels at low pH values is important for the production of products such as dessert jellies containing fruit juices as well as self-structuring satiety based food products which take advantage of the natural digestive processes (Moritaka et al., 1995; Norton et al., 2011). Aqueous systems of gellan maintain the gel state over a wide pH range in comparison with those made from other polysaccharides. Since, gellan is an anionic polyelectrolyte; pH may affect the conformation of the gellan chains in aqueous systems in two ways. One is the shielding effect caused by the electrostatic repulsion between the carboxyl groups found in the gellan units, as reported for other cation species (Miyoshi et al., 1996a; Miyoshi et al., 1998; Nickerson et al., 2003; Tang et al., 1995). The other is the change in anionic nature of the gellan chain as determined by the degree of dissociation of the carboxyl groups, which varies with pH (Horinaka et al., 2004). Research into the development of satiety based food products has demonstrated that acidification with hydrochloric acid (HCl) can be used to control the structure and breakdown of gellan gum acid gels, in acidic environments which modelled the stomach processes (Norton et al., 2011). These methods could also apply to gellan gum fluid gels.

An important requirement of self-structuring systems being incorporated into food products is their ability to remain stable during storage, whether that is during distribution or on the market shelves. Fluid gels have advantages in that they are temperature and time-stable structures, which can be used alone or added to pre-existing food products without structural changes. They can also provide an improved mouthfeel, generating higher consumer satisfaction. Thus, an approach to the aforementioned requirement is to formulate gellan gum fluid gels during process production and to then cyclise them to

achieve stability prior to their placing in food products and during consumption, avoiding any pre-structuring prior to reaching the target structuring stomach environment. It is this approach that generated the key motivation behind the results presented in the second results chapter, “Low Acyl Gellan Gum Fluid Gels”.

Industrial formulation of fluid gels requires a change in process equipment for instance from the rheometer to a more industrially relevant scale production. Studies describing bench scale production of fluid gels using a pin-stirrer heat exchanger, which are often used in industry at elevated scalable dimensions, have been published by Norton et al. (2000), Fernández Farrés et al. (2013) and Garrec & Norton (2012). They describe the production of agar, Ca-alginate and kappa-carrageenan fluid gels. Formulating the fluid gels using either process equipment method does not change the fact that fluid gels are influenced by process controls such as shear and cooling rate (Norton et al., 1999). Thus a comparison of these processing conditions for the respective methods is necessary.

The formation and properties of low acyl gellan gum fluid gels, by applying shear during the gelation process using two common production methods (a rheometer and a pin-stirrer heat exchanger) is discussed. This will aid understanding into the influence of processing conditions on their structure and material response. Additionally, the acid gelation or structuring of the low acyl gellan gum fluid gels is investigated through the direct addition of HCl acid, inducing a range of pH environments, and prolonged exposure to acid. This serves to simulate the stomach environment whilst eating and digesting. A further key aspect of this work is to see whether these fluid gel structures demonstrate similar responses to acid to those exhibited by the quiescent low and high acyl mixed gellan gum systems or whether a changed acid response prevails.

A challenge faced by researchers investigating self-structuring satiety based food products is how to incorporate materials that will modulate the energy delivery and slowly release calories after the meal (slow burn) has been consumed. The use of gel alone is more than capable of providing prolonged satiety but leads to unpleasant sensations for the consumer if there is no delivery of energy to the body to compliment the sensation of satiety. It is particularly important that any additional materials are still organoleptically acceptable to the consumer. The addition of co-solutes such as sugar and the measurement of their subsequent release from hydrocolloid gels could provide a first step to tackling these issues. The content of sugars in foods is of great importance. Both consumers and industry are interested in healthier new products with a decreased amount of sugars present. As the sweetness and the texture of these new products should not be significantly altered, a study on the behaviour of various sugars and their mixtures is necessary.

1.2. Objectives

The overall objective of this project was to find means of controlling the acid-induced gelation of a variety of gellan gum gel forms, in addition to exploring their mechanisms of co-solute release. The purpose of this being to provide optimal polymer selection and the initial breadths of research towards the development of a self-structuring satiety based food product. The key aims and objectives of the work presented in this thesis are as follows:

- Investigate whether the gelation kinetics of a low acyl gellan gum system can be further controlled by introducing high acyl gellan gum as a disrupter biopolymer. Further, investigate the *in-vitro* acid-induced gelation of the low acyl and high acyl gellan gum mixed biopolymer systems, and assess their

reactions over prolonged time periods (1 – 3 hours) in acidic conditions that mimic the stomach processes.

- Formulate a range of low acyl gellan gum fluid gel particulate structures using varying processing methods to ensure stability once incorporated into self-structuring food products, and to avoid premature structuring. Further, investigate whether these fluid gel structures demonstrate similar responses to acid to those exhibited by the quiescent low and high acyl mixed gellan gum systems. The key aspects are as follows:

- the effect of processing conditions: shear and cooling rates
- the influence of the production method: rheometer versus pin-stirrer
- the influence these parameters have on subsequent acid gel structuring

- Incorporate low levels (0 – 50 %) of sugars (glucose, sucrose and fructose) as energy sources in low acyl gellan quiescent and fluid gel structures to work towards providing a solution to consumers experiencing a sense of fullness without satisfaction after the consumption of a self-structuring product. Incorporate the sugars into the gel systems to deliver the energy for everyday functioning between meals, and modulate them so that calories are slowly release post-meal consumption maintaining consumer contentment over time.

The key aspects are as follows:

- the influence of sugar on structuring of acid-sensitive gels
- the energy release mechanism: the sugar release
- the influence of gel structure on the energy release properties

Chapter 2

LITERATURE REVIEW

2.1. Hydrocolloids

Hydrocolloids are widely used in many food formulations to improve quality attributes and shelf-life, with new uses and functions for these unique ingredients constantly being found (Saha & Bhattacharya, 2010; Seisun, 2010).

Hydrocolloids are defined as “a heterogeneous group of long chain polymers (polysaccharides and polypeptides (proteins)) characterised by their property of forming viscous dispersions and/or gels when dispersed in water. The presence of a large number of hydroxyl (-OH) groups markedly increases their affinity for binding water molecules rendering them hydrophilic compounds” (Saha & Bhattacharya, 2010). When dispersed they exhibit properties intermediate between a true solution and a suspension; a colloid. They are termed as ‘hydrophilic colloids’ or ‘hydrocolloids’.

The food industry has seen a large increase in the use of hydrocolloids in recent years. Despite being often present only at concentrations of less than 1%, they can have a significant influence on the textural and organoleptic properties of food products (Williams & Phillips, 2009). The main reason behind their use in foods is their ability to modify the rheology of food systems. This includes the two basic properties of flow behaviour (viscosity) and mechanical solid characteristics (texture). The modification of these properties within a food system helps to modify its sensory properties, and hence hydrocolloids are used as important food additives to perform specific purposes (Saha & Bhattacharya, 2010).

The changes in modern lifestyle, the ever growing awareness of the link between diet and health and new processing technologies have led to a rapid rise in the consumption of ready-made meals, functional foods and the development of high fibre and low-fat food products. In particular, numerous hydrocolloid products have been developed specifically

for use as fat replacers in food (Milani & Maleki, 2012). This has consequently led to an increased demand for hydrocolloids. The world hydrocolloids market is valued at around US\$4.4 billion per annum with a total volume of about 260,000 tonnes. In recent years, the average growth rate has been estimated at 2.5 – 3% (Williams & Phillips, 2009). Pure gellan gum is one of the most expensive hydrocolloids at US\$31 - 33/kg (Seisun, 2010). Gellan gum was approved for food use in Japan in 1988, but much later in the USA and Europe. It was one of the last hydrocolloids to go through a full food additive petition on a global scale, and its approval took many years at high costs. 25 years after its approval, gellan gum has yet to reach commercial volumes that justify the cost of bringing it to market full-scale. These high stakes and high risks could mean that no new hydrocolloid will be taken through a full approval process in the foreseeable future. Overall, the fundamental concept in terms of markets for food hydrocolloids is that the perception of consumers is the reality of hydrocolloid producers.

Hydrocolloids have a wide array of functional properties in foods. These include thickening (Sahin & Ozdemir, 2004), gelling (Milani & Maleki, 2012), emulsifying (Connolly et al., 1988), stabilisation (Phillips et al., 1990), controlling flavour release during mastication (Morris, 1993), and controlling the crystal growth of ice and sugar (Buyong & Fennema, 1988).

All colloids thicken and impart stickiness to aqueous dispersions, the extent of which is dependent on their nature and type. In addition, a few hydrocolloids also have the ability to form gels. Gel formation is the phenomenon involving the association or cross-linking of the polymer chains to form a three dimensional network that traps or immobilises the water within it to form a rigid structure that is resistant to flow (Saha & Bhattacharya, 2010). Essentially, it becomes viscoelastic exhibiting characteristics of both a liquid and a solid. The textural properties (e.g. elastic or brittle, long or

spreadable, chewy or creamy) of a gel vary widely with the hydrocolloid used. Sensory properties such as opacity, mouth feel and taste are also influenced on the hydrocolloid employed. The most common hydrocolloids used as thickening agents are starch, xanthan, guar gum, locust bean gum, gum karaya, gum Arabic and carboxymethyl cellulose (CMC). These are frequently used in soups, gravies, sauces and toppings to provide base texture. Common hydrocolloid gelling agents include alginate, pectin, carrageenan, gelatin, gellan and agar, which are used in food products like jams, jellies, ice-creams, gelled desserts, cakes and candies (Saha & Bhattacharya, 2010).

Mixtures of hydrocolloids are commonly used to impart novel and improved rheological characteristics to food products. The nature of the synergy can be due to association of the different hydrocolloid molecules or to phase separation. Careful selection of hydrocolloid type and concentration can lead to formation of a broad range of gel textures. The search for new synergistic combinations continues and is an area receiving considerable attention, as the understanding of the interactions and phase behaviour of hydrocolloid mixtures increases at the molecular level. New processing procedures are also being introduced and an area of growing interest is the formation of sheared gels to give novel rheological characteristics (Kavanagh & Ross-Murphy, 1998; Picout & Ross-Murphy, 2003). This as previously discussed involves applying shear as the hydrocolloid is undergoing gelation and results in the formation of micron-size hydrocolloid gel particles. At a sufficiently high concentration, the systems formed can have a very high low-shear viscosity and display strong shear thinning characteristics (Sworn et al., 1995).

Much research has been conducted in the nutraceutical benefits of hydrocolloids. Potential benefits range from cholesterol reduction to cancer risk reduction (Seisun, 2010). Their use in weight loss programmes (Paeschke & Aimutis, 2008; Fiszman &

Varela, 2013) is already widespread and likely to expand further. The hydrocolloids inulin and gum Arabic have also recently been shown to have prebiotic effects (Williams & Phillips, 2009). They are resistant to our human digestive enzymes and pass through the stomach and small intestine without being metabolised. They are then fermented in the large intestine to yield short chain fatty acids and stimulate the specific growth of beneficial intestinal bacteria, notably, bifidobacteria, and reduce the growth of harmful micro-organisms such as clostridia.

Genetic engineering could offer a tremendous opportunity for new functional developments in hydrocolloids. Bio-fermentation products such as xanthan and gellan gum could be manipulated to provide specific functional properties not now available (Seisun, 2010). The common approach taken for alteration or control is to change the physiological conditions of fermentation, or to use different strains of the respective bacteria. The genetic approach focuses on the enzymes controlling the biosynthetic pathways, and attempts to produce and isolate in sufficient quantity genetic mutants deficient or defective in one or more of these enzymes to give respective polymer chains with varying residual side chains (Morris & Harding, 2009). Seaweed, seed or other agricultural raw materials could also be genetically enhanced. For example, giant, rapidly growing kelp could be programmed to produce more than alginates. Unfortunately, these scenarios for improved production are restricted by consumer concerns. Although, this is not to say that future generations and future nutritional conditions will not radically change.

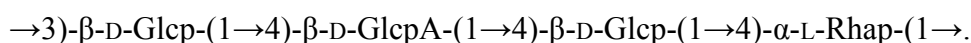
2.1.1. Gellan gum

2.1.1.1. Origin and production

Gellan gum is an extracellular bacterial polysaccharide secreted (Pollock, 1993) by the micro-organism *Sphingomonas elodea* (ATCC31461), formally known as *Pseudomonas elodea*. It was identified as being commercially viable (Sanderson, 1990) in 1978, via a thorough screening process involving soil and water bacteria by Kelco (San Diego, USA), who were seeking naturally occurring hydrocolloids with useful properties. To manufacture gellan gum, the micro-organism is inoculated with a fermentation medium, containing carbon, phosphate and nitrogen sources (Sworn, 2009). The process is performed under sterile conditions with careful management of aeration, agitation, temperature and pH. Pasteurisation follows fermentation, which then enables the polysaccharide to be extracted using varying methods to yield four different product types. Subjecting the pasteurised broth to alcohol precipitation yields the native, high acyl (*HA*) gellan form, whilst pre-treating prior to this with hot alkali yields the deacylated, low acyl (*LA*) form (Sworn, 2009). Gellan gum is currently sold commercially in three basic forms, namely *HA* unclarified (Kelcogel LT100), *LA* unclarified (Kelcogel LT), and *LA* clarified (Kelcogel and Kelcogel F). Tailored grades can also be formed, depending upon the intended use of the product, where properties such as particle size and gel strength can be manipulated. Additionally, gellan gum is often blended with other ingredients to make products with properties that are targeted to the needs of specific applications.

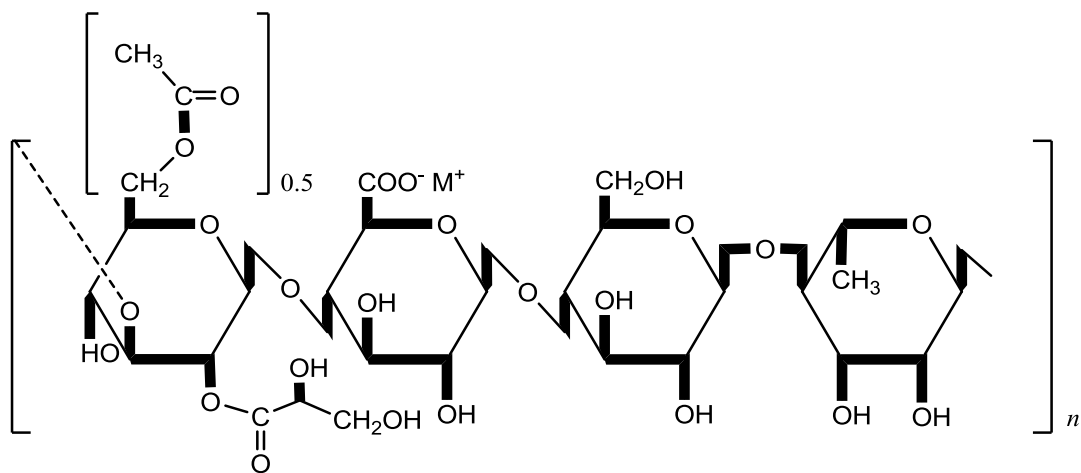
2.1.1.2. Molecular structure

Gellan gum is a “linear anionic polymer with a tetrasaccharide repeating sequence” (Jansson et al., 1983; O’Neill et al., 1983) formed from the residues β -D-glucose, β -D-glucuronate and α -L-rhamnose in the molar ratio 2:1:1:



The native polysaccharide, as biosynthesised, has an L-glycerol substituent on O(2) of the 3-linked glucose residue of the tetrasaccharide sequence and an acetyl group at O(6) of the same residue. On average, there is one glycerate per repeat and one acetate per every two repeats (Kuo et al., 1986). The acyl groups have a profound influence on gel characteristics. The *HA* form produces soft, elastic, non-brittle gels, whereas the *LA* form produces firm, non-elastic, brittle gels. Figure 2.1 shows the molecular structures of a) native or *HA* gellan gum and b) *LA* gellan gum.

(a) Native or high acyl gellan gum



(b) Low acyl gellan gum

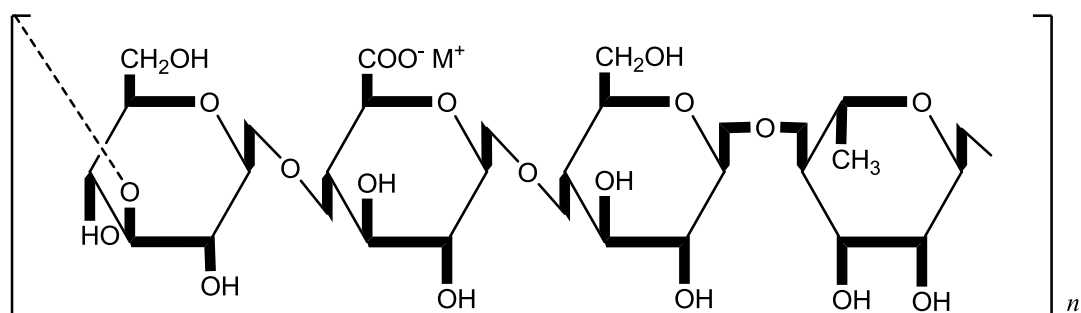


Figure 2.1. Molecular structures of gellan gum in its native (a) and deacylated (b) forms.

2.1.1.3. Gelation

The proposed gelation mechanism of gellan gum is based on the “domain model”, which assumes the formation of distinct junction zones that are connected adjacently by disordered polymer chains (Morris et al., 1980). Gellan gum solutions form gels on cooling, during which “a disorder-order transition” is undertaken. This transition has been attributed to a coil-helix transition (Grasdalen & Smidsrød, 1987). *LA* gellan gum forms a three-dimensional network following aggregation of the gellan double helices, by gel promoting cations to form hard, brittle gels. This mechanism has recently been challenged by studies using atomic force microscopy; Noda et al. (2008) propose “a fibrous model”, where network structures grow through the construction of non-associated fibres or strands via elongation or branching.

The acyl substituents have a profound effect on the structure and rheological characteristics of gellan gum gels (Sanderson et al., 1988b; & Mazon et al., 1999). Native gellan gum solutions proceed with similar disorder to order transitions on cooling, but the “domain model” states that further aggregation of the helices is restricted by the presence of the acetyl group (Morris et al., 1996). The fibrous model suggests that the “acyl groups inhibit end-to-end type intermolecular associations through steric hindrance, resulting in a decrease in the degree of continuity and homogeneity of the gelled system” (Noda et al., 2008). Thus, the *HA* gellan gum gels are soft and elastic.

LA gellan gum forms gels with several cations, particularly calcium (Ca^{2+}), magnesium (Mg^{2+}), sodium (Na^+), and potassium (K^+), in addition to acid (H^+) (Grasdalen & Smidsrød, 1987; & Sanderson & Clark, 1984). Divalent cations are more effective at promoting the gelation of *LA* gellan gum than monovalent ions (Gibson & Sanderson, 1997; Milas & Rinaudo, 1996; Miyoshi et al., 1996b; & Sanderson, 1990).

Gel strength rises with increasing ion concentration until its limit is reached. Addition of ions past this maximum causes a decrease in gel strength due to the “over-conversion” of the *LA* gellan gum with surplus ions. Generally, ion concentration levels for optimum gelation are independent of gellan gum concentration (Morris et al., 2012), but are minimised as the quantity of dissolved solids is increased. When *LA* gellan gum is exposed to pH levels below pH 3.0 it can form gels independently, without mono- or divalent metal ions. Irrespective of the acid used, these gels reach their optimum strength at pH 2.8 – 3.0 (Sworn, 2009). Acid gels tend to have greater gel strengths than ion mediated gels in water and sugar environments (Grasdalen & Smidsrød, 1987; Picone & Cunha, 2011). Acid gel strength however is generally reduced on addition of Na^+ and Ca^{2+} gelling cations (Sworn, 2009).

LA gellan gum is known to have (Sworn, 2009) a “snap” setting due to the rapid gelation occurring immediately after its setting temperature has been reached. Hydration temperature, setting and melting temperatures of the gels each depend on the ion type and concentration in solution, in addition to the grade of gellan gum and the presence of other dissolved solids (Kelco Division of Merck and Co., Inc., 1993). The greater the ion concentration, the greater the setting and melting temperature (Sworn, 2009). In the absence of added cations, *LA* gellan gum gels set at around 25 °C and are typically formed in the range 30 – 50 °C (Kelco Division of Merck and Co., Inc., 1993). Kasapis et al. (1999) reported that *LA* gellan gum gels in the presence of high levels of counterions, exhibit “significant thermal hysteresis between the setting and melting temperature, where the gels melt at a higher temperature than at which they set”. Below 100 °C, *LA* gellan gum gels in the absence of added cations are not thermally reversible (Sworn, 2009). Although, gels produced with a low level of monovalent ions, namely K^+ and milk gels are exemptions. Gel setting time is determined by the rate at which heat is

removed, which is dependent on the dimensions of the system being cooled (Sworn, 2009). After setting, gel modulus does not change significantly over time. Sworn (2009) found that *LA* gellan gum has the ability to form “self-supporting gels at concentrations as low as 0.05 % gum, which do not synerise unless cut or broken”.

Publications on the gelation of *LA* gellan gum in water, in the absence of added salt, have focused on the onset of the disorder-order transitions for varying gum concentrations. Miyoshi & Nishinari (1999a) recorded DSC measurements on both heating and cooling at a rate of 0.5 °C/min for a sodium type gellan called NaGG-3 (with the cation content (wt.%): Na⁺ 2.59; K⁺ 0.009; Ca²⁺ 0.02; Mg²⁺ 0.001) using varying polymer concentrations (1.0 – 5.5 wt.%). The size of the transition peaks increased as the polymer concentration was raised, and the measurements on cooling displayed an individual exotherm that moved gradually to elevated temperatures with increasing polymer concentration. The measurements on heating (≥ 4 wt.%) showed a solitary peak, which was equivalent to the exotherm observed on cooling. A second minor endotherm was detected (4.5 wt.%) which increased in magnitude relative to the first with increasing concentration. This enhancement in thermal stability was attributed to the Na⁺ cations (at their elevated concentration in the NaGG-3 type gellan at 4.5 wt.%), forming aggregated junctions of greater thermal stability. Miyoshi & Nishinari (1999a) also characterised the accompanying rheological changes using low-amplitude oscillatory measurements and comparable temperature cycles to those used in the DSC study. An initial, rapid incline in G'' on cooling coincided with the equivalent material cooling peaks in the DSC traces and also with conformational ordering events recorded (Matsukawa et al., 1999) using circular dichroism. These specific thermal transitions were therefore assigned as the coil-helix transition temperature (T_{ch}). G' also increased rapidly below T_{ch} , however at gellan concentrations under 2 wt.% it remained smaller

than G'' . Raising the concentration caused G' to rise above G'' , and the temperature at which the two curves crossed one another was taken to be the sol-gel transition temperature (T_{sg}). Both T_{ch} and T_{sg} increased with rising gellan concentration, paralleling the corresponding transitions observed in DSC. The rheological events during heating also proceeded via an identical thermal pathway to those on cooling for concentrations up to approximately 4 wt.%, supporting the DSC measurements. At 4.5 wt.%, a final steep decrease in G' and G'' during heating was observed at a greater temperature than the early, rapid incline on cooling, which was in agreement to the second elevated thermal peak recorded using DSC.

Three distinguishable physical conditions of gellan were identified from this work. The region above T_{ch} was ascribed to solutions of disordered coils; the area between T_{ch} and T_{sg} to solutions of ordered gellan; and the area below T_{sg} to continuous gel networks (Morris et al., 2012). Miyoshi & Nishinari (1999a) also found that for the gellan structures produced at < 3.5 wt.%, the rheological data displayed minimal parting between G' and G'' , with each showing large variations with frequency. Gels displaying these trends exhibit typical weak gel behaviour (Morris et al., 2012). However, the mechanical spectra reported by Miyoshi & Nishinari (1999a) for the structures produced at 3.5 wt.% gellan concentrations display a form typical of a true gel, where G' is greater than G'' with minimal changes in frequency. The behaviours of gellan can therefore, be grouped into “true gels” at polymer levels of 3.5 wt.% and over, and “weak gels” at reduced polymer levels down to 2 wt.%, where the sol-gel transition is absent on progressive decline (Morris et al., 2012).

HA gellan gum gels can be formed without the addition of cations and they are much less reliant on aqueous ion levels. The gels order at around 70 °C, and set at approximately 65 °C, showing “no thermal hysteresis” (i.e. their setting and melting

temperatures are identical) (Kelco Division of Merck and Co., Inc., 1993). Rising cation levels result in increased setting temperatures (Huang et al., 2004). *HA* gellan gum has the ability to form “self-supporting gels” at gellan gum levels above $\sim 0.2\%$ gellan gum, and they do not synerise (Sworn, 2009).

2.1.1.4. Conformation

The conformation of gellan gum in its gel form was first investigated by Upstill et al. (1986), who recorded high quality gellan fibre patterns using X-ray diffraction via elongation of gels, to encourage side ordering and configuration prior to drying. Initial models proposed were unconvincing; however re-examination by Chandrasekaran et al. (1988) successfully demonstrated that the solid-state structure of gellan in its ordered form “is a coaxial double helix”. Each strand in this conformation is a “3-fold, left-handed double helix with a pitch of 5.64 nm” (Morris et al., 2012). The helix-polymer chains are positioned parallel to each other and are staggered by a half, to give a repeat distance of 2.82 nm (Morris et al., 2012). Figure 2.1 shows the “tetrasaccharide repeating sequence of gellan”; three of the four glycosidic linkages form “equatorial bonds at C(1) and C(4)” residue positions (Morris et al., 2012). Generally, in long-chained carbohydrates, where each of the connections are “(1 \rightarrow 4)-diequatorial”, a flat, ribbon-like structure is adopted in the solid form (Rees et al., 1982). However, the exceptive connection in the gellan sequence is “(1 \rightarrow 3)”; this induces a regulated rotation in chain direction which encourages helix formation (Morris et al., 2012).

Many different techniques have been explored to examine polysaccharide conformational shifts and ordering mechanisms. With investigations of gellan, the common procedure associated (Morris et al., 2012) is the “conversion of the polymer to a single salt form” and the subsequent addition of salts of the identical cation to manipulate

the overall cation level. This method helps to minimise disruptions caused by the varying cations. Most frequently, “the tetra-methylammonium (M_4N^+) gellan salt form” is used to avoid gel formation mishaps. This is due to the very high added salt concentration (C_s) values required to induce gelation of gellan with M_4N^+ cations (Grasdalen & Smidsrød, 1987).

Crescenzi et al. (1987) used optical rotation (OR) at a wavelength of 302 nm to measure the conformational transitions of M_4N^+ gellan aqueous solutions (1.2 mM \approx 0.086 wt.%) and those with added M_4NCl (30 – 250 mM) on heating and cooling. The solution in water showed only a fractional linear rise in optical activity (-ve) with diminishing heat. Whilst, the aqueous samples with added M_4NCl displayed distinct sigmoidal changes that moved gradually to elevated temperatures with rising salt levels. Thermal hysteresis was also absent between heating and cooling measurements. Comparable sigmoidal profiles using polarimetry methods have also been obtained for other long-chained carbohydrates (Rees et al., 1982). These were shown to “arise from a conformational transition between an ordered structure at low temperature and a disordered coil state at high temperature” (Morris et al., 2012).

Circular dichroism (CD) is an additional technique many researchers (such as Matsukawa et al., 1999; Matsukawa & Watanabe, 2007; Nitta et al., 2001; Nitta et al., 2003; Ogawa et al., 2006; Tanaka et al., 1996) have used to gain an informed understanding of the conformational transitions of M_4N^+ gellan. Large spectral changes were recorded at \sim 202 nm between the high temperature disordered phase and the low temperature ordered phase. The temperature-pathway of conformational change is then monitored using the CD ellipticity data recorded around this wavelength.

Differential scanning calorimetry (DSC) is an additional technique used to study heat-induced conformational transitions. It is advantageous in that it can be performed at high polymer levels, due to optically-clear gel solutions not being necessary. Manning (1992) reported that M_4N^+ gellan aqueous samples (1 – 2 wt.%) in both water and with added M_4NCl at varying levels, gave distinct exo- and endotherms on cooling and heating respectively. The midpoint temperatures (T_m) recorded for each of the solutions from the exo- and endothermic runs were found to extrapolate to the identical reading at zero scan rate. This was agreeable with the lack of measurable thermal hysteresis observed by Crescenzi et al., (1987) using polarimetry.

Manning (1992) also monitored M_4N^+ gellan aqueous sample conformational transitions in both water and in the presence of M_4NCl using optical rotation and circular dichroism. Optical rotation measurements however were recorded using increased polymer levels and a greater wavelength (436 nm) than that employed by Crescenzi et al. (1987). Despite these differences, the values of the midpoint temperatures (T_m) from the respective studies agreed well.

The measurement of temperature-dependence on intrinsic viscosity has also been employed to study gellan structural changes. Ogawa et al. (2006) performed these measurements on sodium gellan with varying molecular weights (120 – 17 kD) in NaCl. High molecular weight samples gave sharp, sigmoidal increases in intrinsic viscosity $[\eta]$ between the high temperature disordered phase and the low temperature ordered phase. Whereas samples with progressively smaller molecular weights followed the same intrinsic viscosity increases on cooling, albeit at lower values. The sample with smallest molecular weight (17 kD) failed to display a sigmoidal profile. This was thought to be due to the polymer chains being too short to form an ordered structure. DSC

measurements reported (Ogawa et al., 2006) for identical gellan specimens on cooling, also displayed progressive reduction in intensity with diminutive molecular weight.

The loss of measurable nuclear magnetic resonance (NMR) signals can also enable conformational arrangements to be monitored (Rees et al., 1982). Generally, solutions containing small molecules (e.g. sugars) give sharp signals, whereas those of disordered polysaccharide coils give rise to broader, yet identifiable lines. When the polymer is converted to its rigid, ordered conformation, these signals are broadened further, flattening them into the baseline making them undetectable. Milas & Rinaudo (1996) reported a sigmoidal fall in their ^1H high-resolution NMR intensity measurements with diminutive temperature for various Na^+ gellan solutions. They used the methyl group resonance from the rhamnose residue (Figure 2.1) to quantify this reduction, which gave emissions that were well resolved compared to other hydrogen atoms in gellan. It was confirmed (Milas & Rinaudo, 1996) that the loss of detectable signal, in addition to the conformational transitions observed using the previously explained techniques, corresponds to the change from a high temperature disordered state to a low temperature, rigid conformation. Additionally, Milas & Rinaudo (1996) reported that the T_m 's for D_2O gellan solutions were approximately 6 °C higher than those of water, suggesting reinforcement of the gellan double helices through interparticulate and water molecule hydrogen bonding.

A plethora of experimental evidence has been used to provide the basis for two gelation models of gellan; presented schematically in Figure 2.2. The first model (Figure 2.2a) used data from DSC and rheology (Robinson et al., 1988, 1991; Morris et al., 1996 ; Manning, 1992), whilst the second (Figure 2.2b) used light scattering evidence of M_4N^+ gellan (Gunning & Morris, 1990). Each model portrays the development of “true gels” by association of “gel-promoting metal cations” (Morris et al., 2012). The associated

helices for the respective models are termed differently; “cation-mediated aggregates” for the Robinson et al. (1991) model and “crystalline junction zones” in Gunning & Morris’ (1990) model. However, both proposals focus on balancing the negative charge of the gellan polysaccharide through the ordered assembly of these metal cation incorporated double helices.

A key element of the first model (Robinson et al., 1991) is the co-existence of “cation-mediated aggregates” and unaggregated regions of double helices within the gellan network (Figure 2.2a, top, RHS). The unaggregated double helices melt initially on heating, to leave a helix-helix aggregated crosslinked network. It is this mechanism that the researchers believe is responsible for the two endothermic transitions noted in the DSC measurements discussed previously. Concomitant regions of unaggregated and aggregated double helices are also evident in Gunning & Morris’ (1990) model (Figure 2.2b, bottom, LHS), although the two-stage network melting is excluded.

A key feature of the second model (Gunning & Morris, 1990) (Figure 2.2b, RHS) is the formation of long “filaments” or “filamentous aggregates (Morris, 1995) with decreasing temperature under non-gelling conditions (primarily M_4N^+ gellan with or without M_4N^+ cations). Selective linear filament branching exists, which is in contrast to the chain assembly’s crosslinked by individual double helices in Robinson et al.’s (1991) ‘weak gel’ model (Figure 2.2a, bottom).

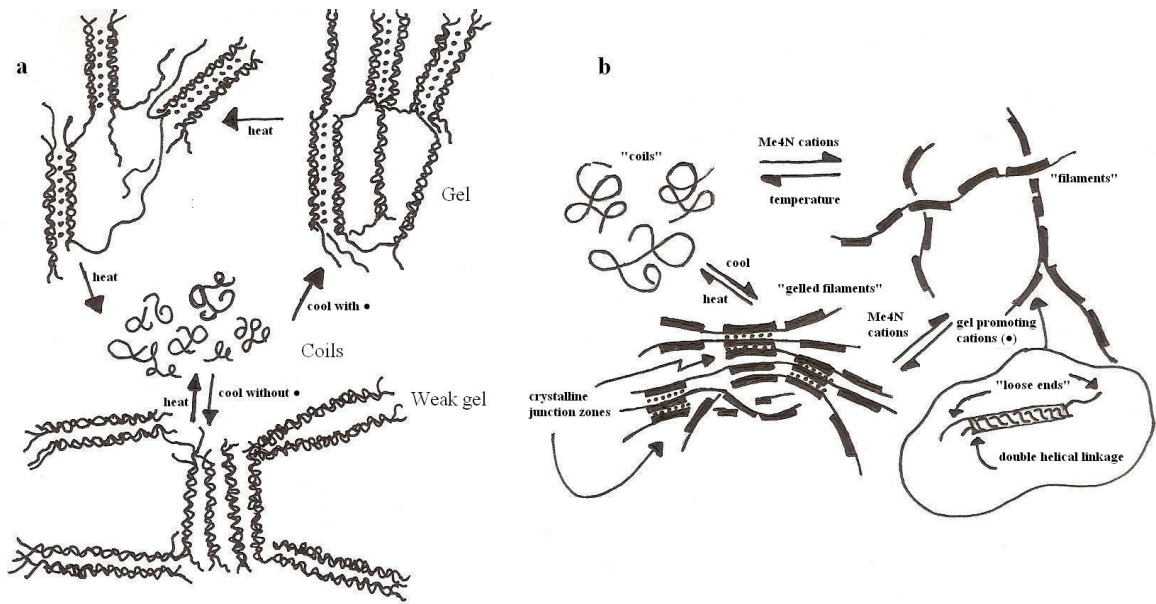


Figure 2.2. Schematic models for the gelation of gellan adapted from those proposed by (a) Robinson et al. (1991) and (b) Gunning & Morris (1990) and presented in Morris et al. (2012). Filled circles in each model denote cations that encourage the aggregation of double helices.

In terms of differences between the two models; regions of disordered polymer chains amongst the gellan double helices are evident in the first model (Figure 2.2a), but do not exist in the second (Figure 2.2b). According to Nishinari et al., (1985), the existence or non-existence of these disordered chains is crucial when considering gel mechanical characteristics. Networks that contain a significant volume of disordered sequences will respond to an applied stress by stretching the flexible regions, reducing the overall conformational entropy. This gives rise to elastic resistance to deformation, which increases for “entropic” networks of this type with increasing temperature (Watase & Nishinari, 1993). This is supportive of changes in entropy (ΔS) becoming progressively more significant as temperature (T) is elevated ($\Delta G = \Delta H - T\Delta S$). Alternatively, for networks created by “lateral association of fibrillar strands” (Figure 2.2b), the elasticity arises mainly from enthalpy (ΔH) elevation “on distortion of the aggregated filaments, or the entire fibrillar network” (Morris et al., 1999).

Gunning and co-workers (Gunning et al., 1996; Gunning et al., 1997) have also provided insight into the gellan network strand dimensions using atomic force microscopy (AFM). They observed branched fibrillar strands for networks that were created by drying aqueous solutions of M_4N^+ or K^+ gellan on freshly-cleaved mica. The micrographs on average showed lengths for the regions between branch points to be around 150 nm. More recently, AFM has been used to gather molecular images of gellan surfaces (at complete gel formation). Representations of a network comprising “long fibrillar strands” were first observed (Gunning et al., 1996, 1997) for firm gellan gels (1.2 wt.%) produced from systematic pH reduction using D-glucono- δ -lactone (GDL). Ikeda et al. (2004) also observed fibrillar strand networks using this technique for 2 wt.% gellan gels formed with 100 mM CsCl or KCl.

In the same study, representations were collected for conformations produced via the placing of aqueous solutions onto freshly-cleaved mica, as described previously for Gunning et al.’s (1996) study. Gellan solutions (0.2 wt.% with 10 mM CsCl or KCl) were prepared, kept at 90 °C (30 min), and cooled to ambient temperature before being diluted and deposited onto the mica surface. A contrast was also formed using M_4N^+ gellan. The M_4N^+ salt form produced images containing “branched clusters of strands with regular (~ 0.5 nm) height, consistent with crosslinking solely through unaggregated double helices” (Morris et al., 2012). For the samples incorporating K^+ , isolated clusters were observed, although the branch heights were lengthened (~ 1.2 nm) and the strands were taller, signifying lateral double helical organisation. The Cs^+ specimens produced a continuous network structure with strand heights that corresponded to aggregates created via side-by-side double helical organisation.

Lastly, Shimizu et al. (2012) have provided further insight into the gellan network dimensions by measuring the diffusion coefficient of an incorporated molecular probe

(pullulan). It was found that the dimensions of the empty gaps amid the polymer chains (mesh size) rise on cooling, as the molecules one-by-one combine to form double helices and helix-helix aggregates.

2.2. Texture of gellan gum: factors affecting gel texture

2.2.1. Effect of cations

In an anionic polysaccharide solution, the only cations present are those acting as counterions to the charged regions of the polymer chains. The positively charged ions are electrostatically attracted to the negatively-charged polymer chains, which in turn reduces their effective concentration (activity) in the bulk solution (Katchalsky, 1971; Manning, 1969a, b). The “strength of attraction is determined by the linear charge density (charge per unit length) of the polyanion and the charge of the individual cations, with divalent cations being attracted twice as strongly as monovalent” (Morris et al., 2012). To experimentally quantify and derive cation activity, a variety of techniques can be employed: “measurement of the transport coefficient (f) from conductivity or free diffusion of counterions, the osmotic coefficient (ϕ) from measurements of osmotic pressure, and activity coefficient measurements (γ) using potentiometry” (Rinaudo, 2009).

The “total concentration of cations (C_T)”, when extraneous salt is added becomes:

$$C_T = C_p + C_s \quad (\text{Eq. 2.1})$$

and the “total cation activity (α_T) in dilute solution” is given by:

$$\alpha_T = \gamma C_p = C_s \quad (\text{Eq. 2.2})$$

where “ C_p is the concentration of charged groups on the polymer, C_s is the concentration of added salt, and γ is the fraction of thermodynamically-free counterions” (Morris et al., 2012). Rochas & Rinaudo (1980) stated that for anionic polysaccharides which on cooling are converted to an ordered double helical form, from a disordered coil arrangement (Rees et al., 1982), “the inverse of the midpoint temperature (T_m) of the disorder-order transition will vary linearly with the logarithm of cation activity” (Morris et al. (2012):

$$d(1/T_m) / d\log \alpha_T = -R(\phi c - \phi h) / \Delta H \quad (\text{Eq. 2.3})$$

This was further defined by Milas et al. (1990) who stated that the slope of $1/T_m$ versus $\log \alpha_T$ is determined by the “transition enthalpy (ΔH)” and the decline in osmotic coefficient from ϕc to ϕh when the polymer is in its coil and ordered conformations respectively. The decline is a consequence of the double-stranded helix having a high linear charge density, which causes the cation activity to be reduced to a greater extent than for the single coil chains.

Milas & Rinaudo (1996) later extended their research to explore the efficacy of varying cations in encouraging conformational ordering of aqueous gellan. The gellan polymer was converted to certain salt compositions using cation exchange, with the overall cation level being adjusted via the addition of chloride salts of identical cations, before recording the disorder-order transition midpoint temperature using optical rotation. Plotting the variation of T_m with total cation activity (α_T) in line with Eq. 2.3 gave good linearity. Divalent cations were found to induce structural ordering at higher temperatures than monovalent, though no significant variations in efficacy were found between Mg^{2+} and Ca^{2+} . No confirmation of selectivity amongst the Group I metal ions investigated (Li^+ , Na^+ , K^+) or collectively against M_4N^+ was found either. However,

converting the polymer from its disordered to ordered conformation resulted in conductivity data (monitoring free K^+ and Na^+ cation depletion) with values of T_m that agreed well with those collected using optical rotation (Milas et al., 1990). Together, these findings provide firm support towards the polyelectrolyte theory (Manning, 1969a, b; Katchalsky, 1971) described previously at the beginning of this section (2.2.1.).

Gellan gelation using alkali metal group I cations has been investigated widely. Manning and co-workers (Robinson et al., 1988; Robinson et al., 1991; Manning, 1992) investigated Na^+ gellan (1 wt.%, $C_p = 15$ mM) with NaCl at varying concentrations (0 – 130 mM) using DSC. The resulting DSC cooling scans revealed an individual exotherm, that gradually moved to superior temperatures as the proportion of Na^+ was increased. Heating at low concentrations also gave single endotherms that were equal and opposite to those observed on cooling. A second endotherm however appeared in the heating traces at a salt level of ~ 50 mM NaCl, which progressively shifted to elevated temperature and expanded in dimension with increasing salt concentration, before becoming the only detectable process at 130 mM NaCl (highest concentration studied). In contrast, the first endotherm stayed in an identical position to the exotherm observed in the equivalent cooling curves, but became gradually smaller with increasing salt concentration. Similar behaviour was also observed for Na^+ gellan at the same concentration by Mazen et al., (1999).

The second thermal process on heating has been accepted (Gunning et al., 1996; Miyoshi & Nishinari, 1999a; Mazen et al., 1999; Nakajima et al., 1996) to be a result of the melting of double helices stabilised by aggregation. Whilst the initial process is said to be due to unaggregated residual helices that melt at an identical temperature at which they are produced on cooling. The stability and quantity of the aggregated helices increased with increasing C_T above a “critical threshold value, C_T^* ” (Morris et al., 2012).

Morris et al. (1999) used the aforementioned DSC thermal data to identify three types of rheological response for gellan in its low temperature ordered conformation over a range of Na^+ concentrations. With low Na^+ concentrations, up to $C_T \approx 25$ mM, the ordered, aqueous gellan samples gave mechanical spectra that were comparable to those observed for entangled polysaccharide coils. Increasing the C_T to ~ 40 mM gave samples that displayed “weak gel” properties. True gels were only formed when C_T became greater than C_T^* , causing the moduli to steeply increase thereafter as the Na^+ proportion was increased. This rise in the degree of aggregation, determined from the size of the second DSC endotherm, together with the stability of the aggregates, indicates that true gellan gels are produced via the association of double helices into stable aggregates (Morris et al., 1999).

Milas & Rinaudo (1996) also observed evidence of hysteresis between midpoint temperature (T_m) values in optical rotation measurements recorded on both heating and cooling at cation (Na^+ and K^+) levels above a minimum threshold. Values of C_T^* of ~ 45 mM and ~ 20 mM were obtained for the Na^+ and K^+ ions respectively. It is clear from the value for K^+ gellan being appreciably lower than the Na^+ form, that the organisation of the double helices into aggregates is dependable on the type of cation used. This is dissimilar to the absence of selectivity between the monovalent cations in encouraging the development of the gellan double helices. Together these results are supportive of the order of effectiveness published by Grasdalen & Smidsrød (1987) for gellan gelation with Group I cations: “ $\text{Li}^+ < \text{Na}^+ < \text{K}^+ < \text{Cs}^+$.”

When a gellan solution is in the disordered state, the coil dimensions “are expanded by intramolecular electrostatic repulsion” (Morris et al., 2012). These repulsions are then gradually shielded by the cations and anions on increasing concentrations of added salt, with subsequent reduction in the polyelectrolyte coil dimensions. This results in a fall in

both viscosity and the dynamic moduli, G' and G'' . Smidsrød & Haug (1971) subsequently used the degree in which the “intrinsic viscosity” decreased on rising salt levels to determine the polyelectrolyte stiffness. When gellan is in its ordered conformation, however, it is “resistant to contraction, and charge screening by added salt has the opposite effect of enhancing rheology, by suppressing repulsion between the ordered structures, facilitating aggregation” (Morris et al., 2012)

Smidsrød & Haug (1971) stated that “non-specific charge screening is determined by ionic strength, and cannot account for the observed selectivity between different monovalent cations in promoting aggregation and gelation of gellan” (Morris et al., 2012). Morris et al. (1996) proposed the interpretation that Group I cations fasten themselves via site-binding entirely to the gellan double helices, with subsequent decrease (or removal) of inter-helical repulsion. The site-binding can also be expressed “as formation of stable ion pairs between the metal cations and the carboxylate groups of gellan” (Morris et al., 2012). Cation site-binding to the conformationally-ordered anionic polysaccharides involves both electrostatic attraction and cation chelation via suitably-spaced oxygen atoms surrounding the polysaccharide charged groups (Grant et al., 1973; Morris et al., 1978; 1982). In terms of the “order of effectiveness of Group I cations in promoting aggregation of gellan double helices”, Cs^+ ions would theoretically give the most-suited “geometric fit to the binding site”, with progressive, reduced coordination efficiency as the cation dimension diminishes (Morris et al., 2012).

It is well-known (Grasdalen & Smidsrød 1987; Gibson & Sanderson, 1997; Miyoshi & Nishinari, 1994, 1995, 1996a; Milas & Rinaudo, 1996; Sanderson, 1990) that the level of divalent cations needed to provoke gellan gelation is considerably smaller than that for monovalent cations, and that the subsequent gels have superior thermal stability. Generally, in commercial gellan, the divalent cation content is enough to yield stable,

strong gels exclusive of added salt. However, mixtures of monovalent and divalent cations within gellan solutions (e.g. CaCl_2 and MgCl_2 salt addition to gellan in a mixed salt or monovalent form), can lead to complex gelation and melting processes with properties that are difficult to interpret.

2.2.2. Effect of excess salt and acids

Many studies (such as Sanderson & Clark, 1984; Moritaka et al., 1991; Kasapis et al., 1999; Sanderson & Clark, 1984; & Morris & Brownsey, 1995) of gellan have shown that the early rise in gel strength with incremental salt addition leads to a subsequent fall at elevated salt levels. Milas & Rinaudo (1996) studied this effect for blends of K^+ gellan (0.8 wt.%, ~ 12 mM) with KCl and Na^+ gellan (0.3 wt.%, ~ 4.5 mM) with MgCl_2 using compression testing of the cylindrical gel samples at 25 °C. Each sample displayed upper-limits in “Young’s modulus (E) and force at break” (which was relative to “breaking stress, σ_b ”), however the molar proportions at which these occurred were “ ~ 30 times higher for K^+ than for Mg^{2+} ” (Morris et al., 2012). For each salt however, the maxima in break stress arose at significantly smaller salt levels than the modulus maxima. The researchers (Milas & Rinaudo, 1996) observed three distinguishable compression fracture patterns as the level of added MgCl_2 or KCl was raised. The first region corresponded to salt levels below the break stress maxima, where “the gels were weak and broke sharply along a single fracture plane” (Morris et al., 2012). Firmer gels were produced in the second area, which was assigned to salt levels between the break stress maxima and the modulus maxima, where the gels proceeded to form several minor fractures during break. The final area corresponded to salt levels above the modulus maxima, where “the gels were softer and their disintegration resembled a coagulation or phase-separation process” (Morris et al., 2012). Phase separation is induced by the

addition of extraneous salt, since the imbalance in counterion concentration becomes progressively less significant as the overall concentration of ions is increased (Morris, 2009).

When the degree of intermolecular association is raised e.g. by pH and ionic environment, biopolymer gels such as gellan are said to “form part of a continuum from solutions of individual molecules at one extreme to close-packed solids at the other” (Morris et al., 2012). Optimum crosslinking occurs at a specific point within this range, with less association giving rise to a fragile network and “greater association giving larger aggregates with consequent reduction in the effective number of individual junctions, until ultimately the network collapses into a solid precipitate” (Morris et al., 2012). This explanation is supportive of the observed “phase separation” noted for gellan gels at low pH levels (Moritaka et al., 1995) or with high salt excesses (Milas & Rinaudo, 1996), in addition to the observation (Ohtsuka & Watanabe, 1996) “that the gels become turbid at the point where their strength begins to decrease” (Morris et al., 2012).

2.2.3. Effect of sugars

The influence of sugars on aqueous sodium gellan (1 wt.%) samples has been investigated by Miyoshi & Nishinari (1999b) and Miyoshi et al. (1998). In each investigation, sugar proportions were changed from 0 – 72 wt.% and the subsequent gel properties studied using DSC and rheological characterisation methods. Miyoshi et al. (1998) used a Na⁺ gellan form called NaGG-2 (with the cation content (wt.%): Na⁺ 3.03; K⁺ 0.19; Ca²⁺ 0.11; Mg²⁺ 0.02) and studied the influence of the sugars; glucose and mannose. Comparisons were made with similar investigations that looked at the variation of gellan concentration in the absence of sugar (Section 2.2.1.4.). The

researchers (Miyoshi et al., 1998) found that when NaGG-2 (1 wt.%) was cooled without sugar, a steep rise in G'' at $T_{ch} \approx 30$ °C was observed, with an associated DSC exotherm; G' was too small to be detected, but was measurable using low concentrations of added glucose (0.18 wt.%). Further increasing the glucose concentration to 28.8 wt.% resulted in cooling and heating curves of G' and G'' virtually the same as those recorded for NaGG-2 (2 wt.%) in water, with a rise in T_{ch} to ~ 37 °C and G' increasing above G'' at $T_{sg} \approx 7$ °C. Continued increase in glucose concentration, then resulted in an increasing T_{ch} value, with an accompanying steeper increase in T_{sg} , “until conformational ordering and gelation occurred simultaneously at $T_{ch} = T_{sg} = 41$ °C with 63 wt.% glucose” (Morris et al., 2012). Thermal hysteresis was observed amongst the heating and cooling measurements at a glucose level of 32.4 wt.%, which amplified in size as the glucose level continued to be elevated.

Comparable variations in T_{ch} and T_{sg} were observed (Miyoshi et al., 1998) using mannose as the sugar, although the co-solute levels needed were considerably greater than for glucose, and thermal hysteresis was absent. The main conclusions from this investigation (Miyoshi et al., 1998) were that “incorporation of sugars promotes conformational ordering and gelation of gellan and that glucose is more effective than mannose” (Morris et al., 2012).

Miyoshi & Nishinari (1999b) in contrast, investigated NaGG-3, the Na^+ gellan form (with the cation content (wt.%): Na^+ 2.59; K^+ 0.009; Ca^{2+} 0.02; Mg^{2+} 0.001) and the sugars; fructose, trehalose, glucose and sucrose. Variations in T_{ch} with rising glucose levels were found to be almost the same as those observed (Miyoshi et al., 1998) for NaGG-2, although the associated rise in T_{sg} was less sharp and gelation (i.e. crossover of G' and G'') was not recorded until ~ 21 °C. It has been proposed (Morris et al., 2012)

that the reason for NaGG-2 having an earlier gelation point, arises from its higher divalent cation content than NaGG-3.

The DSC data (Miyoshi & Nishinari, 1999b) displayed increases in the peak-maximum temperature with increasing sugar concentration, and no evidence of thermal hysteresis. The disaccharides were shown to give greater increases in the peak-maximum temperature with increasing sugar concentration than the monosaccharides. Miyoshi & Nishinari (1999b) combined this data with that equivalent by Miyoshi et al. (1998) to construct an effectiveness order in encouraging ordered gellan association for the respective added sugars: sucrose > trehalose > glucose > mannose >> fructose.

Polymer chain association can be promoted by substituting a high proportion of the solvent in the gel solution with high sugar concentrations (Morris et al., 2012). Miyoshi & Nishinari (1999b) studied this by making comparisons of T_{ch} and T_{sh} for gellan solutions with concentrations expressed relative to the mass of residual water and for equivalent concentrations of gellan in water in the absence of sugars. Most of the samples tested exhibited increases in transition temperature with increasing sugar concentrations, but the values of T_{ch} and T_{sh} for the gellan-disaccharide (trehalose and sucrose) mixtures were greater than for their equivalents with gellan singly. Other exceptions were reported for glucose whose values were marginally greater, and for fructose (higher levels only) where they were smaller. Miyoshi & Nishinari (1999b) ascribed the enhancements seen for glucose, sucrose, and trehalose to “sugar-water associations that were in competition with interactions between water and gellan” (Morris et al., 2012). The respective effectiveness order for the three sugars was then correlated (Miyoshi & Nishinari, 1999b) using the sugar equatorial hydroxyl group number: the “dynamic hydration number” (Nishinari et al., 1990; Nishinari & Watase, 1992; Katsuta et al., 1992). Lastly, the inhibitory effect of fructose was explained

(Miyoshi & Nishinari, 1999b) by the fastening of the fructose units to gellan via hydrogen bonding, and subsequent reduction of polymer self-association. A similar proposal has since been suggested for blends of fructose and high-methoxy pectin (Tsoga et al., 2004).

More recently, research has focused on the influence of co-solutes on commercial gellan at gelling levels typical for gels produced without sugar. Bayarri et al. (2002) studied the effect of sucrose (0 – 25 wt.%) using three Kelcogel samples (0.30, 0.75 and 1.2 wt. %) using compression testing. Raising the level of sucrose was found to cause subsequent increases in break stress (σ_b), Young's modulus (E), and strain at break (ε_b) (i.e. gels became stronger and less brittle). The changes also became more distinguishable when using higher gellan concentrations. At the highest concentrations of gellan and sucrose (1.2 wt.% and 25 wt.%), E was ~ 38% greater than that recorded for gels with no sugar, σ_b was ~ 72% higher and ε_b increased from 17 % strain at break to ~ 23%.

Sworn & Kasapis (1998) noted very similar small increases in gel strength and breaking strain using a higher sucrose concentration of 40 wt.%, which gave a strain at break value of ~ 32%. However, at 60 wt.% sucrose a large increase in ε_b occurred, and up to ~ 65% strain the gels remained intact. Overall, the use of sucrose in reinforcing gellan networks has proved to be very effective (Kawai et al., 2008).

The different responses observed between sugars in mixed gellan systems enable their texture to be varied through the manipulation of the total sugar composition. For example, “partial replacement of sucrose by either glucose or fructose at 60 wt.% sugar concentration results in stronger gels than at 60 wt.% sucrose alone” (Morris et al., 2012). This result was discovered by Gibson & Sanderson (1997) when they were

testing for gellan (0.5 wt.%) degradation with 60 wt.% sucrose under hot (85 °C), acidic conditions (pH 3.4). Unexpectedly, the gel produced on cooling was stronger than that exposed to high temperature and pH, which was assumed (Gibson & Sanderson, 1997) to be due to “partial hydrolysis (inversion) of sucrose to glucose and fructose” (Morris et al., 2012). In addition, the values of modulus at break (σ_b/ϵ_b) were found (Gibson & Sanderson, 1997) to be greater for fructose gellan gels than for the equivalent glucose gellan gels. The effectiveness order for the respective sugars in reinforcing the gellan gels was thus: fructose > glucose > sucrose, which is the opposite to that reported by Miyoshi & Nishinari (1999b). The most likely explanation (Morris et al., 2012) for this difference is that the commercial gellan samples contain greater amounts of divalent cations than in NaGG-3 and NaGG-2 specimens investigated by Miyoshi & Nishinari (1999b) and Miyoshi et al. (1998) respectively.

Morris et al. (2012) also proposed an alternative explanation for the experimental differences, where sugars are thought to promote the “association of gellan in the order: sucrose > glucose > fructose”. Gel strength increases in this order for Na⁺ gellan samples whose degree of association (without sugar) is significantly under the optimum gelation level (Miyoshi et al., 1998, 1999b). However, the use of commercial gellan with its high divalent cation content gives gels that are close to or at, the optimum degree of crosslinking, which in turn causes excessive aggregation when in the presence of added sugar. This weakens the network, so that the gel strength with varying sugar type decreases with progressive, heightened association, leading to the opposite effectiveness order: fructose > glucose > sucrose (Gibson & Sanderson, 1997).

The influence of sugars on high acyl gellan gum is not as well-known. Although, it is accepted (Sworn, 2009) that the “addition of sugars to high acyl gellan generally results

in an increase in the force required to break the gel; and that the setting and melting temperatures increase with increasing sugar concentration”.

2.2.4. Effect of acyl substituents

Chandrasekaran & Thailambal (1990) first explored the acyl groups in the helical gellan conformation (Figure 2.1) using computer modelling. They concluded that the “acetyl substituents lie on the periphery of the duplex, with no further modifications to the underlying helix geometry” (Morris et al., 2012). The glycerol unit however, was said (Chandrasekaran et al., 1992) to “lie in the interior of the helix and force the carboxylate group to rotate through an angle of $\sim 14^\circ$ about the C(5)-C(6) bond, with subsequent major changes in the hydrogen bonding within and between the participating strands” (Morris et al., 2012). Additionally, rotation ($17 \pm 3^\circ$) of the glucuronate residue about the glycosidic bonds connecting it to the two adjacent glucose residues (Figure 2.1), is also undertaken (Chandrasekaran et al., 1992). This enables the required separation between the glycerol substituent and the carboxylate group to be achieved.

The acyl groups during gellan gum commercial formulation, are disconnected via brief alkali (KOH) exposure at elevated temperatures. The mechanism (Morris et al., 2012) can be expressed as:



where R-COO and R' are the substituent and the polymer chain respectively. The volume of alkali used influences the degree of removal. Generally, when performed at high temperature with gellan in its disordered conformation, the glycerol units are released faster than the acetyl groups. Alternatively, hydrolysis can be performed for longer time periods, at lower temperatures, where the polymer is conformational ordered. In these

environments, the liberation of the “acetyl groups from the double helix periphery occurs more rapidly than the removal of the glycerol substituents from the helix interior” (Morris et al., 2012). Baird et al. (1992) stated that through the controlled handling of alkali concentration, hydrolysis time and temperature, it is therefore possible to produce samples with varied proportions of “repeat units carrying residual acetyl (f_a) or residual glyceryl (f_g) substituents” (Morris et al., 2012).

One of the primary strengths of gellan gum is its ability to achieve a diverse range of gel textures through the blending of the two forms. The properties of the mixed system can be manipulated through control of the blend ratio and ion mixture level (Mao et al., 2000; Huang et al., 2003). At low ionic concentrations the *HA* form predominates, but with increasing ionic concentration this is reversed and the *LA* form contributes more to gel texture (Sworn, 2009). Morrison et al. (1999) and Morris et al. (2012) reported that “blends of *HA* and deacylated gellan gives gels with textures that lie between the extreme brittleness of the deacylated form and the extreme extensibility of the *HA* form”. Kasapis et al. (1999) studied the rheological response of the mixtures and found during a high temperature quench, two areas of sharp inclination in G' existed, the first representative of the “sol-gel transition of *HA* gellan at high temperature and the second with the respective transition for the deacylated polymer at low temperature” (Morris et al., 2012). Two distinguishable transitions were additionally noted using DSC (Kasapis et al., 1999; Morris et al., 1996), with peaks coincident with the individual components, and via “the temperature-course of reduction in intensity of detectable ^1H NMR resonances on cooling and associated changes in circular dichroism spectra” (Morris et al., 2012; Matsukawa & Watanabe, 2007). From this evidence, it is apparent that deacylated and *HA* gellan do not produce double helices involving strands of each variant.

Morris et al. (2012) have classified the interactions between two distinguishable polymers “as ‘associative’ if they are thermodynamically more favourable than interactions between the individual polymers of each type and ‘segregative’ if they are less favourable”. Segregative interactions (Morris et al., 2012) are increasingly more common than associative interactions. They occur in virtually all biopolymer mixtures where there is no over-riding drive to heterotypic binding (Morris, 2009). It has been suggested (Manson & Sperling, 1976; Mao et al., 2000, Morris et al., 2012) that the gellan gum blends are composed of segregative interpenetrating rather than cooperative networks of polymers. For polymer mixtures, such as *LA* and *HA* gellan at equivalent concentrations, there are few free molecules free to move independently and the entropy of mixing is much less significant than when compared to smaller molecular mixtures (Morris, 2009). This subsequently causes the mixed polymer systems to phase separate into two co-existing phases, each enriched in one polymer and depleted in the other. Phase separation of biopolymers in the solution state is usually detected by immediate development of turbidity on mixing, due to formation of a ‘water-in-water emulsion’ in which one phase exists as a continuous matrix with the other dispersed through it as small liquid droplets (Morris, 2009). After initial phase separation, for gelling biopolymers, this water-in-water emulsion structure can become trapped by network formation, giving a biphasic co-gel with one phase continuous and the other dispersed. Phase-separated co-gels can also be formed from the gelation of a single-phase mixture. In these cases, the first component to gel gives a continuous network, permeated by a solution of the second polymer. Subsequent gelation of the other component then creates a second gel phase (Morris, 2009). If the first network is weak, there may be an enthalpic advantage from the second, stronger, gel becoming the continuous phase, with the original network being broken down into dispersed particles (Mohammed et al.,

1998). It is more common however, for the first network to remain continuous, and for the second component to form the dispersed phase (Morris, 2009).

Generally in these structures, the *HA* form sets at a higher temperature with the *LA* from setting within the *HA* network on further cooling (Valli & Clark, 2010). This ‘gel within a gel’ structure then allows for the smooth transition of one form to another as the *LA* to *HA* gellan gum ratio is varied, which is accountable for the wide texture range observed.

2.3. Rheology of solutions and gels

Compression testing is a widespread technique employed to characterise the mechanical properties of gels. The procedure measures the “variation of resistance to deformation (stress, σ) as the extent of compression (strain, ϵ) is increased” (Morris et al., 2012). Low-amplitude oscillatory deformation resistance measurements, used to monitor gel network formation and melting, provide a versatile alternative to compression testing. (Ross-Murphy, 1984; Te Nijenuis, 1997; Morris, 1985). The different regions of the oscillatory cycle have distinguishable consequences on characteristics such as solid-like resistance and deformation rate. The cycle limits (where strain displacement is highest) provide the greatest elastic resistance, but the middle of the cycle causes it to drop to zero. The reverse is true for the deformation rate, which is greatest in the centre of the cycle, and drops to zero at the extremes. For ideal solids, the stress generated is precisely “in-phase with the oscillatory strain”, whilst for ideal liquids it is precisely “90° out-of-phase” (Morris et al., 2012).

The total stress generated “for ‘viscoelastic’ materials can be resolved into an in-phase component and an out-of-phase component; dividing these by the applied strain

gives, respectively, the ‘storage modulus’ (solid-like response), and the ‘loss modulus’ (liquid-like response)” (Morris et al., 2012). The moduli are given the following symbols based on shear strain: G' (storage modulus) and G'' (loss modulus). Any “unresolved stress to the applied strain is totalled and expressed as a ratio termed the complex modulus, $|G^*|$ ” (Morris et al., 2012). This is related to G' and G'' by:

$$|G^*| = (G'^2 + G''^2)^{1/2} \quad (\text{Eq. 2.5})$$

When $|G^*|$ is divided by “the frequency of oscillation (ω), the complex dynamic viscosity, $|\eta^*|$ is obtained, which is regarded as the oscillatory analogue of steady-shear viscosity (η) from rotational measurements” (Morris et al., 2012).

$$|\eta^*| = \frac{|G^*|}{\omega} = \frac{(G'^2 + G''^2)^{1/2}}{\omega} \quad (\text{Eq. 2.6})$$

The loss tangent, $\tan \delta$, is another useful parameter (Morris et al., 2012), given by:

$$\tan \delta = G''/G' \quad (\text{Eq. 2.7})$$

A materials’ ‘mechanical spectrum’ is produced when the variation of G' and G'' is plotted logarithmically with frequency; $|\eta^*|$ is often also included in the spectrum. Figure 2.3 shows mechanical spectra obtained by Morris et al. (2012) that is typical for polysaccharide gels and solutions. Figure 2.3a shows the mechanical spectra for gels, in which the elastic properties (G') take precedence over the viscous response (G''). Each modulus displays minimal change with varying frequency (ω), and $\log |\eta^*|$ decreases linearly (~ -1 slope) as $\log \omega$ is increased (Morris et al., 2012). In dilute solutions, where the disordered coils move freely and independently a different mechanical spectrum is observed (Figure 2.3c), where G'' predominates over G' , due to the “resistance to deformation occurring from the movement of polymer molecules through the solvent”

(Morris et al., 2012). Both $\log G''$ and $\log G'$ increase linearly with increasing $\log \omega$ with respective slopes of +1 and +2. The steeper slope exhibited by $\log G'$ reflects the “progressively greater storage of energy by the contortion of individual polymer coils with increasing frequency of oscillation” (Morris et al., 2012).

Raising the polymer concentration forces these polymer coils to eventually interpenetrate one another and produce an entangled network (Graessley, 1974). The “concentration at which this occurs is known as C^* , and solutions of higher concentration are termed ‘semi-dilute’” (Morris et al., 2012).

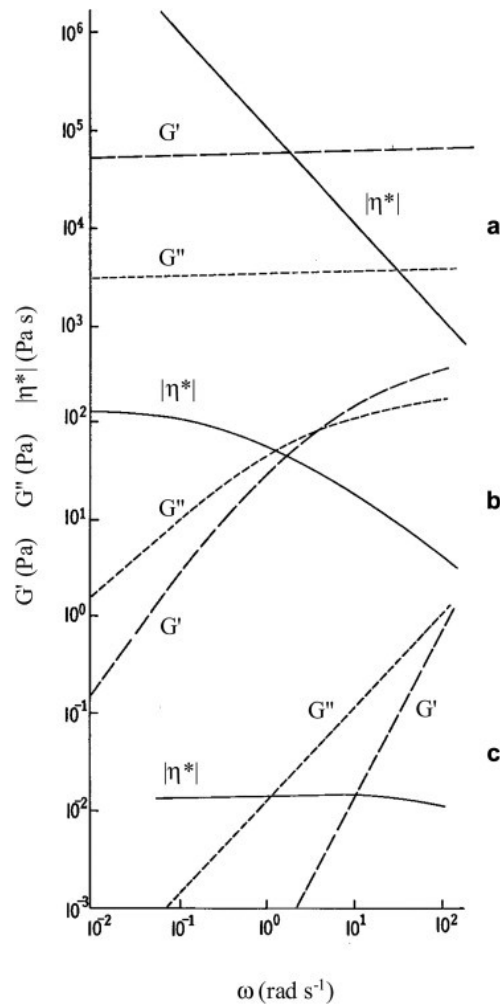


Figure 2.3. Typical mechanical spectra (taken directly from Morris et al. (2012)) of (a) a true gel, (b) a semi-dilute solution of entangled polymer coils, and (c) a dilute polymer solution.

Disentanglement of the polymer coils during oscillation exposure is particularly dependent on the degree of frequency applied; low frequencies allow time for entanglements to separate, whilst at higher frequencies the time is restricted. This is evident within the mechanical spectra for semi-dilute solutions (Figure 2.3b) where at low frequencies they respond by flow and show similarities observed for dilute solutions (Figure 2.3c). At higher frequencies however, the entangled network of the semi-dilute solutions becomes distorted in response to the oscillatory strain and the mechanical spectra (Figure 2.3b) begins to resemble those for gels (Figure 2.3a).

2.4. “Weak gels” (fluid gels)

Several polysaccharide solutions have the ability to flow freely, whilst having mechanical spectra similar to those of typical gel networks, as shown in Figure 2.3a. When small perturbations are applied to these systems, their response is mostly elastic or ‘gel-like’. This property, together with the fact that they generally are unable to support themselves, and can be poured and stirred like standard solutions explains why they are often termed “weak gels” (Ross-Murphy, 1984; Picout & Ross-Murphy, 2003; Morris, 1985; Kavanagh & Ross-Murphy, 1998). Conventional gels that display ‘weak’ properties in that they have low moduli are not classified as “weak gels”. The main difference being, that conventional gels (or “true gels”) “respond to high stress by fracturing, whereas “weak gels” flow” (Morris et al., 2012). Other terms ascribed to these gels are “structured liquid” (Ross-Murphy, 2008); “fluid gels” (Sworn et al., 1995); and “pourable gels” (Morris, 1991). Weak gel mechanical spectra differs from conventional gels in that they tend to have a greater frequency-dependence of G' and G'' , and a reduced parting between the two moduli. Each gel responds quite differently to unidirectional stress however (Morris et al., 2012). Subjecting polysaccharide solutions

which produce conventional gels under quiescent conditions on cooling, to shear during the sol-gel transition temperature-course can also produce microscopic gel particle dispersions with “weak gel” characteristics (Harris & Pointer, 1986; & Norton et al., 1999). Sworn et al. (1995) used this approach to obtain “weak gel” networks of gellan gum that were able to suspend small particles at minute polymer levels (0.125 wt.%).

Gellan microgel particle rheology of this type has been evaluated against the overall “weak gel” macroscopic characteristics (Caggioni et al., 2007). In this study, blends of aqueous NaCl and commercial gellan were made (80 °C) and cooled (0.5 °C/min) to 25 °C, either under shear (100 s⁻¹ constant shear rate) or quiescently. The conventional “gels formed on quiescent cooling had greater moduli (G' and G'') than the “weak gels” formed under shear” (Morris et al., 2012). Video imaging was also used to probe the “microrheology” (micro-metre scale) of 1 µm polystyrene beads (tracer particles) integrated within the aqueous gellan solutions (minimum 0.05 wt.%) prior to cooling. No distinguishable properties were found between the sheared and non-sheared solutions, indicating “that the microgel particles created from cooling under shear have identical internal structures as the continuous gel networks obtained on quiescent cooling” (Morris et al., 2012). Caggioni et al. (2007) also probed the deformation of the “weak gels” by applying small steady and oscillatory stresses. This was found to increase directly in proportion to the stress. However, “above a critical stress, the strain rose sharply, displaying “weak gel” network failure, with elastic deformation being replaced by viscous flow” (Morris et al., 2012). These failure stress points rose proportionally with gellan concentration, and the failure strain was found to decrease inversely. The researchers (Caggioni et al., 2007) attributed the production of the “weak gel” microgel particle network “to a shear-induced transition from a ‘jammed’ to a ‘un-jammed’ state” (Morris et al., 2012).

Garcia et al. (2011) most recently investigated the failure of gellan gum “weak gel” networks formed under shear. Commercial gellan solutions (0.025 – 0.25 wt.%) were used alongside a fixed NaCl concentration (0.22 M) at 80 °C, and the onset gelation temperature on cooling was recorded at ~ 41 °C. “Weak gels” were then formed by shearing (700 rpm) at 41 °C for 1 min to give cloudy preparations. Fluorescently labelling the gellan using fluoresceinamine then enabled the observation of irregularly-shaped particles (0.1 – 1mm dimension at 0.25 wt.% gellan) using CSLM, which were roughly 10 times larger than those reported by Caggioni et al. (2007) where vigorous and prolonged shearing was ensued. Garcia et al. (2011) reported mechanical spectra of the “weak gels” that was comparable to the true gel spectrum in Figure 2.3a, with G' being “approximately an order of magnitude greater than G'' ”, and with both moduli displaying fractional decreases with decreasing frequency (ω)” (Morris et al., 2012). “Equilibrium” measurements of G' (G_e) were then shown to vary with gellan concentration similarly to the “elastic moduli of conventional (un-sheared) biopolymer gels with $G_e \sim C^2$ for $C = 0.25 - 0.05$ wt.%” (Morris et al., 2012). “Weak gel” microgel particle network failure was also identified using transient rheology measurements in response to shear (Garcia et al., 2011). Following the application of constant shear (10 s^{-1} for 5 min), a large increase in resistance (stress, τ) to an abrupt maximum was observed, which then declined steadily towards a stable reading of steady-shear viscosity. The recovery of “weak gel” rheology gradually became slower with rising gellan concentration.

The peak viscosity relating to the stress required to induce “weak gel” flow is a crucial factor in industrial processes and dispensing applications (Garcia et al., 2011) for example pumping sheared networks from tanks where they were formulated, and from the final product containers for consumer use (Morris et al., 2012). The energy required

however to do so is often substantially greater than that expected from steady-shear viscosity.

2.5. *Future developments: Gellan gum*

Many further advances are likely to be made that exploit gellan gum's full potential as a gelling agent. These will without doubt include identification of new areas of application, and formulation of novel or improved products.

An alternative research pathway is the manipulation of gellan acyl content, by variant cultures or controlled deacylation, to target specific gel textures and product functionalities. Gellan gums with intermediate acyl content tend to show a wider variation in texture and single homogeneous setting behaviour (Baird et al., 1992; Morrison et al., 2002), when compared to blends of the two gellan variants. Methods for creating these partially acylated products (as discussed in Section 2.3.4.) exist, but they are yet to be produced on a commercial scale (Sworn et al., 1999).

It may also be possible to produce gellan gum with significantly greater molecular weight (Valli & Clark, 2010). Gellan gum with extremely high gel strength would result from the higher molecular weight. This property could make gellan more cost-effective in numerous applications, and would expand its subsequent functionalities.

2.6. *Food processing in the human digestive system*

Foods undergo significant transformations when processed through the human digestive system. The chemical reactions and mechanical forces the foods are subjected to during transit reduce their sizes dramatically, in order to help release nutrients to be

absorbed by the body. The kinetics of digestion depends on both the chemical and physical properties of food and their interaction with the physiological events occurring within the gastrointestinal (GI) tract (Cox et al., 2009). Foods are disintegrated into their small size in the mouth and stomach, whilst nutrient absorption mainly occurs in the small intestine (Kong & Singh, 2008).

Hydrocolloids are well known to have substantial effects on the processing of foods in the GI tract. A new area of research is focusing on adding hydrocolloids to foods, so that they undergo physical transformations at specific sites during natural biological processes within the human body (Cox et al., 2009). Insight into the types of processing involved inside people has the potential to offer scientists the capability to design and formulate foods that could either impact texturally or break down and release their micro- and macronutrients in a controlled manner.

In terms of the food processing that occurs in the mouth, food is subjected to a complex series of manipulations by the tongue, teeth, lips and cheeks, during which it is converted into a form suitable for swallowing (Guinard & Mazzucchelli, 1996). Mastication is the initial digestion stage and the main process by which solid food is broken down into smaller particles. It is a complex function that utilizes the muscles, teeth, lips, cheeks, tongue, palate, and salivary glands, and involves controlled compressive, shearing and tensile forces produced by the intermittent movements of the teeth (Malone et al., 2003). The forces applied to food during mastication depend on the texture properties of the food itself (i.e. food of brittle, elastic and/or plastic behaviour) and range from approximately 30 – 60 N (Cox et al., 2009).

A further important factor in the oral processing of solid foods is the effect of mixing with saliva. Saliva is secreted as soon as food is placed in the mouth, in response to

mechanical stimulation (chewing) and to the taste qualities of the food (e.g. pH) (Cox et al., 2009). During the mastication process, saliva mixes with the food acting as a lubricant, but also influencing the textural changes induced to the food during oral manipulation. Mixing with saliva also affects bolus formation, thus the decision for swallowing, and in turn influences the residence time of the food in the mouth (Guinard & Mazzucchelli, 1996).

Foods typically structured with hydrocolloids are soft food materials, which include liquid, semi-liquid and semi-solid foods; none of which rely heavily on mastication during digestion in the mouth, since they do not involve fragmentation by the teeth (Cox et al., 2009). Instead, the structural changes during oral processing resulting from heating (or cooling) to mouth temperature, mixing with saliva (dilution and chemical breakdown) and the flow involved in squeezing and shearing between palate and tongue are more crucial. During oral processing, food is also subjected to the flow conditions in the mouth. These are of particular importance to liquid and semi-liquid foods as they determine how the food is perceived and broken down in the mouth (Cox et al., 2009). Research on mixing and its dependence on hydrocolloid structure is an important area of study (Koliandris et al., 2008). Fluid gels and mixed gels are expected to have a major impact within this field, although no systematic studies have been carried out to date (Cox et al., 2009). This gap in the research highlights the importance and novelty of the work presented in this thesis on mixed *LA* and *HA* gellan gel systems and *LA* gellan fluid gels.

Gastric disintegration of foods, compared to oral mastication has received less research attention, due to its complexity; it involves several influencing factors such as fed/fast state, gastric acid, bile salts, enzymatic reactions, and hydrodynamic and mechanical forces (Cox et al., 2009). Stomach physiology however, has still not been

fully understood; the stomach wall movement, rheological properties of gastric content, the flow state of gastric fluid, and hydrodynamic/mechanical forces acting on foods require further clarification.

After in-mouth processing of the food is complete the formed bolus is transported through the oesophagus to the stomach where gastric digestion occurs. The stomach performs three functions: storage, mixing, and emptying its contents into the small intestine and it is divided into four main regions: fundus, body, antrum and pylorus (Kong & Singh, 2008). The proximal part of the stomach (fundus and body) acts as a reservoir for undigested material and is responsible for the emptying of liquids, whereas the distal stomach (antrum) is the grinder, mixer, and sieve of solid food, and acts as a pump for gastric emptying of solids by propelling actions (Arora et al., 2005). The volume of the reservoir part of the stomach is flexible with the ability to expand from as low as 25 mL (in the fasted state) to approximately 4 L (Kong & Singh, 2008). The function of mixing and homogenizing is achieved through the secretion of gastric juice and stomach contraction that produces grinding and crushing of the food. The stomach contraction imposes a considerable mechanical force on food particulates and thus plays a significant role on the disintegration of solids (Cox et al., 2009). Peristaltic waves originate from the stomach wall and spread toward the antrum, mixing and forcing the antral contents toward the pylorus. The contraction frequency is approximately 3 cycles per minute (Marciani et al., 2001a). Concurrently, the pylorus contracts and the sphincter narrows, so that the pyloric opening is small on the arrival of the peristaltic wave. Retropulsion then occurs; an action where the contents are squirted back into the stomach. Repeated propulsion, grinding, and retropulsion, together with the function of enzymes and acids, reduce the size of food particles (Cox et al., 2009). In the gastric antrum, solids are ground to particles of size less than 1 – 2 mm (Carneiro et al., 1999).

Researchers have measured the contraction forces present in the stomach using magnetic resonance imaging (MRI). Marciani et al. (2001b) used this technique to directly visualise the breakdown of agar gelled beads in the antrum and reported forces close to 0.65 N exerted by the antral walls of the stomach.

Hydrocolloid structures can both influence and be influenced by the biological, chemical and physical processes occurring in the stomach. The self-structuring foods concept discussed in detail in the previous chapter, where foods are produced that structure the stomach contents and thus provide a feeling of satisfaction followed by prolonged satiety is a prime example. If the structuring is successful the meal then provides a pleasant sensation of ‘fullness’ for a prolonged period and so snacking on high-fat/calorie foods may be reduced (Norton et al., 2011). To fully achieve this requires design rules to manipulate new foods and give a reduced calorie intake within a day and as a function of time between meals (Cox et al., 2009)

Consumption of liquid-like foods structured with a hydrocolloid that is sensitive to a shift in pH, so that it self structures in the stomach and gels (acid gelation) part of the stomach’s content, has been shown to increase satiety (Hoad et al., 2004; Norton et al., 2006). The observed fullness effect was found to be directly related to the strength of the formed gel; i.e. weak gels only provoked a weak response similar to that of a viscous meal, while stronger gels, which were more resistant to breakdown in the stomach, were more successful in extending satiation.

Rather than using liquid-based products to provide the above-mentioned satiety effect, a similar approach can be adopted for a solid food formulation (e.g. a cereal bar) which may provide a more suitable system. Three kinetic processes must be controlled for this formulation to be explored. These are the process of dissolution of the product

throughout the stomach, the gelation rate of the food, and the process by which the de-structuring of the stomach's contents occurs (to allow for the emptying and loss of stomach distension and satiety) (Cox et al., 2009). The rate of gelation must be controlled, so as to ensure that the whole of the food structure is saturated with gastric juice prior to gelation. Rapid gelation can lead to the structuring material only gelling on the outer surface, resulting in the formation in the stomach of enlarged 'fish eye' forms which involve the partial wetting of hydrocolloid powders when dissolved (Cox et al., 2009). Eventually these structures should be slowly broken down via physical, chemical or enzymatic processes to expose new surfaces, which will then gel and break (in cycle), resulting in the required loss of the structuring process. The kinetics of gelation and the process of stomach content destructuring can be controlled by the use of an acid-sensitive biopolymer with a non-acid-sensitive biopolymer. This is explored in Chapter 4 with the mixed *LA* and *HA* gellan gum systems, where the kinetics are controlled by the molecular structures of the two biopolymers and their phase volumes. It is paramount that all of the factors affecting stomach emptying and satiety are controlled in a co-ordinated fashion, to ensure that the structured materials are meta-stable and breakdown appropriately at the right time to relieve stomach distension, and allow the feeling of hunger to return progressively (Cox et al., 2009).

Self-structuring systems, the notion of healthy foods and bioavailability are gaining wide recognition (Norton et al., 2007). Future developments within these areas are likely to include: structures designed for GI tract processing, subsequent process control using mixed biopolymer systems, and the use of fluid gels as delivery systems (Cox et al., 2009). These support fittingly the work presented in this thesis on mixed *LA* and *HA* gellan gel systems and *LA* gellan fluid gels, in an attempt to provide the initial breadths of research towards formulating a self-structuring food product.

Chapter 3

EXPERIMENTAL

3.1. Materials

3.1.1. Biopolymer solutions

The aqueous phase for the preparation of all the aqueous hydrocolloid solutions was deionised double distilled water.

3.1.1.1. Low Acyl and High Acyl Gellan Gum

Low (*LA*) and high (*HA*) acyl gellan gum (Kelcogel F and Kelcogel LT100) samples were kindly supplied by CPKelco (San Diego, USA) and were used with no further purification. Gellan gum is commercially available as a fine mesh, free-flowing white powder.

3.1.1.2. Hydrochloric Acid

38 % (12.4 mol dm^{-3}) hydrochloric acid (HCl) was purchased from Fisher Scientific (Loughborough, UK), and diluted to form a 0.5 % (0.137 mol dm^{-3}) stock solution, which was used for both the direct and post-production acidification of all the produced acid gel structures.

3.1.1.3. Gelatin

Gelatin (from porcine skin) was purchased from Sigma Aldrich Company Ltd (Dorset, UK), and used as it was supplied with no further purification.

3.1.1.4. Sugars

'D-(+)-Glucose' (ACS reagent) was purchased from Sigma Aldrich Company Ltd (Dorset, UK), and used as it was supplied with no further purification.

The sucrose (ACS reagent) was purchased from Sigma Aldrich Company Ltd (Dorset, UK), and used as it was supplied with no further purification.

'D-(−)-Fructose' was purchased from Sigma Aldrich Company Ltd (Dorset, UK), and used as it was supplied with no further purification.

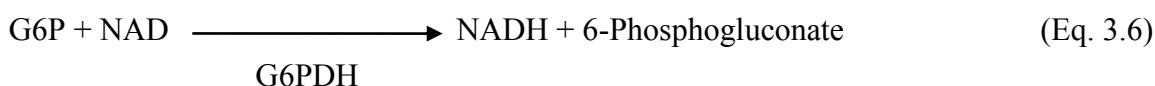
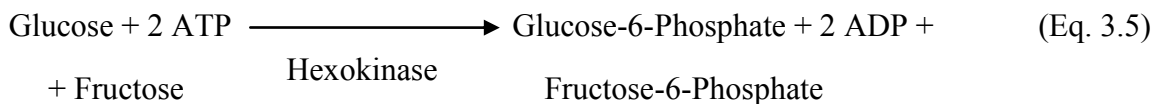
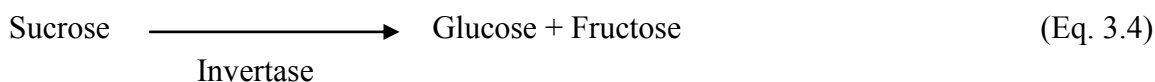
3.1.1.5. Sodium Azide

Sodium azide (NaN_3) was purchased from Sigma Aldrich Company Ltd (Dorset, UK), with purity $\geq 99\%$ and used as it was supplied with no further purification. It was added to all of the aqueous solutions during preparation at a concentration level of 0.05 % of the total specific biopolymer concentration used, serving as a preservative.

3.1.1.6. Starch Assay Kit

Starch glucose oxidase/oxidase (GO/P) assay kits were purchased from Sigma Aldrich Company Ltd (Dorset, UK), and were used as supplied with no further modification. Each kit was sufficient for 20 assays and enabled for the quantitative, enzymatic determination of glucose in low acyl gellan gum and glucose mixed quiescent and fluid gels. Glucose is oxidised to gluconic acid and hydrogen peroxide by glucose oxidase. Hydrogen peroxide reacts with *o*-dianisidine in the presence of peroxidase to form a coloured product. Oxidised *o*-dianisidine reacts with sulphuric acid to form a more stable coloured product. The intensity of the pink colour measured at 540 nm is proportional to the original glucose concentration. Equations 3.1 – 3.3 subsequently portray these reactions.

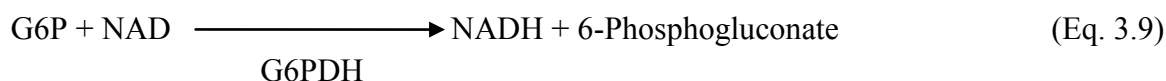
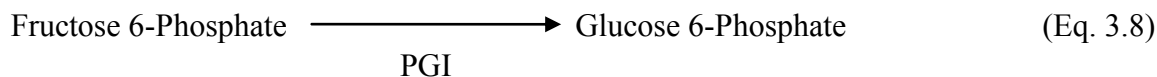
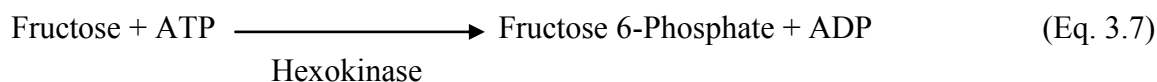
Further details of the experimental procedures are described in Sections 3.2.7.4 and 3.2.8.3.



3.1.1.8. Fructose Assay Kit

Fructose assay kits were purchased from Sigma Aldrich Company Ltd (Dorset, UK), and were used as supplied with no further modification. Each kit was sufficient for 20 assays and enabled for the quantitative, enzymatic determination of fructose in low acyl gellan gum and fructose mixed quiescent gels. Fructose is phosphorylated by adenosine triphosphate (ATP) in the reaction catalyzed by hexokinase. Fructose 6-phosphate is converted to glucose 6-phosphate by phosphoglucose isomerase (PGI). Glucose-6-phosphate (G6P) is then oxidised to 6-phosphogluconate in the presence of nicotinamide adenine dinucleotide (NAD) in the reaction catalyzed by glucose-6-phosphate dehydrogenase (G6PDH). During this oxidation, an equimolar amount of NAD is reduced to NADH. The consequent increase in absorbance at 340 nm is directly proportional to fructose concentration. Equations 3.7 – 3.9 subsequently portray these reactions.

Further details of the experimental procedures are described in Section 3.3.7.4.



3.2. Methodology

3.2.1. Study of low acyl and high acyl mixed and mixed acid gellan gum quiescent gels

3.2.1.1. Preparation of mixed gels

Mixed hydrocolloid aqueous solutions of the two gellan variants with concentration varying from 0.5 - 3 wt.% were formulated by dispersing the specified hydrocolloid proportions in double distilled water at 85 °C. The gellan solution pH was recorded as 5.4, and was independent of gellan concentration. The natural pH of the mixed gellan solutions was altered by the drop wise direct addition of 0.5 % (0.137 mol dm⁻³) HCl. The acidified solutions were then transferred to cylindrical moulds (22.5 mm internal diameter and 50 mm height), and stored at either room temperature or 5 °C for 24 hours enabling gel formation. Texture analysis of all mixed acid gel specimens was performed directly following the 24 hour setting period.

3.2.1.2. Texture analysis

The structures of the fully-formed mixed acid gels were characterised by performing compression tests using a TA XT plus Texture Analyser (Stable Micro Systems Ltd.,

UK), with a 40-mm diameter cylindrical aluminium probe. Each sample had a 22.5 mm diameter and 10 mm length. All measurements were performed in triplicate with a compression rate of 1 mm/s.

The force/distance data, obtained from the texture analyser, was converted into true strain (ϵ_H) and true stress (σ_T) data using the following equations (Moresi & Bruno, 2007):

$$\epsilon_E = (H_o - h)/H_o \quad (\text{Eq. 3.10})$$

$$\epsilon_H = \ln(1 + \epsilon_E) \quad (\text{Eq. 3.11})$$

$$\sigma_E = F/A_o \quad (\text{Eq. 3.12})$$

$$\sigma_T = \sigma_E(1 + \epsilon_E) \quad (\text{Eq. 3.13})$$

where ϵ_E and ϵ_H are the engineering and true (Hencky) strain, σ_E and σ_T are the engineering and true stress, H_o and A_o are the initial height and cross-sectional area of each specimen and F and h are the compressive force applied and sample height resulting from the compression tests.

The gradient of the initial linear region (up to strain values of 0.05) in the true stress/true strain curves can be used to calculate the Young's modulus (Smidsrød et al., 1972) whilst the gradient of the second linear section, culminating in structure failure can be used to calculate the bulk modulus (Nussinovitch, 2004). These calculated moduli give information relating to the deformation mechanisms connected to the individual linear regions. Sample loading causes the connections amongst the hydrocolloid molecules in the gel network to deform, due to the stress applied. Within this initial

compression phase the gel matrix displays elastic behaviour, which is assessed by the Young's modulus. When a threshold stress is met the links in the hydrocolloid network break, and deformation proceeds via a second much steeper linear section. Within this compression phase the demonstrated behaviour is non-elastic and the gradient of the linear section in the true stress/true strain curve, "relates to the stiffness/deformability of the gel matrix, until structure failure occurs" (Norton et al., 2011).

Lastly the "total work to failure" (Kaletunc et al., 1991) is the total work (given as work per unit area) that is needed to induce structure failure and is determined from the area under the true strain/true stress curve, up to the point of failure. Figure 3.1 shows a typical true strain/true stress curve and also how the data in the plot is interpreted to give the total work to failure, bulk modulus and Young's modulus for the acid gel structures.

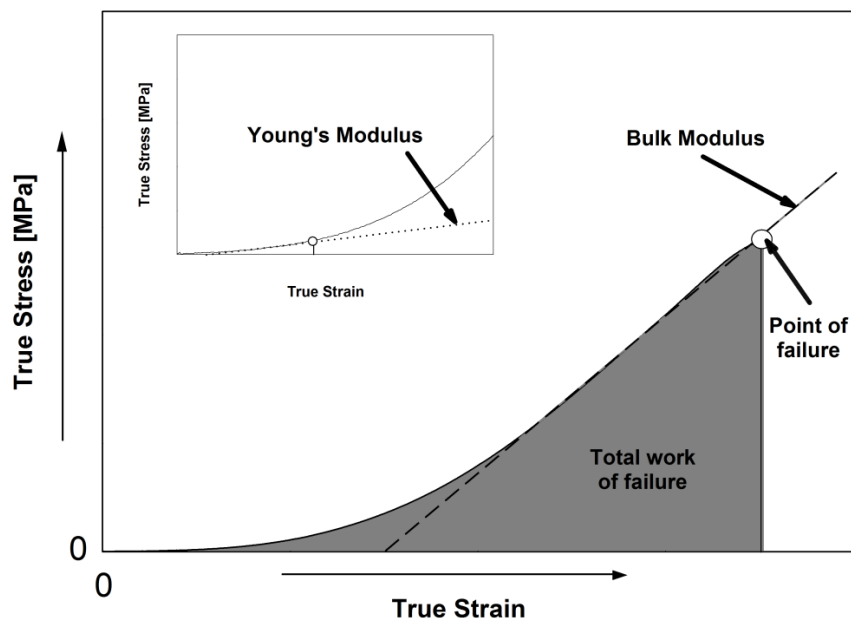


Figure 3.1. A typical true strain/true stress curve obtained during uniaxial compression of gellan gum acid gels adapted from Figure 1, Norton et al. (2011). Also shown is how the data in the plot is interpreted to give the total work to failure, bulk modulus and Young's modulus for the acid gel structures.

3.2.1.2.1. Post-production exposure to an acidic environment

The 3 wt.% mixed gellan gels were exposed to acid conditions by inserting the 10 mm long samples (as prepared for texture analysis) into an acid solution (pH 1) for time periods up to 3 hours. Texture analysis of these samples was performed immediately after exposure. Experiments were performed in triplicate to ensure reproducibility.

3.2.1.3. Rheological analysis

Rheological measurements on the aqueous mixed gellan solutions in their natural and pH adjusted forms were carried out using a Gemini HR nano stress-controlled rheometer using a 4°, 40 mm cone and plate, as illustrated in Figure 3.2. Cone and plate geometry was selected as it provides a well-defined and uniform shear field during experimentation. The aqueous mixed gellan samples were heated to 90 °C, before loading on to the pre-heated plate of the rheometer. All experiments were carried out within a ‘humidity trap’ (Figure 3.2), and using a silicon oil moisture barrier to reduce evaporation. A constant shear rate of 0.5 s⁻¹ was applied whilst cooling at 2 °C/min to 5 °C to obtain viscosity. Frequency response in the range 0.1 – 10 Hz was obtained under constant stress (0.1 Pa) at 10 °C intervals from 90 °C to 10 °C.

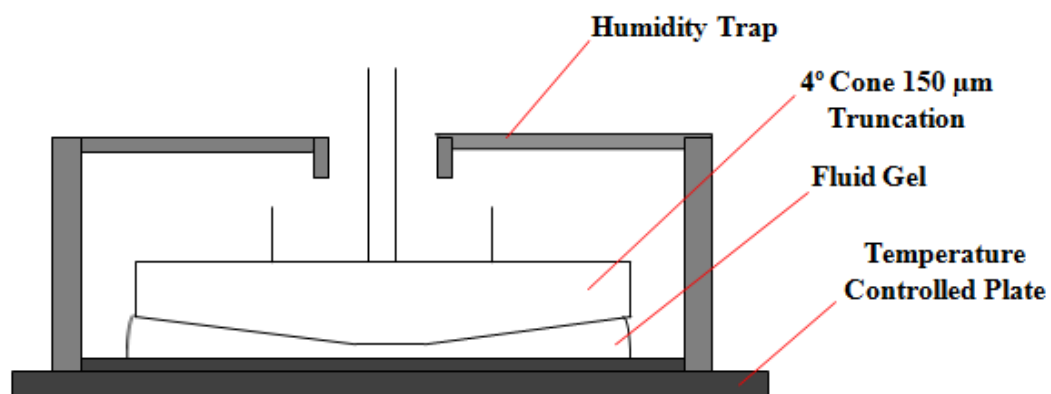


Figure 3.2. Rheometer peltier plate and cone and plate geometry with the fixed humidity trap to reduce evaporation.

3.2.1.4. Differential scanning calorimetry

Differential scanning calorimetry measurements were performed using a Setaram μ -DSC3 evo Dynamic Scanning Calorimeter (DSC) to measure the enthalpies and temperatures of thermal transitions. Screw-top, stainless steel ‘closed-batch cells’ were used where sample cells were filled (~ 75 %) with 0.76 g of the aqueous mixed gellan acid sample solution and the water-filled reference cell matched to this within 1 mg. The reference cell was used with double distilled water so as to cancel out the temperature dependence of the specific heat capacity, thus providing ‘non-sloping’ baselines. At the beginning of each experiment both sample and reference were isothermally held at 10 °C for 10 min, then heated to 95 °C (3 °C/min) to eliminate errors caused by thermal history during sample preparation and loading. Each were then cooled to 5 °C, and then heated back to 95 °C using a constant rate of 0.2 °C/min. The total test time of this procedure was 15 hours, 40 minutes. Hence, in most cases only one test was performed per sample.

3.2.1.5. Polarimetry

An Anton Paar Gyromat automatic Polarimeter was used to measure optical rotations of the mixed gellan solutions in their natural pH forms at 365 nm. Temperature was controlled via a recirculating water bath flowing around the cell annulus and was measured using a thermocouple situated in the sample fluid. The cell path length was 5 cm.

For control purposes, the optical rotation for gelatin (5 wt.%), a known optically active material that displays thermal hysteresis, was measured at 578 nm.

3.2.2. Kinetic studies of low acyl gellan gum fluid gels produced using a scraped surface heat exchanger and a jacketed pin-stirrer

Initially, a scraped surface heat exchanger (SSHE) combined in series with a jacketed pin-stirrer was used to produce the *LA* gellan gum fluid gels. The equipment was chosen for this purpose based on established research by Norton & Frith (2001), who demonstrated through the manipulation of the pin-stirrer rotating shaft velocity, that different fluid gels could be obtained. The SSHE and pin-stirrer employed in this work closely resembles the standard unit equipment used in the food industry to formulate products such as water-in-oil based low-fat spreads that are stabilised by fat crystals e.g. margarine or mayonnaise.

3.2.2.1. The scraped surface heat exchanger

A schematic diagram of the model scraped surface heat exchanger (SSHE) used in this work is shown in Figure 3.3. The SSHE's incorporate an internal mechanism which periodically removes the formulated product from the heat transfer wall. The product side is scraped by blades that are attached to a moving shaft, as depicted in Figure 3.3. The blades are made of a rigid plastic material to prevent damage to the scraped surface. This material is FDA approved, allowing a wide range of possibilities for food applications, in addition to the well established chemical, petrochemical and pharmaceutical industrial applications. A primary function of current SSHE's is to improve heat transfer. The ideal goal is to exchange the maximum amount of heat per unit area by generating maximum turbulence possible below given pumping power limits. This is primarily achieved through the extension of the SSHE shaft surface via the addition of blades. Optimum mass flow and turbulence extremities however, become

diminished for many of these technologies when fouling appears; obliging designers to fit significantly larger heat transfer areas. Fouling generally constitutes as sample particulate accumulation; precipitation or crystallisation; or sedimentation.

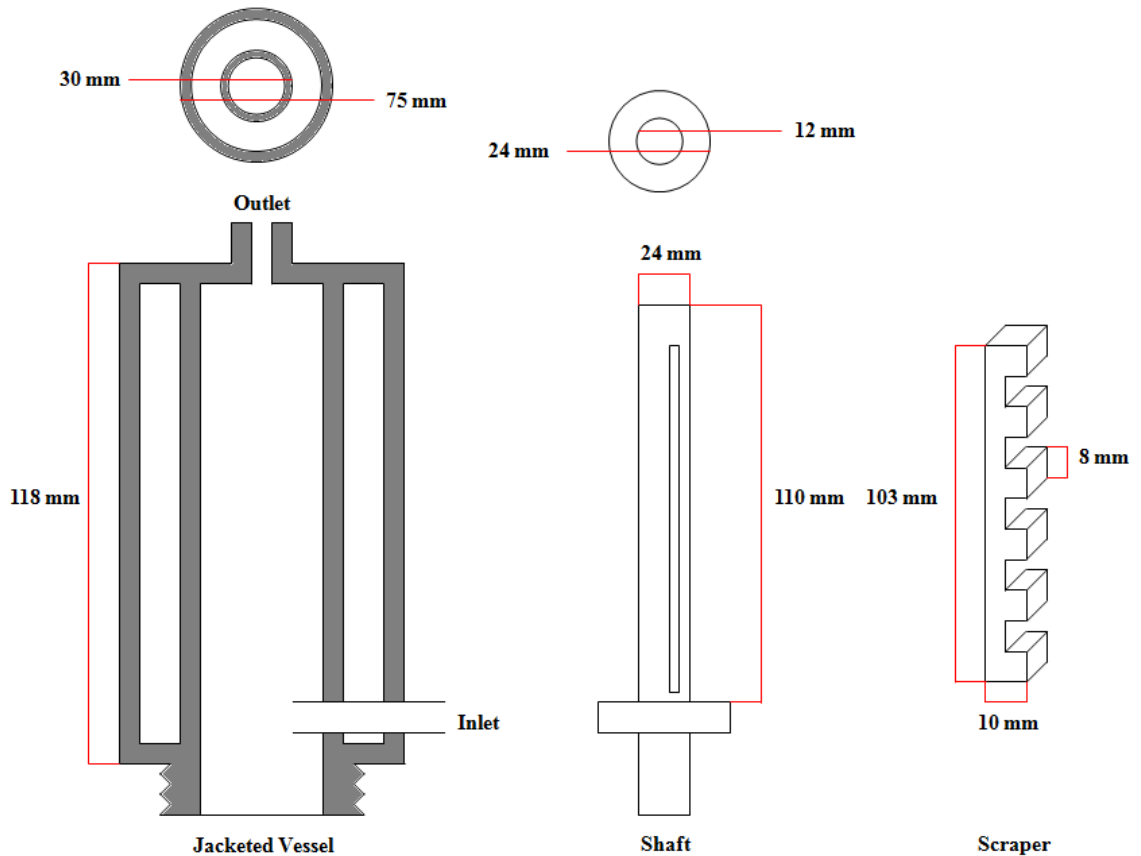


Figure 3.3. Schematic diagram of the scraped surface heat exchanger (a-unit). Units are expressed in mm.

A second factor that often poses difficulties to heat transfer within SSHE's is viscosity. Highly viscous fluids tend to generate deep laminar flow; a condition with poor heat transfer rates and high pressure losses involving considerable pumping powers which often exceed the exchanger design limits. The current SSHE's including the one incorporated within this work, have been designed to resolve the aforementioned problems. They increase heat transfer by removing the fouling layers; increasing

turbulence in the case of high viscosity flow; and help to avoid the generation of ice and other process by-products.

The SSHE (Figure 3.3) consists of a rotating shaft (24 mm diameter) fixed with two detachable plastic blades (103 mm long) that are positioned parallel to a sealed jacketed vessel when fully constructed. The internal volume of the SSHE was measured by flooding it with water; with the shaft inserted it measured 40 mL.

The smallest gap between the rotational blades fixed to the shaft and the outer sealed vessel wall is approximately 0.5 mm, and is found when the rotating blades ‘scrape’ the formulated product from the heat transfer wall. The shear rate at this position can be estimated for a rotating velocity of 1500 rpm (Table 3.1) to be $\sim 558 \text{ s}^{-1}$ as calculated using Eq. 3.14 below.

$$\dot{\gamma} = \frac{\pi R_1^2 n_1}{15 (R_2^2 - R_1^2)}$$

Where R_1 = inner cylinder radius of the rotating SSHE shaft = 12 mm; and R_2 = outer cylinder radius of the SSHE = 15 mm. n = rotations per minute (rpm) of the SSHE shaft, which was set to 1500 rpm (refer to Section 3.2.5.2). The shear rate for the SSHE rotating shaft set at this speed is thus:

$$\dot{\gamma} = 560 \text{ s}^{-1}$$

(Eq. 3.14) Calculating the approximate shear rate (s^{-1}) for the SSHE rotating shaft, set at a speed of 1500 rpm.

3.2.2.2. The pin-stirrer

A schematic diagram of the model pin-stirrer used in this work is shown in Figure 3.4. The pin-stirrer consists of a rotating shaft (14 mm diameter) with 16 pins evenly distributed along its length, which is inserted into a jacketed vessel with 16 stators running up the inside wall (as depicted in Figure 3.4).

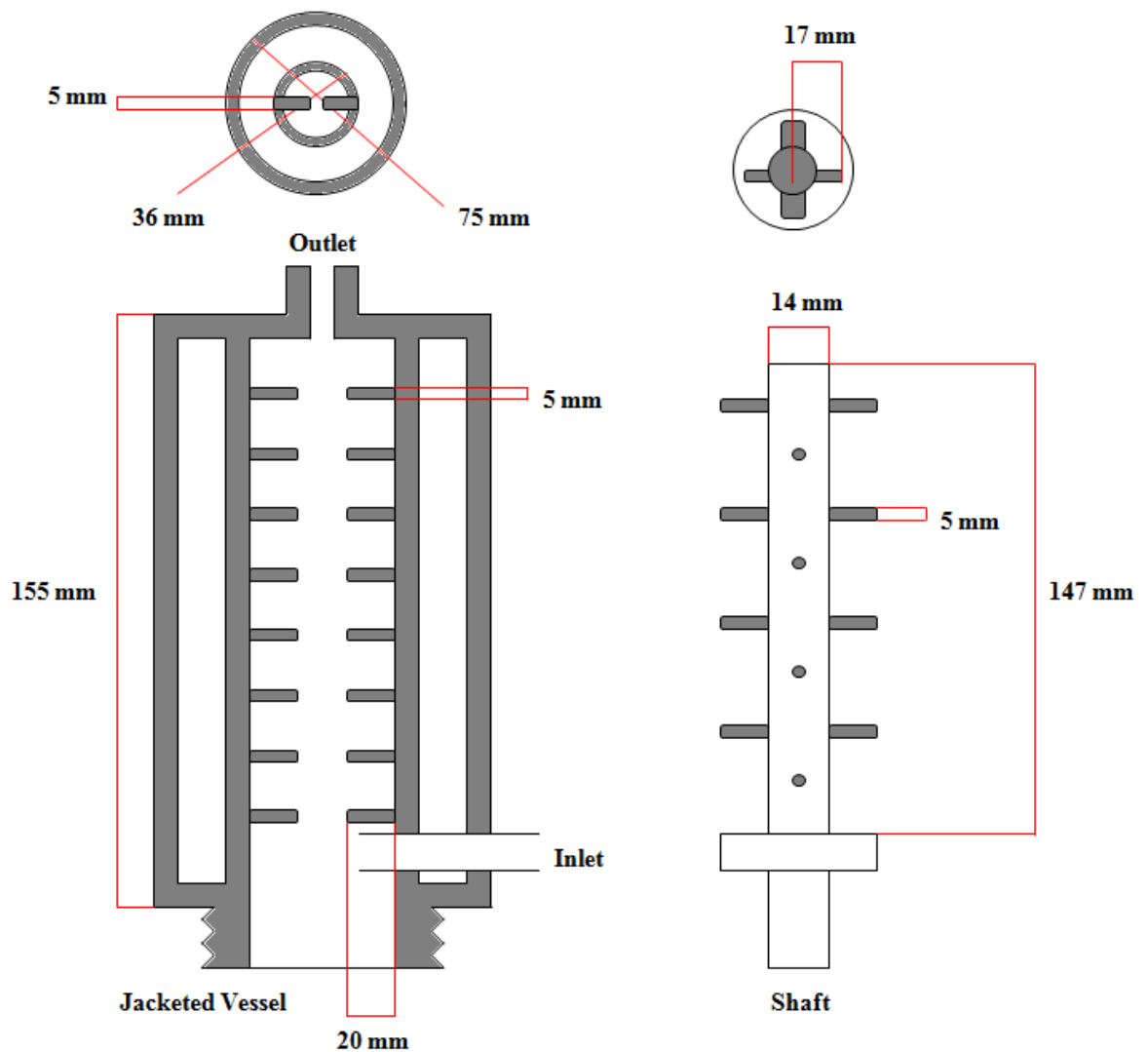


Figure 3.4. Schematic diagram of the pin-stirrer (c-unit). Units are expressed in mm.

The stators are designed to be positioned between the rotating pins, which in turn break the flow created against them and increase the anisotropy of the flow field. The smallest gap between the stationary pins and the rotational pins is approximately 3 mm

and is found when the rotating pins pass between the stationary pins. The shear rate at this position can be estimated for a rotating velocity of 1500 rpm (Tables 3.1 & 3.2) to be $\sim 56 \text{ s}^{-1}$ (refer to Section 3.2.5.2 and Eq. 3.15 for a more in depth discussion and calculation). The highest shear is expected to be found in the small region of swept volume between the rotating pins and the outer wall. The shear in this region can be estimated to be $\sim 112 \text{ s}^{-1}$ based on extrapolating rates calculated using computational fluid dynamic (CFD) measurements (Gabriele, 2011) to those obtained within this work.

3.2.2.3. Set-up

The schematic in Figure 3.5 displays the set-up adopted together with the associated components. The hot *LA* gellan gum aqueous solutions (1 – 2 wt.%) were prepared and fed from a sealed jar (containing a specially adapted jar-lid to prevent water evaporation) on the stirred hot-plate firstly into the SSHE, and then into the pin-stirrer. Silicon tubing was used to connect all of the units within the process, and material flow was induced via a peristaltic pump (Masterflex® L/S®), with the flow rate being maintained at 100 ml/min. The temperature of the fluid entering the SSHE was maintained above the melting point of the *LA* gellan biopolymer (approximately 85 °C), and T_{exit} was controlled via two recirculating water baths (each set to 20 °C) that ran through the annulus (jacket) of the SSHE and the annulus of the pin-stirrer respectively. The SSHE and the pin-stirrer were both used at shaft rotation speeds of 1500 rpm. The speeds were measured using a digital laser tachometer (Cole-Parmer Instruments Ltd., UK), and were chosen due to them each being the maximum rotation speeds capable for the respective equipment pieces.

Prior to sample collection, the aqueous fluid was pumped through the SSHE and pin-stirrer unit circuit (as shown in Figure 3.5) filling their internal volumes, whilst being

timed to do so. Immediately following this a proportion of ‘waste material’ was collected (~ 300 – 400 mL) for the time recorded to complete the circuit. This procedure allowed for the system to transition from an initial non-steady state condition to an equilibrium period in which the temperatures of the inlet biopolymer and outlet fluid gel solutions have time to stabilise. The samples were then collected, refrigerated (3 °C) and stored for at least 24 h, before testing, to allow post processing ripening effects to fully take place. Table 3.1 summarises the set up parameters for the varying *LA* gellan gum concentrated solutions formulated.

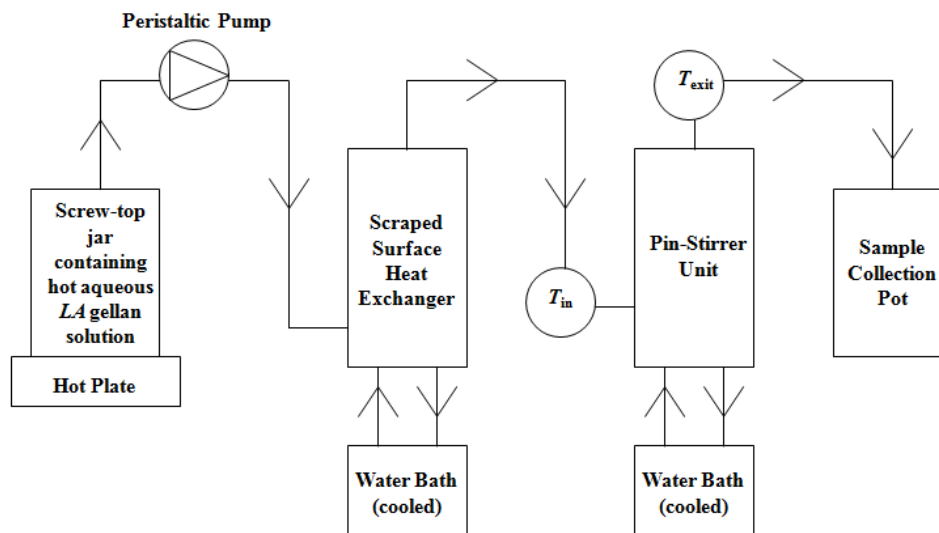


Figure 3.5. Schematic diagram of the scraped surface heat exchanger and pin-stirrer experimental set-up employed for fluid gel production.

<i>LA</i> Gellan Gum Concentration [wt. %]	Recirculating Water Bath Temperature [°C]	Flow Rate [ml/min]	a-unit Shaft Speed [rpm]	c-unit Shaft Speed [rpm]
1	20	100	1500	1500
2	20	100	1500	1500

Table 3.1. Set up parameters for the *LA* gellan gum fluid gel solutions formulated using scraped surface heat exchanger and the pin-stirrer unit under consistent flow rate and shaft speed conditions.

3.2.2.4. *Viscosity measurements post fluid gel production*

The post-production flow behaviour of the fluid gel samples was investigated approximately 24 hours after their production by performing viscosity measurements using the rheometer. The tests were performed at 25 °C using a cone and plate (cp) 4°, 40 mm geometry (Figure 3.2), and a shear rate range of 0.1 – 100 Hz.

3.2.2.5. *Examination of the fluid gel physical properties*

To examine the physical properties of the fluid gels, the samples were subjected to small deformation, low-amplitude oscillatory measurements during temperature cooling and heating ramps, with an intermittent table of frequencies test. The low-amplitude oscillatory measurements were performed at 10 rad/s at 1 % strain, using a 4° truncated cone and plate geometry, 40 mm in diameter (Figure 3.2). Samples (heated to 90 °C) were loaded (~ 1.25 ml) on to the pre-heated plate of the rheometer and cooled to 20 °C at 1 °C/min. All experiments were carried out within a ‘humidity trap’ (Figure 3.2), and using a silicon oil moisture barrier to reduce evaporation. Cooling was immediately followed by a frequency table from 0.1 – 100 rad/s at 20 °C. The last part of the rheological routine (based on that performed by Kasapis et al. (1999)) involved heating scans (1 °C/min) to the highest accessible temperature of the machine (95 °C).

3.2.3. Kinetic studies of low acyl gellan gum fluid gels produced using a jacketed pin-stirrer

Following the preliminary experiments described in Section 3.2.2., a decision was made to eliminate the SSHE in the fluid gel production process, and instead to use the pin-stirrer alone. This change of focus is explained in greater detail in Chapter 5, but primarily was due to most of the cooling taking place within the SSHE and significant loss of temperature control incurring between the transfer links connecting the respective units. More efficient mixing is also thought to take place within the pin-stirrer (Garrec & Norton, 2012).

3.2.3.1. Set-up

The schematic in Figure 3.6 displays the set-up adopted together with the associated components. The hot *LA* gellan gum aqueous solutions (1 – 2 wt.%) were prepared and fed from a sealed jar (containing a specially adapted jar-lid to prevent water evaporation) on the stirred hot-plate into the pin-stirrer. The temperatures of the fluid entering (T_{in}) and exiting (T_{exit}) the pin-stirrer were recorded using thermocouples, and T_{exit} was controlled via a recirculating water bath (set to 20 °C) that ran through the annulus (jacket) of the pin-stirrer. Silicon tubing was used to connect all of the units within the process, and material flow was induced via a peristaltic pump (Masterflex® L/S®). The internal volume of the pin-stirrer was measured by flooding it with water; with the shaft inserted it measured 150 mL. The pin-stirrer was used at a shaft rotation speed of 1500 rpm with the flow rate being maintained at 100 ml/min. The shaft rotation speed was measured using a digital laser tachometer (Cole-Parmer Instruments Ltd., UK). Prior to sample collection, the aqueous fluid was pumped through the pin-stirrer unit circuit (as shown in Figure 3.6) filling the internal volume, whilst being timed to do so. Following

this a proportion of ‘waste material’ was collected (~ 300 – 400 mL) for the time recorded to complete the circuit. This procedure allowed for the system to transition from an initial non-steady state condition to an equilibrium period in which the temperatures of the inlet biopolymer and outlet fluid gel solutions have time to stabilise. The samples were then collected, refrigerated (3 °C) and stored for at least 24 h, before testing, to allow post processing ripening effects to fully take place. Table 3.2 summarises the set up parameters, together with the T_{in} and T_{exit} recorded for the varying *LA* gellan gum concentrated solutions formulated.

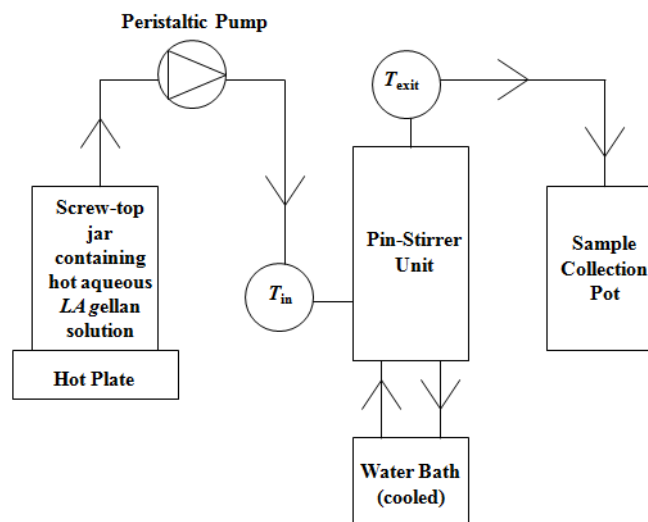


Figure 3.6. Schematic diagram of the pin-stirrer heat exchanger experimental set-up employed for fluid gel production. ‘ T ’ denotes the thermocouples measuring the temperatures of the fluid entering (T_{in}) and exiting (T_{exit}) the pin-stirrer.

<i>LA</i> Gellan Gum Concentration [wt. %]	T_{in} [°C]	T_{exit} [°C]	Recirculating Water Bath Temperature [°C]	Flow Rate [ml/min]	c-unit Shaft Speed [rpm]
1	74.7	29.7	20	100	1500
2	75.5	33.6	20	100	1500

Table 3.2. Set up parameters for the *LA* gellan gum fluid gel solutions formulated using the pin-stirrer unit under consistent flow rate and shaft speed conditions. Each of the T_{in} and T_{exit} values are based on a single sample measurement.

3.2.3.2. Viscosity measurements post fluid gel production

The post-production flow behaviour of the fluid gel samples was investigated by performing viscosity measurements using the rheometer 24 hours after their production. The tests were performed at 25 °C using a 4°, 40 mm cone and plate geometry (Figure 3.2), and a shear rate range of 0.1 – 100 Hz.

3.2.3.3. Study of the microstructure recovery

In order to investigate whether inter-particle interactions are involved during the production of fluid gels formulated using the pin-stirrer method, and whether these persist post-processing during structure development, the following kinetic studies were performed.

3.2.3.3.1. Structure development

Structural ripening or “strengthening” of the fluid gel structures, is affected by the cooling rates applied during processing, with more extended interactions taking place for those structures produced at higher cooling rates. To understand the time scales over which this “strengthening” process occurs, the samples (1 – 2 wt.%) were subjected to a linear viscoelastic table of frequencies test (0.1 – 100 rad/s), 24 hours after their production, measuring their viscoelastic modulus response, as a function of time. Each test was performed at 25 °C using a 4°, 40 mm cone and plate geometry.

3.2.3.3.2. Strain-recovery test

Each of the *LA* gellan gum fluid gel samples (1 – 2 wt.%) were subjected to a strain-recovery test. The elastic (G') and viscous (G'') modulus were measured initially during

an applied stress sweep ramp, which served to fully ‘break’ the inter-particle bonds by plastically deforming the structure. The samples were then subjected to a ‘rest period’ of 10 minutes, allowing for structural recovery. Immediately after this, a second stress sweep was performed. Each stress sweep had an amplitude range of 0.5 – 30 Pa, with constant frequency of 1 Hz.

3.2.3.4. Examination of the fluid gel properties

To examine the physical properties of the fluid gels, the samples (1 – 2 wt.%) were subjected to the same rheological routine (under identical conditions) performed on the 1 – 2 wt.% *LA* gellan fluid gel samples formulated using the SSHE and jacketed pin-stirrer (Section 3.2.2.5).

3.2.3.5. Differential scanning calorimetry

Differential scanning calorimetry (DSC) measurements (Setaram μ -DSC3 evo Dynamic Scanning Calorimeter) were performed on each of the samples (1 – 2 wt.%) to measure the enthalpies and temperatures of thermal transitions. The screw-top, stainless steel ‘closed-batch’ sample cell was filled (~ 75 %) with 0.74 – 0.75 g of the *LA* gellan gum fluid gel samples and the water-filled reference cell matched to this within 1 mg. Initially, both sample and reference were isothermally held at 10 °C for 60 min. The procedure then commenced as follows: heating to 90 °C, cooling to 10 °C, heating to 90 °C, and then finally cooling to 10 °C; all at a constant rate of 0.5 °C/min. This experimental procedure allows for a direct comparison of quiescent and fluid gels to be made. The first scan investigates the thermal transition of melting a fluid gel. The cooling scan thereafter forms a quiescently cooled gel within the cell, since no external shear force was applied during the DSC testing. This is then melted during the third

scan, thus probing the thermal transition of melting a quiescent gel. Cooling again is then used to gauge the accuracy of the data, since the second and forth scans (both cooling) should be similar. The first and third (heating) scans were used to directly compare the melting profiles of fluid and quiescent gels.

Note that the scanning rate used in this procedure (0.5 °C/min) is faster than the rate previously used for the mixed gellan gum systems (0.2 °C/min) noted in Section 3.2.1.4. The justification for raising this rate was to reduce the total time of the experimental procedure (from 15 hours, 40 minutes to 11 hours, 40 minutes), whilst also improving the data to be collected by improving the detected signals with the increased heat flow sensitivity. One test per sample however, was still performed due to the lengthy test period.

3.2.4. Effect of processing conditions on low acyl gellan gum fluid gels

To probe the effect of how manipulating the processing conditions during fluid gel production influences their subsequent gel properties; a selection of *LA* gellan gum fluid gels were formulated using the pin-stirrer set up (as described in Section 3.2.3.1 and Figure 3.6) using varying pump- and shaft-rate speeds.

3.2.4.1. Set-up

The hot *LA* gellan gum aqueous solutions (0.25 and 1 wt.%) were prepared and fed from a sealed jar on the stirred hot-plate into the pin-stirrer (Figure 3.6). The temperatures of the fluid entering (T_{in}) and exiting (T_{exit}) the pin-stirrer were recorded using thermocouples, and T_{exit} was controlled via a recirculating water bath (set to 20 °C) that ran through the annulus of the pin-stirrer. The pin-stirrer was used at shaft rotation

speeds ranging from 275 - 1500 rpm, with the flow rate being varied from 50 - 200 ml/min. The shaft rotation speeds were measured using a digital laser tachometer (Cole-Parmer Instruments Ltd., UK).

For each sample, prior to collection, the aqueous fluid was also pumped through the pin-stirrer unit circuit (Figure 3.6) filling the internal volume, whilst being timed to do so. 'Waste material' was then collected (~ 300 – 400 mL) for the times recorded to complete the respective circuits, to allow for steady-state equilibration of the systems. The samples were then collected, refrigerated (3 °C) and stored for at least 24 h, before testing, to allow post processing ripening effects to fully take place. Tables 3.3 and 3.4 summarise the set up parameters, together with the T_{in} and T_{exit} recorded for the varying *LA* gellan gum concentrated solutions formulated.

3.2.4.2. *Viscosity measurements post fluid gel production*

The post-production flow behaviour of the fluid gel samples was investigated by performing viscosity measurements using the rheometer 24 hours after their production. The tests were performed at 25 °C using a 4°, 4mm cone and plate geometry (Figure 3.2), and a shear rate range of 0.01 – 100 Hz.

3.2.4.3. *Strain-recovery test*

Each of the *LA* gellan gum fluid gel samples (0.25 and 1 wt.%) were subjected to the same strain-recovery test (under identical conditions), as described for the *LA* gellan gum fluid gel samples (1 – 2 wt.%) produced using the jacketed pin-stirrer in Section 3.2.3.3.2.

<i>LA</i> Gellan Gum Concentration [wt.%]	T_{in} [°C]	T_{exit} [°C]	Recirculating Water Bath Temperature [°C]	Flow Rate [ml/min]	c-unit Shaft Speed [rpm]
0.25	78.4	23.3	20	50	1500
0.25	88.5	26.0	20	100	1500
0.25	90.2	27.5	20	150	1500
0.25	94.8	30.2	20	200	1500
0.25	67.4	22.8	20	50	1000
0.25	79.6	25.8	20	100	1000
0.25	87.4	32.4	20	150	1000
0.25	88.6	33.1	20	200	1000
0.25	70.3	23.2	20	50	500
0.25	82.3	26.2	20	100	500
0.25	87.5	30.6	20	150	500
0.25	90.2	32.4	20	200	500
0.25	71.6	22.9	20	50	275
0.25	86.1	26.4	20	100	275
0.25	90.5	31.1	20	150	275
0.25	93.5	33.5	20	200	275

Table 3.3. Set up parameters for the 0.25 wt.% *LA* gellan gum fluid gel solutions formulated using the pin-stirrer unit under varying flow rate and shaft speed conditions. Each of the T_{in} and T_{exit} values are based on a single sample measurement.

<i>LA</i> Gellan Gum Concentration [wt.%]	T_{in} [°C]	T_{exit} [°C]	Recirculating Water Bath Temperature [°C]	Flow Rate [ml/min]	c-unit Shaft Speed [rpm]
1	71.0	22.3	20	50	1500
1	83.7	30.8	20	100	1500
1	86.6	33.5	20	150	1500
1	88.3	34.9	20	200	1500
1	73.9	25.0	20	50	1000
1	86.6	32.2	20	100	1000
1	92.4	35.2	20	150	1000
1	93.3	36.1	20	200	1000
1	69.2	25.1	20	50	500
1	80.6	28.5	20	100	500
1	88.8	31.9	20	150	500
1	90.8	33.7	20	200	500
1	71.5	25.5	20	50	275
1	86.8	30.5	20	100	275
1	88.7	34.0	20	150	275
1	89.2	36.0	20	200	275

Table 3.4. Set up parameters for the 1 wt.% *LA* gellan gum fluid gel solutions formulated using the pin-stirrer unit under varying flow rate and shaft speed conditions. Each of the T_{in} and T_{exit} values are based on a single sample measurement.

3.2.4.4. Differential scanning calorimetry

DSC measurements (Setaram μ -DSC3 evo Dynamic Scanning Calorimeter) were performed on a selection of the 0.25 wt.% *LA* gellan gum fluid gel samples to measure the enthalpies and temperatures of thermal transitions. Each of the samples were prepared in an identical manner and subjected to the same experimental procedure described for the *LA* gellan gum fluid gel samples (1 – 2 wt.%) in Section 3.2.3.5. This experimental procedure allowed for a direct comparison of quiescent and fluid gels to be made.

3.2.4.5. Particle size determination

To investigate whether varying pump rates and biopolymer concentration influence *LA* gellan gum fluid gel particle size, micrographs were obtained for the samples (0.25 and 1 wt.%) formulated using a shaft speed of 1000 rpm and pump rates ranging from 50 – 200 ml/min. Precise measurement of the sizes of the formulated fluid gel particles proved to be difficult, due to the small dimensions of the particles, and also because of the close similarity between their refractive index and that of the suspending medium. For these reasons, the particle sizes were determined from images obtained using an optical microscope (Leica DMRBE, Leica Microsystems Imaging Solution LTD) equipped with a camera (3CCD, Colour Vision Camera Module, Donpisha) for micrograph acquisition. The length scales on the micrographs were calibrated using micrometer-scale graticules, which gave a conversion factor of 18.55 pixel/ μm . The dimensions of the particles in the micrographs were then measured in pixels using public software ImageJ (NIH, Maryland, USA), and converted into μm using the aforementioned calibration. Samples were taken from the fluid gel systems under investigation in their pure forms, with no further manipulation via dilution or staining.

3.2.5. Kinetic studies of low acyl gellan gum fluid gels produced using a rheometer

3.2.5.1. Rheometer configuration and set-up

LA gellan gum fluid gel production and rheological measurements (both during and after fluid gel production) were carried out in a Gemini HR nano stress-controlled rheometer using a 4°, 40 mm cone and plate geometry (Figure 3.2). This approach allows for the precise control of the temperature, rate of cooling and the applied rate of shear, which determine the structure of the produced systems. The cone and plate geometry was chosen since it provides a well-defined and uniform shear field during experimentation. Solutions of 2 wt.% *LA* gellan gum were transferred via pipette to the rheometer peltier plate set to 90 °C. The sample temperature was allowed to reach equilibrium (2 minutes) after the geometry was lowered and excess material removed. All experiments were carried out within a ‘humidity trap’ (Figure 3.2), and using a silicon oil moisture barrier to reduce evaporation. Whilst the volume of the samples used for all of the measurements was kept constant at 1.18 ml in order to be consistent and obtain reproducible data.

3.2.5.2. Viscosity measurements during fluid gel production

Following the rheometer set-up (Section 3.2.5.1), shear cooling profiles were conducted using a variation of shear rates ranging from 0.5 – 1000 s⁻¹, whilst cooling from 90 – 5 °C, using rates of 0.5 – 4 °C/min. By conducting these sheared cooling profiles to *LA* gellan gum solutions, fluid gels are formed and their viscosities can be probed. The primary focus of these viscosity profiles was to investigate the subsequent effects of the applied shear and cooling rates on the formation and properties of the *LA* gellan gum fluid gels.

Performing the shear cooling profiles at 50 s^{-1} has been calculated (Eq. 3.15) to be approximately the average shear that particles are exposed to within the pin-stirrer experimental setup (Section 3.2.2.2) when the rotating shaft is set at a speed of 1500 rotations per minute (rpm). Calculating the equivalent shear rate for the pin-stirrer shaft rotation speed, thus allows direct comparison to be made for the fluid gels samples formulated using the respective productive methods.

$$\dot{\gamma} = \frac{\pi R_1^2 n_1}{15 (R_2^2 - R_1^2)}$$

Where R_1 = inner cylinder radius of the rotating pin-stirrer shaft = 7 mm; and R_2 = outer cylinder radius of the pin-stirrer = 18 mm. n = rotations per minute (rpm) of the pin-stirrer shaft, which for the samples produced using the method described in Section 3.2.3.1 was set to 1500 rpm.

The shear rate for the pin-stirrer set at this speed is thus:

$$\dot{\gamma} = 56 \text{ s}^{-1}$$

(Eq. 3.15) Calculating the approximate shear rate (s^{-1}) for the jacketed pin-stirrer rotating shaft, set at a speed of 1500 rpm.

The calculated average cooling rate that the particles are exposed to within the pin-stirrer experimental setup (Section 3.2.2.2) under the conditions listed in Table 3.2 is $\sim 30 \text{ }^\circ\text{C}/\text{min}$. This high cooling rate makes it very difficult to make a direct comparison of the fluid gel samples formulated using the respective production methods, due to the cooling constraints of the rheometer equipment (maximum rate = $6 \text{ }^\circ\text{C}/\text{min}$). Thus, comparisons of the respective fluid gel samples were based solely on their shear rates during production.

3.2.5.3. Viscosity measurements post fluid gel production

To investigate the post-production flow behaviour, viscosity tests were performed on a selection of the 2 wt.% *LA* gellan gum fluid gels produced using the rheometer immediately after their production. Eight shear rates (0.5, 1, 5, 50, 200, 400, 600 and 1000 s⁻¹) were selected from the twelve that were initially used to produce the samples from the shear range 0.5 – 1000 s⁻¹; and a cooling rate of 3 °C/min was implemented during sample production. The tests were performed at 25 °C using a 4°, 40 mm cone and plate geometry (Figure 3.2). All data is presented in Chapter 5.

3.2.5.4. Particle size determination

To investigate whether the applied rate of shear during *LA* gellan gum fluid gel production has an influence on fluid gel particle size, micrographs were obtained for the samples (2 wt. %) formulated using shear rates of 1, 5, 50 and 100 s⁻¹, with a cooling rate of 1 °C/min. The same method described for the 0.25 and 1 wt.% *LA* gellan fluid gel samples (Section 3.2.4.5.) was adopted.

3.2.5.5. Study of the microstructure recovery

It is known (Gabriele et al., 2009) that for fluid gel systems produced using the rheometer method that inter-particle interactions are involved during production, and that these persist post-processing, before further developing for significant time periods after processing completion. This continuous “strengthening” of the fluid gel structures, is affected by the cooling rates applied during processing, with more extended interactions or bridging generally taking place for those structures produced at higher cooling rates. The reason for this is that higher cooling rates result in faster fluid gel production

processes. Decreasing the processing time causes the particles in the produced system to have less time to form, culminating in a greater reactivity once the shear environment is removed, at the end of the production process (i.e. during quiescent cooling). This then leads to the particles to interact with each other to a greater extent (via inter-particle bridging, as well as within the particles themselves) than if produced more slowly at lower cooling rates, to complete the remainder of the molecular ordering.

In order to understand the time scales over which this “strengthening” process occurs, the following kinetic studies were implemented.

3.2.5.5.1. *Microstructure ripening*

The tests were performed on fluid gel samples that were produced using the eight shear rates selected in Section 3.2.5.3 and formed using a cooling rate of 3 °C/min, following the same controlled methods previously discussed. The microstructure ripening test began immediately after fluid gel production had ceased, i.e. once the shear had stopped and the temperature had equilibrated to 25 °C. The samples were then subjected to a “pseudo-resting” stage, during which an oscillatory frequency of 1 Hz was used in a controlled stress mode (with the stress being set to be within the linear viscoelastic region (1 % strain)) was applied, and the elastic (G') and viscous (G'') modulus response of the samples were measured as a function of time. The viscoelastic moduli measured represent the changes within the fluid gel structure under the assumption that the controlled stress applied does not affect the structure’s subsequent aging process.

3.2.5.5.2. Strain-recovery test

Three of the fluid gel samples produced using varying combinations of controlled shear and cooling regimes were subjected to a strain-recovery test. The elastic (G') and viscous (G'') modulus were measured initially during an applied stress sweep ramp, which served to fully 'break' the inter-particle bonds by plastically deforming the structure. The samples were then subjected to a 'rest period' of 10 minutes, allowing for structural recovery. Immediately after this, a second stress sweep was performed. Each stress sweep had an amplitude range of 0.5 – 30 Pa, with constant frequency of 1 Hz. The three fluid gel samples were produced using the following conditions:

- 2 wt.% LA gellan cooled at 1 °C/min with an applied shear rate of 5 s⁻¹
- 2 wt.% LA gellan cooled at 4 °C/min with an applied shear rate of 100 s⁻¹
- 2 wt.% LA gellan cooled at 6 °C/min with an applied shear rate of 100 s⁻¹

3.2.5.6. Study of the gel de-structuring and restructuring

The *LA* gellan gum fluid gel de-structuring and restructuring after sample formation was explored, as a function of temperature versus G' and G'' . The 2 wt.% *LA* gellan gum fluid gel samples formed using a cooling rate of 3 °C/min at the eight selected shear rates (Section 3.2.5.3), were subjected to frequency tables from 0.1 – 10 Hz, performed every 10 °C during a temperature heating (20 – 90 °C) and cooling ramp (90 – 20 °C). Each test was performed using a 4°, 40 mm cone and plate geometry (Figure 3.2).

3.2.6. Acid exposure of low acyl gellan gum fluid gels

3.2.6.1. Direct acid addition

Norton et al. (2011) found that it is possible to successively structure acid-sensitive solutions, such as *LA* gellan gum at pH values found in the stomach and to break (de-structure) the resulting gels within a desired time frame by forces typically found in the stomach. There is a requirement however, for these types of structures to be temperature and time stable, so that they can be transported and / or added to pre-existing food products without any structural changes. Forming acid fluid gels could satisfy this, thus a natural progression of this work was to investigate the acid gelation (structuring) process of *LA* gellan gum fluid gels, in order to gain an insight into the acid gel structures that can be produced by direct addition of acid, inducing a range of pH environments. 1 wt.% *LA* gellan gum aqueous solutions were prepared. Following, the 30 minute stirring period at 80 °C, the natural pH of the gellan solution was adjusted by the drop wise direct addition of 0.5 % (0.137 moldm³) HCl (also at 80 °C) to the desired pH level (pH 4 – 2) using a pH meter to monitor the progress.

<i>LA</i> Gellan Gum Concentration [wt.%]	pH (acidity) Level	T _{in} [°C]	T _{exit} [°C]	Recirculating Water Bath Temperature [°C]	Flow Rate [ml/min]	c-unit Shaft Speed [rpm]
1	5.4	75.6	26.0	15	100	1500
1	4	74.0	22.1	15	100	1500
1	3	72.3	21.6	15	100	1500
1	2	73.9	22.9	15	100	1500

Table 3.5. Set up parameters for the 1 wt.% *LA* gellan gum acid fluid gel solutions formulated using the pin-stirrer unit using varying recirculating water bath temperatures. Each of the T_{in} and T_{exit} values are based on a single sample measurement.

The acidified solutions were then processed using the pin-stirrer method (described in Section 3.2.3.1) following the set-up parameters enclosed in Table 3.5. Four control *LA* gellan gum quiescent acid gel samples (pH natural – pH2) were also formulated for comparison purposes.

3.2.6.1.1. Viscosity measurements post fluid gel production

The post-production flow behaviour of the *LA* gellan gum acid fluid gel and acid quiescent gel samples was investigated by performing viscosity measurements using the rheometer approximately 24 hours after their production. The tests were performed at 25 °C using a parallel plate geometry (40 mm in diameter) and a shear stress range of 0.001 – 1000 Pa, following an applied pre-shear at 100 s^{-1} for 60 seconds with an equilibrium period (120 seconds) immediately after. The parallel plate geometry was used because the fluid gel samples were gradually expelled from the gap in a cone and plate geometry. The disadvantage however, when using a parallel plate geometry is that the shear rate varies across the sample, so that an average value is given by the rheometer software.

3.2.6.1.2. Study of the gel de-structuring

The *LA* gellan gum acid fluid gel and acid quiescent gel de-structuring after sample formation was explored, as a function of temperature versus G' and G'' . Each sample was subjected (24 hours after formation) to frequency tables from 0.1 – 10 Hz, performed every 10 °C during a temperature heating (10 – 90 °C) ramp. Each test was performed using a 4°, 40 mm cone and plate geometry (Figure 3.2).

3.2.6.2. *Post-production acid exposure*

All of the *LA* gellan gum fluid gels formulated using the jacketed pin-stirrer units (Sections 3.2.3 and 3.2.4) together with the *LA* gellan gum acid fluid and acid quiescent gels (Section 3.2.6.1) were assessed post-production in terms of their response to a prolonged exposure to HCl acid. This served to simulate the stomach environment whilst eating and digesting. Immediately after their formulation, the respective aqueous gel solutions were placed into visking dialysis tubing (23mm ID, 14000 Da pore size, Medicell International, Ltd.), which was then allowed to soak in a 0.5 % HCl acid solution (corresponding to ~ pH 1) for 24 hours. Texture analysis of these systems was then performed to assess their structural properties. The procedure followed was identical to that described for the compression tests performed on the mixed gellan gels in Section 3.2.1.2.

3.2.7. Study of % co-solute (sugar) release from low acyl gellan gum and co-solute mixed quiescent gels

A challenge faced by researchers investigating self-structuring satiety based food products is how to incorporate materials that will modulate the energy delivery and slowly release calories after the meal (slow burn) has been consumed. It is particularly important that these additional materials are still organoleptically acceptable to the consumer. The addition of co-solutes such as sugar and the measurement of their subsequent release from hydrocolloid gels could provide a first step to tackling these issues. The content of sugars in foods is of great importance. Both consumers and industry are interested in healthier new products with a decreased amount of sugars present. As the sweetness and the texture of these new products should not be significantly altered, a study on the behaviour of various sugars and their mixtures is necessary. Thus, the final part of this work focused on studying the structuring, the energy (sugar) release, and the influence of gel structure on these release properties for *LA* gellan quiescent gels containing low levels (0 – 50 %) of the co-solutes glucose, sucrose and fructose using rheological, UV-Vis spectrophotometric, and compression tests.

3.2.7.1. Preparation of the low acyl gellan gum and co-solute mixed quiescent gels

Heated aqueous gel solutions (2 – 4 wt.%) were prepared by dispersing the required amounts of the *LA* gellan gum (CPKelco (San Diego, USA)) and co-solute (0 – 50 % glucose, sucrose or fructose) in double distilled water at 90 °C, whilst stirring for 30 minutes until dissolved. No further modifications to the materials were implemented.

3.2.7.2. Gel texture

To assess the gel texture of the *LA* gellan gum and co-solute mixed quiescent gels, the heated aqueous solutions prepared in Section 3.2.7.1 were poured into cylindrical moulds (22.5 mm internal diameter and 50 mm height), and then stored at 5 °C for 24 hours to allow for gel formation. Texture analysis of these systems was then performed immediately after the 24 hour setting period to assess the structural properties. The procedure followed was identical to that described for the compression tests performed on the mixed gellan gels in Section 3.2.1.2.

3.2.7.3. Kinetic study of the low acyl gellan gum and co-solute mixed quiescent gels

To assess the gel formation behaviour of the *LA* gellan gum and co-solute mixed quiescent gels, the 18 aqueous solutions (90 °C) prepared in Section 3.2.7.1 were loaded onto the pre-heated rheometer plate (90 °C), and then subjected to oscillatory frequency tables from 0.1 – 10 Hz at 10 °C intervals, during a temperature quench (90 – 10 °C). All measurements were performed using a 4°, 40 mm cone and plate geometry, fitted with a “humidity trap” to reduce evaporation (Figure 3.2), and sample volumes were kept constant (1.18 ml) in order to be consistent and obtain reproducible data.

3.2.7.4. Measuring the % co-solute release using spectrophotometry

To measure the % co-solute release (0 - 50 % glucose, sucrose and fructose respectively) from the *LA* gellan gum quiescent gels (2 – 4 wt.%), a diffusion method was adopted. This was then used together with co-solute specific enzymatic assay kits and spectrophotometry measurements to accurately monitor the co-solute release. The

decision to use the enzymatic assay kits as a tool for measuring the co-solute release was based on the widespread use of enzymes as analytical tools in the food, biochemical, and pharmaceutical industries. Enzymatic methods are specific, reproducible, sensitive, rapid, and therefore, ideal for analytical purposes.

The diffusion method involved preparing the heated aqueous gel solutions as described in Section 3.2.7.1 and placing each sample into visking dialysis tubing (23mm ID, 14000 Da pore size, Medicell International, Ltd.), which were then secured and individually allowed to soak in beakers filled with double distilled water for 18 hours. During this soaking time, the co-solutes are able to diffuse from the gel solutions through the dialysis membranes and into the double distilled water. The amount of co-solute in the double distilled water samples were then assessed using the co-solute specific enzymatic assay kits, following the specific instructions supplied. These instructions detailed the procedures to perform the reactions detailed in Sections 3.1.1.6; 3.1.1.7; and 3.1.1.8 for the starch, sucrose, and fructose assay kits respectively. Following these reactions, a 2000 Series Cecil CE2040 UV-Vis spectrophotometer was used to measure the intensity of the pink colour measured at 540 nm (starch assay kit and glucose co-solute samples only); and the increase in absorbance at 340 nm (sucrose and fructose assay kits and sucrose and fructose co-solute samples only) which were proportionate to the % glucose, sucrose and fructose released from the original *LA* gellan gum and co-solute samples.

Equations 3.16, 3.17, and 3.18 respectively show examples of how the spectrophotometric absorbencies recorded for the 2 wt.% *LA* gellan – 50 % glucose; 2 wt.% *LA* gellan – 50 % sucrose; and 2 wt.% *LA* gellan – 50 % fructose double distilled water samples following diffusion (18 hours) and enzymatic assay analysis, were used to calculate the % co-solute release levels from their original mixed gel solutions.

$$\Delta A_{\text{STANDARD}} = A_{\text{STANDARD}} - A_{\text{STANDARD BLANK}}$$

$$\Delta A_{\text{TEST}} = A_{\text{TEST}} - A_{\text{REAGENT BLANK}}$$

$$\% \text{ Glucose} = \frac{(\Delta A_{\text{TEST}})(F)(V)(VGA)(MWF)(100)}{(\text{Conversion Factor for } \mu\text{g to mg})(\text{Sample Weight in mg})}$$

$$\% \text{ Glucose} = \frac{(\Delta A_{\text{TEST}})(50/\Delta A_{\text{STD}})(350)(1.0)(0.9)(100)}{(1000)(\text{Sample Weight in mg})}$$

$$\% \text{ Glucose} = \frac{(\Delta A_{\text{TEST}})(1575)}{(\Delta A_{\text{STD}})(\text{Sample Weight in mg})}$$

$$F = \mu\text{g glucose in standard} \div \Delta A_{\text{STANDARD}} \text{ at } 540 \text{ nm} = 50/\Delta A_{540}$$

V = Initial Sample Volume (from sample preparation)

VGA = Initial Sample Volume from Glucose Assay

MWF = Molecular Weight of Starch Monomer/Molecular Weight of Glucose =
162/180 = 0.9

For the 2 wt.% LA gellan – 50 % glucose mixed gel solution:

$$\% \text{ Glucose} = \frac{(0.931)(1575)}{(1.103)(1000)}$$

$$\% \text{ Glucose} = 1.329 \text{ (4 s.f.)}$$

(Eq. 3.16) Calculating the % glucose released from the 2 wt.% LA gellan – 50 % glucose mixed gel solution, following an 18 hour diffusion period.

$$A_{\text{TOTAL BLANK}} = (A_{\text{SAMPLE BLANK}} - A_{\text{GLUCOSE ASSAY REAGENT BLANK}}) + A_{\text{SUCROSE ASSAY REAGENT BLANK}}$$

The total blank takes into account the contribution to the absorbance of the sample, the Glucose Assay Reagent, and the Sucrose Assay Reagent used within the sucrose enzymatic assay kit. The absorbance of the Glucose Assay Reagent is subtracted from

the sample blank, so that the absorbance of the Glucose Assay Reagent is only counted once in the total absorbance, since it is in both the sample blank and the Sucrose Assay Reagent blank.

$$\Delta A = A_{\text{TEST}} - A_{\text{TOTAL BLANK}}$$

$$\text{Sucrose concentration (mg/ml)} = \frac{(\Delta A)(TV)(\text{Molecular Weight of Sucrose})(F)}{(\epsilon)(d)(SV)(\text{Conversion Factor for } \mu\text{g to mg})}$$

$$\text{Sucrose concentration (mg/ml)} = \frac{(\Delta A)(2.2)(342.3)(F)}{(6.22)(1)(0.1)(1000)}$$

$$\text{Sucrose concentration (mg/ml)} = (\Delta A)(F)(1.21)$$

A = Absorbance at 340 nm

ϵ = Millimolar Extinction Coefficient for NADH at 340 nm. Units = millimolar⁻¹ cm⁻¹
or (ml/μmoles)(1/cm)

d = Light path (cm)

TV = Total Assay Volume

SV = Sample Volume

F = Dilution Factor from sample preparation

For the 2 wt.% LA gellan – 50 % sucrose mixed gel solution:

$$A_{\text{TOTAL BLANK}} = (0 - -0.023) + -0.001 = 0.022$$

$$\Delta A = 0.359 - 0.022 = 0.337$$

$$\text{Sucrose concentration (mg/ml)} = (0.337)(F)(1.21)$$

$$\text{Sucrose concentration (mg/ml)} = 0.4078$$

To convert the sucrose concentration (mg/ml) into % sucrose released:

$$\% \text{ Sucrose} = \frac{(\text{Sucrose concentration (mg/ml)}) (\text{Volume of water gels were soaked in})}{\text{mg Sucrose added when forming initial mixed gel}} \times 100$$

Therefore, for the 2 wt.% *LA* gellan – 50 % sucrose mixed gel solution:

$$\% \text{ Sucrose} = 14.273 \text{ (4 s.f.)}$$

(Eq. 3.17) Calculating the % sucrose released from the 2 wt.% *LA* gellan – 50 % glucose mixed gel solution, following an 18 hour diffusion period.

$$A_{\text{TOTAL BLANK}} = (A_{\text{SAMPLE BLANK}} - A_{\text{GLUCOSE ASSAY REAGENT BLANK}}) + A_{\text{PGI BLANK}}$$

$$\Delta A = A_{\text{TEST}} - A_{\text{TOTAL BLANK}}$$

$$\text{Fructose concentration (mg/ml)} = \frac{(\Delta A)(TV)(\text{Molecular Weight of Fructose})(F)}{(\epsilon)(d)(SV)(\text{Conversion Factor for } \mu\text{g to mg})}$$

$$\text{Fructose concentration (mg/ml)} = \frac{(\Delta A)(2.12)(180.2)(F)}{(6.22)(1)(0.1)(1000)}$$

$$\text{Fructose concentration (mg/ml)} = (\Delta A)(F)(0.614)$$

A = Absorbance at 340 nm

ϵ = Millimolar Extinction Coefficient for NADH at 340 nm. Units = millimolar⁻¹ cm⁻¹
or (ml/μmoles)(1/cm)

d = Light path (cm)

TV = Total Assay Volume

SV = Sample Volume

F = Dilution Factor from sample preparation

For the 2 wt.% *LA* gellan – 50 % fructose mixed gel solution:

$$A_{\text{TOTAL BLANK}} = (0 - 0) + 0 = 0$$

$$\Delta A = A_{\text{TEST}} - 0$$

$$\text{Fructose concentration (mg/ml)} = (0.806)(0)(0.614)$$

$$\text{Fructose concentration (mg/ml)} = 0.4949$$

To convert the fructose concentration (mg/ml) into % sucrose released:

$$\% \text{ Fructose} = \frac{(\text{Fructose concentration (mg/ml)}) (\text{Volume of water gels were soaked in})}{\text{mg Fructose added when forming initial mixed gel}} \times 100$$

Therefore, for the 2 wt.% *LA* gellan – 50 % fructose mixed gel solution:

$$\% \text{ Fructose} = 17.322 \text{ (4 s.f.)}$$

(Eq. 3.18) Calculating the % fructose released from the 2 wt.% *LA* gellan – 50 % glucose mixed gel solution, following an 18 hour diffusion period.

3.2.7.4.1. Measuring the % co-solute release over time

Additionally, to explore the variation of % co-solute release over time for varying diffusion periods, the 2 wt. % *LA* gellan – (10 – 50 %) glucose and 2 wt. % *LA* gellan – (10 – 50 %) sucrose samples were selected and exposed to diffusion times of 1h, 5h and 10h. The procedure detailed in Section 3.2.7.4 was then followed to measure the % co-solute release levels for the individual samples. Comparisons of the samples with those exposed to 18h diffusion times were also conducted (Section 3.2.7.4). The methods for

calculating the % co-solute release levels for the respective samples were identical to those shown in Equations 3.16 and 3.17.

The *LA* gellan – (10 – 50 %) fructose samples were omitted from these tests, since the initial results from the experiments conducted in Section 3.2.7.4 were very similar and had no key distinguishable differences to the *LA* gellan - sucrose mixed samples. Direct comparison between the disaccharide and monosaccharide sugars systems also wanted to be maintained.

3.2.8. Study of % co-solute (sugar) release from low acyl gellan gum and co-solute mixed fluid gels

3.2.8.1. Preparation of the low acyl gellan gum and co-solute mixed fluid gels

Heated aqueous gel solutions (0.5 – 2 wt.%) were prepared by dispersing the required amounts of the *LA* gellan gum (CPKelco (San Diego, USA)) and co-solute (0 – 50 % glucose or sucrose) in double distilled water at 90 °C, whilst stirring for 30 minutes until dissolved. Fluid gels were then produced by feeding the solutions from a sealed jar on the stirred hot-plate into the pin-stirrer (Figure 3.6). The temperatures of the fluid entering (T_{in}) and exiting (T_{exit}) the pin-stirrer were recorded using thermocouples, and T_{exit} was controlled via a recirculating water bath (set to 20 °C) that ran through the annulus of the pin-stirrer. The pin-stirrer was used at a consistent shaft rotation speed of 1500 rpm, with a flow rate of 100 ml/min.

For each sample, prior to collection, the aqueous fluid was also pumped through the pin-stirrer unit circuit (as shown in Figure 3.6) filling the internal volume, whilst being timed to do so. ‘Waste material’ was then collected (~ 300 – 400 mL) for the times

recorded to complete the respective circuits, to allow for steady-state equilibration of the systems. The samples were then collected, refrigerated (3 °C) and stored for 24 h, before testing, to allow post processing ripening effects to fully take place. Tables 3.6 and 3.7 summarise the set up parameters, together with the T_{in} and T_{exit} values recorded for the varying *LA* gellan gum – glucose and *LA* gellan gum – sucrose concentrated solutions formulated.

3.2.8.2. Study of the low acyl gellan gum and co-solute mixed fluid gel de-structuring

To assess the gel de-structuring behaviour of the *LA* gellan gum and co-solute mixed fluid gels after sample formation, the refrigerated samples were loaded onto the pre-set rheometer plate (10 °C), and then subjected to oscillatory frequency tables (0.1 – 10 Hz; 0.1 Pa shear stress) at 10 °C intervals, during a temperature heating (10 – 90 °C) ramp. Each test was performed using a 4°, 40 mm cone and plate geometry, fitted with a “humidity trap” to reduce evaporation (Figure 3.2). Sample volumes were kept constant (1.18 ml) in order to be consistent and obtain reproducible data.

3.2.8.3. Measuring the % co-solute release using spectrophotometry

To measure the % co-solute release (0 – 50 % glucose and sucrose respectively) from the *LA* gellan gum fluid gels (0.5 – 2 wt.%), the same diffusion method described in Section 3.2.7.4 was followed. This was then used together with co-solute specific enzymatic assay kits and spectrophotometry measurements to accurately monitor the co-solute release. The % co-solute release levels were then calculated using the recorded absorbencies and Equations 3.16 and 3.17.

<i>LA</i> Gellan Gum Concentration [wt.%]	% Glucose Level	T_{in} [°C]	T_{exit} [°C]	Recirculating Water Bath Temperature [°C]	Flow Rate [ml/min]	c-unit Shaft Speed [rpm]
0.5	0	78.5	25.7	20	100	1500
0.5	10	81.9	26.9	20	100	1500
0.5	20	80.0	27.2	20	100	1500
0.5	30	80.6	26.9	20	100	1500
0.5	40	78.9	26.6	20	100	1500
0.5	50	81.1	27.6	20	100	1500
1	0	77.6	28.3	20	100	1500
1	10	82.7	29.5	20	100	1500
1	20	79.4	28.0	20	100	1500
1	30	75.4	26.8	20	100	1500
1	40	76.8	26.8	20	100	1500
1	50	78.7	26.4	20	100	1500
2	0	77.0	34.4	20	100	1500
2	10	78.4	33.9	20	100	1500
2	20	79.7	34.1	20	100	1500
2	30	78.8	32.8	20	100	1500
2	40	78.9	32.9	20	100	1500
2	50	76.5	27.2	20	100	1500

Table 3.6. Set up parameters for the 0.5 – 2 wt.% *LA* gellan gum – glucose fluid gel solutions formulated using the pin-stirrer unit under consistent flow rate and shaft speed conditions. Each of the T_{in} and T_{exit} values are based on a single sample measurement.

<i>LA</i> Gellan Gum Concentration [wt.%]	% Sucrose Level	T_{in} [°C]	T_{exit} [°C]	Recirculating Water Bath Temperature [°C]	Flow Rate [ml/min]	c-unit Shaft Speed [rpm]
0.5	0	80.6	26.0	20	100	1500
0.5	10	80.4	23.9	20	100	1500
0.5	20	80.9	23.6	20	100	1500
0.5	30	81.8	24.2	20	100	1500
0.5	40	80.0	22.4	20	100	1500
0.5	50	81.2	22.8	20	100	1500
1	0	85.4	28.8	20	100	1500
1	10	82.3	23.8	20	100	1500
1	20	80.2	21.7	20	100	1500
1	30	75.8	19.3	20	100	1500
1	40	76.4	18.4	20	100	1500
1	50	74.6	15.4	20	100	1500
2	0	78.7	30.8	20	100	1500
2	10	73.4	24.1	20	100	1500
2	20	74.5	22.8	20	100	1500
2	30	74.1	20.5	20	100	1500
2	40	75.9	16.4	20	100	1500
2	50	72.1	14.2	20	100	1500

Table 3.7. Set up parameters for the 0.5 – 2 wt.% *LA* gellan gum – sucrose fluid gel solutions formulated using the pin-stirrer unit under consistent flow rate and shaft speed conditions. Each of the T_{in} and T_{exit} values are based on a single sample measurement.

Chapter 4

ACID-SENSITIVE LOW AND HIGH ACYL MIXED GELLAN GUM SYSTEMS

4.1. Introduction

The aim of this chapter was to investigate whether the gelation kinetics of a *LA* gellan gum system can be further controlled by introducing *HA* acyl gellan gum as a disrupter biopolymer. Further, the *in-vitro* acid-induced gelation of the *LA* and *HA* gellan gum mixed biopolymer systems was investigated, and their reactions over prolonged time periods (1 – 3 hours) in acidic conditions that mimic the stomach processes assessed.

4.2. Results & Discussion

4.2.1. Characterisation of mixed gellan gels

4.2.1.1. Gel structure

To explore the range of gel structures that could be obtained prior to acid exposure, mixed gellan gels were produced initially to 3 wt.% total biopolymer, by combining the *LA* and *HA* gellan variants in different ratios. The textural properties of the gels were then assessed by performing compression tests. Figure 4.1 shows these values of bulk modulus (a) and work up to fracture (b) for 3 wt.% mixed gellan gels as a function of increasing *HA* gellan percentage. Texture analysis (Figure 4.1) shows that the ratio of *HA:LA* variants affected the resulting gel structure. The mechanical properties of the mixtures depend on the ratio of the two biopolymers used. At natural pH mixtures with *HA* gellan weight fractions >30 % produce higher bulk moduli gels than those with lower *HA* content. The gels in Figure 4.1 display mechanical properties between those exhibited for the *HA* and *LA* gellan variants, despite the *HA* gellan used behaving differently to that reported in the literature (Sanderson et al., 1988b). Sanderson et al. (1988b) also used texture profile analysis to study the mixed gellan gels, but contrastingly, found that *HA* gellan gave gels with lower modulus and lower hardness

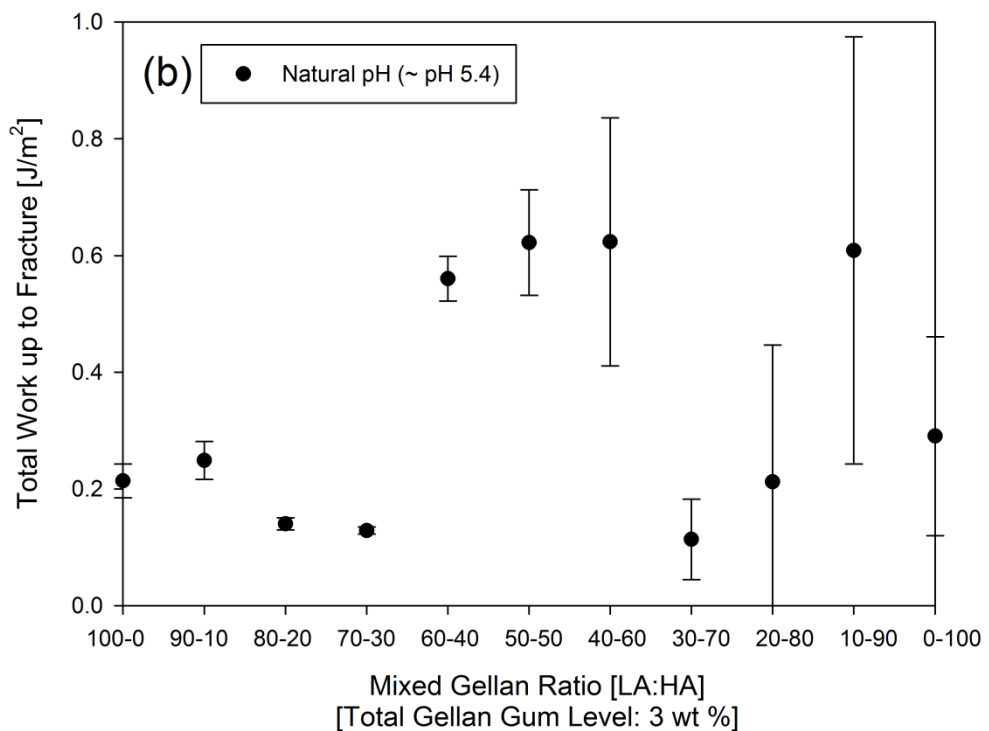
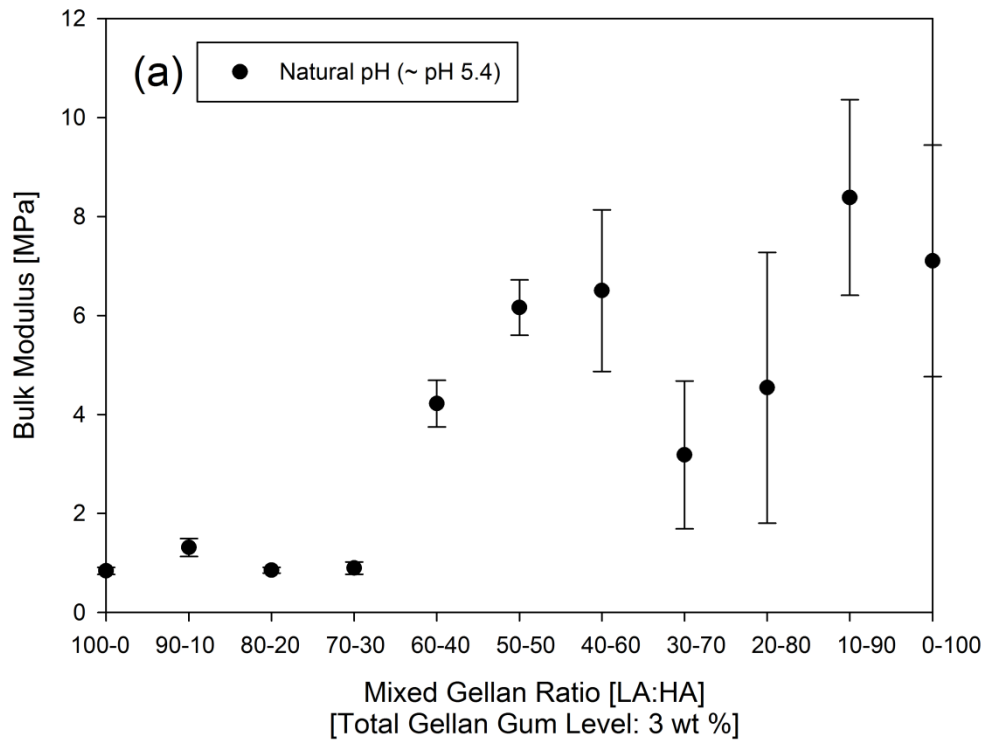


Figure 4.1. Bulk modulus (a) and work up to fracture (b) for 3 wt.% low acyl gellan gels as a function of increasing high acyl gellan percentage (0 – 100 % of the total biopolymer added). All measurements were carried out in triplicate with a compression rate of 1 mm/s. The error bars were determined from the standard deviations of these measurements collectively. Where error bars cannot be observed, they are smaller than the data points.

than those formed by commercial *LA* gellan gum. The elasticity and brittleness values for the *HA* gellan gels were reported to be much greater however. The large error bars observed in Figure 4.1 for the gels with *HA* gellan weight fractions >30 %, clearly reflect a progressive increase in brittleness of the mixtures, and in turn lower reproducibility with increasing *HA* gellan content. Each error bar is a reflection of the degree of brittle fracture propagation through the gel matrix, and its random behavioural nature.

These results (Figure 4.1) show a constant bulk modulus and total work up to fracture with *HA* proportions from 0 % to 30 %, indicating that the addition of *HA* gellan in this range is not changing the overall structure; this implies that up to this point the gel structure is phase separated with the *LA* form continuous. Between 30 % and 60 % *HA* gellan, the bulk modulus and work to fracture results increase gradually, reaching a maximum at 60 % *HA* gellan. This suggests that the biopolymers are now forming a full-interpenetrating network structure, whereby the *HA* and *LA* gellan polymers form continuous networks separately. The formation of double helices does not involve strands of both types (Morris et al., 1996); instead each of the gellan polymer chains is cross-linked. Alternatively, the biopolymers could be forming a bi-continuous phase separated structure at this point, with the *HA* and *LA* gellan polymers still forming continuous networks separately. This would allow for the smooth transition of one type of phase-separated structure to another as the *LA* to *HA* gellan gum ratio is varied. However, due to the lack of microstructural microscopy evidence in the literature clearly demonstrating one type of structure over the other and the majority of evidence, including that presented in this chapter siding towards a segregative interpenetrating network of polymers (Manson & Sperling, 1976; Mao et al., 2000; Morris et al., 2012) it is unlikely that this is the case.

Past this maximum the bulk modulus and work to fracture results fall dramatically with very low values at 70 % and 80 % *HA* gellan. This suggests a phase separation at these values, with neither variant able to form a continuous matrix, leading to a weak gel structure. At 90 % *HA* gellan and above, the *HA* gellan is continuous, with rheology the same as (bulk modulus and work to fracture within error bounds) the rheology of the *HA* variant alone. These results (Figure 4.1) are in contrast to the smooth increase of bulk modulus values observed by Morrison et al. (1999) as the proportion of *HA* gellan was increased.

4.2.1.2. Viscometric material response

To further investigate the material properties of the mixed gels and to identify molecular ordering events, viscosity measurements were recorded for five of the mixed gellan weight ratios: 0 %, 30 %, 50 %, 70 % and 100 % *HA* gellan proportions. Figure 4.2 shows the viscosity profiles on cooling for 0.5 wt.% mixed gellan aqueous solutions at their natural pH, as a function of increasing *HA* proportion. The decision to reduce the total biopolymer concentration from 3 wt.% to 0.5 wt.% for these tests was based on the fact that the mixed gellan aqueous solutions were easier to work with at reduced concentrations, whilst having little impact on the subsequent results.

Increasing the proportion of *HA* gellan results in an increase in viscosity. The rheological onset of gel formation on cooling is apparent for both of the gellan types within the mixed systems at their respective transition temperatures of approximately 25 °C (*LA*) and 65 °C (*HA*). This agrees with the rheological measurements taken from mixed gellan systems by Kasapis et al. (1999), who on cooling from high temperature observed two regions of steep increase in G' , the first coincident with the sol-gel

transition of *HA* gellan at high temperature and the second with the corresponding transition of the deacylated polymer at much lower temperature.

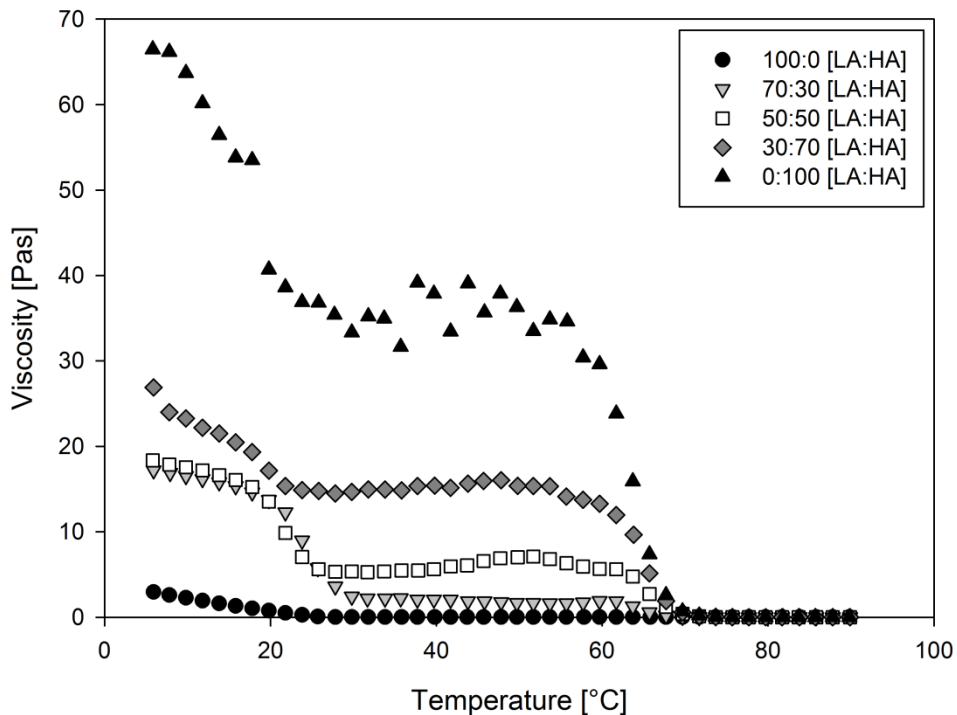


Figure 4.2. Viscosity measurements of 0.5 wt.%, pH 5 mixed gellan aqueous solutions during a temperature cooling ramp (90 – 5 °C) at 2 °C/min, using a constant shear rate of 0.5 s⁻¹. Each of the viscosity readings are based on a single sample measurement.

The mixed gellan solutions with 30 – 70 % *HA* gellan each show two distinct coil-helix transition temperatures on cooling for the *HA* and *LA* gellan variants, which shows that the problems associated with the high gelation temperature of the *HA* gellan gum (for example them being difficult to handle at high temperatures, due to their increased viscosity) are present in the mixed systems.

At 100 % *HA* gellan the coil-helix transition of the *HA* gellan is at approximately 65 °C, but a second step transition is also observed at around 25 °C. The first step at 65 °C corresponds to the conversion of the polymer from the disordered coil state to the double-helix form (García et al., 2011; Yamamoto & Cunha, 2007; Chandrasekaran & Radha, 1995). However, conformational ordering does not in itself give a cohesive

network. Formation of true gels requires association of double helices into stable aggregates (Morris et al., 2012). The carboxyl side groups of gellan gum molecules repulse each other by electrostatic interaction, which in turn hinder the tight binding and aggregation of helices (Grasdalen & Smidsrød, 1987). Introduction of cations can shield this electrostatic repulsion, thereby permitting tight binding and aggregation of helices at lower temperatures, or lead to the reduction of coil dimensions at higher temperatures (Morris et al., 1980; Kobayashi et al., 1994). A possible explanation for the appearance of the low temperature transition at 100 % *HA* gellan is that a delayed salt ordering (Miyoshi et al., 1995; Ogawa et al., 2002) is occurring following the initial *HA* gellan conformational ordering. This phenomenon occurs most strongly in *HA* gellan systems, whereby the high coil-helix transition temperature is distinct from the salt ordering at lower temperatures, unlike *LA* gellan. Additionally, the L-glycerol groups in *HA* gellan increase the stability of the double helix by forming additional hydrogen bonds within and between the participating strands, but destroy the binding site for metal cations by changing the orientation of the adjacent carboxyl group. This suggests that no cation-mediated aggregation occurs directly with *HA* gellan, but any salt that may be present within the initial *HA* gellan sample composition is likely to be forced to order and aggregate within the gel matrix. This additional salt ordering at 100 % *HA* gellan contributes to the overall high viscosity observed in Figure 4.2, whereby a considerably more aggregated, true gel form exists consisting of a larger number of elastically active network chains and junction zones than the remaining mixed gellan solutions. The small plateau in viscosity observed at 100 % *HA* gellan at the end of the low temperature transition, also suggests that a threshold concentration for the formation of the true *HA* gel has been reached and that prior to this progressive suppression of the electrostatic repulsion between the gellan double helices was taking place.

Alternatively at these low temperatures ($< 7\text{ }^{\circ}\text{C}$) some extended ordering of the *HA* gellan network chains could be occurring, as a result of the water present increasing in density. This would in turn, increase the concentration of the *HA* gellan forcing the network chains closer together until maximum ordering and aggregation is achieved.

4.2.1.3. Viscoelastic material response

Rheological measurements were extended to investigate the viscoelastic material response of the mixed gels to frequency sweeps during a temperature cooling ramp. Stress controlled oscillation measurements were performed at 0.1 Pa from $90 - 10\text{ }^{\circ}\text{C}$ on the same range of samples as the viscometric tests, by performing frequency tables from $0.1 - 10\text{ Hz}$ at $10\text{ }^{\circ}\text{C}$ intervals. Figures 4.3a and b show the resulting elastic and viscous modulus versus temperature for 0.5 wt.%, pH 5 mixed gellan aqueous solutions. The data plotted was taken at 1.06 Hz from the frequency sweeps that were performed within the LVR for gellan (1% strain). Figure 4.3a shows that increasing the proportion of the *HA* variant causes an increase in G' . This increase begins at $70\text{ }^{\circ}\text{C}$ and continues with further cooling, a consequence of the *HA* gellan coil helix transition. This behaviour is not apparent at 0 % *HA* gellan (100 % *LA* gellan), and there is no apparent change in G' due to the *LA* variant, which would show as a change in value at around $25\text{ }^{\circ}\text{C}$. The G'' shown in Figure 4.3b shows a sharp increase beginning at $80\text{ }^{\circ}\text{C}$, increasing in magnitude with increasing *HA* gellan proportion, again corresponding to the *HA* gellan coil-helix transition. In all the gels containing the *LA* variant there is a further, much larger increase in G'' at $30\text{ }^{\circ}\text{C}$ corresponding to the *LA* gellan coil-helix transition. This highlights the different characters of the two variants, the *LA* gellan having an inelastic brittle gel, and the *HA* gellan a more elastic and less stiff behaviour.

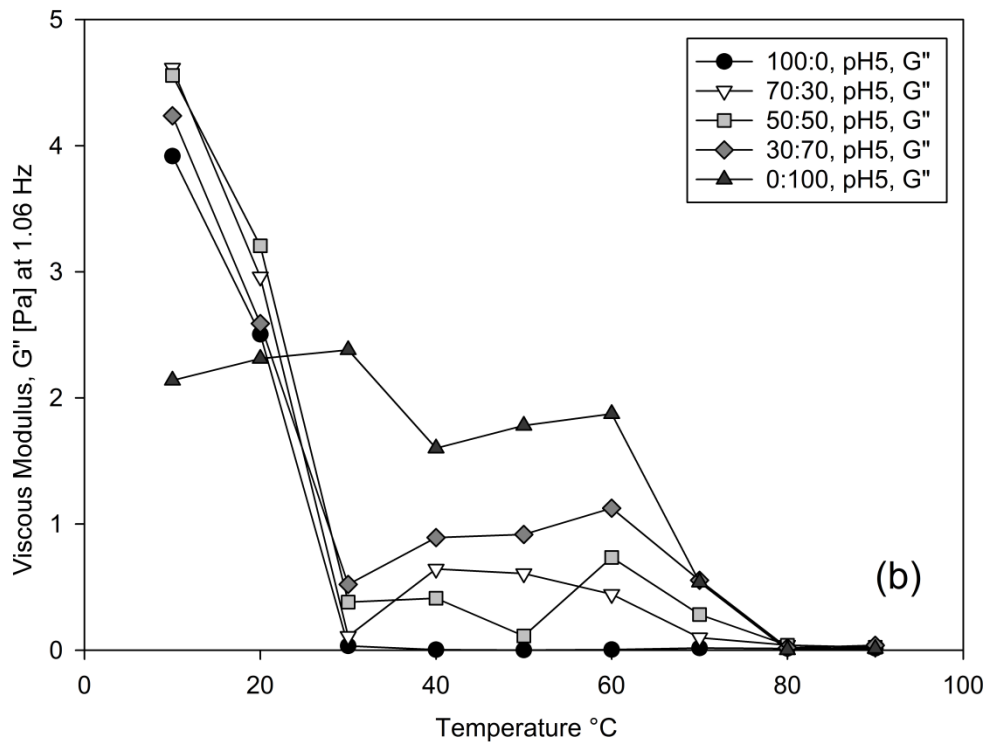
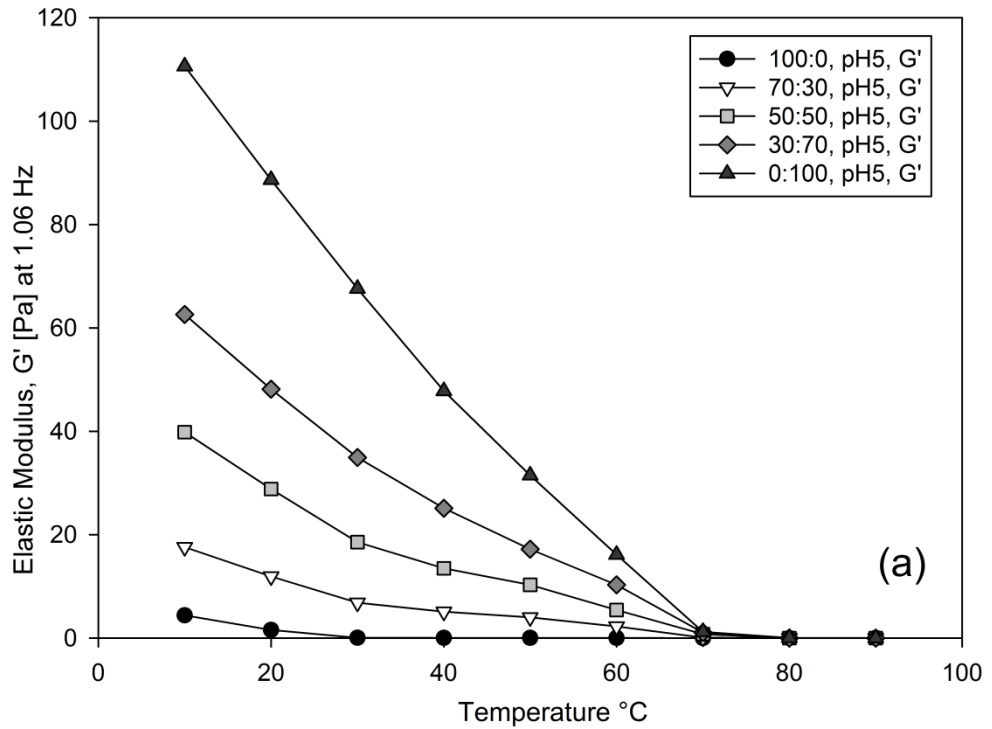


Figure 4.3. Elastic modulus (a) and viscous modulus (b) measurements at 1.06 Hz versus temperature for 0.5 wt.%, pH 5, low acyl gellan aqueous solutions as a function of increasing high acyl gellan proportion (0, 30, 50, 70, and 100 %) during a temperature cooling ramp (90 – 10 $^{\circ}\text{C}$), whilst performing frequency tables from 0.1 – 10 Hz at 10 $^{\circ}\text{C}$ intervals. Each of the modulus readings are based on a single sample measurement.

4.2.1.4. Identification of enthalpic conformational transitions using DSC

DSC was used to identify the enthalpies and maximum heat flow temperatures (T_{\max}) of the coil-helix transitions on both heating and cooling for the mixed gel solutions. The technique is often used to detect the transmutations in a mixed system with the heterotypic interactions usually manifesting themselves by distorting the peaks of the individual gels and generating a new thermal event (Kasapis et al., 1999). Figures 4.4a and b show the cooling and heating, exothermic and endothermic μ -DSC curves for the 0.5 wt.% *LA* gellan gum solutions with 0, 50, and 100 % *HA* gellan, at their natural pH values using a scanning rate of 0.2 °C/min.

The *LA* gellan cooling curve showed a single, sharp, exothermic peak with a T_{\max} of 23.7 °C, and the heating curve (Figure 4.4b) showed a single, sharp, endothermic peak with a T_{\max} of 24.3 °C. These peaks denote the cooperative conformational transition of the *LA* gellan molecule. Each peak also coincides with the *LA* gellan coil-helical transition temperature observed with the viscosity measurements at the same total gellan concentration (Figure 4.2). At 100 % *HA* gellan, the cooling curve (Figure 4.4a) showed a single, broader, exothermic peak with a T_{\max} of 62.6 °C, and the heating curve (Figure 4.4b) showed a single, broader, endothermic peak with a T_{\max} of 64.3 °C. The appearance of broader peaks is a reflection of the gradual development of the *HA* gellan network, and indicates that the transition is less cooperative. No thermal peaks were recorded at around 25 °C for *HA* gellan, which could correspond to the low temperature viscosity transition observed in Figure 4.2. The peaks observed in Figures 4.4a and b can therefore be confidently attributed to the coil-helix transitions of the gellan gum molecules and the subsequent aggregation of these helices.

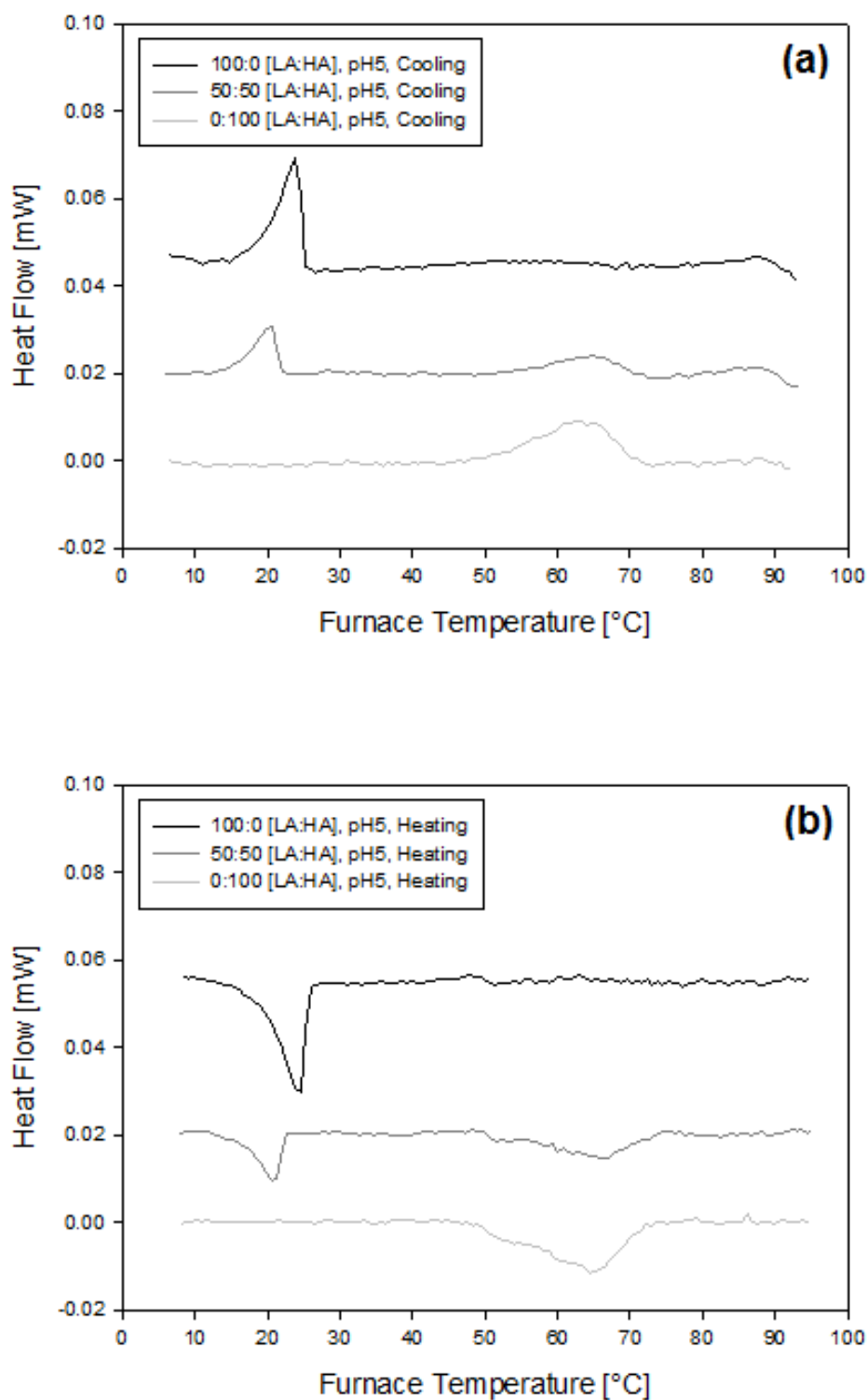


Figure 4.4. μ -DSC exothermic (a) and endothermic (b) peaks (baseline subtracted) for 0.5 wt.% low acyl gellan gum solutions with 0, 50, and 100 % high acyl gellan, at their natural pH. A cooling and heating rate of 0.2 °C/min was implemented. Note that heat flow y-values have been added and subtracted to separate the curves from each other for clarity. Each curve is based on a single sample measurement, due to the lengthy experimental procedure of 15 hours, 40 minutes.

This is generally in agreement of what has previously been reported for gellan gum gels in the presence of small amounts of monovalent cations (Miyoshi et al., 1996b). It is only with added salt to the mixed gellan systems that one would expect to observe bimodal character and splitting of the single μ -DSC endothermic heating peak into multiple peaks, with the single μ -DSC exothermic peak remaining.

At 50 % *HA* gellan, the cooling curve (Figure 4.4a) showed two exothermic peaks with T_{\max} 's of 64.5 °C and 20.3 °C, whilst the heating curve (Figure 4.4b) showed two endothermic peaks with T_{\max} 's of 66.3 °C and 20.9 °C. These two separate transitions occur in the same peak positions as those shown in Figure 4.4 for the individual *LA* and *HA* gellan components; a result which argues that they each gel independently as in isolation. The peak observations are also in agreement with the high and low temperature coil-helical transitions observed for the 50 % *HA* gellan mixed solution in Figure 4.2. Kasapis et al. (1999) and Morris et al. (1996) also reported two separate coil-helix transitions observed by DSC for blends of *HA* and deacylated (*LA*) gellan gum that were coincidental with the peak positions for the individual constituents. Morris et al. (2012) later stated that this was firm evidence that *HA* and deacylated gellan (*LA*) do not form double helices incorporating strands of both types.

A final observation from Figure 4.4 is that for each of the three mixed gellan solutions, the heating curves are essentially equal and opposite to the cooling curves, with no indication of thermal hysteresis. This in turn provides additional support for the two gellan components gelling independently.

Table 4.1 encloses the μ -DSC enthalpy and maximum heat flow temperature (T_{\max}) values on heating and cooling for the *LA* gellan solutions with 0, 50, and 100 % *HA* gellan at pH 5, where ΔH is the amount of heat energy gained or lost by the solutions.

Ratio	& pH	Gelation (LA), ΔH (J/g) [$T_{\max.}$ ($^{\circ}\text{C}$)]	Gelation (HA), ΔH (J/g) [$T_{\max.}$ ($^{\circ}\text{C}$)]	Melting (LA), ΔH (J/g) [$T_{\max.}$ ($^{\circ}\text{C}$)]	Melting (HA), ΔH (J/g) [$T_{\max.}$ ($^{\circ}\text{C}$)]
100:0	100:0				
	Natural pH	-0.0400 [23.7]	-	0.0400 [24.3]	-
	pH 4	-0.0310 [19.5]	-	0.00732 [18.6]	-
	pH 3	*	-	*	-
	pH 2	*	-	*	-
50:50	50:50				
	Natural pH	-0.0160 [20.3]	-0.0200 [64.5]	0.0150 [20.9]	0.0230 [66.3]
	pH 4	-0.0130 [14.4]	-0.0230 [64.8]	0.00316 [38.3]	0.0230 [65.2]
	pH 3	-0.0140 [47.9]		0.00712 [50.0]	
	pH 2	-0.0920 [35.2]		0.00708 [51.6]	
0:100	0:100				
	Natural pH	-	-0.0430 [62.6]	-	0.0400 [64.3]
	pH 4	-	-0.0530 [64.3]	-	0.0520 [65.1]
	pH 3	-	-0.0160 [44.4]	-	0.00538 [45.6]
	pH 2	-	*	-	0.00318 [52.1]

Table 4.1. Table of differential scanning calorimetry measurements (to 3 s.f.) for 0.5 wt.% low acyl gellan aqueous solutions with 0, 50, and 100 % high acyl gellan, for a variety of pH values, where ΔH is the amount of heat energy gained or lost by the solutions. The asterisks (*) in the table indicate where no clear peak detection was observed for the corresponding material components. Each of the ΔH and $T_{\max.}$ values are based on a single sample measurement.

4.2.2. Post-production exposure of gels to an acidic environment

Mixed gellan gels were soaked in 0.5 % (0.137 mol/dm³) HCl acid for varying time periods up to 3 hours. This simulated stomach conditions during digestion and allowed investigation of the effects of prolonged acid exposure on the mechanical properties of the mixed gellan gels after formation at their natural pH. Gastric acid that is secreted in the stomach during digestion is composed of 0.5 % HCl acid, which lowers the pH to the desired pH of 1-3 (Kong, & Singh, 2008). Hence, a concentration of 0.5 % HCl used for the HCl acid soak baths. Soaking periods of up to 3 hours were chosen to mimic the typical human digestion gastric phase duration and average solid food retention time in the stomach of approximately 3 – 4 hours (Versantvoort et al., 2004). Although, residence times as short as 1 and as long as 5 hours have been reported depending on circumstances (Mojaverian et al., 1985).

Figure 4.5 shows that exposing the gels to an acidic environment altered their mechanical properties. Irrespective of the *LA:HA* gellan weight fractions in the mixtures, the total work to fracture the gels increased after 1 hour of exposure to acid. This suggests that the cross-links between the hydrocolloid chains are reinforced by acid exposure. Gels containing higher proportions of *HA* gellan take longer in the acid soak to achieve maximum work to fracture, although the bulk modulus decreases between 1 and 3 hours exposure to acid. The step change in the bulk modulus between 60 and 70 % *HA* gellan, suggests a change in which variant is forming the continuous matrix. The smooth linear increase of moduli between 0 – 60 % *HA* gellan after 1 hour of acid exposure indicates a semi-interpenetrating network structure. The *LA* gellan forms a continuous gel matrix in which, small amounts of the *HA* gellan are dispersed, as opposed to the phase-separated structure seen at natural pH.

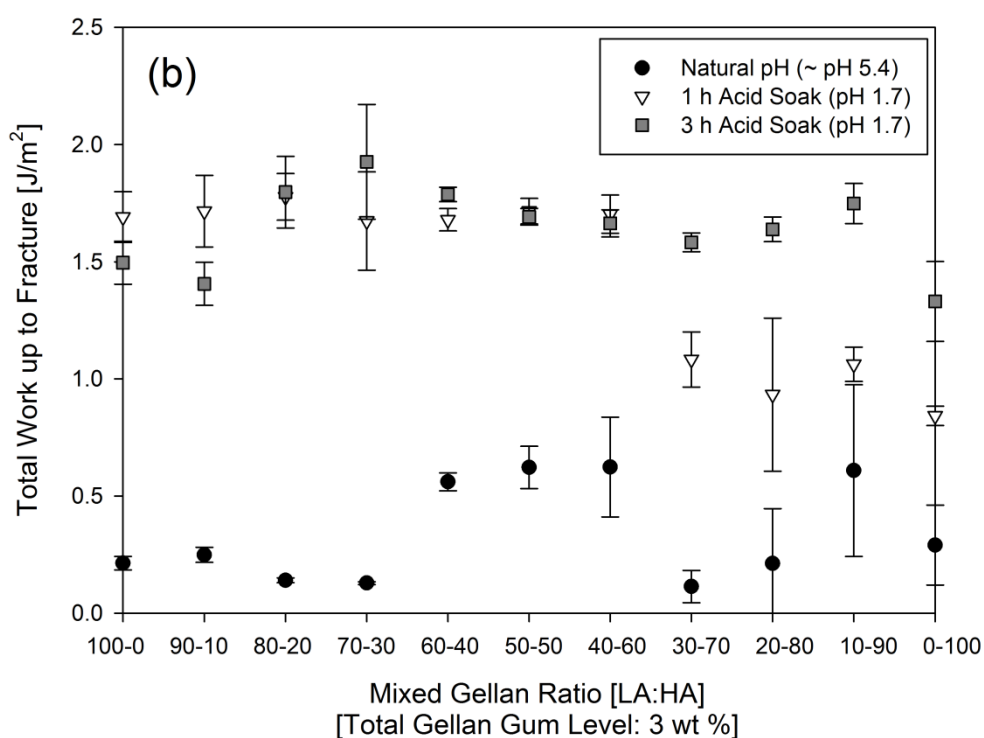
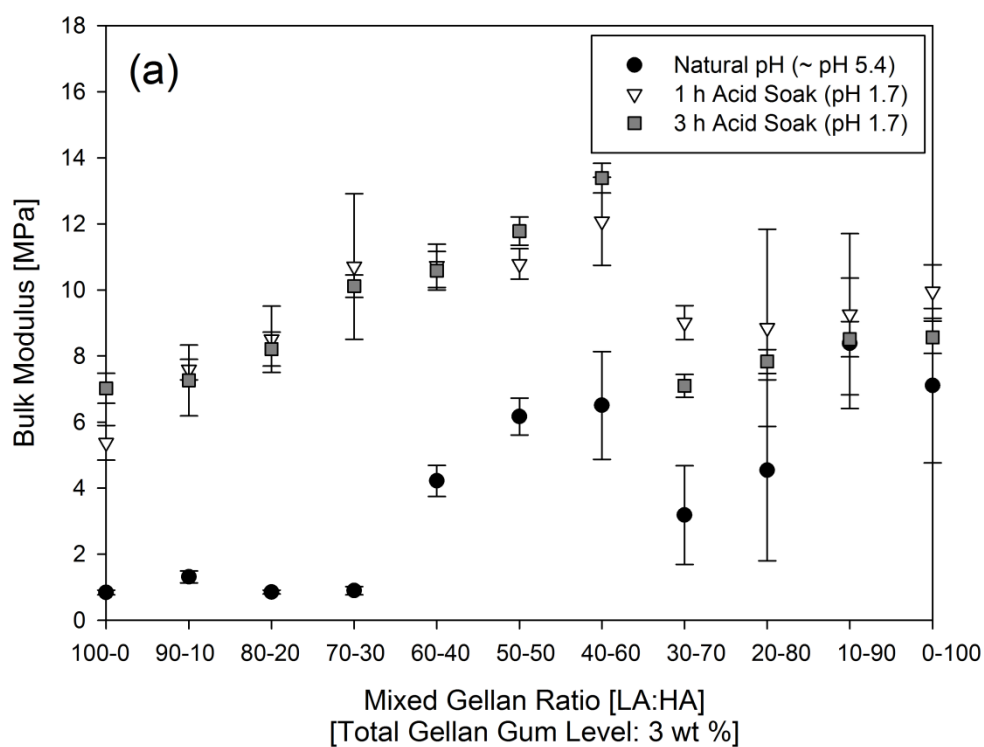


Figure 4.5. The bulk modulus (a) and work up to fracture (b) data for mixed gellan gels after production, and after exposure to acid. All measurements were carried out in triplicate with a compression rate of 1 mm/s. The error bars were determined from the standard deviations of these measurements collectively. Where error bars cannot be observed, they are smaller than the data points.

This once again follows from the observations of Morris et al. (2012) that when there is no indication of discontinuity in properties (as would be expected from phase separation), an interpenetrating network structure is dominant. Above 60 % *HA* gellan, the network formation remains semi-interpenetrating, but the opposite structure is suggested, with discrete *LA* gellan polymers being dispersed in a continuous *HA* gellan matrix as suggested by Mao et al. (2000). With each of these proposed network structures, only the continuous phase gellan polymer chain is cross-linked, with the other remaining linear.

It is widely reported that the *LA* gellan is acid sensitive, whilst the *HA* gellan form is not (Yamamoto & Cunha, 2007; Norton et al., 2011). Thus, it may be questioned why the post-production acid exposure of the mixed gellan is causing the high proportion *HA* gel strength to increase at all. One possible explanation is that the L-glycerol groups in *HA* gellan increase the stability of the double helix by forming additional hydrogen bonds within and between the participating strands, but remove the binding site for metal cations by changing the orientation of the adjacent carboxyl group (Morris et al., 2012). The consequent loss of cation-mediated aggregation reduces gel strength, but makes the *HA* gellan more susceptible to the positively charged protons from the acid, encouraging the formation of additional hydrogen bonds resulting in an overall gel strength increase (Horinaka et al., (2004); Miyoshi et al., (1996); Miyoshi et al., (1998); Nickerson et al., 2003); Tang et al., (1997) Yamamoto & Cunha, (2007)).

Increasing the acid exposure time from 1 hour to 3 hours does not seem to further affect the structure or mechanical properties of the gels that contain a large proportion of *LA* gellan. The gels with a higher proportion of *HA* gellan however, are beginning to show signs of structural weakening after exposure for 3 hours, with the bulk modulus values beginning to fall. This effect is possibly caused by the acyl groups becoming

charged at low pH, and repelling each other. This in turn causes a conformational change in the glycosidic bond between sugars, exposing the oxygen to acid attack and subsequent hydrolysis. This could be confirmed in the future by subjecting the samples (composed of *HA* gellan proportions > 60 %, following varying acid exposure times) to polarimetry tests, to assess their conformational ordering.

The result is promising for the discussed application of these mixed systems in self-structuring foods and their controlled breakdown and release of food nutrients at desired sites in the GI tract.

During food digestion in the stomach, the HCl acid assists with the acid protein denaturation of digested food, provides an optimum pH for the activation of pepsinogens to release the enzyme pepsin, and kills most of the ingested bacteria (Kong, & Singh, 2008). It is the gastric juices secreted from the glands lining the stomach, containing the digestive enzymes (e.g. pepsin) and bile salts that are responsible for the breakdown of solid foods into particles small enough to be emptied into the intestine. Soaking the mixed gels in baths formulated from HCl acid, digestive enzymes and bile salts for similar time periods to those already tested may help to gain a more realistic *in-vitro* perspective of their structural weakening and breakdown mechanisms that are comparable to that *in-vivo*. *In vitro* digestion models need to be developed however, to enable detailed investigations of food disintegration of such systems, as related to the influences of hydrodynamic and mechanical contraction forces that are present *in vivo* (Kong, & Singh, 2008). Studies are also needed to explore the relationships between food texture, microstructure, and chemical properties and the digestion properties such as disintegration rate and gastric emptying rate. Research in these areas should contribute to the development of innovative processing methods for optimal delivery of nutrients in the GI tract (Kong, & Singh, 2008).

4.2.3. Acid exposure during gelation

4.2.3.1. Viscometric material response

Adjusting the acidity of the mixed gellan solutions via direct, dropwise addition of 0.5 wt.% HCl at 80 °C during production, altered the measured viscosity during network formation. Figure 4.6 shows the viscosity measurements of 0.5 wt.%, 70 % *HA* mixed gellan aqueous solutions at varying pH's, over a range of temperatures under a constant shear rate of 0.5s^{-1} . At pH 4 and 5 we observed the two high and low temperature coil-helix transitions of the *HA* gellan gum and *LA* gellan gums respectively, as also presented in Figure 4.2. However, at pH 3 – 2, no structuring was evident across the temperature range. This same trend was also observed with the 0 %, 30 %, 50 % and 100 % *HA* mixed gellan solutions.

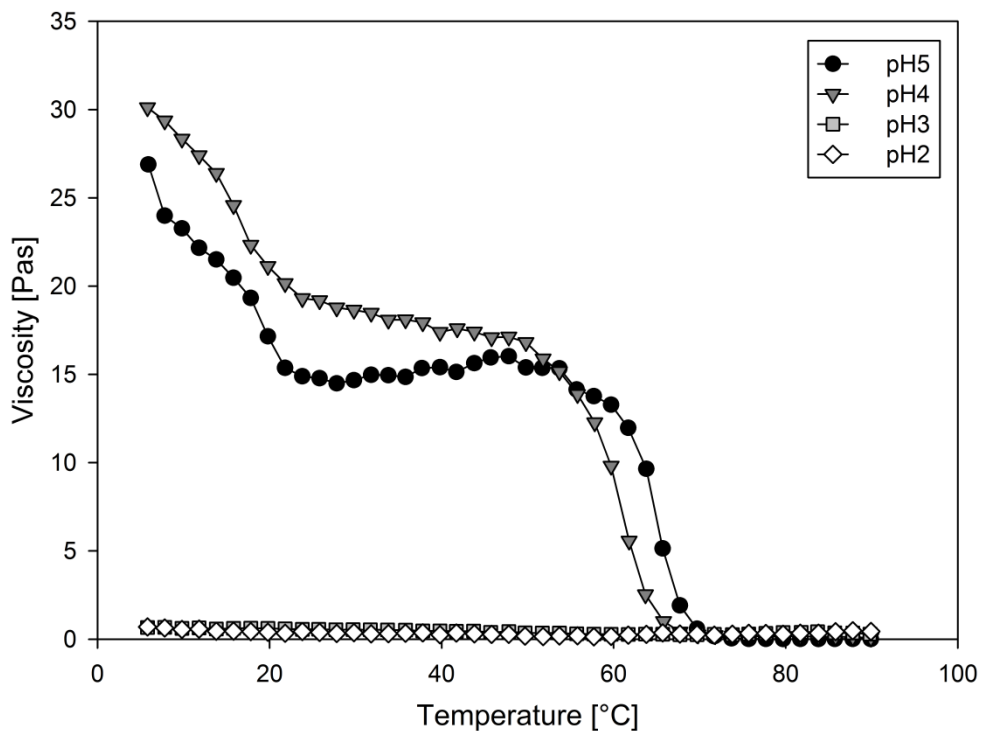


Figure 4.6. Viscosity measurements of 0.5 wt.%, 70 % high acyl mixed gellan aqueous solutions at varying pH values during a temperature cooling ramp (90 – 5 °C) at 2 °C/min, using a constant shear rate of 0.5s^{-1} . Each of the viscosity readings are based on a single sample measurement.

The gelation of gellan can be induced by the reduction in pH, with Grasdalen and Smidsrød (1987) describing HCl as ‘the most potent gel-former’. However, the variation in gel strength with increasing concentration of acid is not monotonic. Initial acidification from neutral pH to pH 3.5 causes a large increase in work to fracture (Picone & Cunha, 2011). Decreasing the pH below the pK_a of the glucuronate residues in gellan at pH 3.4 (Haug, 1964), decreases the work to fracture (Norton et al., 2011). At pH 2 the gels are extremely weak and turbid, and show phase separation of polymer and solvent (Moritaka et al., 1995). Under these low pH conditions, ordering and aggregation between the individual gellan chains occurs immediately upon acidification; “over-structuring”. A weak, sponge-like structure is created, rather than a stronger, homogeneous one. It is likely that gel structuring at pH 2 is disrupted by the shear applied during the acidification process. However, much lower levels of shear-induced disruption would be expected to occur for the mixing conditions found in the stomach. Singh (2007) reported that the shear force on the surface of a food particle (~ 0.00043 N) is insignificant in comparison to the crushing or grinding force of the stomach walls (0.2 N).

A possible explanation for the flat viscosity observed at acidic pH’s in Figure 4.6 is that the shear rate used to measure the viscosity of the mixed gel solutions is subsequently causing the gel to break during its formation or is preventing it from forming. Alternatively fluid gels could be being produced at these low pH values. However, if this was the case we would still observe some increase in viscosity, together with evidence at the higher pH values. The fact that we do not suggests that fluid gels are unlikely to be responsible for the flat viscosity trends observed. A final possibility is that the effects of gelation are being hindered at these low pH values, providing fewer particles (via nucleation and growth) to undergo structural ordering and aggregation.

4.2.3.2. Viscoelastic material response

Adjusting the acidity of the mixed gellan solutions via direct, dropwise addition of 0.5 wt.% HCl at 80 °C during production, also had an impact on the G' and G'' during network formation. Figures 4.7a and b show the G' and G'' versus temperature measurements for 0.5 wt.%, 70 % *HA* mixed gellan aqueous solutions as a function of pH over a range of temperatures at constant stress. Figure 4.7 shows that with lower pH's, the G' and G'' increased on cooling, despite no observed changes in the corresponding viscosity measurements. As was observed with the un-acidified gels, only a single increase in the G' was observed at 70 °C at pH 5, corresponding to the *HA* gellan coil-helical transition, instead of the two transitions present in the viscosity data for the respective pH value. This is attributed to the elastic and non-elastic natures of the *HA* and *LA* gellan gels respectively. Figure 4.7b shows the two distinct regions of increase in the G'' coincidental with the *HA* and *LA* gellan coil-helical transitions for pH 4 and 5 at 75 °C and 30 °C respectively. The *LA* gellan low temperature transition becomes less pronounced as the pH is lowered. At low pH values, no significant rises in the G'' were observed at a specific temperature. A steady increase in the G'' with decreasing temperature was observed in a similar fashion to the G' .

Direct addition of HCl acid to the natural pH mixed gellan aqueous solutions in this way is a fast method of acidification that is novel for biopolymers of this type, where slower and alternative methods using different acids have been investigated. Alginate acidification has been undertaken by slow exposure of alginate to a D-glucono- δ -lactone (GDL) produced acid environment (Draget et al., 2006), where acid gels are produced progressively during a two-hour period. The rate of aggregation using this direct HCl acid addition method is expected to be much higher than the rate achieved by thermally induced gelation.

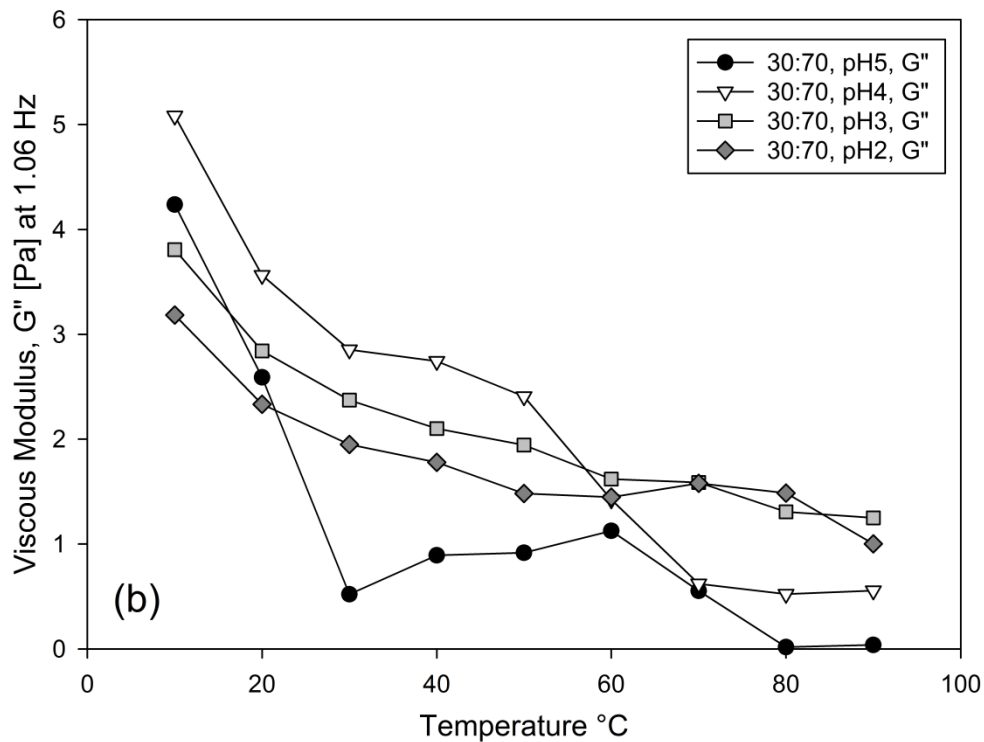
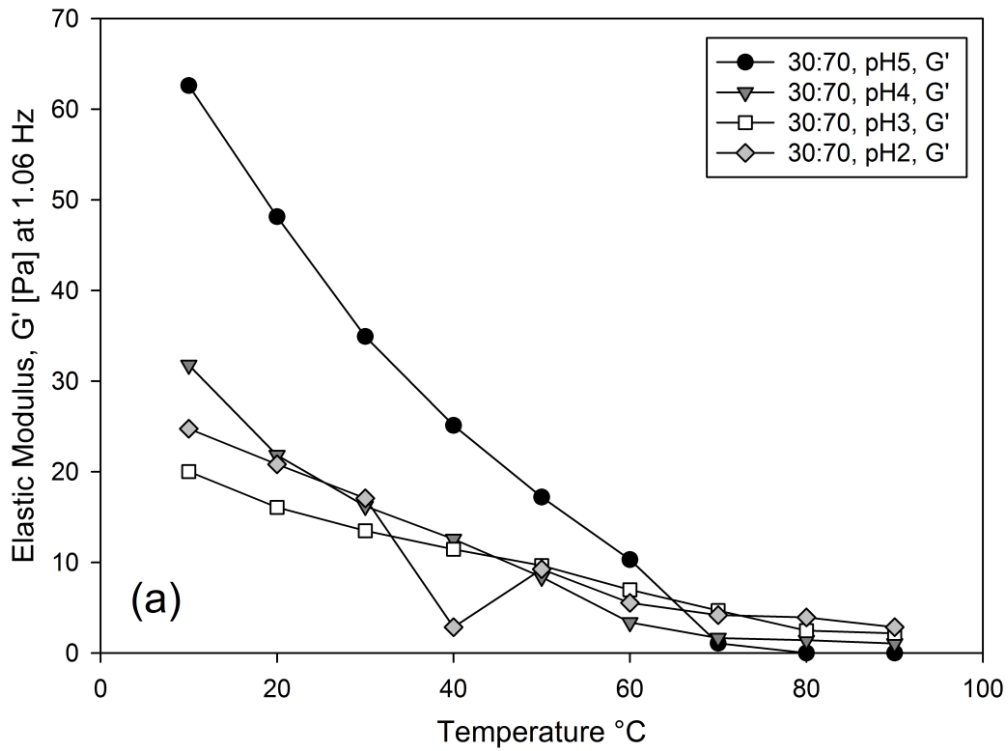


Figure 4.7. Elastic modulus (a) and viscous (b) measurements at 1.06 Hz versus temperature for 0.5 wt.%, 70 % high acyl mixed gellan aqueous solutions as a function of pH (natural – 2) during a temperature cooling ramp (90 – 10 °C), whilst performing frequency tables from 0.1 – 10 Hz at 10 °C intervals. Each of the modulus readings are based on a single sample measurement.

This suggests that the extent of cross-linking between the polymer chains in the case of direct addition of HCl acid becomes lower than when cross-linking occurs in the case of thermally set gels. This results in altered elasticity and strength of the overall mixed gellan acid structure.

For each of the pH's tested, it was the 50 % *HA* mixed gellan solutions that produced the gels with the highest bulk moduli and work to fracture. Similar behaviour has been reported by Mao et al. (2000), who suggest that a strong synergistic interaction may exist between *LA* and *HA* gellan at the 50:50 ratio, where each of the hydrocolloids form continuous networks separately, resulting in strong full-interpenetrating network structures, where both polymers are self cross-linked. It is likely that the biopolymers could be forming a bi-continuous phase separated structure at this ratio instead, with the *HA* and *LA* gellan polymers still forming continuous networks separately. However, the evidence, as discussed in Section 4.2.1.1. suggests otherwise.

4.2.3.3. Identification of enthalpic conformational transitions using DSC with decreasing pH

Adjusting the acidity of the 0.5 wt.% mixed gellan gels via direct, dropwise addition of 0.5 % HCl acid to the natural pH mixed gellan aqueous solutions during production, had a notable effect on the subsequent thermal transitions observed in the cooling and heating μ -DSC curves. Figures 4.8a, c, e and b, d, f show the cooling and heating, exothermic and endothermic μ -DSC curves respectively, for the 0.5 wt.% *LA* gellan gum solutions with 0, 50, and 100 % *HA* gellan, as a function of pH (4 – 2) using a scanning rate of 0.2 °C/min. Table 4.1 encloses the corresponding μ -DSC enthalpy (ΔH) and maximum heat flow temperature (T_{\max}) measurements for these gellan aqueous solutions.

The addition of 0.5 % HCl acid to the gellan aqueous solutions during production disrupts the subsequent gellan network structure formation by protonating the exposed negatively charged carboxylate groups and in turn converting them to the uncharged COOH form. The network structure overall becomes less charged, and electrostatic repulsions between the negatively charged carboxylate groups are minimised by the protonation. This allows aggregation of the double helices to proceed, which was previously hindered due to the electrostatic repulsions. Excessive aggregation is gradually promoted with the subsequent addition of increasing protons from the HCl acid, which eventually leads to the collapse of the gel structure and, ultimately, precipitation of the polymer.

Reducing the acidity of the 0 % *HA* (100 % *LA*) gellan aqueous solution from its natural pH of 5.4 to pH 4, caused the subsequent *LA* gellan exothermic and endothermic peaks to shift to lower temperatures with T_{\max} 's of 19.5°C and 18.6 °C respectively (Table 4.1, Figures 4.8a and b). A reduction in the amount of heat energy lost and gained at this pH level was also observed. At pH values below pH 4, no gelation or melting peaks were observed for the 0 % *HA* (100 % *LA*) gellan aqueous solution at 0.5 wt.% within the tested temperature range of 95 – 5 °C. The 0 % *HA* gellan (100 % *LA*), pH 3 aqueous solution was re-tested using an increased hydrocolloid concentration of 2 wt.% under identical conditions, to see if any thermal peaks were detectable. A clear *LA* gellan gelation peak (plotted in Figure 4.8a) was observed ($\Delta H = - 0.0240$ J/g; $T_{\max} = 21.2$ °C), but again an equal and corresponding melting peak failed to be observed. This suggests that the appearance of thermal transitions for the 0 % *HA* (100 % *LA*) gellan aqueous solution at reduced pH levels, is dependent on the hydrocolloid concentration. The absence of clear melting peaks in the 0 % *HA* (100 % *LA*) gellan aqueous solution

heating μ DSC curves however, suggests that the gels have become more heat resistant at these reduced pH values, after having already formed firm gels on cooling to below the setting temperature. It is possible that at a very high concentration of protons (from the addition of acid to the gellan solution) this may cause the endothermic and exothermic conformational transitions of the *LA* gellan, to shift to temperatures higher than 100 °C. It has been reported that hydrogen bond junction zones can be unzipped on heating to 120 °C (Miyoshi et al., 1996a). To test this theory, one would need to repeat the corresponding μ DSC measurements at an increased temperature range than the one currently implemented.

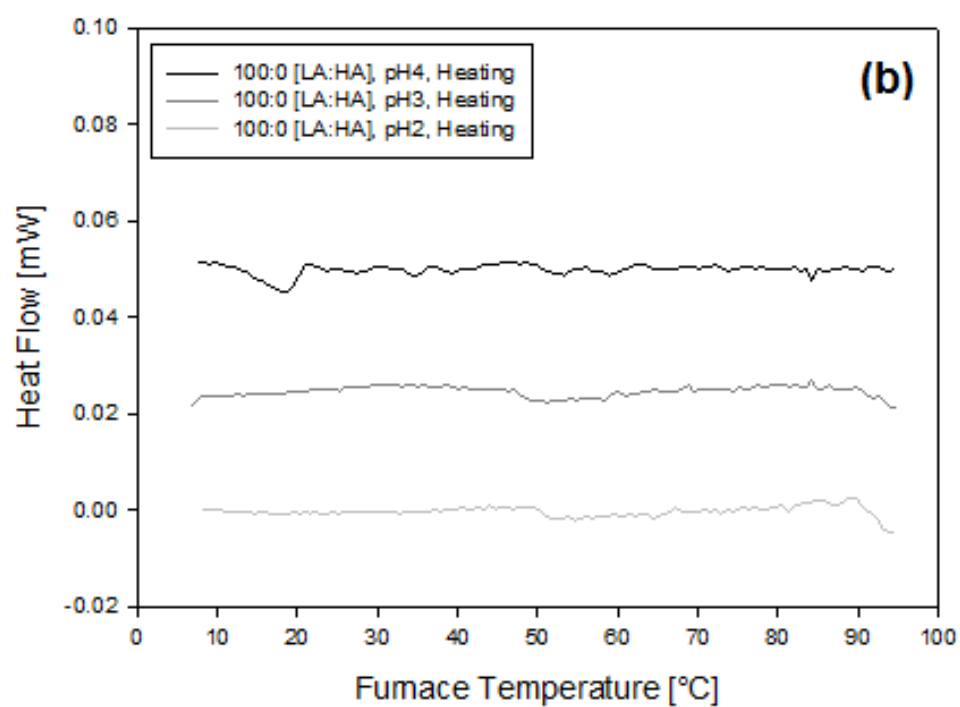
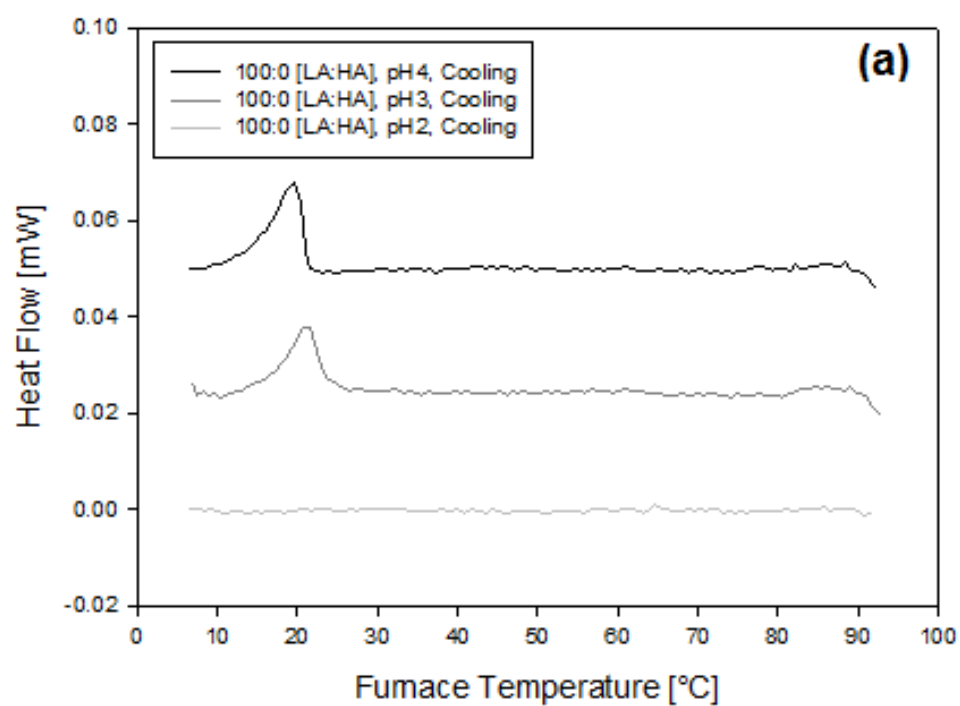
Reducing the acidity of the 50 % *HA* mixed gellan gel solution from its natural pH of 5.4 to pH 4, also caused the subsequent *LA* gellan exothermic and endothermic peaks to shift temperatures with T_{\max} 's of 14.4 °C and 38.3 °C respectively (Table 4.1, Figures 4.8c and d). As with the 0 % *HA* (100 % *LA*) gellan gels, a reduction in the amount of heat energy lost and gained was also observed. The latter 50 % *HA* mixed gellan aqueous solution, *LA* melting peak is believed to be an anomalous result, since it differs so much to that of the corresponding gelation peak; and because the exothermic and endothermic peaks corresponding to the *HA* gellan shifted very little on reduction of pH (T_{\max} of 64.8 °C and 65. 2 °C respectively). Further reduction of the acidity to pH 3 leads to the appearance of a single gelation, and a single melting peak with T_{\max} 's of 47.9 °C and 50.0 °C respectively. The same trend was also observed at pH 2 with a single gelation peak with T_{\max} of 35.2 °C and a single melting peak with T_{\max} of 51.6 °C. The latter gelation peak for pH 2 shifted to a significantly lower temperature than that reported for pH 3, which suggests that this is also likely to be an anomalous result. Particularly since, splitting of the peak is observed (Figure 4.8c). Repeating this

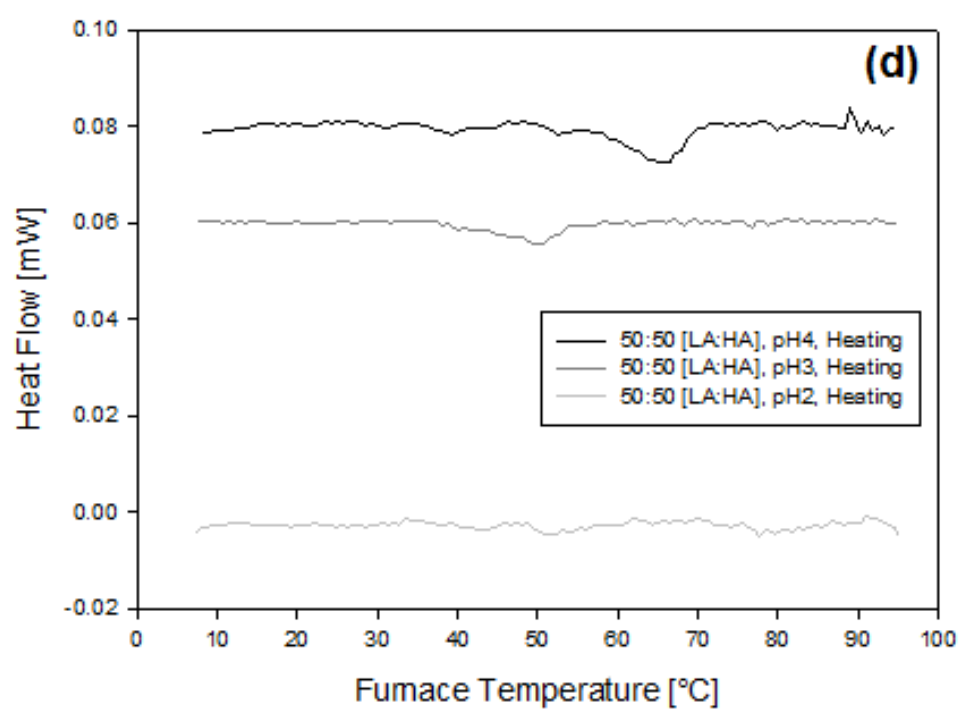
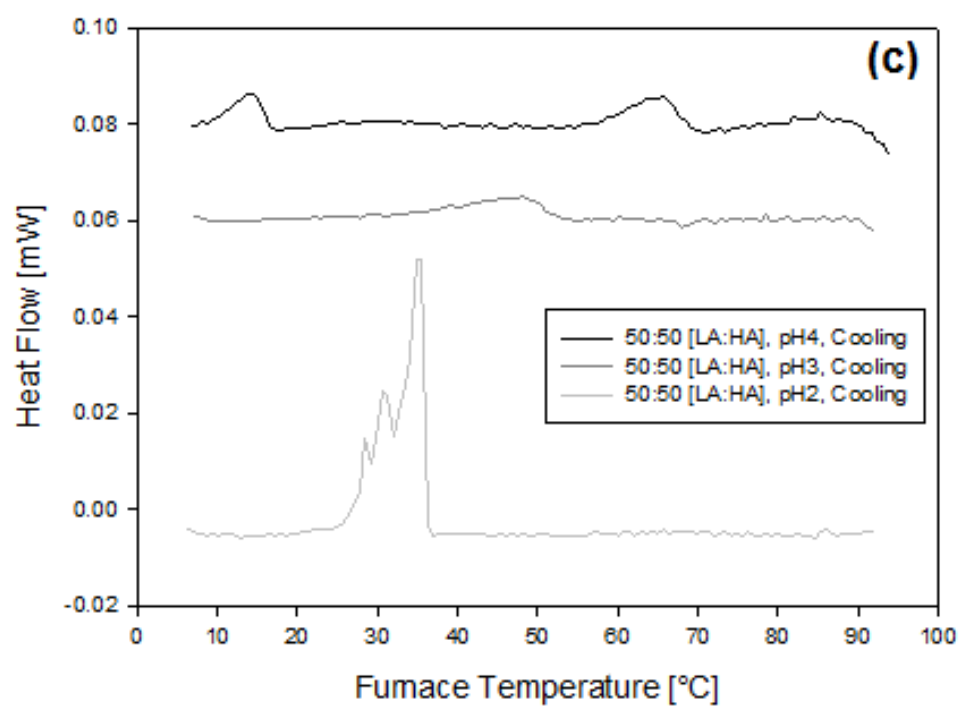
measurement would identify more representative thermal behaviour. Despite this result, the appearance of these single gelation and melting peaks for this specific mixed gellan composition suggests that they are a result of the merging of the two gellan variants to form an intermediate temperature transition. This is supportive of the mixed gellan network structure hypothesis for the 50 % *HA* mixed gellan gel at reduced pH values. The observation implies that the *HA* and *LA* gellan form helices that incorporate strands of both types at pH values lower than pH 4. However, this is contradictory to that reported for 1 wt.% *LA* gellan gels at reduced pH values by Moritaka et al. (1995), who observed no peaks during DSC cooling and heating curves at pH 2, and peak shifts to lower temperatures together with decreasing enthalpy values with decreasing pH (pH 6 - 4). The latter two observations were attributed (Moritaka et al., 1995) to the acid hydrolysis of the *LA* gellan gum molecules at lower pH values (via the acid disintegration of the gellan gum junction zones) during the DSC measurements.

This results implies for the 50 % *HA* mixed gellan gel at reduced pH values in Figures 4.8c – d that rather the single peaks observed at pH 3 - 2 being a result of the merging of the two gellan variants to form an intermediate temperature transition, extensive acid hydrolysis of the *LA* gellan molecule takes place causing the peak signals to be lost. This then leaves only the *HA* gellan molecule peak signal to be detected at these reduced pH values (with shifts in its position to lower temperatures compared to the higher pH values), whose junction zones are more stable at reduced pH levels (Moritaka et al., 1995) and whose structure is known (Yamamoto & Cunha, 2007; Norton et al., 2011) to be less acid sensitive.

Reducing the acidity of the 100 % *HA* gellan gel solution from its natural pH of 5.4 to pH 4, caused the corresponding *HA* gellan exothermic and endothermic peaks to shift

temperatures slightly with T_{\max} 's of 64.3 °C and 65.1 °C respectively, with an increase (\sim \pm 0.01 J/g) in the amount of heat energy lost and gained (Table 4.1, Figures 4.8e and f). Further reduction of the acidity to pH 3 results in a reduction in the T_{\max} for both the gelation and melting peaks observed at pH natural – pH 4 by approximately 20 °C, in addition to a reduction in the amount of heat energy lost and gained. At pH 2, only a single melting peak corresponding to the *HA* gellan polymer is observed, but it is recorded at a higher temperature with T_{\max} of 52.1 °C. This temperature however, is at an intermediate value to the temperature reported for the corresponding melting peak at pH values 4 and 3 suggesting that at pH 2, the high concentration of acid has disrupted the *HA* gellan network formation, and/or it has caused the gelation peak to shift to a temperature higher than 100 °C. Repeating this μ DSC measurement at an increased temperature range than the one currently implemented, would indeed test which explanation is likely to be correct.





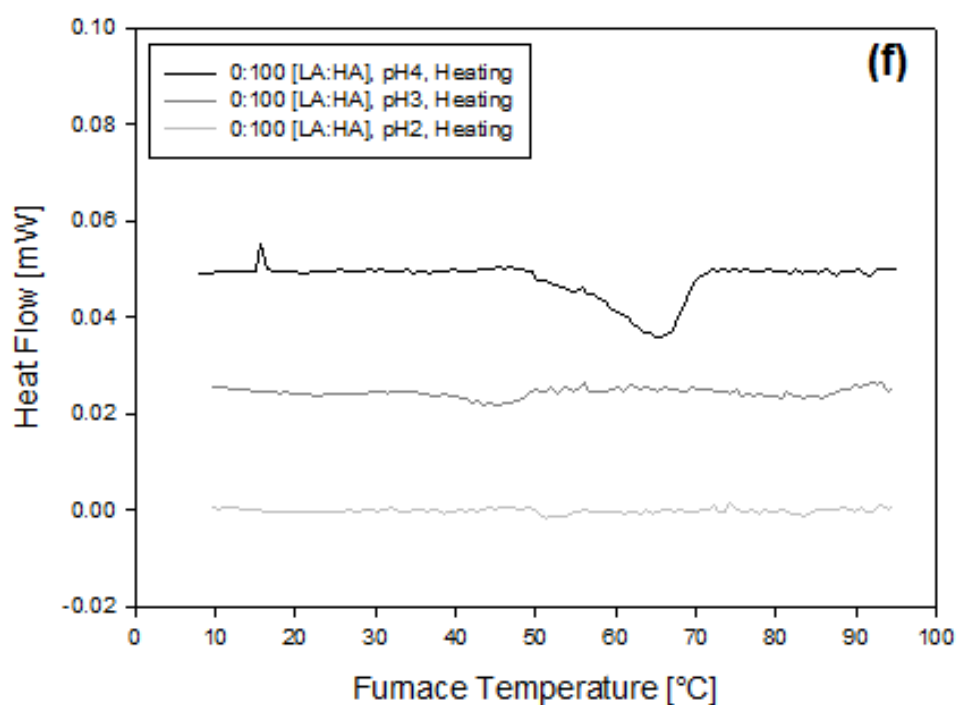
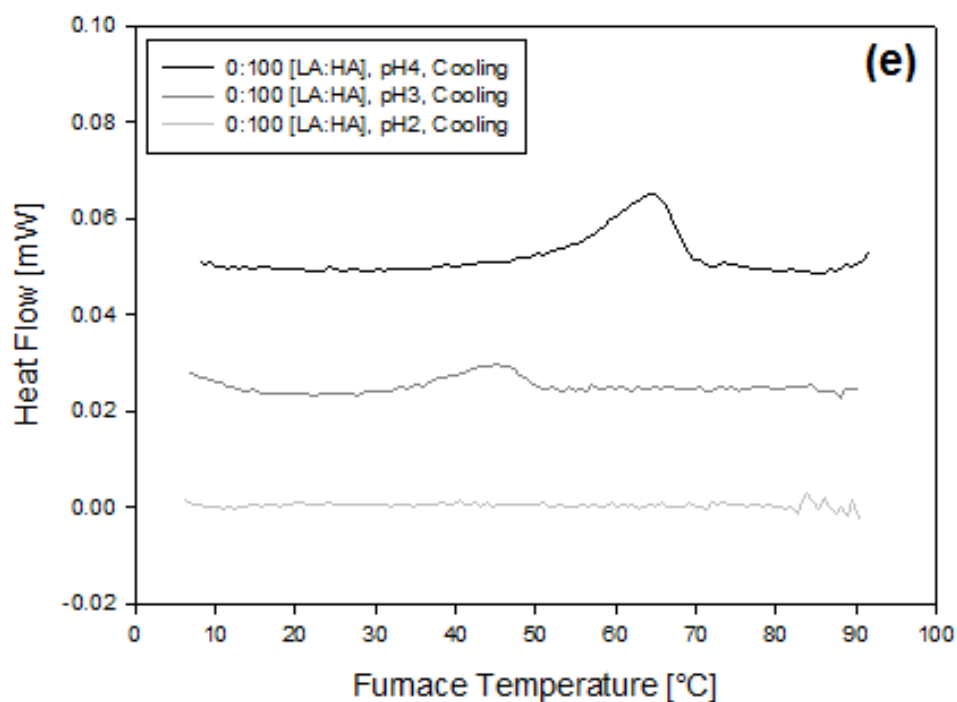


Figure 4.8. μ -DSC exothermic (a, c, e) and endothermic (b, d, f) peaks (baseline subtracted) for 0.5 wt.% low acyl gellan gum solutions with 0, 50, and 100 % high acyl gellan, as a function of pH (4 – 2). A cooling and heating rate of 0.2 °C/min was implemented. Note that heat flow y-values have been added and subtracted to separate the curves from each other for clarity. Further, the 100:0 (LA:HA), pH 3 cooling curve in Figure 4.8a is representative of a 2 wt.% concentrated sample. Each curve is based on a single sample measurement, due to the lengthy experimental procedure of 15 hours, 40 minutes.

4.2.4. Effect of biopolymer concentration

4.2.4.1. Gel structure

Addition of acid to the mixed gellan solutions during production has a significant influence on their resulting rheological properties. Figure 4.9 shows the true stress/strain curves for the 50 % *HA* mixed gellan gels at pH 4, as a function of increasing gellan concentration (1 – 2 wt.%) and the bulk modulus and work of fracture values calculated from this data are plotted in Figure 4.10.

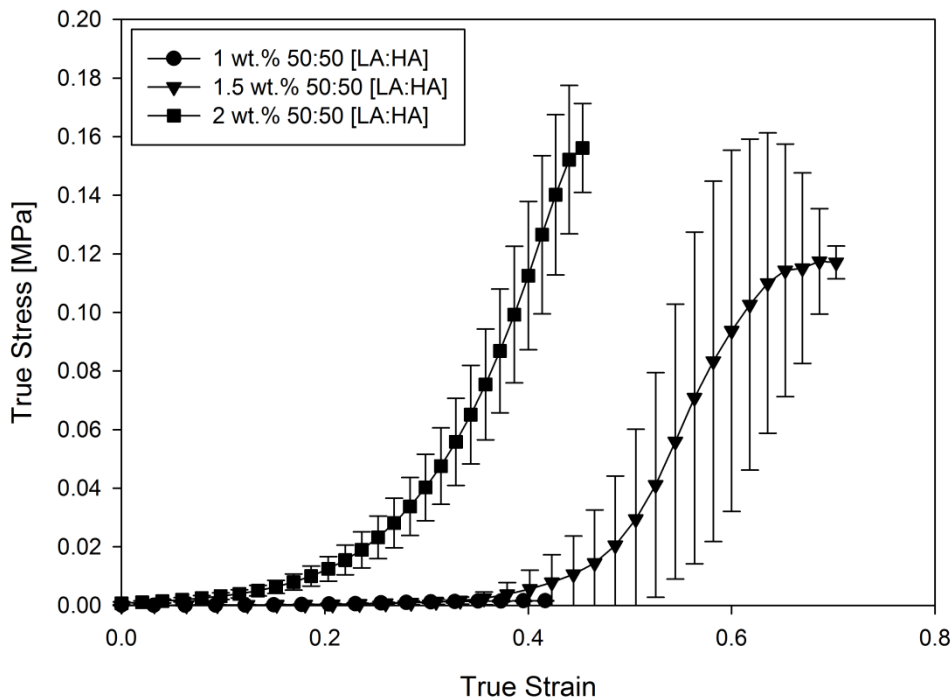


Figure 4.9. True stress/true strain curves for the 50 % high acyl mixed gellan gels at pH 4, as a function of increasing gellan concentration (1 to 2 wt.%). All measurements were carried out in triplicate with a compression rate of 1 mm/s. The error bars were determined from the standard deviations of these measurements collectively. Where error bars cannot be observed, they are smaller than the data points.

The bulk moduli and work to fracture both increase as the concentration of the gellan in the mixed acid gels is increased. Each of the mixed gel samples displayed purely brittle fracture behaviour, with a rapid decrease in the applied stress once the gels fail at

strains typically between 0.4 and 0.45, where a clear fracture point is observed. This behaviour is observed for the gellan concentrations 1 and 2 wt.% in Figure 4.9, however a shifted failure strain is visible for the 1.5 wt.% gellan concentration. Shift in strain values are generally indicative of an increase in gel brittleness (strain at break).

Both Figure 4.9 and Figure 4.10 display concentration dependence, that with increasing biopolymer concentration, firmer gels are produced as a result of the increased interactions occurring between the hydrocolloid chains. The error bars for all measurements until failure are relatively small, which further supports the fact that the performed compression tests give a genuine representation of the behaviour of these systems. Error bars on the data recorded after the structures have failed are larger due to the random nature of fracture propagation through the gel matrix.

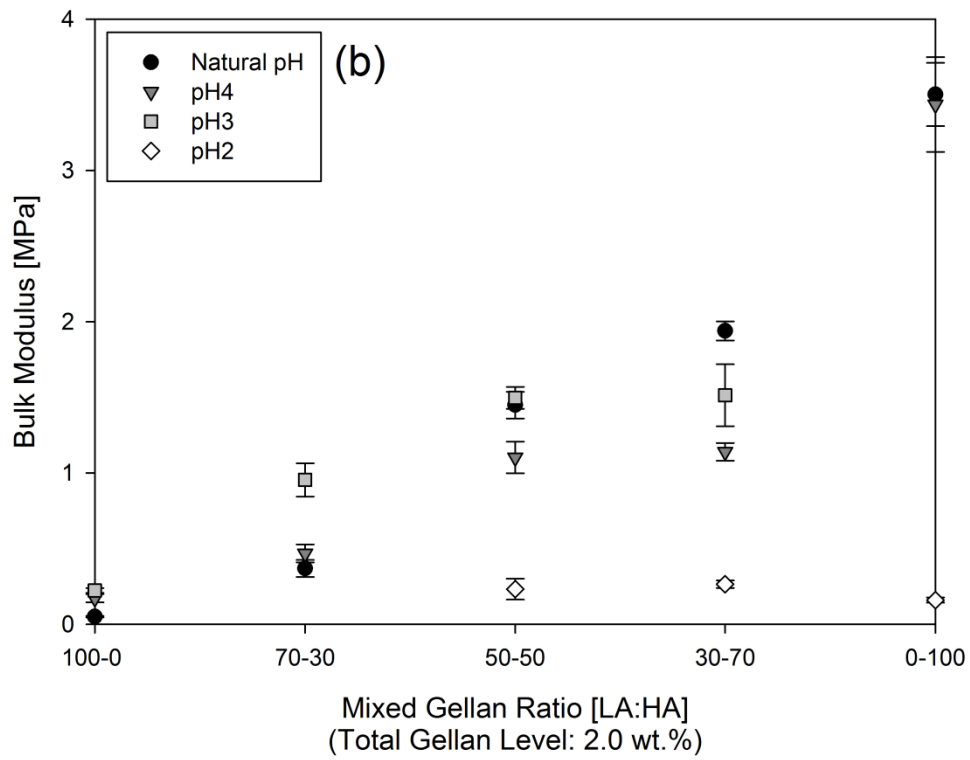
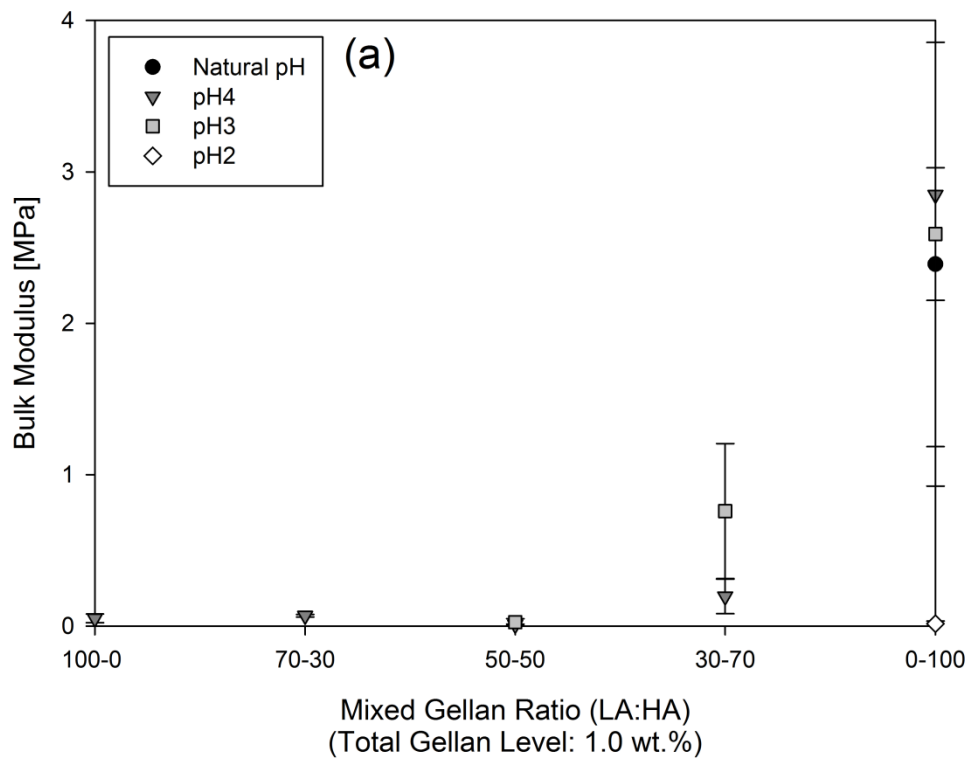
Increasing the total biopolymer concentration normally increases gel firmness; increasing the absolute amount of *HA* gellan in the mixed gels also has a significant impact on the corresponding gel firmness. Figure 4.10 shows the data for the 1 wt.% and 2 wt.% mixed gellan acid gels, indicating that the proportion of each hydrocolloid is more influential over the mechanical properties than total biopolymer concentration. Irrespective of the total biopolymer concentration, the gels with higher *HA* proportions retain their mechanical properties better at low pH. The gels show an increase in bulk modulus as more of the *HA* gellan is added and the mixed gellan acid gels become more turbid as the proportion of *HA* gellan is increased, demonstrating the presence of highly aggregated structures

Figure 4.10 shows that adjusting the acidity of the 1 wt.% and 2 wt.% mixed acid gels during their production has an influence on the resulting gel properties. The natural pH of the gellan solutions was measured at 5.4 and this was not dependent upon the gellan

concentrations used. Mixed acid gels with pH's 3 – 4 were more resistant to fracture than those at pH 2. Although some overlap was observed between the natural pH, pH 4, and pH 3 calculations for the 1 wt.% mixed gellan gels, presumably due to the greater difficulty in molecular ordering within their weak gel environments. This demonstrates that the gels become more resistant to deformation as a result of greater numbers of cross-links between the hydrocolloid chains promoted at the lower pH conditions.

Control of the physical properties of mixed gellan acid gels can be implemented by changing their biopolymer concentration and proportion of *HA* and *LA* types, but it is this *LA:HA* ratio that is the most influential.

A final study was performed on these mixed gellan acid gel samples to investigate the influence of storage temperature on their material properties. 1 and 2 wt.% mixed gellan acid gels with varying pH (natural – pH 2) were formulated and stored at 5 °C and at room temperature for 24 hours, before being subjected to compression tests. Textural analysis revealed very little difference in the textural properties between the two temperatures, indicating that the gel storage temperature did not affect their gel network structure significantly. Before, the mixed gel samples can be used as satiety increasing agents in formulation of foods, however, this would need to be further investigated, along with the effects of excess water and how acidification changes their water holding capacity.



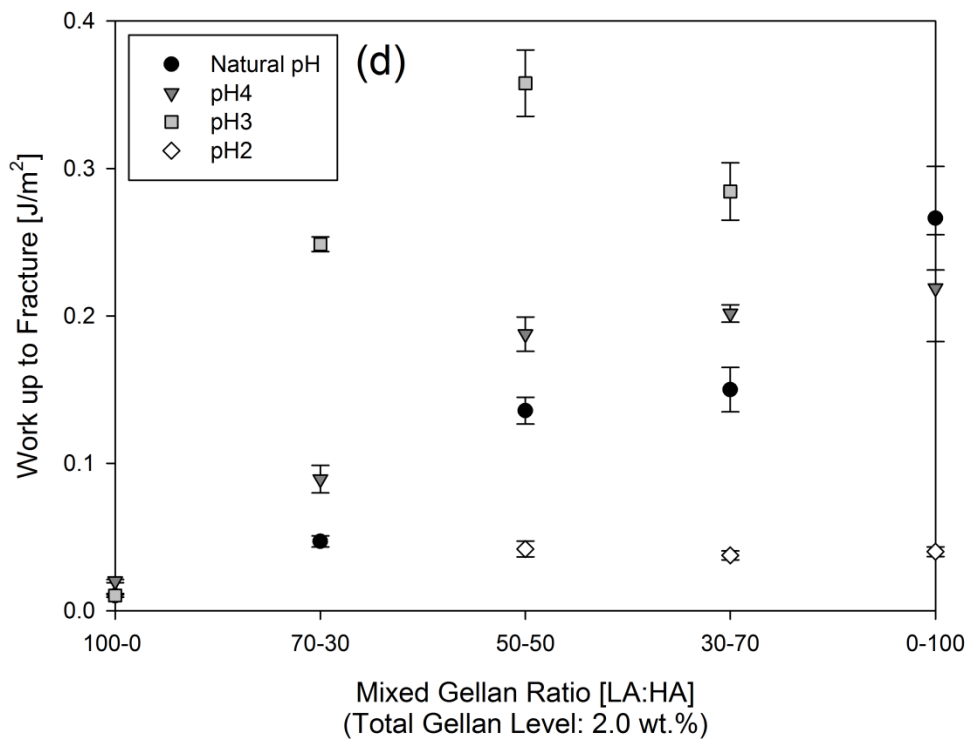
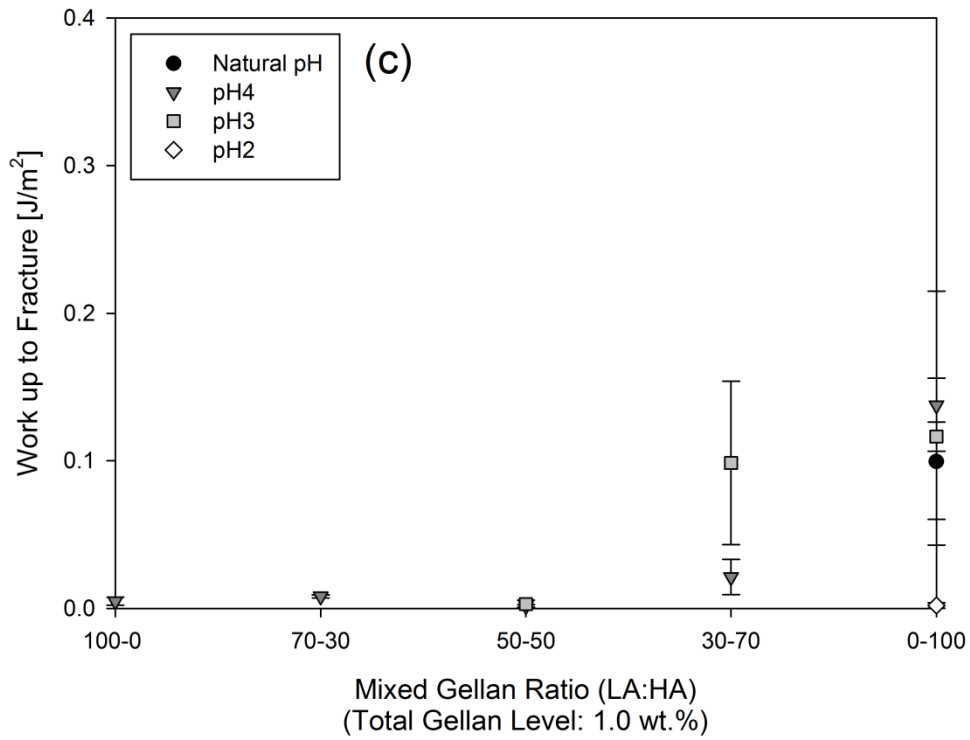


Figure 4.10. Bulk modulus (a – b) and work up to fracture (c – d) for the mixed gellan gels, as a function of pH at gellan concentrations 1 wt.% and 2 wt.% respectively, each stored at 5 °C. Note, where data plots are missing, the gels formed were not strong enough to be tested. All measurements were carried out in triplicate with a compression rate of 1 mm/s. The error bars were determined from the standard deviations of these measurements collectively. Where error bars cannot be observed, they are smaller than the data points.

4.2.4.2. *Enthalpic ordering of gellan gum*

Molecular ordering events were investigated as a function of temperature using polarimetry. The optical rotation of ultraviolet light has previously been demonstrated to show temperature dependence in accordance with the conformational disorder-to-order transition of *LA* gellan gum, regardless of its macromolecular consequence (Kasapis et al., 1999). Figure 4.11a shows the variation of optical rotation (365 nm) with temperature for *LA* gellan (0.025 wt.%) on cooling (two runs) and heating, using a scan rate of 2 °C/min. At high temperatures a linear entropic effect on the optical activity of the disordered gellan chains is observed. However, when measurements are extended to below 7.5 °C a sharp decrease is observed in the optical activity, which should correspond to the enthalpic ordering of the gellan molecule. The ordering temperature is significantly lower than that expected, based on the previous rheological and calorimetry temperature transitions observed within this chapter. Subsequent heating follows back the cooling profile albeit with a temperature lag, due to the additional energetic requirement of melting the aggregated structures. The thermal hysteresis persists at the top of the temperature range thus rendering part of the gellan network thermally irreversible, in agreement with the rheological T_{melt} in Figure 4.3a. A second cooling run confirms that the gellan structure cannot reform after melting. This suggests that rather than the individual double helices breaking during melting, the majority of the structure in fact, remains intact, and it is the inter-helical hydrogen bonds adjoining the double helical aggregates that are broken instead. These results were not expected, after having gained a perspective of the associated gellan molecule enthalpic ordering from Kasapis et al. (1999). They found that when measurements are extended to below 43 °C for a gellan sample with 100 mN added NaCl, a sigmoidal trace is recorded which corresponds to the enthalpic ordering of the gellan molecule. We would have expected to observe this same

sigmoidal trace, but at a lower temperature in the range of 20 – 30 °C in the absence of added salt. Several attempts using a variety of gellan concentrations (from the range 0.025 – 0.5 wt.%) and cooling and heating sequences were made to achieve this trace. The best obtained result was observed for 0.025 wt.% *LA* gellan as depicted in Figure 4.11a. A possible explanation as to why we could not reproduce the same sigmoidal trace for the *LA* gellan molecule is the difference in jacketed quartz cell length used. Kasapis et al. (1999) used a cell of pathlength 1 cm, whereas we used one that had a larger pathlength of 5 cm. Generally, optical rotation is directly proportional to path length; the longer the tube, the greater the overall accuracy. It is therefore desirable to use the longest tube possible. However, exceptions are made with darker samples or those prone to turbidity, for example gellan gum. In these cases, a shorter tube will allow sufficient light through to make a measurement. Transmission decreases logarithmically with path length and optical rotation directly, thus halving the path length will give much more light while reducing the accuracy by only 50 %.

Figure 4.11b shows the variation of optical rotation (365 nm) with temperature for *HA* gellan (0.025 wt.%) on cooling (two runs) and heating, using a scan rate of 2 °C/min. At high temperatures a very slight linear entropic effect on the optical activity of the disordered gellan chains is observed, but this is significantly less pronounced than that observed for the *LA* gellan sample. When measurements are extended to below 11 °C, a sharp decrease (sharper than that observed for the *LA* gellan) is observed in the optical activity. As for the *LA* gellan, subsequent heating follows back the cooling profile albeit with a temperature lag, due to the additional energetic requirement of melting the aggregated structures. The thermal hysteresis persists at the top of the temperature range, thus rendering part of the gellan network thermally irreversible. A second cooling run also confirms that the gellan structure cannot reform after melting.

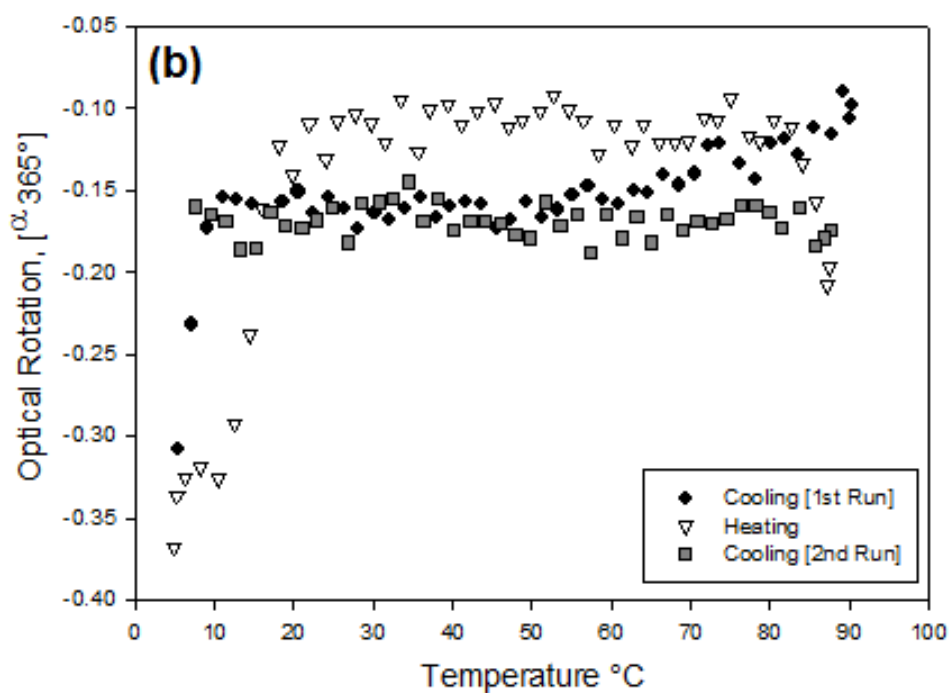
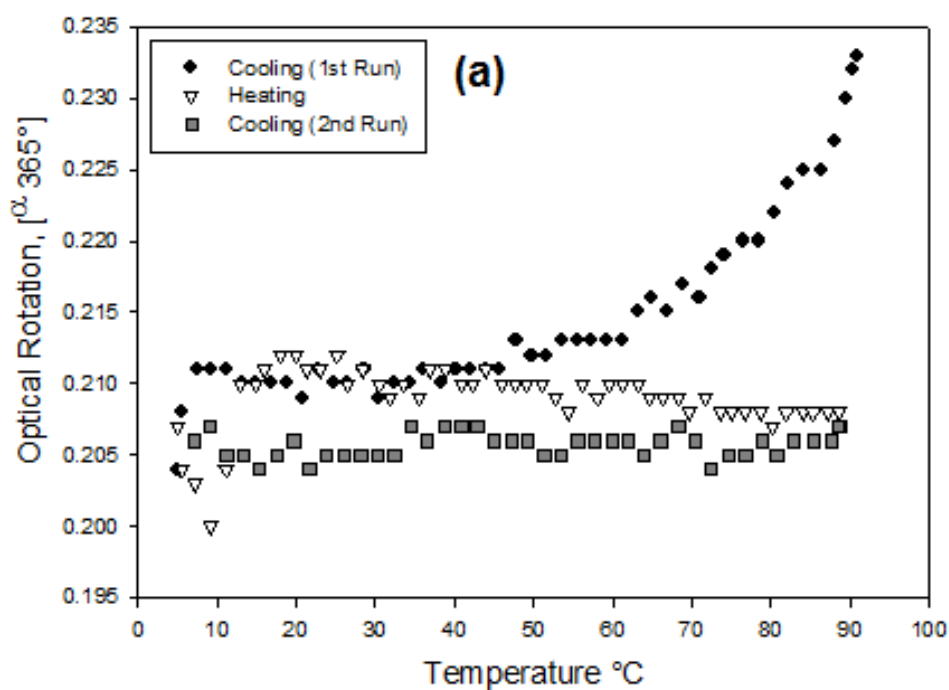


Figure 4.11. Variation of optical rotation (365 nm) with temperature for 0.025 wt.% low acyl gellan gum solutions with 0 (a), and 100 (b) % high acyl gellan on cooling (two runs) and heating in double distilled water, using a scan rate of 2 °C/min.

It was proposed that the sharp decreases in optical activity observed in Figures 4.11a and 4.11b for the *LA* and *HA* gellan at 7.5 °C and 11 °C respectively could be the result of the formation of ice from the water present in the gellan aqueous solutions. However, Figure 4.12 clearly shows that the enthalpic ordering of double distilled water at ~ 5 °C occurs in the small optical rotation range of - 0.030 - - 0.010, which is out of range for the two transitions observed in Figures 4.11a and 4.11b. Incidentally, water is one of the common solvents that is not optically active and so when solutions are prepared, it is the dissolved optically active chemical that causes the rotation, not the solvent.

Errors with the polarimeter equipment were also ruled out by measuring the optical activity of a known optically active material: gelatin. Figure 4.13 shows the variation of optical rotation (578 nm) with temperature for a 5 wt.% gelatin aqueous solution on cooling and heating. The expected sigmoidal enthalpic ordering trace is observed. This leads one to conclude that the reason for comparable results not being obtained for the *LA* and *HA* gellan aqueous solutions is due to their higher level of opacity at much lower concentrations. Performing the measurements at lower concentrations than those tested in this work, using a shorter cell pathlength (e.g. 1 cm) should yield the desired result.

The optical rotation profiles for the mixed gellan samples containing the two variants display very different results, with a constant level of optical activity at high temperatures being seen up until 15 °C, where a sharp drop in optical activity then proceeds. Subsequent heating once again follows back the cooling profiles in these mixed systems, with the temperature lag remaining. This is in agreement with the behaviour reported for *HA* gellan gels by Morris et al., (1996), who observed no detectable thermal hysteresis in the conformational transitions that accompany the formation and melting of the gels, either in water or in 100 ml NaCl.

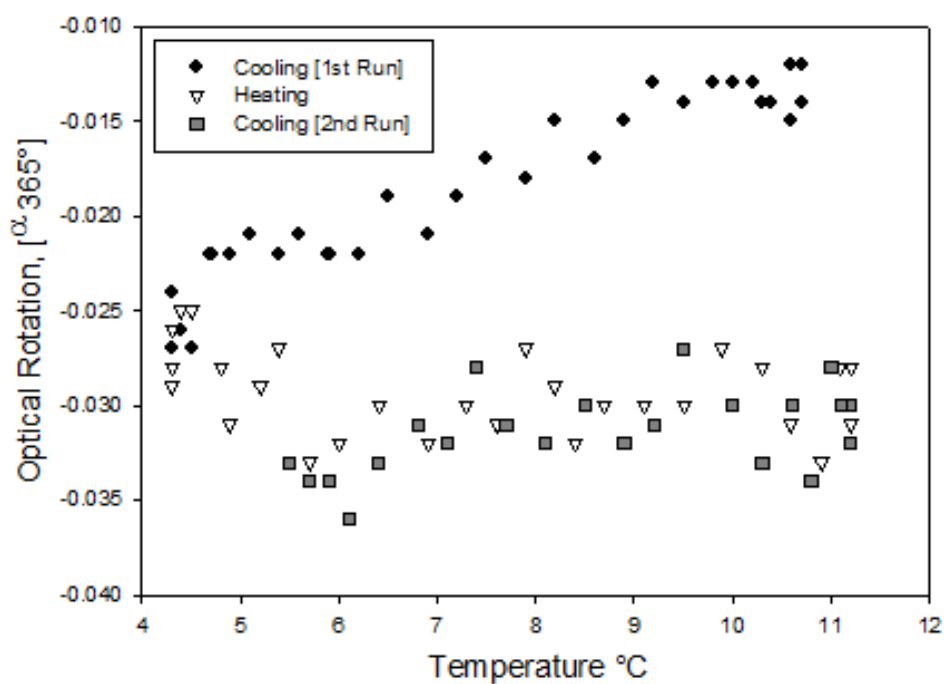


Figure 4.12. Variation of optical rotation (365 nm) with temperature for double distilled water on cooling (two runs) and heating. Each reading is based on a single sample measurement.

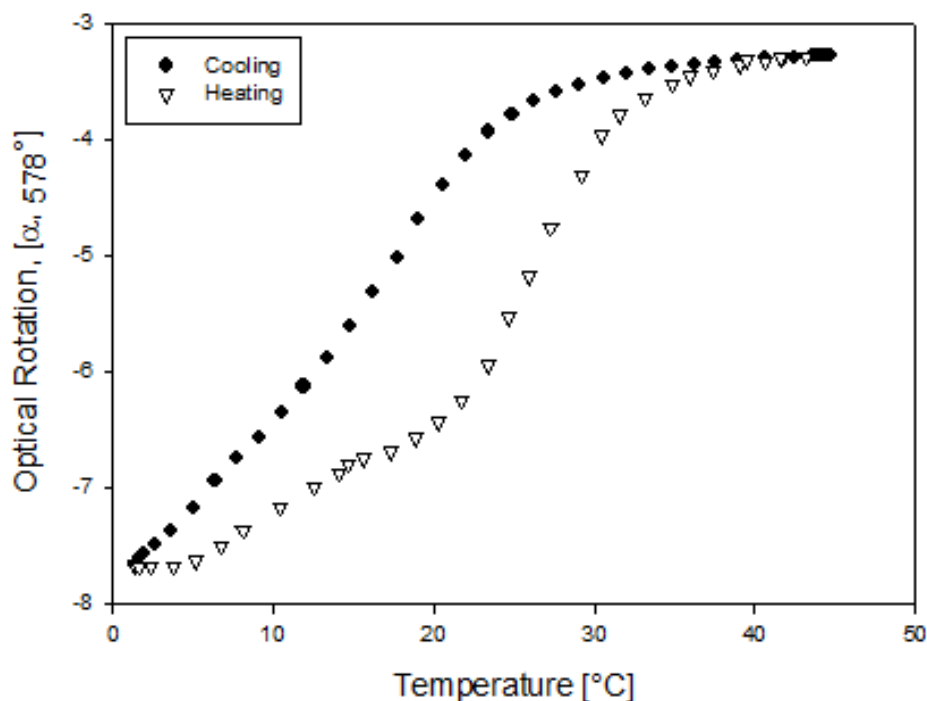


Figure 4.13. Variation of optical rotation (578 nm) with temperature for 5 wt.% gelatin (from porcine skin) aqueous solution on cooling and heating in double distilled water. Each reading is based on a single sample measurement.

4.3. Conclusions

The *in vitro* acid-induced gelation of mixed systems of two biopolymers; *LA* and *HA* gellan gum has been investigated. Rheological and texture analysis showed that these mixed gels displayed textures that lay between the material properties exhibited for the *LA* and *HA* gellan variants. DSC analysis showed that mixtures of the *LA* and *HA* gellan forms exhibit two separate conformational transitions at temperatures coincident with each of the individual biopolymers.

Various metabolically relevant pH environments and hydrocolloid concentrations were investigated. These resulted in very different acid gelled structures, which were characterised by texture analysis. The structures of the acid gels were shown to depend upon the pH, hydrocolloid concentration and proportion of each biopolymer used during their production. A selection of these mixed gellan structures were assessed post-production in terms of their response to prolonged exposure to an acidic (pH 1), stomach-like, environment. This resulted in a significant increase in the gel strength, regardless of the biopolymer proportions. The *HA* gellan was less acid sensitive, and subsequently no evidence of acid gelation was observed with *HA* gellan at a proportion greater than 60 % of the total biopolymer.

The findings presented demonstrate that structuring as well as de-structuring of mixed gellan acid gels can be controlled in acidic environments similar to those that are present in the stomach after food consumption.

Chapter 5

LOW ACYL GELLAN GUM FLUID GELS

5.1. Introduction

This chapter presents the results of the microstructure investigations on low acyl (*LA*) gellan gum fluid gels. Their formation and properties, by applying shear and cooling during gelation using two common production methods (a rheometer versus a pin-stirrer) is discussed. Further, the influence these parameters have on subsequent acid gel structuring, and whether these fluid gel structures demonstrate similar responses to acid to those exhibited by the quiescent low and high acyl mixed gellan gum systems is also investigated.

5.2. Results & Discussion

5.2.1. Kinetic studies of low acyl gellan gum fluid gels produced using a jacketed pin-stirrer

5.2.1.1. Viscometric material response post fluid gel production

The post-production flow behaviour of the fluid gel samples was investigated 24 hours after their production by performing viscosity measurements using the rheometer. Figure 5.1 shows viscosity flow curves for the 1 and 2 wt.% *LA* gellan fluid gel samples, as a function of the increasing number of processing cycles. Each of the samples displayed non-Newtonian shear-thinning flow behaviour, where the fluids decreased in viscosity with increasing shear rate. Fluid gels reported in Figure 5.1 showed no distinguishable differences between the sample flow behaviours, with an increasing number of processing cycles. For each gellan concentration, the samples displayed almost identical shear thinning behaviour with increasing shear exposure time. This implies that homogeneous fluid gel samples are formed rapidly using the pin-stirrer unit, as a result of efficient mixing. It also suggests that they are then resistant to break-up by shear with continued processing, presumably due to the smaller, more spherical nature of

the fluid gel particles, and increased packing and volume fraction caused by the rapid gelation process.

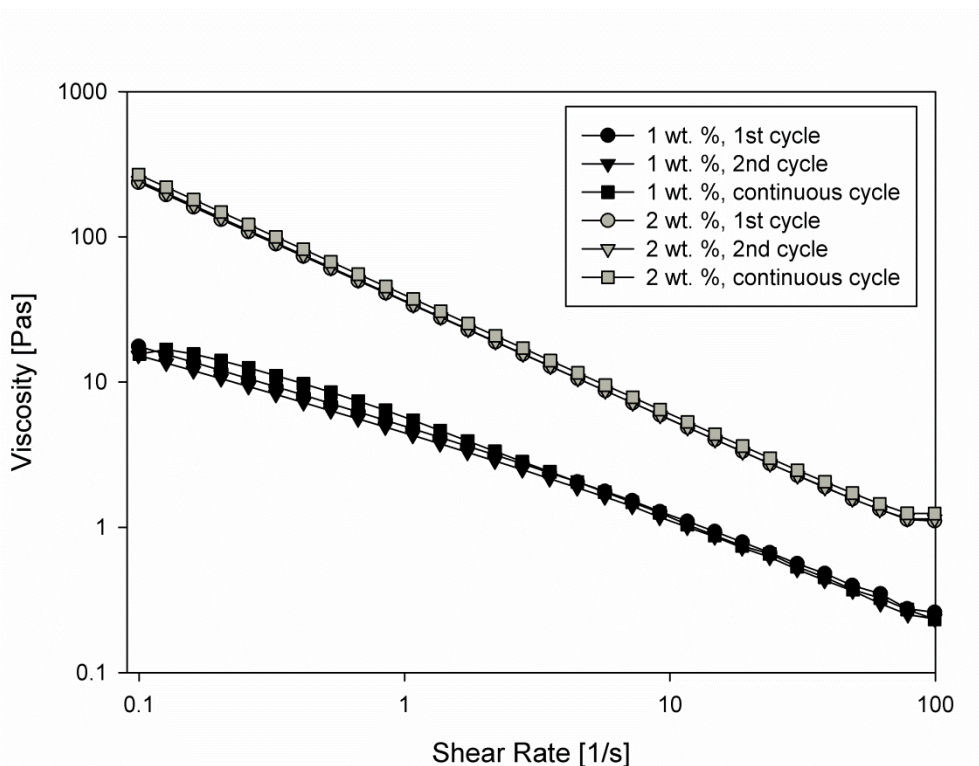


Figure 5.1. Viscosity flow curves for 1 and 2 wt.% low acyl gellan gum fluid gels produced using a jacketed pin-stirrer (1500 rpm shaft speed, 100 ml/min pump rate, 20 °C water bath, ~ 30 °C/min cooling rate), as a function of increasing shear exposure time. 1 cycle is equal to one full pass through the pin-stirrer unit. The continuous cycle is when the inlet and outlet solution tubes are fed from the final sample container to create a linked system. Samples were collected from each after equilibrium had been achieved. Each of the viscosity readings are based on a single sample measurement.

An increased resistance to flow behaviour was however, observed when increasing the gellan polymer concentration from 1 wt.% to 2 wt.% *LA* gellan (Figure 5.1). Polymer concentration controls fluid gel particle stiffness (Frith et al., 2002) and volume fraction (Norton et al., 1999). On increasing polymer concentration the particle elasticities (Frith et al., 2002) and volume fraction (Norton et al., 1999) increase, as a result of ordering and aggregation occurring within the fluid gel particles. These factors are responsible for the observed marked increase in gel viscosity with *LA* gellan concentration.

5.2.1.2. Structure development

In order to investigate whether inter-particle interactions were involved during the production of fluid gels formulated using the pin-stirrer method, and whether these persist post-processing during structure development, structural ripening tests were performed. Structural ripening of the fluid gel structures is affected by the cooling rates applied during processing, with more extended interactions taking place for those structures produced at higher cooling rates. The tests enabled the time scales over which the structural ripening or “strengthening” of the fluid gel structures occurred to be determined. Figure 5.2 shows the resulting viscoelastic modulus data as a function of time from the linear viscoelastic table of frequencies test (0.1 – 100 rad/s), performed on the samples (1 – 2 wt.%), 24 hours after production.

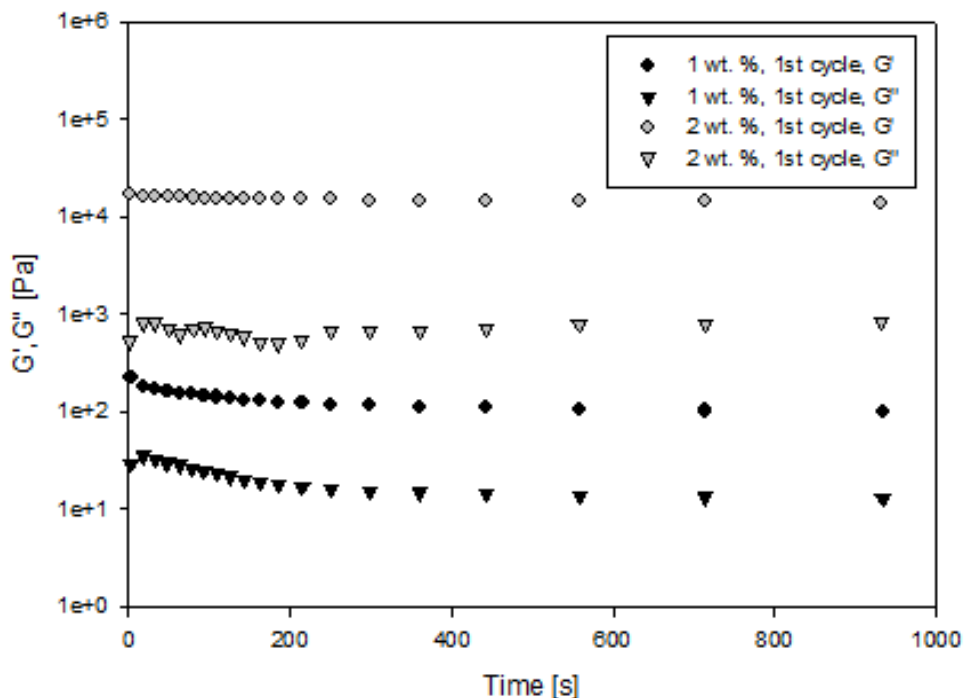


Figure 5.2. Storage (G') and loss (G'') moduli as a function of time for 1 and 2 wt.% low acyl gellan gum fluid gels produced using a jacketed pin-stirrer, during a table of frequencies test (0.1 – 100 rad/s at 20 °C). Each of the modulus readings are based on a single sample measurement.

The viscoelastic data for the 1 and 2 wt.% *LA* gellan samples in Figure 5.2 demonstrated the typical fluid gel responses to a table of frequencies test of this type. Fluid gels should display characteristics that lie somewhere between a ‘weak gel’ and a ‘strong gel’ in terms of the dependence of the storage and viscous modulus on frequency, and the phase angle values. The weak gel behaviour of fluid gels can be ascribed structurally; closely packed particle interactions allow an elastic network to form at rest, whilst under shear, they are disrupted allowing material flow. The strong gel component arises from the strong elasticities of the gel particles, and increases with particle stiffness (Garrec & Norton, 2012). Strong dependencies of the viscous modulus on the phase angle were evident for the 1 and 2 wt.% *LA* gellan samples in Figure 5.2, suggesting weak gel criteria. However, the phase angle values were fairly low (between 2 – 4 °), as a result of the storage moduli being significantly higher than the viscous moduli across the frequency range in each case, indicating strong gel characteristics.

The corresponding initial decrease and increase observed in the storage and viscous moduli respectively, at the start of the kinetic experiment for the 1 and 2 wt.% *LA* gellan samples, suggest that the elastic networks formed at rest have reached their maximum inter-particle interaction level prior to testing, and are subsequently disrupted whilst under shear. This incidentally leads to material flow, hence the observation of the initial increases in the respective viscous moduli. The results imply that all or most of the inter-particle structural ordering of the samples takes place during cooling in the pin-stirrer unit whilst under shear, rather than quiescently post-production. Structural ripening of the fluid gel structures is affected by the cooling rates applied during processing, with more extended interactions taking place for those structures produced at higher cooling rates. More efficient mixing and cooling is thought to take place within the pin-stirrer unit when used alone (rather than in conjunction with a scraped surface heat exchanger,

SSHE), giving rise to fluid gel samples consisting of spherical-shaped particles (Garrec & Norton, 2012) that have strong elasticities and increased particle stiffness's. These spherical-shaped particles allow for a greater packing fraction within the fluid gel solutions, enabling closely packed particle interactions and an elastic network to form at rest. In contrast, producing fluid gel samples using SSHE and pin-stirrer processing units involves significant disruption of the cooling rates. Most of the cooling takes place in the SSHE prematurely with significant losses of temperature control occurring between the transfer links connecting the respective units. These factors together with the less efficient processing nature of the equipment results in a reduction in the amount of structural ordering of the samples that can take place during cooling, whilst under shear. Thus, strengthening and growth of fluid gel particles formulated using SSHE and pin-stirrer processing units, is more likely to occur quiescently.

In terms of concentration dependencies the 1 and 2 wt.% *LA* gellan fluid gel samples in Figure 5.2 exhibited the expected trends, with the 2 wt.% samples producing firmer gels with a greater elastic response. This is reflective of the principle, that with increasing gellan concentration, firmer gels (as proven using dispersion rheology) are produced, as a result of the subsequent increase in particle elasticity (Frith et al., 2002) and volume fraction (Norton et al., 1999).

5.2.1.3. Structure recovery

Each of the *LA* gellan gum fluid gel samples (1 – 2 wt.%, collected after the 1st, 2nd and continuous processing cycles) were subjected to a strain-recovery test, 24 hours post-production, to further assess the degrees of ordering. The elastic (G') and viscous (G'') moduli were measured initially during an applied stress sweep ramp, which served to fully ‘break’ the inter-particle bonds by plastically deforming the structure. The samples were then subjected to a ‘rest period’ of 10 minutes, allowing for structure recovery. Immediately after this, a second stress sweep was performed to study whether the behaviour of the structure, observed during the first sweep had fully recovered. Each stress sweep was performed within a stress range of 0.5 – 30 Pa, and at a frequency of 1 Hz (which was in the plateau region as measured by the table of frequencies test in Figure 5.2). Figures 5.3a and 5.6b show the resulting storage and loss moduli data for the 1 and 2 wt.% *LA* gellan gum fluid gel samples respectively, collected after the 1st processing cycle.

For the 1 wt.% *LA* gellan sample (Figure 5.3a), it was observed that the storage (G') and loss (G'') moduli remain constant until a shear stress of ~ 1.4 Pa is applied. The absence of fluid gel structural change within this shear stress range implies that no inter-particle interactions are occurring in the system. Increasing the applied shear stress above ~ 1.4 Pa however, leads to the failure and eventual collapse of the original fluid gel structure. The G' and G'' values measured for the two separate stress sweeps resembled each other qualitatively, with differences of ~ 3 Pa and ~ 2 Pa respectively. This suggests that the structure of the fluid gel system partially recovered to its initial state during the 10 minute ‘rest period’. It is expected that with a longer ‘rest period’, little changes in the G' and G'' between the two stress sweeps would be observed, indicating full structural recovery.

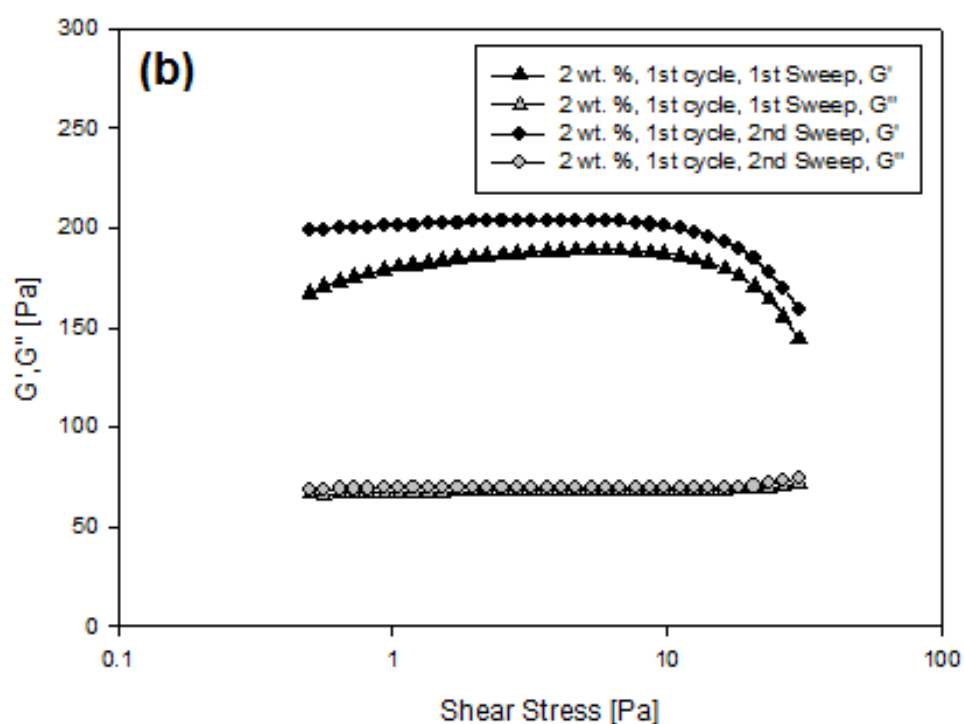
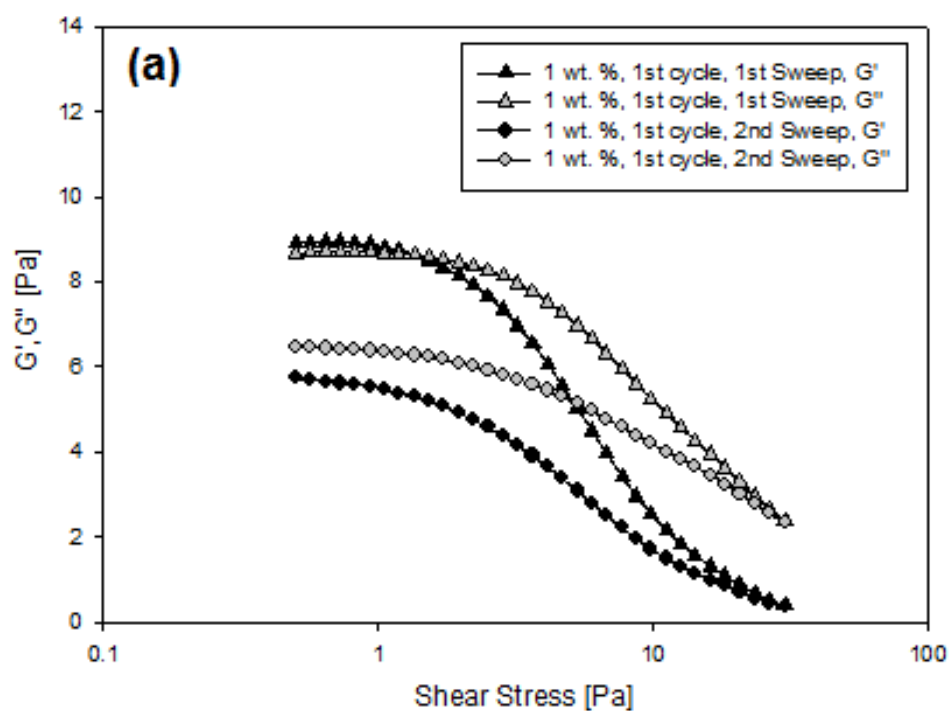


Figure 5.3. Storage (G') and loss (G'') moduli from stress-sweep measurements for 1 and 2 wt.% low acyl gellan gum fluid gels produced using a jacketed pin-stirrer (1st cycle samples only), performed at 1 Hz. The 1st sweep was carried out 24 hours after the production of the fluid gels and, after a “resting” stage of 10 min, it was followed by a 2nd sweep. Each of the stress-sweep moduli values are based on a single sample measurement.

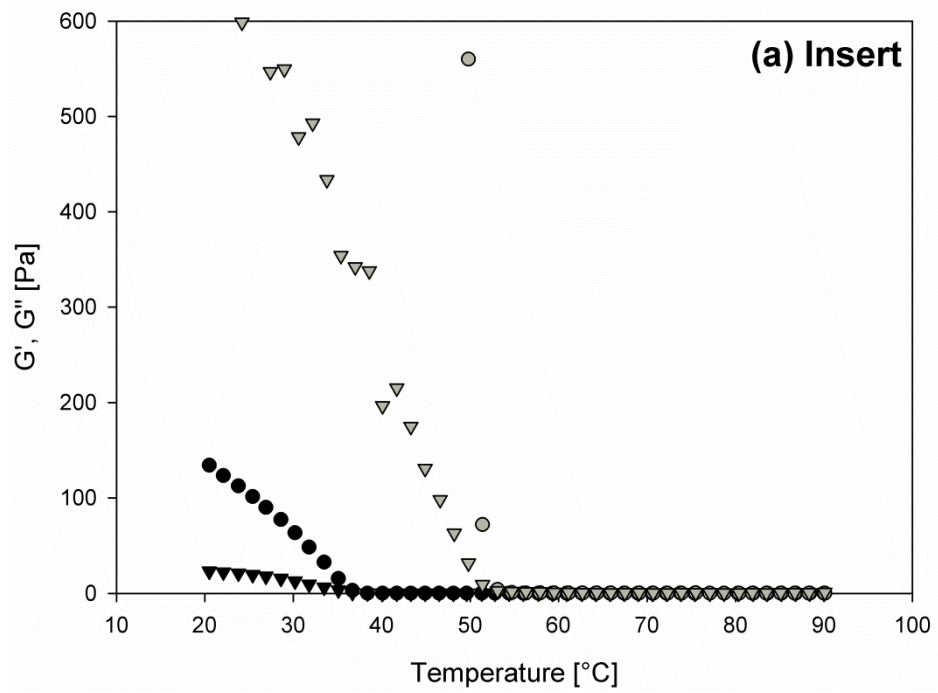
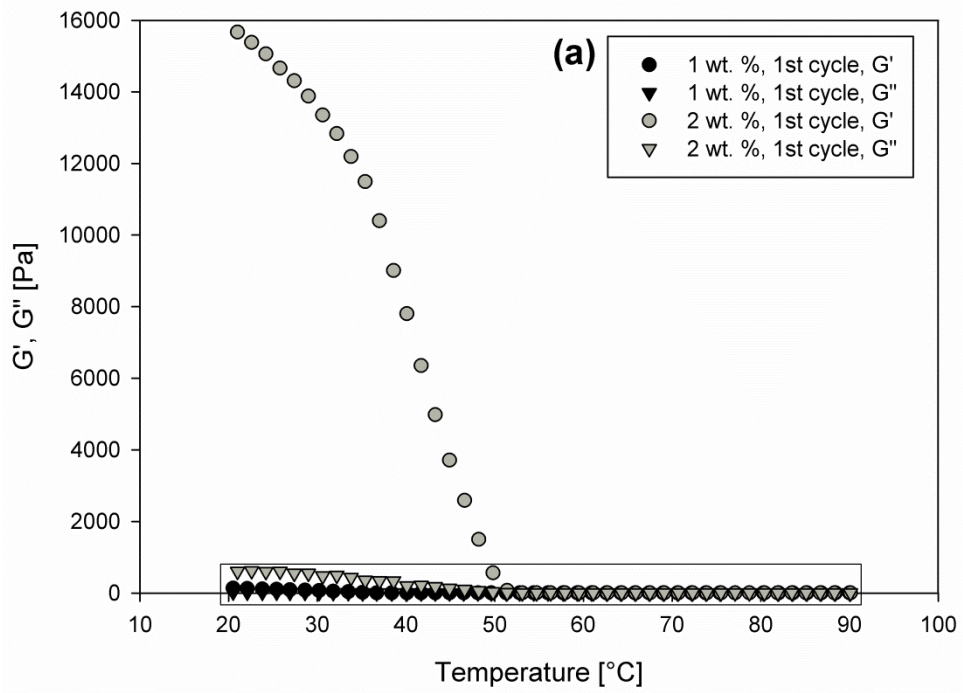
For the 2 wt.% *LA* gellan sample (Figure 5.3b), the behaviour observed was slightly different. During the 1st sweep, an increase in the storage modulus is observed until a shear stress of ~ 1 Pa is applied. This indicates that the structure of the fluid gel is changing due to inter-particle interactions in the system continuing to occur after its production and during the 1st stress sweep experiment itself. Between shear stresses of ~ 1 Pa and ~ 9 Pa, the G' and G'' moduli remain constant. Thereafter, the fluid gel structure begins to fail and finally collapses. Allowing the system to rest, before performing the 2nd stress sweep, revealed little change in the G' and G'' values, and the initial increase in the G' observed in the 1st sweep was absent. The structure of the fluid gel system, therefore fully recovered to its initial state during the relaxation period, with no structural ripening.

In terms of the respective sample strengths, the 2 wt.% *LA* gellan fluid gels exhibited much higher G' and G'' values (Figure 5.3b) than those reported for the 1 wt.% *LA* gellan fluid gels (Figure 5.3a). Comparing the results for the 1 and 2 wt.% *LA* gellan gum fluid gel samples, collected after the 1st processing cycle (Figure 5.3) with those collected after the 2nd and continuous processing cycles (not shown), minimal differences in their recovery responses were found. This demonstrates that increasing exposure to constant applied shear and cooling during fluid gel production has minimal impact on subsequent gel recovery.

5.2.1.4. The coil-helix transition

To examine the physical properties of the fluid gels, the samples (1 – 2 wt.%, collected after the 1st processing cycle) were subjected to small deformation, low-amplitude oscillatory measurements during temperature cooling and heating ramps, with an intermittent frequency sweep test. Performing the low-amplitude oscillation temperature cooling ramp first meant that the fluid gel post-production, had to be heated to 90 °C prior to sample testing. This effectively destroyed the fluid gel structure and the viscoelastic properties actually assessed were those of the formation of the equivalent quiescent gel. The frequency sweep performed at 20 °C also therefore, assessed the properties of the newly formed quiescent gel, and the subsequent low-amplitude oscillation heating ramp monitored its breakdown during melting. To rectify the rheological routine so that it examines the viscoelastic properties of the fluid gel samples post-production, the cooling and heating low-amplitude oscillation temperature ramps should be reversed (i.e. heating then cooling). The intermittent frequency sweep could then either be performed at 90 °C, post-melting of the fluid gel, or at 20 °C post-production of the quiescent gel on cooling.

The results of the small deformation, low-amplitude oscillatory measurements (10 rad/s or 1.585 Hz; 1 % strain) performed on the samples during the temperature cooling (90 – 20 °C) and heating ramps (20 – 95 °C) respectively, are shown in Figures 5.4a and 5.4b. These monitored the viscoelastic responses during the formation of the equivalent quiescent gel on cooling, and its subsequent breakdown on heating; enabling the coil-helix and helix-coil transition temperatures to be identified and the gels' structural ordering and disordering assessed.



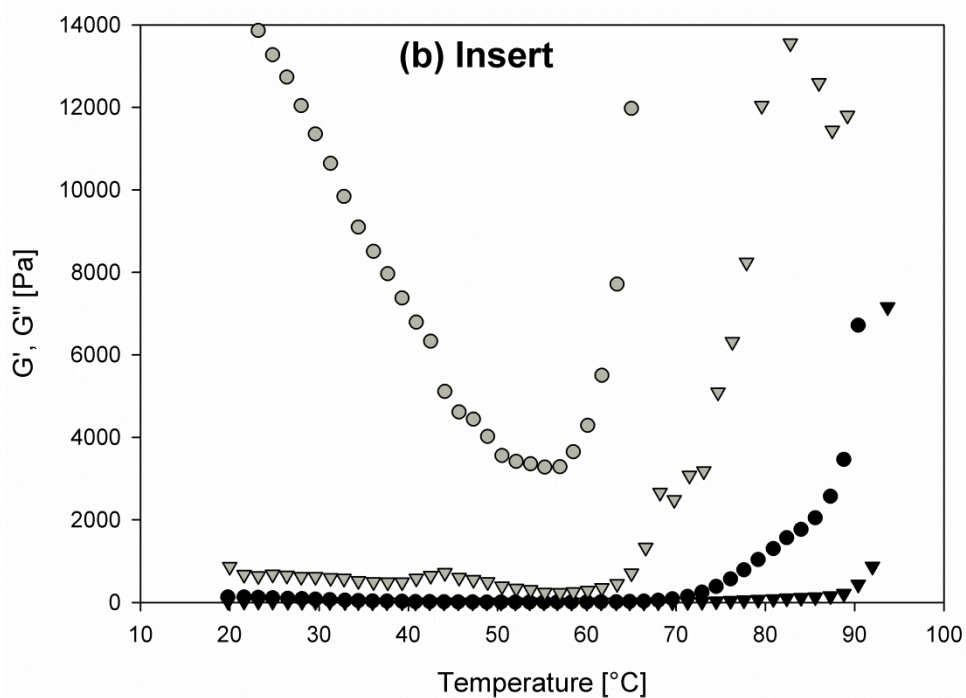
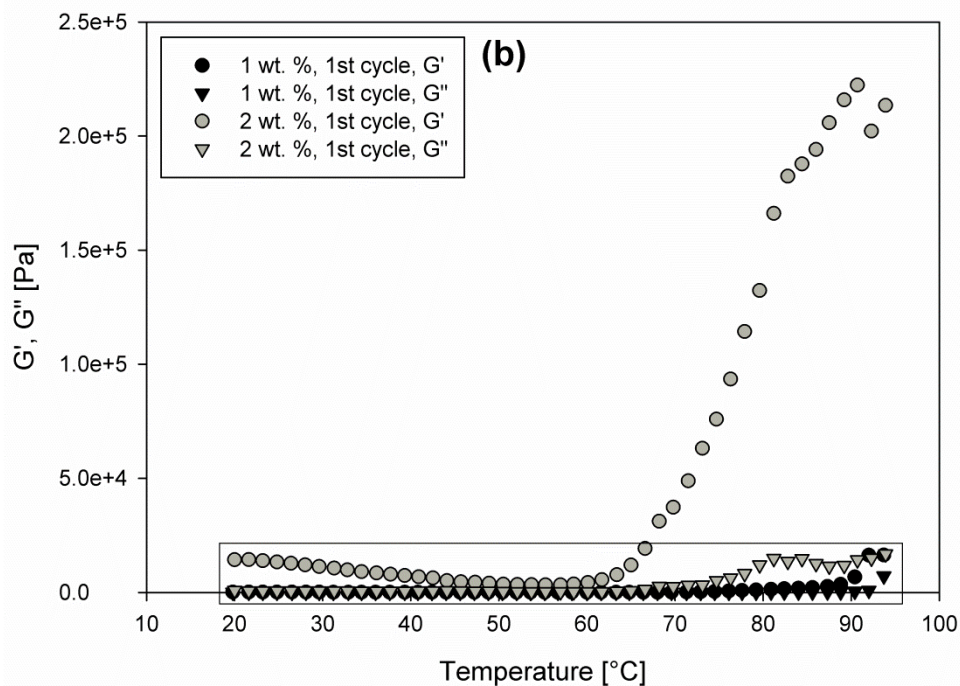


Figure 5.4. Storage (G') and loss (G'') moduli for 1 and 2 wt.% low acyl gellan gum fluid gels produced using a jacketed pin-stirrer, during a low-amplitude oscillation temperature cooling ramp (a) (90 – 20 °C) and heating ramp (b) (20 – 95 °C) at 1 °C/min (10 rad/s at 1 % strain). Each of the modulus readings are based on a single sample measurement. Note that the data enclosed in the boxed region in each of the figures ((a) and (b)) is representative of the respective inserts shown.

LA gellan gum is described as having a ‘snap’ setting due to the rapid gelation occurring immediately after its setting temperature has been reached. The setting and melting temperatures of the gels depends on the ion type and concentration in solution, in addition to the grade of gellan gum and the presence of other dissolved solids (Kelco Division of Merck and Co., Inc., 1993). In the absence of added cations, *LA* gellan gum gels set at around 25 °C and are typically formed in the range 30 – 50 °C (Kelco Division of Merck and Co., Inc., 1993).

LA gellan gum gels are thermally reversible below 100 °C (Sworn, 2009). The ordered form adopted by gellan on cooling in the solution state is the double-stranded helical structure, which then reverts to the single-stranded disordered coil state on heating. Significant thermal hysteresis is observed between the coil-helix and helix-coil transitions for *LA* gellan gum gels, when the gels melt at a higher temperature than at which they set (Kasapis et al., 1999). During cooling, the coil-helix transition involves dimerization of two polymer chains into a double helix (Goodall & Norton, 1987). This is followed by lateral helix aggregation, where counterions to the charged groups of the polymer chains, screen the electrostatic repulsion between chains and bridge neighbouring helices at the sites of their specific chain interactions (Morris et al., 2012).

On cooling, three distinct conformational regions were observed in the G' , G'' data for the 1 and 2 wt.% *LA* gellan samples. These were: 90 – 40 °C (1 wt.%) and 90 – 55 °C (2 wt.%), where the solutions existed in their disordered state; 40 – 25 °C (1 wt.%) and 55 – 30 °C (2 wt.%), occurrence of the coil-helix transitions; and 25 – 20 °C (1 wt.%) and 20 – 30 °C (2 wt.%), where ordered structures are formed via aggregation. The midpoint temperature (T_m) is the midpoint between the two linear regions corresponding to disordered and ordered polymer conformations. The temperatures of the start of these two linear regions for each gellan concentration were identified for the

coil-helix transitions in Figure 5.4a and the mid-point temperatures between them calculated to give $T_m = \sim 32.5$ °C (1 wt.%) and $T_m = \sim 42.5$ °C (2 wt.%). T_m represents the temperature at which the numbers of moles of saccharide residues in the disordered and ordered state are equal, and where the events of helix growth ('zipping-up') and decay ('un-zipping') are occurring at equal rates (Goodall & Norton, 1987). In Figure 5.4, the scales shown were minimised during analysis to fully observe the curve transitions, in order for the T_m values to be approximated. The coil-helix transition has been described as a dynamic equilibrium where the rate constant at T_m is zero, and on decreasing temperature the likelihood of growth events is increased relative to those of decay (Norton et al., 1983). Thus molecular rearrangements to both quiescent and fluid gels, via decay and growth mechanisms are reduced on decreasing temperature below T_m . The growth mechanism that is most likely to be responsible for the formation of the quiescent *LA* gellan gels in Figure 5.4a, involves intermolecular association of the polymer molecules in the solution during the coil-helix transition, which result in the formation of small, soluble clusters of chains. As the extent of association increases these clusters grow, until ultimately one becomes large enough to span the entire volume of the solution and form a continuous crosslinked network (Morris et al., 2012).

On heating, three distinct conformational regions were also seen in the G' , G'' data, as observed on cooling. These were: 20 – 40 °C (1 and 2 wt.%), disassembling and melting of the thermally unstable, ordinary double helical aggregates; 40 – 65 °C (1 wt.%) and 40 – 60 °C (2 wt.%), occurrence of the helix-coil transitions; and 65 – 95 °C (1 wt.%) and 60 – 90 °C (2 wt.%), where the solutions existed in their disordered coil state, and exhibited extensive thermal hysteresis. For the helix-coil transitions in Figure 5.4b, $T_m = \sim 52.5$ °C (1 wt.%) and $T_m = \sim 50$ °C (2 wt.%). The higher T_m and helix-coil transition

temperature ranges for the samples on heating, confirm that thermal hysteresis does indeed take place.

For both Figures 5.4a and 5.4b, the G' values across the temperature range were greater than those recorded for the viscous modulus, G'' from the point of gel ordering completion to the region where the solution is first in the disordered coil state. During this latter region, the values follow identical pathways. Interestingly, the G' values reported for the melting of the quiescent gels (Figure 5.4b) were of a much higher magnitude (~ 14 times), than those for the formation of the quiescent gels (Figure 5.4a). These greater elasticity values reflect the higher magnitude of energy required to melt the extensive quiescent gel interparticulate and thermally-stable aggregated helices and junction zones, than is needed to form them. This supports the principle bond-making process being exothermic, and the bond-breaking process being endothermic. The higher G' values on melting are also likely to be a result of heterogeneous quiescent gel samples formed of a mixture of broken gel fragments and gel particles, created during the frequency sweep prior to heating. Alternatively, the greater elasticity values could be a consequence of a temperature lag error in the rheometer equipment.

In terms of concentration dependencies, there were minimal differences between the temperature ranges of the conformational regions with increasing gellan concentration on cooling and heating separately. Increasing the gellan concentration did however result in the expected increase in gel elasticity observed on both heating and cooling (Figures 5.4a and 5.4b). This is due to greater particle stiffness's (Frith et al., 2002) and volume fractions (Norton et al., 1999) with increasing polymer concentration, together with increased ordering and aggregation occurring between and within the gel particles.

5.2.1.5. Identification of enthalpic conformational transitions using DSC

DSC measurements were performed on each of the samples (1 – 2 wt.%, collected after the 1st processing cycle) using a Setaram μ -DSC3 evo Dynamic Scanning Calorimeter (DSC) to identify the enthalpies and temperatures of the coil-helix transitions on both heating and cooling. Figure 5.5 shows the resulting endothermic and exothermic curves on heating (5.5a) and cooling (5.5b) for the 1 and 2 wt.% *LA* gellan gum fluid gels. The heat flow y-values have been manipulated to separate the respective curves for clarity. The corresponding calculated heat enthalpies (lost or gained by the solutions), and maximum heat flow temperature ($T_{\max.}$) values of the thermal transitions are displayed in Table 5.1.

<i>LA</i> Gellan Gum Fluid Gel Concentration [wt.%]	Melting (Fluid Gel), ΔH (J/g) [$T_{\max.}$ (°C)]	Gelation (Fluid Gel), ΔH (J/g) [$T_{\max.}$ (°C)]	Melting (Quiescent Gel), ΔH (J/g) [$T_{\max.}$ (°C)]	Gelation (Quiescent Gel), ΔH (J/g) [$T_{\max.}$ (°C)]
1	0.616 [28.4]	-0.840 [28.8]	0.566 [28.6]	-0.803 [28.8]
2	0.646 [32.2]	-0.487 [33.1]	0.705 [32.7]	-0.444 [33.2]

Table 5.1. Table of differential scanning calorimetry measurements (to 3 s.f.) for 1 and 2 wt.% low acyl gellan gum fluid gels produced using a jacketed pin-stirrer (1st cycle samples only), where ΔH is the amount of heat energy gained or lost by the solutions. Each of the ΔH and $T_{\max.}$ values are based on a single sample measurement.

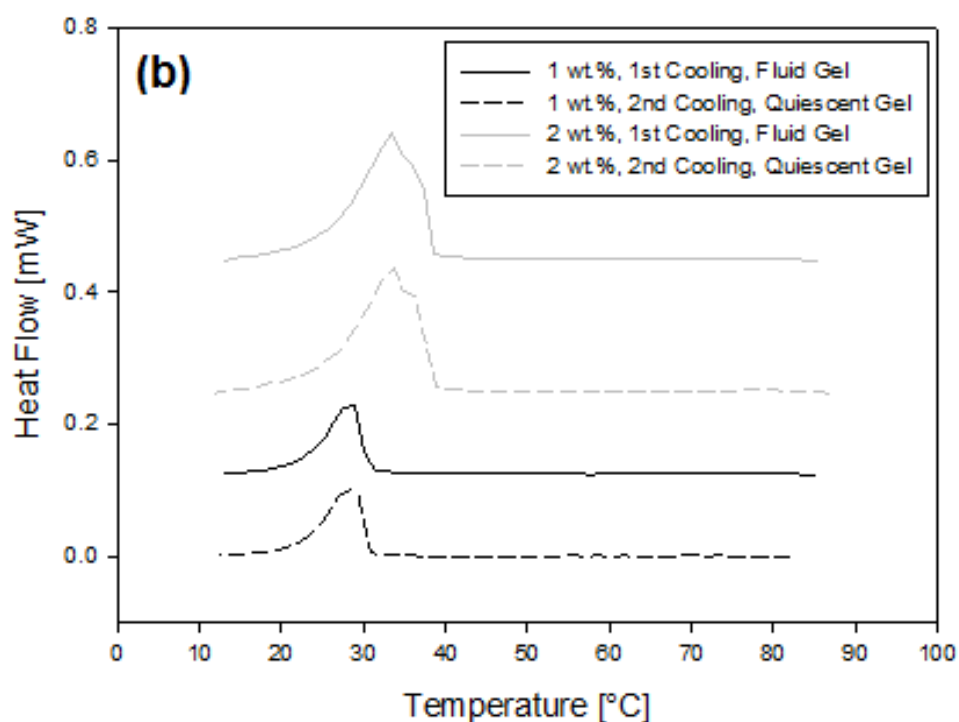
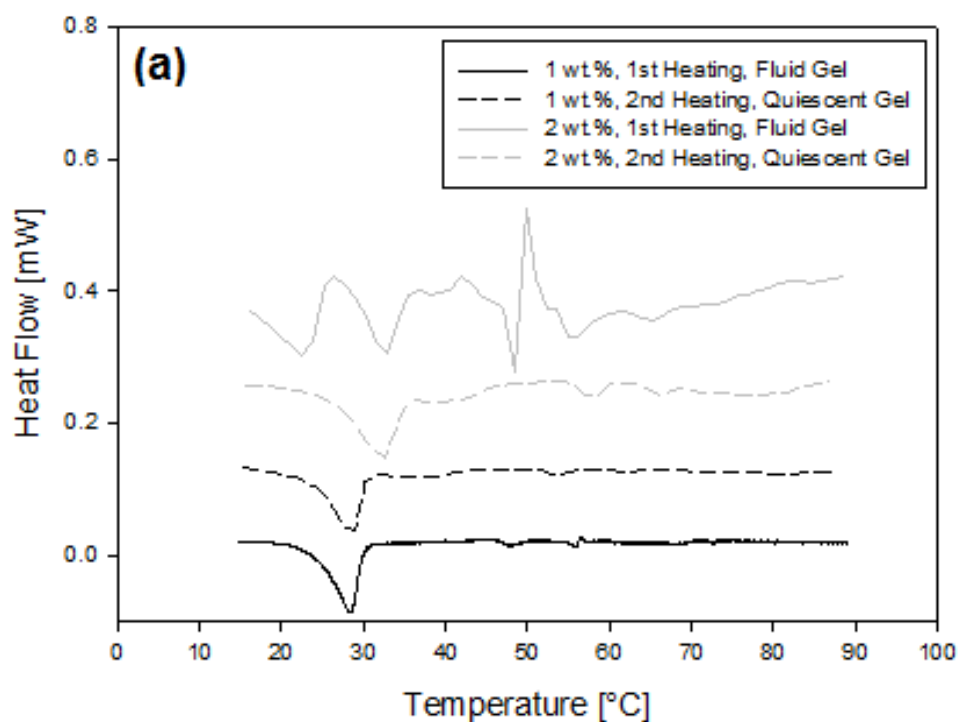


Figure 5.5. μ -DSC endothermic (heating) (a) and exothermic (cooling) (b) peaks (baseline subtracted) for 1 and 2 wt.% low acyl gellan gum fluid gels produced using a jacketed pin-stirrer (1st cycle samples only). A cooling and heating rate of 0.5 °C/min was implemented. The first heating scan shows melting of a fluid gel; the second, a quiescent gel. Note that heat flow y-values have been added and subtracted to separate the curves from each other for clarity. Each curve is based on a single sample measurement, due to the lengthy experimental procedure of 11 hours, 40 minutes.

Note that in Figure 5.5a, an additional melting peak is observed for the 2 wt.% *LA* gellan fluid gel that has been omitted from Table 5.1. This was attributed to an error caused by thermal history during sample preparation and loading, that had failed to be eliminated during the initial 60 min isothermal test period. Failure to observe this peak on subsequent cooling and heating scans, confirm its dissociation with the *LA* gellan system.

The energy gained by the 2 wt.% fluid gel sample on melting (0.646 J/g) was lower than that for the 2 wt.% quiescent gel (0.705 J/g), whilst the energy gained by the 1 wt.% fluid gel sample on melting (0.616 J/g) was slightly higher than that for the 1 wt.% quiescent gel (0.566 J/g). The fluid gel melting peak temperatures for each however, (28.4 °C (1 wt.%) and 32.2 °C (2 wt.)) were lower than those for the quiescent gels (28.6 °C (1 wt.%) and 32.7 °C (2 wt.)). The close similarities between the first and second cooling peaks (Figure 5.5b) for the 1 and 2 wt.% samples, where the gels are formed quiescently (and effectively equivalent events monitored), indicate a strong accuracy of the data. Thus it was suggested (Garrec & Norton, 2012) that the differences observed between the heating scans can confidently be related to the differences between gels formed under sheared and quiescent conditions. It has been reported (Garrec & Norton, 2012) that when the energies gained by fluid gels on melting are smaller than those gained by the quiescent gels (as observed for the 2 wt.% sample), that the total number of helical domains are fewer in the former. This was said to be reinforced (Garrec & Norton, 2012) when the melting temperatures of the fluid gels are lower than the quiescent gels, indicating fewer or weaker, aggregated helices (resulting from their shorter lengths). Although, the fluid gel melting peaks (1 and 2 wt.%, Table 5.1) were lower than those for the quiescent gels (1 and 2 wt.%, Table 5.1) in this data, the differences between them were very small (0.2 °C (1 wt.%) and 0.5 °C (2 wt.)). This

suggests that they are reflective of an alternative theory where the fluid gel internal particle polymeric network, and therefore the elasticity of individual particles, is equivalent to that of their quiescently cooled counterparts (Caggioni et al., 2007; Frith et al., 2002).

Comparing the DSC data from the 1 and 2 wt.% *LA* gellan fluid gels, increases in the volumes of heat energy gained by the systems, and in the melting and gelation temperatures on heating and cooling, were observed on increasing polymer concentration (Table 5.1). As previously mentioned, with increasing polymer concentration, particle elasticity (Frith et al., 2002), and volume fraction (Norton et al., 1999) increase, as a result of ordering and aggregation occurring within the fluid gel particles. It would therefore, be expected that if the fluid gels were formed of fewer helical regions and smaller helix aggregates, (thus having lower particle elasticity compared to the bulk quiescent gels) then significant differences in both the heat energies and gelation temperatures would be evident and on par to those observed with increasing gellan concentration.

5.2.2. Kinetic studies of low acyl gellan gum fluid gels produced using a scraped surface heat exchanger and jacketed pin-stirrer

Preliminary kinetic studies were conducted (described in detail in Section 3.2.2. and Sections 3.2.2.4 – 3.2.2.5.) on low acyl gellan gum fluid gels (1 – 2 wt.%) produced using a scraped surface heat exchanger and jacketed pin-stirrer, prior to the work presented in Section 5.2.1. The results from the post fluid gel production viscometry, and small deformation, low-amplitude oscillatory measurements (during cooling and heating ramps) however, proved to be very similar to the equivalent results presented in

the previous section (Section 5.2.1.1. Viscometric material response post fluid gel production, Figure 5.1; Section 5.2.1.2. Structure Development, Figure 5.2; Section 5.2.1.4. The coil-helix transition, Figure 5.4). Since the results did not present anything new, and to avoid repetition of data a decision was made to eliminate these results from this thesis.

Formulating *LA* gellan fluid gels using these two different processing unit variations, did however highlight their advantages and disadvantages. For example, when formulating a fluid gel using a SSHE in conjunction with a pin-stirrer unit, most of the cooling takes place within the SSHE prematurely and significant losses in temperature control occur between the transfer links connecting the respective units. An increased, less efficient processing nature is also involved with formulating fluid gel samples using this unit combination, compared to when using the pin-stirrer unit alone. Passing an aqueous *LA* gellan solution through a SSHE unit causes the gel particles to start forming instantly with exposure to the shear and cooling regime. Continued shear and cooling in the connected pin-stirrer unit then allows the formed particles to develop, whilst also competing with particle break up phenomena induced by the more intrusive nature (caused by the shaft and vessel ‘pin’ obstructions) of the pin-stirrer shear-field. This regime tends to produce heterogeneous fluid gel samples that consist of gel particles and broken-up fragments, which yield high gel viscosities (and greater G' characteristics). More efficient processing takes place when producing fluid gel samples using the pin-stirrer alone, due to the absence of premature cooling (leading to gel pre-structuring) and unnecessary processing (leading to heterogeneous samples). According to Garrec & Norton (2012), under these conditions, fluid gel samples consisting of spherical-shaped particles are formed. Despite these differences however, the preliminary results and those presented in Section 5.2.1. showed that comparable results can be achieved.

5.2.3. Effect of processing conditions on low acyl gellan gum fluid gels

To probe the effect of how manipulating the processing conditions during fluid gel production influences their subsequent gel properties; a selection of *LA* gellan gum fluid gels (0.25 and 1 wt.%) were formulated using the pin-stirrer only set up (Section 3.2.3.1) using shaft rotation speeds from 275 – 1500 rpm, and flow rates from 50 – 200 ml/min.

5.2.3.1. Viscometric material response post fluid gel production

The post-production flow behaviour of the fluid gel samples, 24 hours after their production was investigated by performing viscosity measurements using the rheometer. Figure 5.6 shows the resulting viscosity flow curves for the 0.25 wt.% (5.6a and 5.6b) and 1 wt.% (5.6c and 5.6d) *LA* gellan gum fluid gel samples, produced using the jacketed pin-stirrer when set to shaft speeds of 1500 and 1000 rpm (5.6a and 5.6c) and 500 and 275 rpm (5.6b and 5.6d), using varying pump rate speeds (50 – 200 ml/min).

After production, each of the 0.25 wt.% samples (Figures 5.6a and 5.6b) exhibited virtually identical shear thinning behaviour, with no significant differences between the viscometric responses for the samples produced with increasing pump rates or decreasing shaft speeds. Each sample, however, towards the end of the viscosity measurements at ~ 14 Pa displayed a decrease in viscometric response; indicating structural failure as a result of increasing the applied stress.

When the gellan polymer concentration is raised to 1 wt.%, the expected increased resistance to flow behaviour is observed with each sample (Figures 5.6c and 5.6d). Polymer concentration controls fluid gel particle stiffness (Frith et al., 2002) and volume fraction (Norton et al., 1999). On increasing polymer concentration the particle elasticity (Frith et al., 2002) and volume fraction (Norton et al., 1999) increase, as a result of ordering and aggregation occurring within the fluid gel particles. These factors are

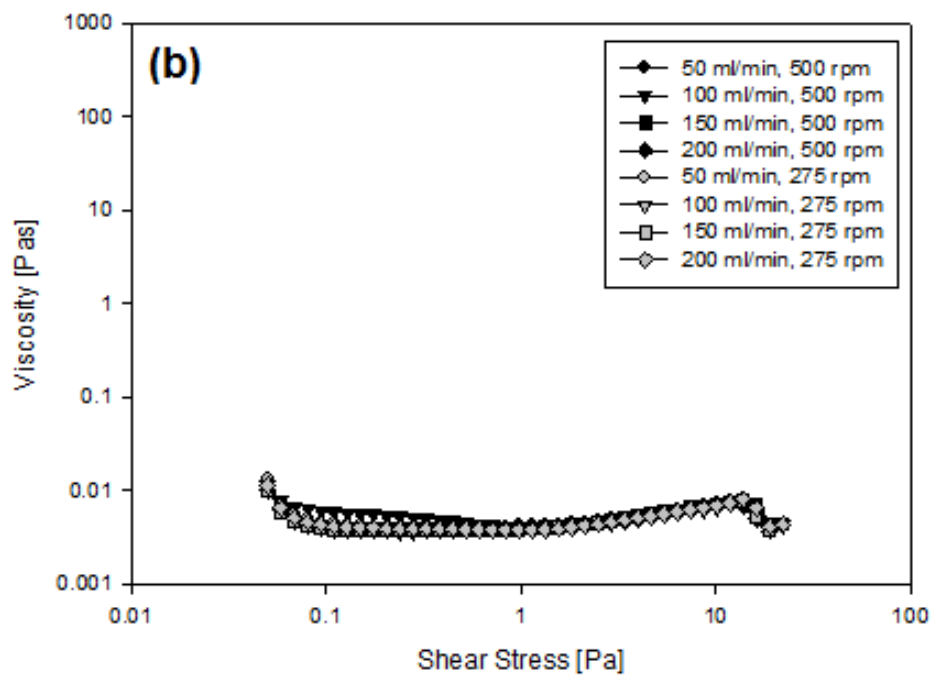
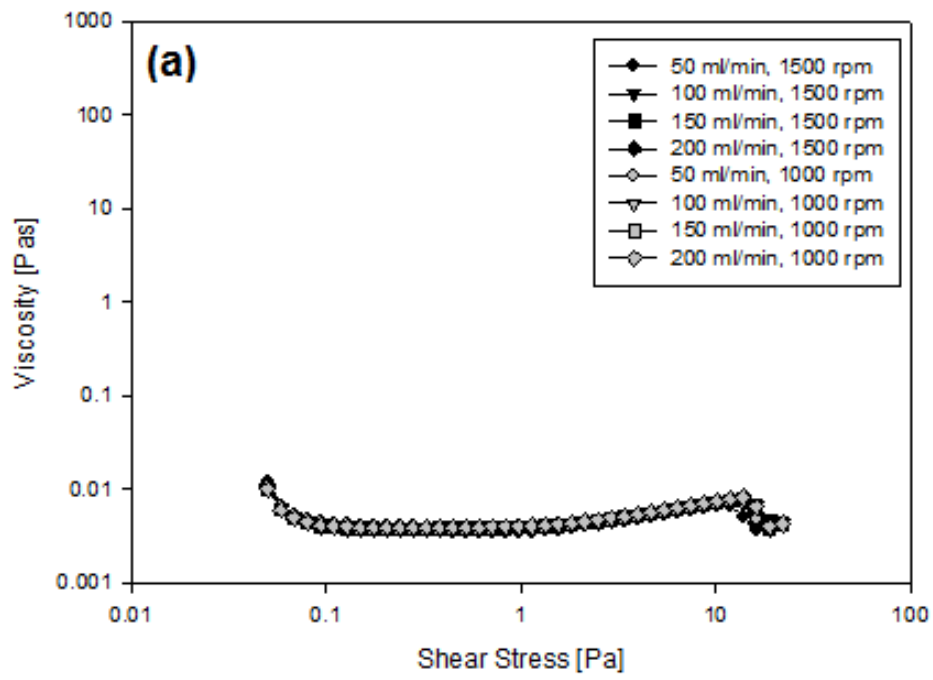
responsible for the observed marked increase in gel viscosity with *LA* gellan concentration.

For the 1 wt.% samples, formulated using shaft speeds of 1500 and 1000 rpm (Figure 5.6c), virtually identical shear thinning behaviour is observed for each pump speed, but with increasing pump rate (50 – 200 ml/min), a lower resistance to flow behaviour is apparent. This can be explained using the theory that by forming fluid gels using low pump rates, the gels are exposed to longer periods of processing (and in turn greater exposure to the applied shear and cooling environment in the pin-stirrer), which result in extensive interactions and bridging between the particles, and the formation of more extensive helical networks. These extended networks are however, more likely to be broken up by the shear during processing, causing structural disruption. As a result, a heterogeneous fluid gel sample is produced, consisting of gel particles and broken-up fragments, culminating in a weaker gel with increased gel viscosity.

For the 1 wt.% samples formulated using shaft speeds of 500 and 275 rpm (Figure 5.6d), virtually identical shear thinning behaviour is observed for each pump speed, and no significant differences between the viscometric responses for the samples produced with increasing pump rates were apparent. The overall viscometric behaviour was very similar to that observed for the 1 wt.% samples formulated using the shaft speeds of 1500 and 1000 rpm (Figure 5.6c), albeit the viscosity values were ~ 10 times smaller in magnitude. This reduction in viscosity for the samples produced using the lower pin-stirrer shaft speeds when compared to those using the higher speeds, can be attributed to the fact that lower particle packing and volume fractions exist, which lead to reduced resistances in flow behaviour.

Since, only small differences in the viscometric responses with samples produced with increasing pump rate, were observed for the 1 wt.% samples formulated using shaft

speeds of 1500 and 1000 rpm (Figure 5.6c), and no comparable differences were observed for the remaining 0.25 and 1 wt.% fluid gel samples (Figures 5.6a, 5.6b and 5.6d), identical shear thinning behaviour was assumed. The reason behind this behaviour is that in highly concentrated systems of particles, the flow is characterised on the micro scale by the relative flow of particles “squeezing” past each other. The bulk viscosity would thus be a direct function of the deformability (intrinsic elasticity) and packing of the particles, similarly to the behaviour of highly “packed” emulsions (Mason et al., 1996).



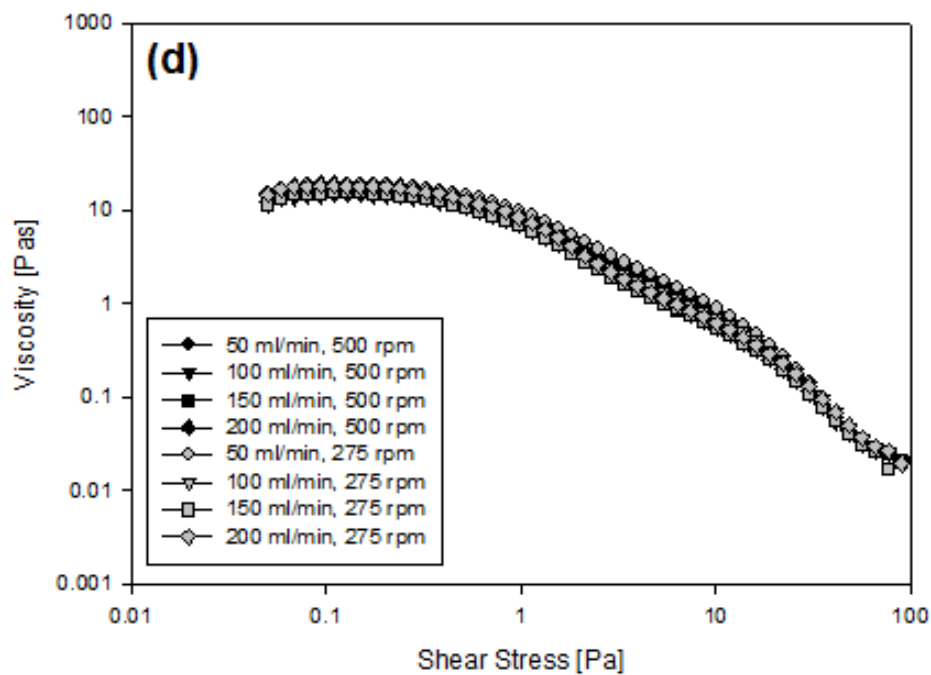
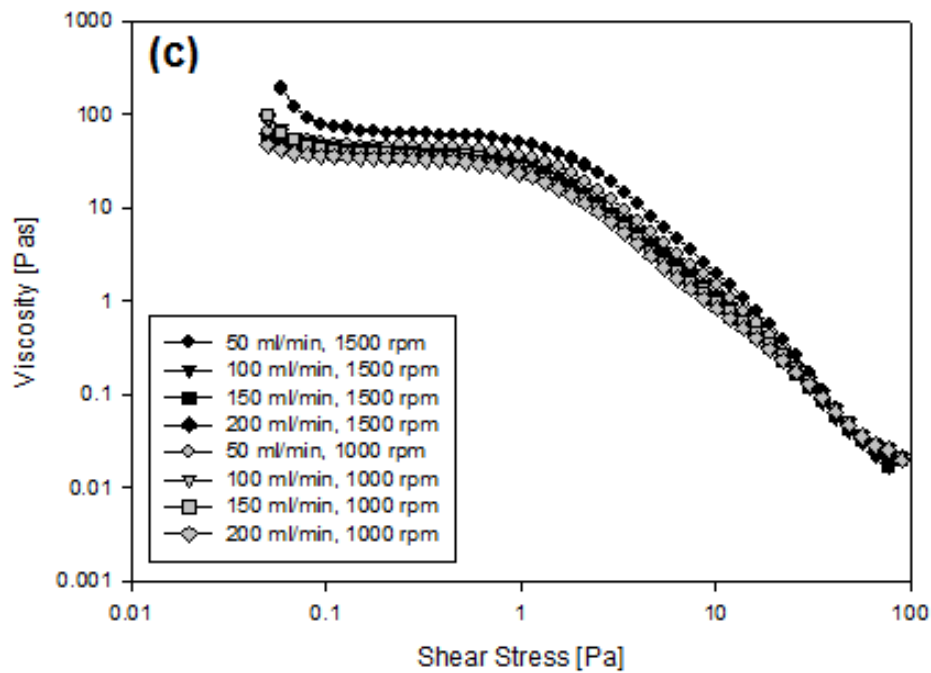


Figure 5.6. Viscosity flow curves for 0.25 (a, b) and 1 wt.% (c, d) low acyl gellan gum fluid gels produced using a jacketed pin-stirrer (average cooling rate, °C/min (per pump rate): 15 (50), 40 (100), 60 (150), 75 (200)) with shaft speeds of 1500 and 1000 rpm (a, c) and 500 and 275 rpm (b, d) and varying pump rate speeds (50 – 200 ml/min). Each of the viscosity readings are based on a single sample measurement.

5.2.3.2. Structure recovery

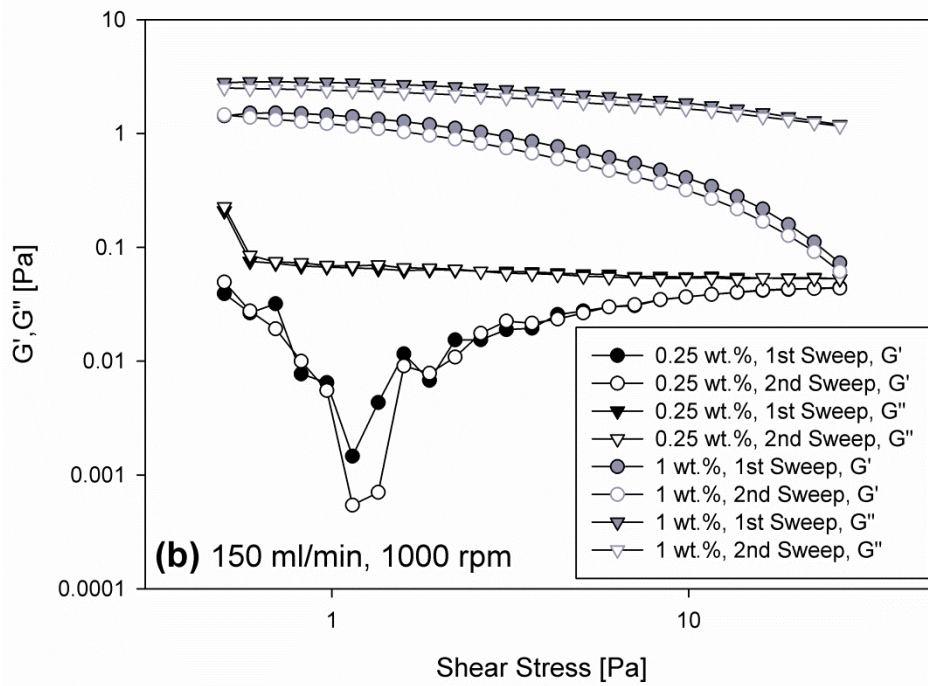
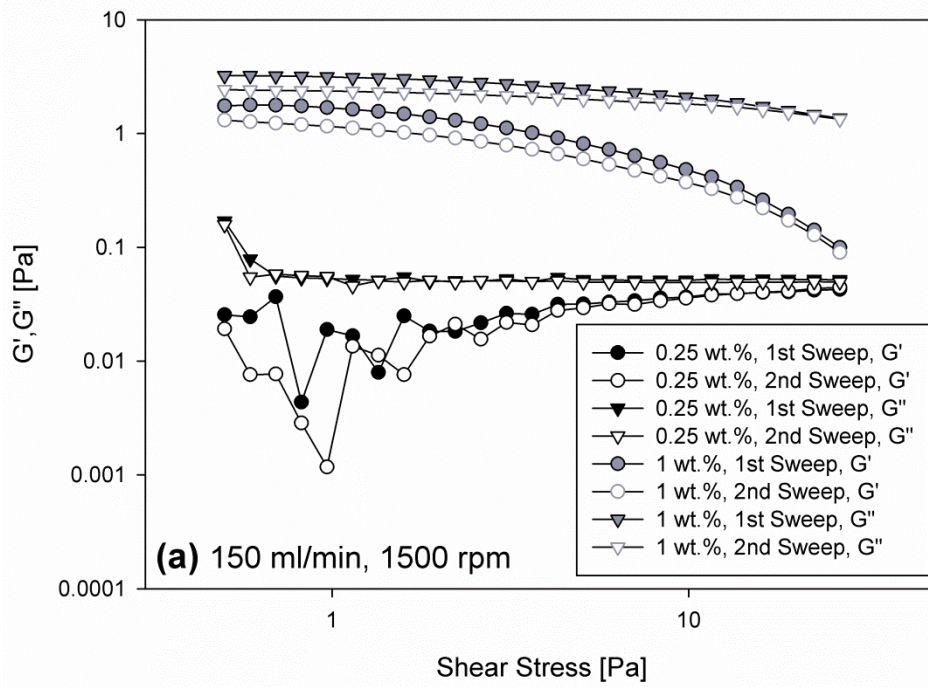
Each of the *LA* gellan gum fluid gel samples (0.25 and 1 wt.%, collected after one processing cycle) were subjected to a strain-recovery test (Section 3.2.4.3.), 24 hours after production, to assess the post-production extent of ordering. Figure 5.7 shows the resulting storage and loss moduli data for the 0.25 and 1 wt.% *LA* gellan gum fluid gel samples, produced using the jacketed pin-stirrer when set to shaft speeds of 1500 (5.7a), 1000 (5.7b), 500 (5.7c) and 275 rpm (5.7d), each using a pump rate speed of 150 ml/min.

For the 0.25 wt.% *LA* gellan gum fluid gel samples formulated using the shaft speeds of 1500 and 1000 rpm (Figures 5.7a and 5.7b) the structural recovery behaviours observed were almost identical, implying that decreasing the pin-stirrer shaft speed during production has minimal impact on the subsequent gel recovery. For each sample, immediate collapse of the structure with applied shear stress took place during the 1st sweep, up until shear stress levels of ~ 0.6 Pa and $\sim 0.7 - 0.8$ Pa for the loss (G'') and storage (G') moduli, respectively. Thereafter, the loss moduli remained constant, whilst the storage moduli were observed to increase up until shear stress values of ~ 10 Pa, where it then too remained constant. The storage moduli increases could be attributed to one of two mechanisms. The first being the system's attempt to re-build the fluid gel structures after failure, as a result of inter-particle interactions occurring during the stress sweep experiment. And the second, being a result of the heterogeneous gel samples post-collapse, that consist of large, broken gel fragments which are continually destroyed under shear. The constant storage moduli values after these increases indicate an absence of fluid gel structural change. Thus, in terms of these proposed mechanisms, the fluid gel structures have either been reformed to one closely resembling the original sample prior to collapse; or uniform homogeneous samples exist, where the large gel fragments have been broken to the smallest size capable under the applied shear.

Allowing the systems to rest and then performing the 2nd stress sweeps, revealed little changes in the G' and G'' values. Thus, the structures of the fluid gel samples (as monitored during the 2nd sweep) fully recovered to their initial state (as monitored during the 1st sweep) during the relaxation period.

For the 0.25 wt.% *LA* gellan gum fluid gel samples formulated using the shaft speeds of 500 and 275 rpm (Figures 5.7c and 5.7d), the structural recovery behaviours observed were almost identical to those found for the previous 0.25 wt.% samples (Figures 5.7a and 5.7b), for the storage and loss moduli, albeit with the former where the initial structural collapse took place over a slightly longer and broader shear stress range up until levels of $\sim 0.8 - 1$ Pa. These differences could be related to the reduced particle packing and volume fractions of the samples, associated with using lower shear rates during production, resulting in more elastic gels that either take longer to rupture, or are more influenced by the test-shear.

Increasing the *LA* gellan polymer concentration from 0.25 wt.% - 1 wt.%, yielded structural recovery behaviours at much higher G' and G'' values. This was once again reflective of the principle, that with increasing gellan concentration, firmer gels are produced, due to the subsequent increase in particle elasticity (Frith et al., 2002) and volume fraction (Norton et al., 1999).



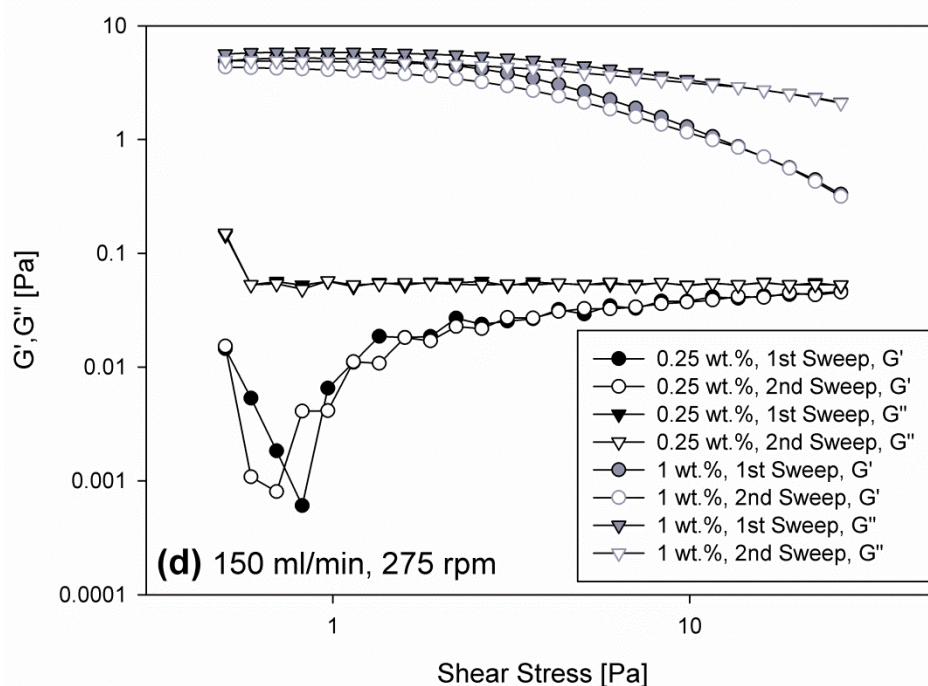
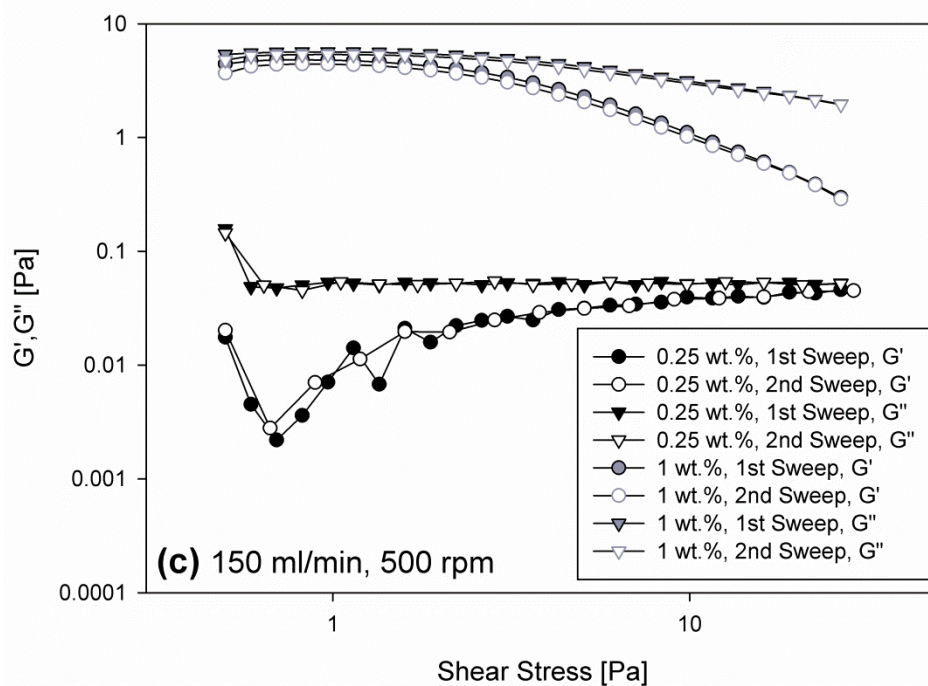


Figure 5.7. Storage (G') and loss (G'') moduli from stress-sweep measurements (1 Hz) for 0.25 and 1 wt.% low acyl gellan gum fluid gels produced using a jacketed pin-stirrer (20 °C at water bath, ~60 °C/min cooling rate) with a pump rate of 150 ml/min and shaft speeds of 1500 (a), 1000 (b), 500 (c) and 275 rpm (d). The 1st sweep was carried out 24 hours after the production of the fluid gels and, after a “resting” stage of 10 min, it was followed by a 2nd sweep. Each of the stress-sweep moduli values are based on a single sample measurement.

For the 1 wt.% *LA* gellan gum fluid gel samples formulated using the shaft speeds of 1500 and 1000 rpm (Figures 5.7a and 5.7b) the structural recovery behaviours observed were very similar; reinforcing that decreasing the pin-stirrer shaft speed during production has minimal impact on the subsequent gel recovery. For each sample, it was observed that the storage (G') and loss (G'') moduli remained constant until a shear stress of ~ 1 Pa was applied. The absence of fluid gel structural changes within this shear stress range implies that no inter-particle interactions are occurring within the systems. Increasing, the applied shear stress above ~ 1 Pa however, led to the failure and eventual collapse of the original fluid gel structures. Allowing the systems to rest and then performing the 2nd stress sweeps, revealed little changes in the G' and G'' values. Thus, the structures of the fluid gel samples fully recovered to their initial state during the relaxation period.

For the 1 wt.% *LA* gellan gum fluid gel samples formulated using the shaft speeds of 500 and 275 rpm (Figures 5.7c and 5.7d) the structural recovery behaviours observed were extremely similar to those found for the previous 1 wt.% samples (Figures 5.7a and 5.7b), although the G' and G'' values across the shear stress range were found to be slightly lower. These differences can be attributed to the reduced sample particle packing and volume fractions emanating from using low shear rates, and the fewer inter-particle interactions and bridging phenomena occurring, yielding weak gels.

The structural recovery behaviours were also assessed for the 0.25 and 1 wt.% *LA* gellan gum fluid gel samples formulated using the pump rates 50, 100 and 200 ml/min, at each shaft speed in Figure 5.7. The same trends observed for the two concentrations in Figure 5.7, as a function of decreasing shaft speed were also evident for each of the samples at the individual pump rates. In terms of recovery response, as a function of decreasing pump rate, minimal differences were found. This demonstrated that

increasing the exposure to a constant applied shear and cooling environment during fluid gel production, has minimal impact on subsequent gel recovery.

5.2.3.3. Identification of enthalpic conformational transitions using DSC

DSC measurements were performed on a selection of the 0.25 wt.% *LA* gellan gum fluid gel samples using a Setaram μ -DSC3 evo Dynamic Scanning Calorimeter (DSC) to identify the enthalpies and temperatures of the coil-helix transitions on both heating and cooling. Initially, the effect of increasing pump flow rate and consequently the applied cooling rate, of the hot *LA* gellan aqueous solution entering the pin-stirrer unit on the subsequent fluid gel thermal transitions was investigated. Figure 5.8 shows the endothermic and exothermic curves on heating (5.8a and 5.8b) and cooling (5.8c and 5.8d) for the 0.25 wt.% *LA* gellan fluid gels formulated within the pin-stirrer, using a constant shaft speed of 1500 rpm and pump rates of 50 and 100 ml/min (5.8a and 5.8c) and 150 and 200 ml/min (5.8b and 5.8d) respectively. The heat flow y-values have been manipulated to separate the respective curves for clarity. The corresponding calculated heat enthalpies (lost or gained by the solutions) and maximum heat flow temperature ($T_{\max.}$) values of the thermal transitions are displayed in Table 5.2.

On heating of the fluid gel samples, formulated using pump rates of 100, 150 and 200 ml/min (Figures 5.8a and 5.8b), no distinguishable differences in the temperatures of the melting peaks for both the fluid and quiescent equivalent gels, with increasing pump rate were observed. Each melting peak was in the range of ~ 19 °C (Table 5.2). There was also no evidence of the energies gained by the quiescent gel samples on melting, being greater than those of the fluid gels; identical energies were in fact, reported for the fluid and quiescent gels produced using the pump rates of 150 and 200 ml/min respectively

(Table 5.2). These results further support the notion that the fluid gel internal particle polymeric network, and therefore the elasticity of individual particles, is equivalent to that of their quiescently cooled counterparts (Caggioni et al., 2007; Frith et al., 2002).

0.25 wt.% Fluid Gel Sample: Pump Rate [ml/min] & Shaft Speed [rpm]	Melting (Fluid Gel), ΔH (J/g) [$T_{\max.}$ (°C)]	Gelation (Fluid Gel), ΔH (J/g) [$T_{\max.}$ (°C)]	Melting (Quiescent Gel), ΔH (J/g) [$T_{\max.}$ (°C)]	Gelation (Quiescent Gel), ΔH (J/g) [$T_{\max.}$ (°C)]
50, 1500	0.0190 [35.3]	-0.0200 [25.5]	0.0150 [26.1]	-0.0170 [25.5]
100, 1500	0.00884 [19.0]	-0.0110 [17.5]	0.00960 [19.2]	-0.0110 [17.7]
150, 1500	0.0110 [19.1]	-0.00961 [17.4]	0.0110 [18.9]	-0.00960 [17.3]
200, 1500	0.0100 [18.7]	-0.0110 [17.3]	0.0100 [18.7]	-0.0100 [17.1]
50, 1000	0.0250 [18.1]	-0.0100 [17.1] -0.00650 [25.0]	0.0200 [18.5]	-0.0110 [17.3] -0.00581 [24.8]
50, 500	0.00783 [18.5]	-0.00851 [17.1]	0.00682 [18.7]	-0.00790 [16.7]

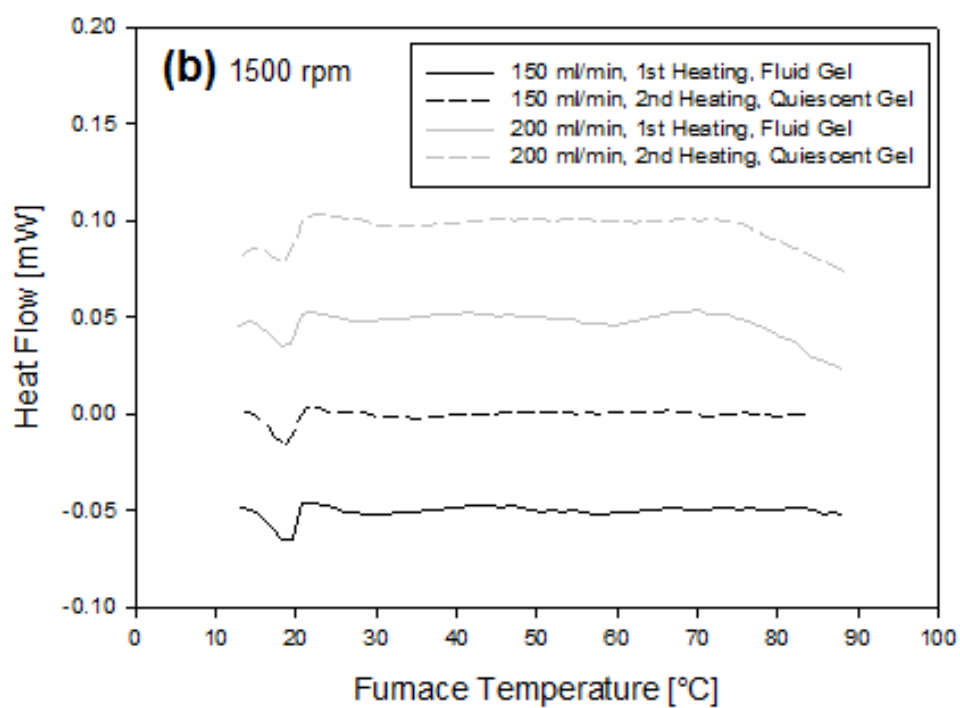
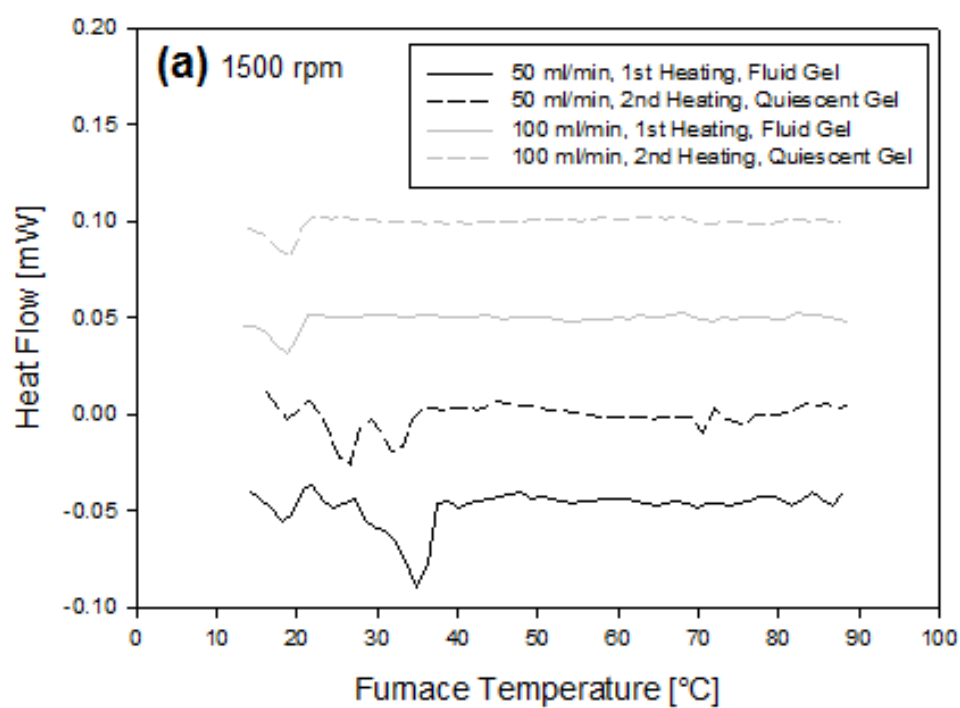
Table 5.2. Table of differential scanning calorimetry measurements (to 3 s.f.) for a selection of 0.25 wt.% low acyl gellan gum fluid gel samples produced using a jacketed pin-stirrer (average cooling rate, °C/min (per pump rate): 15 (50), 40 (100), 60 (150), 75 (200)) with varying pump rates (50 – 200 ml/min) and shaft speeds (1500 – 500 rpm), where ΔH is the amount of heat energy gained or lost by the solutions. Each of the ΔH and $T_{\max.}$ values are based on a single sample measurement.

On cooling of these samples (pump rates of 100, 150 and 200 ml/min), no distinguishable differences in the temperatures of the gelation peaks between the first and second runs, where the gels were formed quiescently, were observed either with increasing pump rate. Each peak was in the range of ~ 17 °C (Table 5.2), and indicates

a strong accuracy of the data. Thus, the observations made for the samples during the heating scans can confidently be assumed to be sound representations of the gels formed under sheared and quiescent conditions. The 2 °C shift in the temperature of the sample peak transitions on cooling also provides support for the results of the 1 and 2 wt.% *LA* gellan fluid gels formulated using the pin-stirrer (Section 5.2.1.5), where higher T_m 's and helix-coil transition temperature ranges were reported for the samples on heating, compared to those on cooling.

These DSC results imply that by increasing the pump rate during fluid gel formation and thus reducing the applied cooling rate and processing exposure time, no significant impacts to the measured thermal transitions (and therefore structure) post-production are made. It is expected that when forming fluid gels using the higher pump rates, greater bridging potential persists post-processing. Although, for these samples the structural ordering and stage at which it occurs during fluid gel formation does not seem to influence the DSC thermal transitions greatly.

A clear exception to the thermal trends observed for the fluid gel samples formulated using the pump rates of 100, 150 and 200 ml/min (Figures 5.8a – 5.8d), was found with the fluid gel sample formulated using the pump rate of 50 ml/min (Figures 5.8a and 5.8c). On melting of the fluid and equivalent quiescent gels formed using this condition, large peaks at higher temperatures of 35.3 °C and 26.1 °C respectively were observed (Figure 5.8a). The energies gained by each of the gels on melting, were also of a higher magnitude than those reported for the gels produced using the higher pump rates (Table 5.2). Analysing the thermal traces on heating for the 50 ml/min fluid and quiescent gel samples (Figure 5.8a) in greater detail however, it is clear that three coincidental peaks are evident. These melting peaks occur at ~ 19 °C, ~ 25 °C and ~ 35 °C.



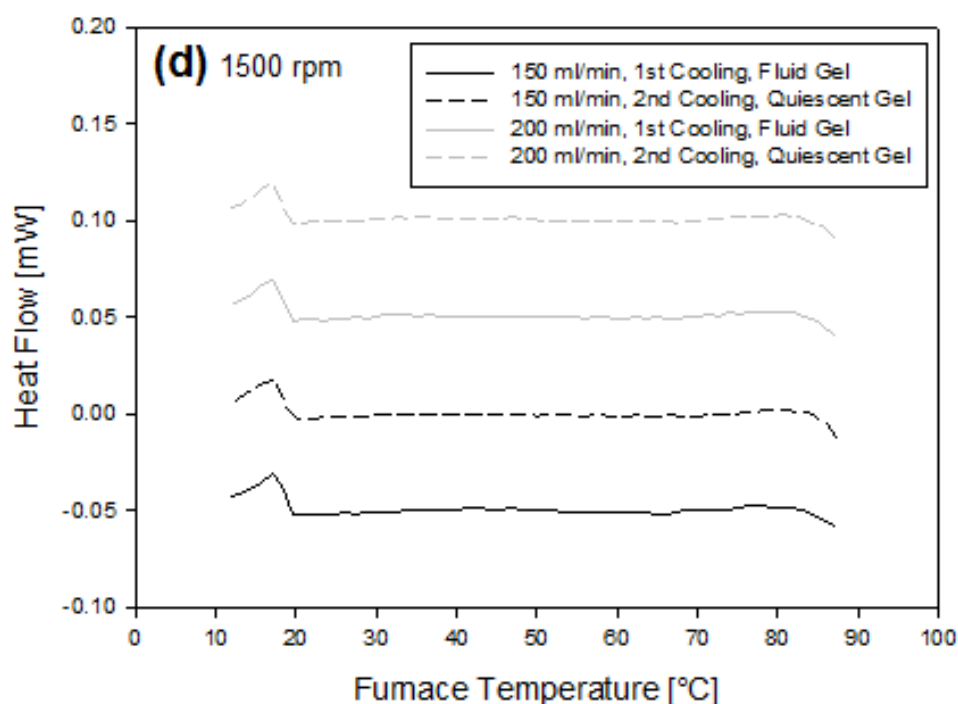
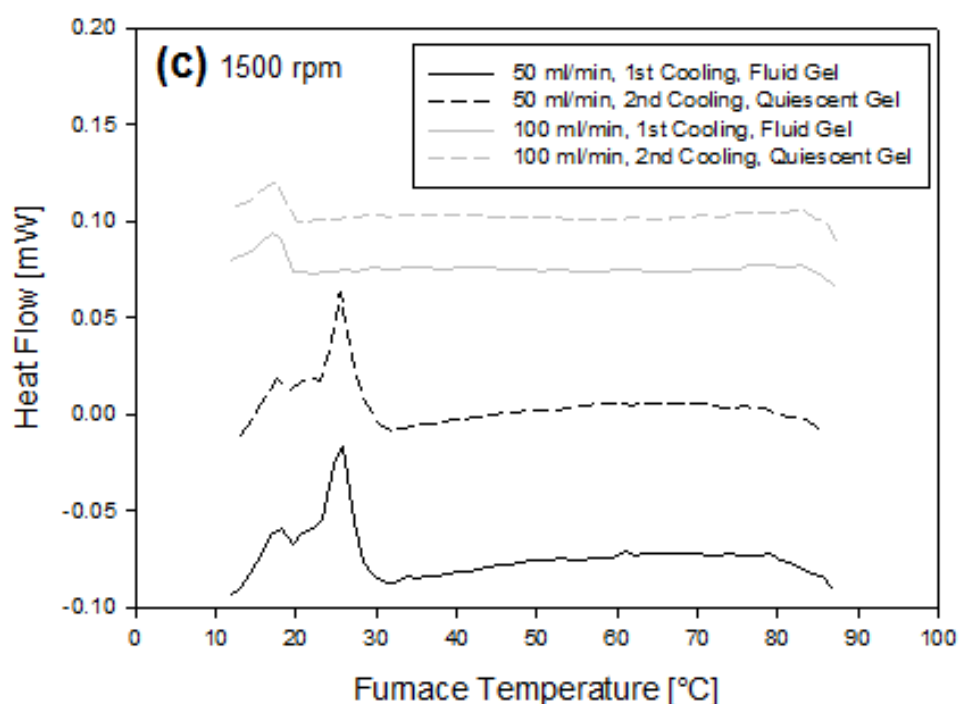


Figure 5.8. μ -DSC endothermic (heating) (a, b) and exothermic (cooling) (c, d) peaks (baseline subtracted) for 0.25 wt.% low acyl gellan gum fluid gels produced using a jacketed pin-stirrer (average cooling rate, $^{\circ}\text{C}/\text{min}$ (per pump rate): 15 (50), 40 (100), 60 (150), 75 (200)) with a shaft speed of 1500 rpm and pump rates of 50 and 100 ml/min (a, c) and 150 and 200 ml/min (b, d). A cooling and heating rate of $0.5\text{ }^{\circ}\text{C}/\text{min}$ was implemented. The first heating scan shows melting of a fluid gel; the second, a quiescent gel. Each curve is based on a single sample measurement, due to the lengthy experimental procedure of 11 hours, 40 minutes. Note that the curves have been separated (on the heat flow axis) for clarity.

The first melting temperature at $\sim 19\text{ }^{\circ}\text{C}$ is supportive of the previous thermal transition peaks observed for the gel samples formulated using the pump rates of 100, 150 and 200 ml/min. This suggests that the traces presented for the 50 ml/min fluid and quiescent gel samples (Figure 5.8a) are not a result of experimental error. The second and third melting peaks at $\sim 25\text{ }^{\circ}\text{C}$ and $\sim 35\text{ }^{\circ}\text{C}$ imply that at this lower pump rate, the fluid gels during their formation are exposed to longer periods of processing, which result in extensive inter-particle interactions and bridging. Thus, a more extensive and different helical network is formed, which is reflected in the subsequent DSC melting traces (Figure 5.8a). The low temperature peak at $\sim 19\text{ }^{\circ}\text{C}$ can be attributed to the melting of unaggregated helices, and the high temperature peaks at $\sim 25\text{ }^{\circ}\text{C}$ and $\sim 35\text{ }^{\circ}\text{C}$ to the melting of aggregated helices formed (Manning et al., 1992).

On cooling of the 50 ml/min fluid gel sample, two peaks were observed in both the first and second gelation traces (Figure 5.8c); a large one prominent at $\sim 25\text{ }^{\circ}\text{C}$, and a smaller one at $\sim 17\text{ }^{\circ}\text{C}$ (enthalpies and transition temperatures omitted from Table 5.2). The first gelation peaks at $\sim 17\text{ }^{\circ}\text{C}$ are similar to the previous cooling peaks observed at the same temperature, for the gel samples formulated using the pump rates of 100, 150 and 200 ml/min. Thus, the low ($\sim 17\text{ }^{\circ}\text{C}$) and high temperature ($\sim 25\text{ }^{\circ}\text{C}$) transition peaks were assigned to the melting of the unaggregated and aggregated helices formed, respectively.

A general finding from this data is that using only low pump rates (50 ml/min) during fluid gel production leads to gels that have extensive networks with aggregated and unaggregated helices, that each exhibit characteristic thermal transition behaviours.

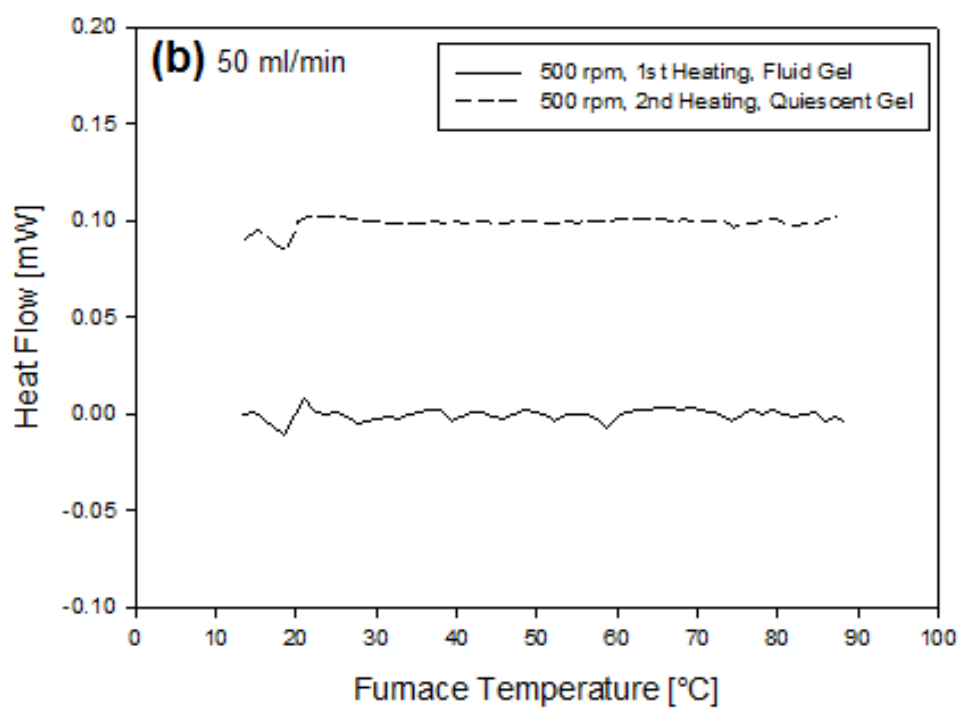
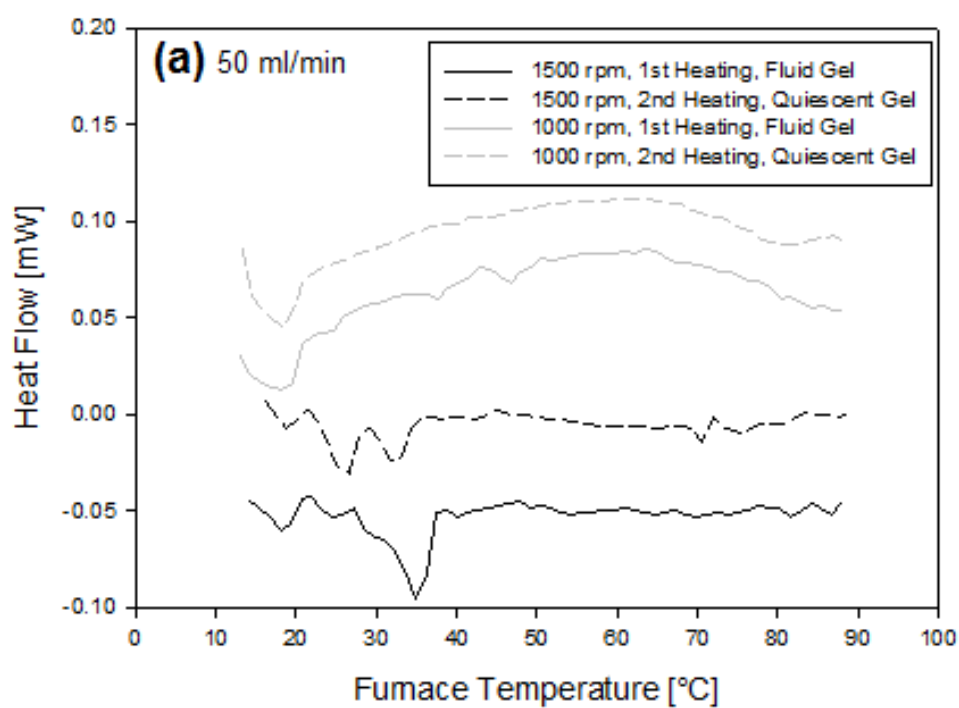
To investigate whether the trends for the 50 ml/min fluid gel samples were also evident for fluid gels formulated using reduced pin-stirrer shaft speeds and whether they

were influenced by them, DSC scans were performed on samples formulated using shaft speeds of 1000 and 500 rpm. Figure 5.9 shows the resulting endothermic and exothermic curves on heating (5.9a and 5.9b) and cooling (5.9c and 5.9d) for the 0.25 wt.% *LA* gellan fluid gels formulated within the pin-stirrer, using a constant pump rate of 50 ml/min and shaft speeds of 1500 and 1000 rpm (5.9a and 5.9c) and 500 rpm (5.9b and 5.9d) respectively. The heat flow y-values have been manipulated to separate the respective curves for clarity. The calculated heat enthalpies (lost or gained by the solutions), and maximum heat flow temperature (T_{\max}) values of the thermal transitions are enclosed in Table 5.2.

On heating, each of the fluid gel samples, formulated using shaft speeds of 500 and 1000 rpm displayed melting peaks at ~ 18.5 °C for both the fluid and quiescent equivalent gels (Figures 5.9a and 5.9b). Similar energies gained by the fluid and quiescent gel samples on melting were also reported (Table 5.2). No traces of higher melting peak transitions at ~ 25 °C and ~ 35 °C (as reported for the 50 ml/min, 1500 rpm sample in Figure 5.9a) were found for either sample. This suggested that unaggregated helical network regions are only evident when formulating fluid gel samples using a pump rate of 50 ml/min, in combination with reduced pin-stirrer shaft speeds.

On cooling however, identical gelation peaks were observed for the 50 ml/min, 1000 rpm sample at ~ 17 °C and ~ 25 °C for each run, as found for the 50 ml/min, 1500 rpm sample (Figure 5.9c). Although, the peak sizes at each temperature, and the energies lost by the former sample were much smaller. For the 50 ml/min, 500 rpm sample, only small, gelation peaks at ~ 17 °C were observed for each run (Figure 5.9d). These results suggest that, the combination of a low pump rate with a high pin-stirrer shaft speed is

needed to form a more comprehensive gel network that is formed of aggregated and unaggregated helices, which melt and form over several different temperatures. Formulating fluid gel samples using shaft speeds below 1000 rpm do not appear to satisfy a high enough proportion of inter-particle interactions (despite the low pump rate used) to form similar extended networks created with the higher shaft rates. This concept is reinforced by the failure to observe the higher melting peaks on heating for the 50 ml/min, 1000 rpm fluid gel sample, despite their appearances on cooling. This suggests that 1000 rpm is an intermediate rate that yields samples having packing fractions close to the threshold, producing extended gel networks.



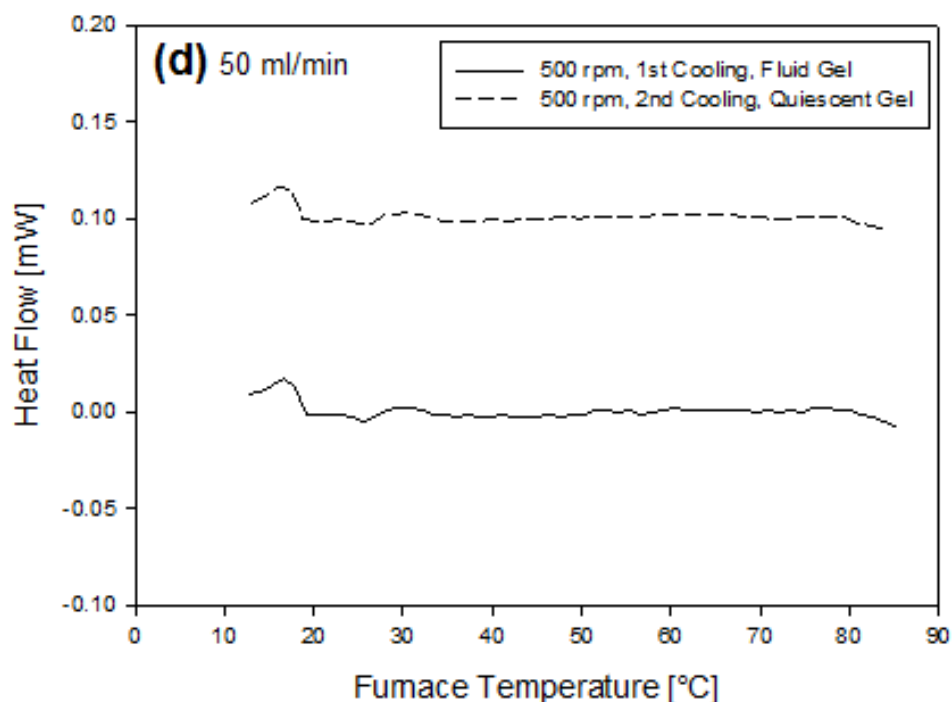
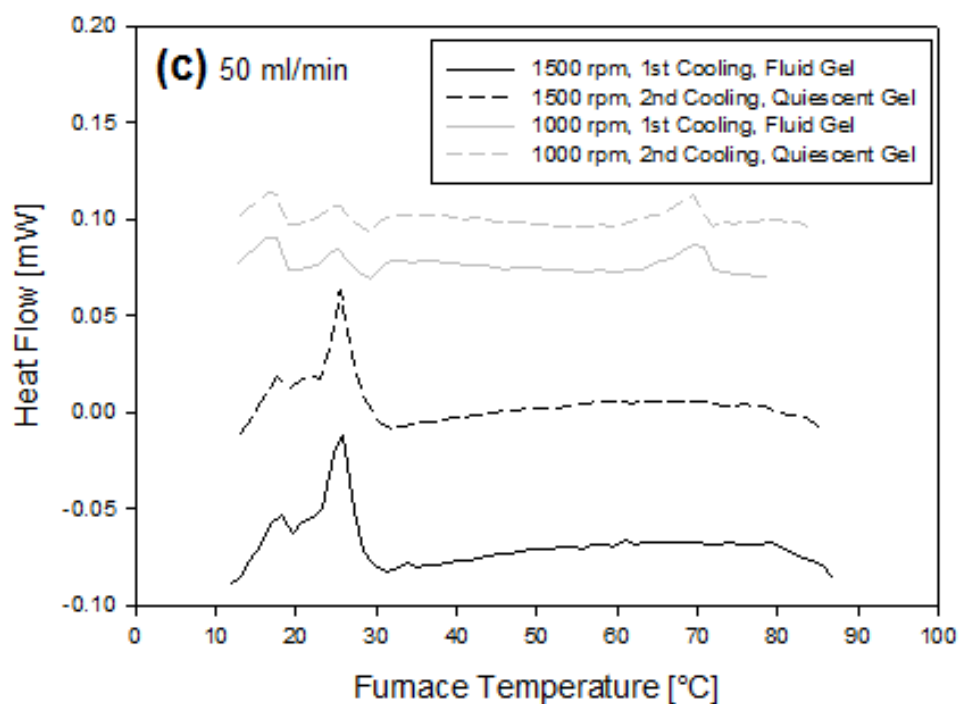
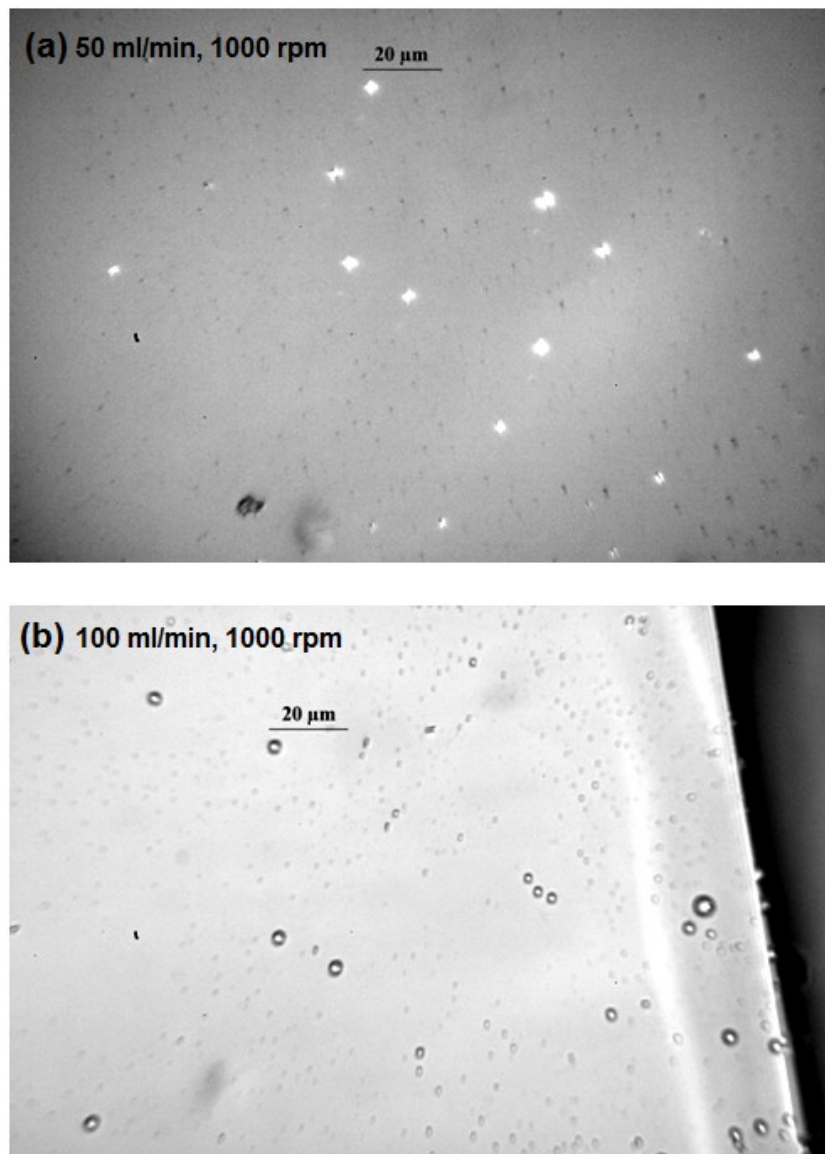


Figure 5.9. μ -DSC endothermic (heating) (a, b) and exothermic (cooling) (c, d) peaks (baseline subtracted) for 0.25 wt.% low acyl gellan gum fluid gels produced using a jacketed pin-stirrer (average cooling rate, $^{\circ}\text{C}/\text{min}$ (per pump rate): 15 (50), 40 (100), 60 (150), 75 (200)) with a pump rate of 50 ml/min and shaft speeds of 1500 and 1000 rpm (a, c) and 500 rpm (b, d). A cooling and heating rate of $0.5^{\circ}\text{C}/\text{min}$ was implemented. The first heating scan shows melting of a fluid gel; the second, a quiescent gel. Each curve is based on a single sample measurement, due to the lengthy experimental procedure of 11 hours, 40 minutes. Note that the curves have been separated (on the heat flow axis) for clarity.

5.2.3.4. Particle size determination

To investigate whether varying the pump flow rate, and in turn the applied cooling rate during *LA* gellan gum fluid gel production, effects fluid gel particle size and shape; optical observation was performed on samples (0.25 wt.%) formulated using a shaft speed of 1000 rpm, as a function of increasing pump rate (50 – 200 ml/min). The respective micrographs are shown in Figure 5.10.



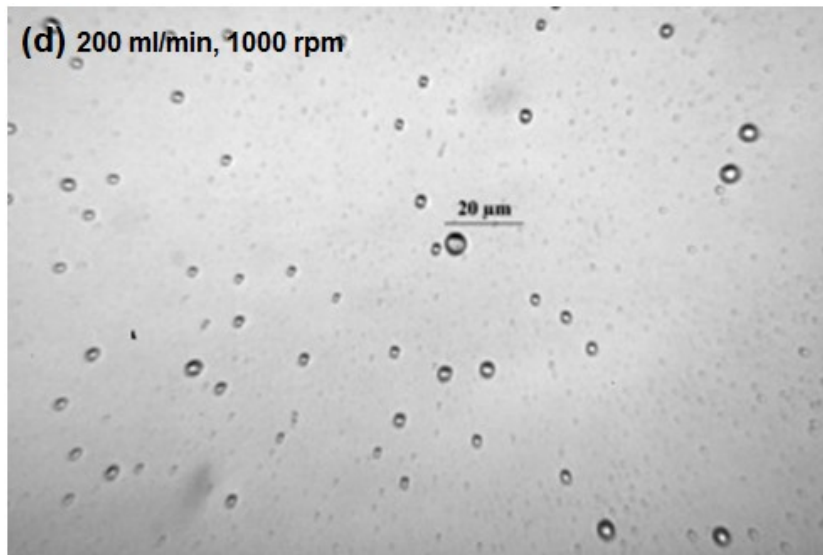
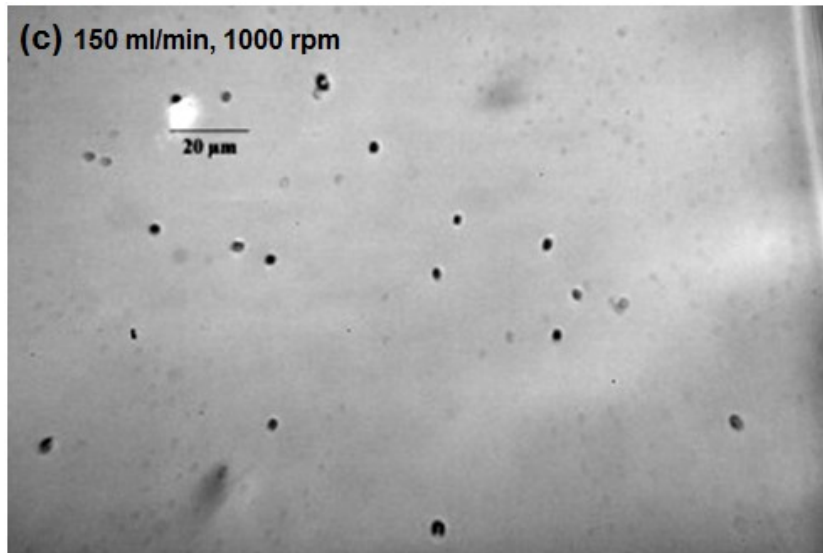


Figure 5.10. Micrographs for 0.25 wt.% low acyl gellan gum fluid gels produced using a jacketed pin-stirrer (average cooling rate, °C/min (per pump rate): 15 (50), 40 (100), 60 (150), 75 (200)) with a shaft speed of 1000 rpm and pump rates of 50 (a), 100 (b), 150 (c) and 200 ml/min (d). Scale = 20 μm .

Each micrograph revealed that irrespective of the applied pump rate, small particles of nearly spherical shape were obtained. In addition, it was also apparent for each fluid gel system, that even smaller ‘pin-like’ particles were present. This supports the mechanism suggested previously during rheological analysis of the fluid gels produced with the pin-stirrer using comparable shear (Section 5.2.1.4); that particles are formed from the growth of small gel nuclei, the size of which are determined by the shear environment. The shear environment for each of the *LA* gellan fluid gel samples represented in Figure

5.10 was kept constant by using a pin-stirrer shaft speed of 1000 rpm. The suggestion that particle size is determined by the shear environment is reinforced by the particle sizes obtained for these samples. Variable particle sizes for each sample were found; the effect of increasing pump rate (and thus the residence time of the aqueous solutions to the exposed shear) seemingly unrelated. The average size of the particles for the samples produced using the pump rates of 50, 100, 150 and 200 ml/min were $\sim 5.3 \mu\text{m}$, $\sim 4.7 \mu\text{m}$, $\sim 6.7 \mu\text{m}$ and $\sim 5.3 \mu\text{m}$ respectively. These experimental findings are in agreement with the theories published in the literature that state, that the size of the fluid gel particles is dictated by the dynamic equilibrium between two competing processes (Carvalho & Djabourov, 1997). These are the process by which the small gel nuclei grow (controlled by the cooling rate during fluid gel production), and the coalescence and break-up processes (controlled by the shear environment applied), which occur during the early stages of the process. In this work, the applied cooling rate was varied whilst using a constant shear rate of 1000 rpm, and was found to have no significant influence over particle size. This suggests therefore, that it is only the applied shear that determines the equilibrium particle size. Gabriele et al. (2009) reported that during the initial stages of fluid gel formation within the aggregation process, the gel nuclei are expected to behave as water-in-water emulsion droplets. Thus, increasing the applied shear rate during fluid gel production, should lead to a size reduction of the obtained particles; as demonstrated by Gabriele et al. (2009). Small, uniform fluid gel particles were obtained during this study when using the high pin-stirrer shaft speed, 1000 rpm, which suggests that this is indeed the case. Future work however, will need to focus on the influence of varying shear rate, in particular low shear rates, during *LA* gellan fluid gel production to see if the particles size dimensions can be manipulated in similar ways to those reported for kappa-carrageenan and agar by Gabriele et al. (2009, 2010).

5.2.4. Kinetic studies of low acyl gellan gum fluid gels produced using a rheometer

5.2.4.1. Effect of shear rate during fluid gel production

The effect of applied shear on the production of *LA* gellan gum fluid gels was initially investigated. This was assessed by measuring the viscosity of the fluid gel systems during their production process as a function of temperature and applied shear rate (0.5 – 1000 s⁻¹); the resulting viscosity profiles on cooling from 90 °C are shown in Figures 5.11a and 5.11b. All fluid gels were produced from the same 2 wt.% *LA* gellan gum “primary” solution, while the cooling rate during the production process was kept constant at 3 °C/min.

The obtained data across all shear rates shows that as the temperature of the system is lowered, a sharp increase in viscosity occurs at ~ 42 °C. This viscosity increase has been ascribed (Norton et al., 1998, 1999) to the formation of small gel nuclei (initiation of ordering), which begins close to the gelation temperature for the used hydrocolloid (30 – 50 °C). On continued cooling, the initially formed gel nuclei continue to grow until an equilibrium particle size, as determined by the shear regime, is reached. It is at this point that a fluid gel is considered to be formed.

The initial formation of the small gel nuclei is thought to be a consequence of a demixing process resulting in the formation of polymer-rich and polymer-poor regions in the system. Norton et al. (1998) suggested that demixing occurs either via spinodal decomposition or nucleation and growth. Either way, it is apparent that particles start to form in the early stages of the aggregation process, during which the nuclei are subjected to the applied shear forces and will appear to behave as water-in-water emulsion droplets; thus it is expected for both droplet coalescence and droplet break-up

phenomena to take place within the system (Gabriele et al., 2009). In terms of the growth of the fluid gel particles, it has been suggested (Norton et al., 1999) that this occurs either via an “enrichment” process of the initially small nuclei from the surrounding non-gelled matrix, or due to the coalescence/agglomeration of the particles being forced to unite under the applied shear flow. Thus, it is clear that the observed rapid increase in viscosity is a direct result of the continual increase in both the number and volume fraction of the formed particles, which occurs within a temperature range near the hydrocolloid’s gelation temperature.

Further reduction (below 30 °C) in the temperature of the systems presented in Figures 5.11a and 5.11b, results in the observed “sudden” viscosity increase to become much more gradual for all of the applied shear rates, except at 0.5 s⁻¹ where the viscosity is more irregular. For applied shear rates above 0.5 s⁻¹, the observed change in viscosity could be a result of further ordering of a small number of remaining disordered polymer chains within the particles and/or at their surface; conformational ordering persists even at temperatures much lower than the gelling temperature. This is expected to increase the size of the particles and thus the viscosity during their production. Additionally, the observed behaviour could be a consequence of the inter-particle interactions that take place as a result of the presence of disordered charged polymer chains at their surface (Norton et al., 1998) which bind to free ions in the surrounding and form inter-particle bridges. As the applied shear rate is increased these chains tend to cyclise towards the particle forming a much smoother surface and thus limiting the likelihood of any inter-particle interactions, which in turn results in the observed decrease in the “end” viscosity as a function of the applied shear. Consideration should also be taken to the contribution to the increase in viscosity with decreasing temperature, typically known to obey an Arrhenius model.

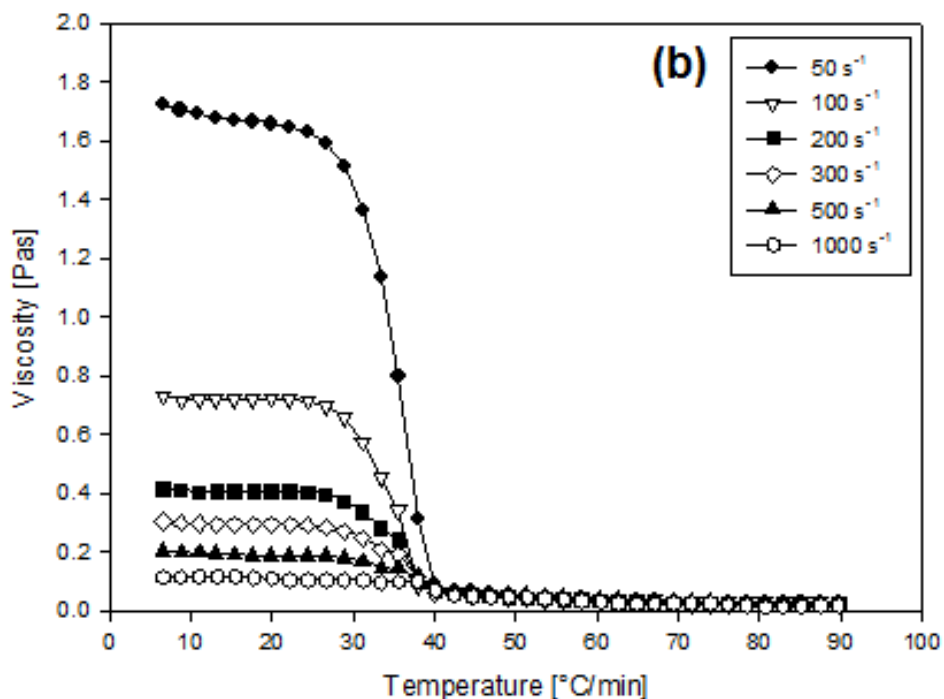
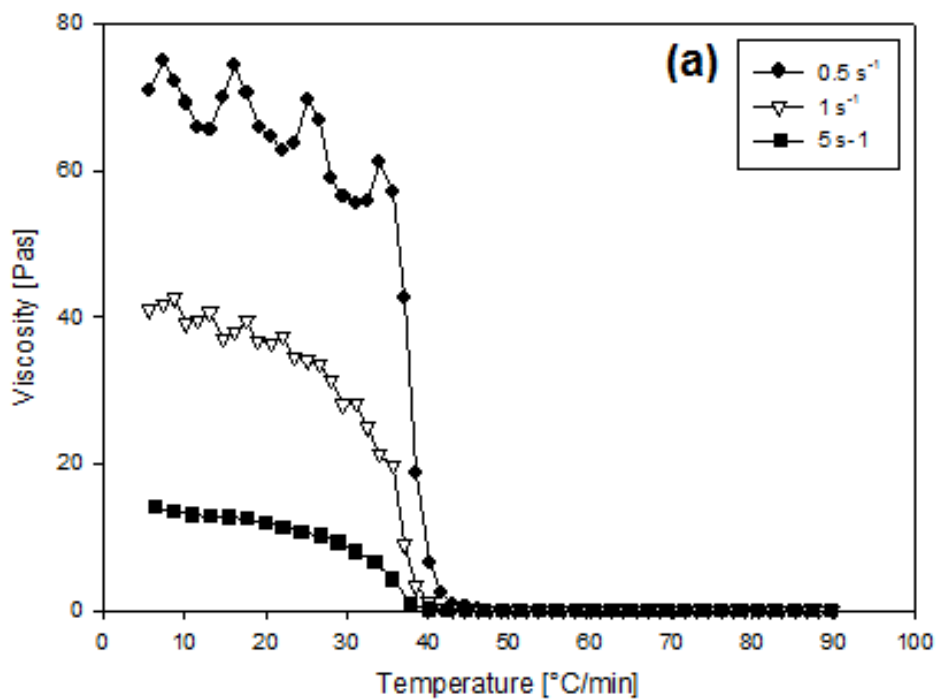


Figure 5.11. Viscosity profiles of 2 wt.% low acyl gellan gum fluid gels, during their production process, as a function of the applied shear rate ($0.5 - 1000 \text{ s}^{-1}$). All systems were subjected to a constant cooling rate of $3 \text{ }^{\circ}\text{C}/\text{min}$ from $90 - 5 \text{ }^{\circ}\text{C}$. Each of the viscosity readings at each shear rate are based on a single sample measurement.

The irregular viscosity behaviour observed for the 0.5 s^{-1} (Figure 5.11a) applied shear rate as the temperature is reduced below $30 \text{ }^{\circ}\text{C}$, can be explained by the notion suggested by Gabriele et al. (2009) that “due to the low shear involved, the fluid gel particles are growing in size much faster and are much more “reactive” in terms of interacting with each other and creating aggregates. As a result their viscosity increases much more rapidly with decreasing temperature”. The formed fluid gel particles also reach large dimensions (100’s of micrometres) that become increasingly affected by the applied shear forces. Therefore, they are more likely to be broken up into gel particulate fragments, resulting in the erratic viscosity decrease-increase regions observed below $30 \text{ }^{\circ}\text{C}$.

5.2.4.2. The coil-helix transition

Low-amplitude oscillatory deformation tests were performed on the 2 wt.% *LA* gellan gum fluid gel samples formulated in the rheometer using a cooling rate of $3 \text{ }^{\circ}\text{C}/\text{min}$ and a range of shear rates ($0.5 - 1000 \text{ s}^{-1}$) after their formation, during heating and cooling. These enabled the helix-coil and coil-helix transition temperatures to be identified, allowing an improved understanding into the molecular ordering.

Figure 5.12 shows the G' and G'' at 1.585 Hz for the 2 wt.% *LA* gellan gum fluid gel, produced within a rheometer using an applied shear rate of 50 s^{-1} and a cooling rate of $3 \text{ }^{\circ}\text{C}/\text{min}$, following frequency tables from $0.1 - 10 \text{ Hz}$ every $10 \text{ }^{\circ}\text{C}$ during temperature heating (a) and cooling (b) ramps between $20 - 90 \text{ }^{\circ}\text{C}$. On heating, the aggregated regions must be disassembled before the helix-coil transition can occur. This is represented by the steep decrease in G' between $20 - 30 \text{ }^{\circ}\text{C}$, with the helix-coil transition occurring thereafter between $30 - 70 \text{ }^{\circ}\text{C}$. Above $70 \text{ }^{\circ}\text{C}$, the solution exists in the disordered coil state. However, a steep increase in G' is evident between $80 - 90 \text{ }^{\circ}\text{C}$.

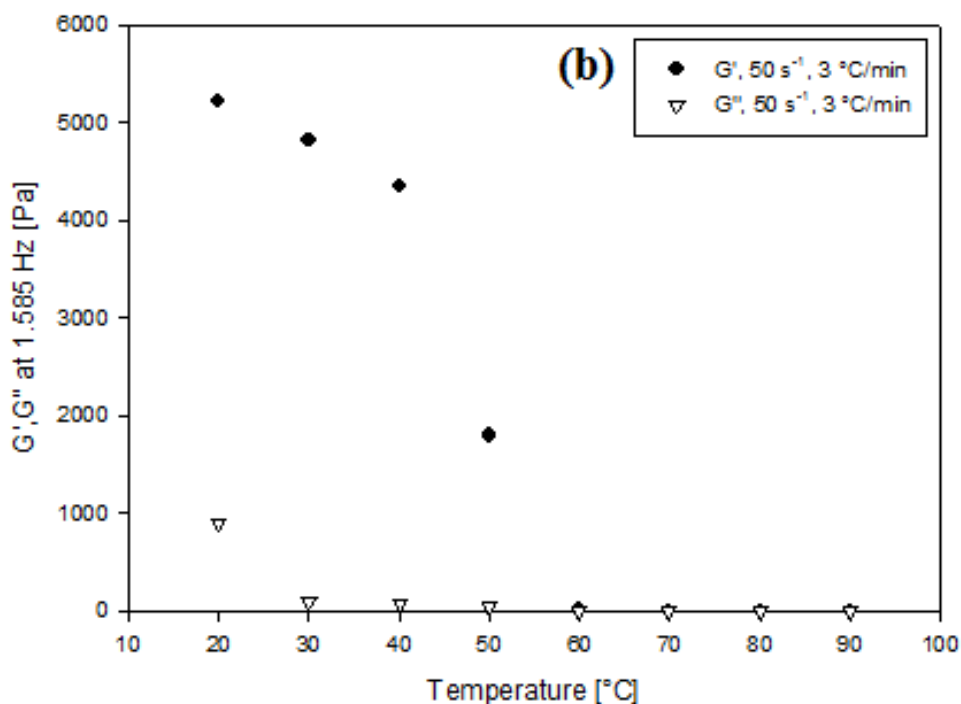
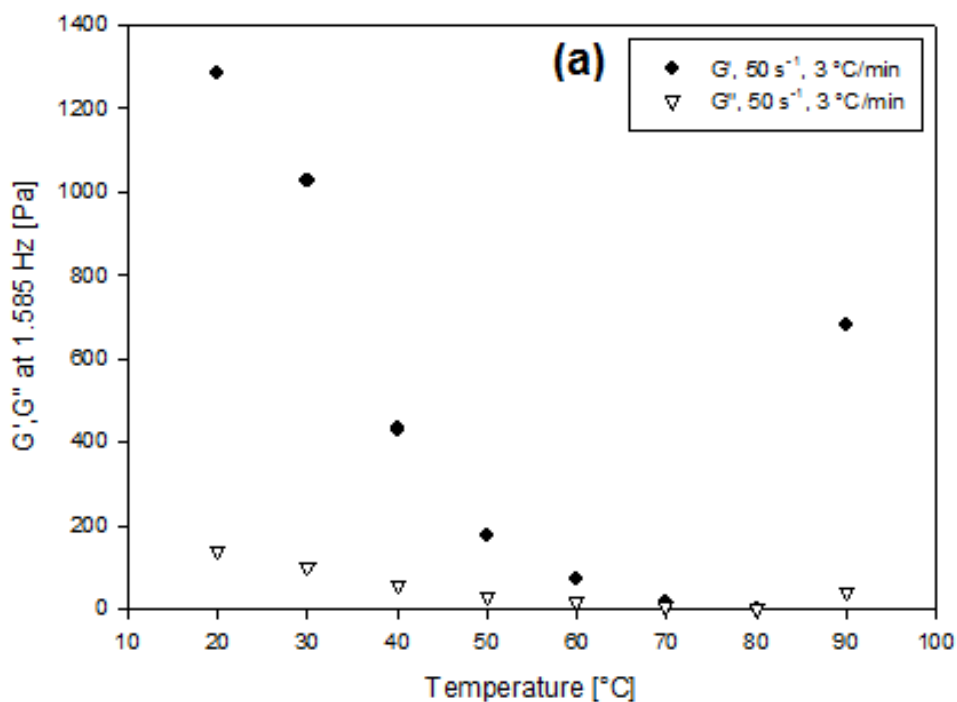


Figure 5.12. Storage (G') and loss (G'') moduli at 1.585 Hz for 2 wt.% low acyl gellan gum fluid gels produced within a rheometer (50 s^{-1} applied shear rate, $3 \text{ }^\circ\text{C}/\text{min}$ cooling rate) following frequency tables from 0.1 – 10 Hz every $10 \text{ }^\circ\text{C}$ during temperature heating (a) and cooling ramps (b) between 20 – 90 $^\circ\text{C}$. Each of the modulus readings are based on a single sample measurement.

The G' data point at 90 °C however, is most likely to be a result of sample evaporation at this high temperature. This leads to an increased concentration of the gellan aqueous solution, forcing the disordered coils closer together causing them to have restricted mobility, and hence increased solid-like character.

The midpoint temperature (T_m) is the midpoint between the two linear regions corresponding to disordered and ordered polymer conformations. The temperatures of the start of these two linear regions for each gellan concentration were identified (30 °C and 70 °C, respectively) for the coil-helix transitions in Figure 5.12a and the mid-point temperature between them calculated to give $T_m = \sim 50$ °C. Note that with this method of broadly assigning the respective ordering transitions, it is impossible to give a more accurate result of the T_m than an approximation. T_m represents the temperature at which the numbers of moles of saccharide residues in the disordered and ordered state are equal, and where the events of helix growth ('zipping-up') and decay ('un-zipping') are occurring at equal rates (Goodall & Norton, 1987).

During the frequency test on cooling (Figure 5.12b), one monitored the formation of a quiescently cooled gel, since the test was performed immediately after fluid gel production with no external shear force applied, from 90 – 20 °C, and the sample had to be heated to 90 °C first (i.e. melting the fluid gel). As with heating, three distinct conformational regions exist in the G' data: 90 – 60 °C, the solution exists in the disordered state; 60 – 40 °C, the coil-helix transition occurs; 40 – 20 °C, formation of an ordered structure via aggregation. For the coil-helix transition, the $T_m = \sim 50$ °C. The coil-helix transition has been described as a dynamic equilibrium where the rate constant at T_m is zero, and on decreasing temperature the likelihood of growth events is increased relative to those of decay (Norton et al., 1983). Thus molecular rearrangements to both quiescent and fluid gels, via decay and growth mechanisms are reduced on decreasing

temperature below T_m . The growth mechanism likely to be responsible for the formation of the quiescent *LA* gellan gel in Figure 5.12b, involves intermolecular association of the polymer molecules in the solution during the coil-helix transition, which result in the formation of small, soluble clusters of chains. As the extent of association increases (as the temperature is reduced) these clusters grow, until ultimately one becomes large enough to span the entire volume of the solution and form a continuous crosslinked network (Morris et al., 2012).

For both Figures 5.12a and 5.12b, the G' values across the temperature range are greater than those recorded for G'' , from the point of gel ordering completion to the region where the solution is first in the disordered coil state. During this latter region, the values follow identical pathways. Interestingly, the G' values reported for the formation of the quiescent gel (Figure 5.12b) are of a higher magnitude (~ 5 times), than those for the melting of the fluid gel (Figure 5.12a). In the absence of shear, interparticulate helices form, thus the products require a greater force to allow the particles to move past one another and store more energy (greater G') (Norton et al., 1998; Garrec & Norton, 2012).

It has been suggested that the *LA* gellan gum fluid gel internal particle polymeric network, and therefore the elasticity of individual particles, is equivalent to that of their quiescently cooled counterparts (Caggioni et al., 2007). The fact that very similar viscoelastic responses with temperature were observed for the fluid gel produced under shear using the rheometer, and with the quiescent gel formed on cooling in the absence of shear (Figures 5.12a and 5.12b) suggests that this is correct. Particularly, since the study also found that the true gels formed on quiescent cooling had higher moduli than the “weak gels” formed under shear.

Referring back to the fluid gel samples (2 wt.%) produced using the jacketed pin-stirrer, the probing of their subsequent quiescent gels, exhibited similar viscoelastic responses (Section 5.2.1.4, Figures 5.4a and 5.4b) with temperature on cooling and heating to the fluid gels formed using the rheometer. On cooling and heating the three distinct conformational regions were observed in the G' data, with very slight range variations. On heating these were: 20 – 40 °C, disassembling and melting of the thermally unstable, ordinary double helical aggregates; 40 – 60 °C, helix-coil transition; and 60 – 90 °C, where the solution existed in the disordered coil state. A direct comparison can be made between the melting of the quiescent gel (Figure 5.4b) from the fluid gel sample produced using the jacketed pin-stirrer method, and the melting of the fluid gel (Figure 5.12a) formulated using the rheometer method. Each display expected thermal hysteresis trends, where the gels melt at higher temperatures than at which they form. The distinguishable difference however, is the larger temperature ranges recorded for the quiescent gel (Figure 5.4b) during the initial disassembly and latter disordered coil-state respectively. These reflect the longer time periods needed to melt the more extensive helical bridging connections and thermally-stable, aggregated helices and junction zones prevalent in the quiescent gels. The greater elasticity values recorded, when compared to those for the melting of the fluid gel also reflect the higher energy magnitude required to achieve this.

The mid-point temperatures on cooling and heating for the quiescent gels from the fluid gel samples (2 wt.%) produced using the jacketed pin-stirrer were $T_m = \sim 42.5$ °C and $T_m = \sim 50$ °C respectively. These, in addition to the helix-coil and coil-helix transition ranges recorded for both fluid gel production methods agree well with the gel phase transition temperatures reported in the literature for *LA* gellan gum (García et al., 2011). They also reinforce the ordering initiation temperature of 42 °C from the

viscosity measurements during *LA* gellan gum fluid gel formation (2 wt.%) within the rheometer (Figures 5.11a and 5.11b).

The quiescent gels from the fluid gel samples formulated using the jacketed pin-stirrer also had G' values across the temperature range that were greater than those recorded for G'' (Figure 5.4a and 5.4b). Additionally, the viscoelastic measurements reported for the fluid gels using the rheometer method were found to be approximately 3 times smaller than those reported in Figures 5.4a and 5.4b for the pin-stirrer gel samples. These observations can be explained through the fact that the fluid gel samples formed using the jacketed pin-stirrer were allowed to rest for 24 hours after production, prior to rheological testing to allow for post-ripening effects to occur. Thus, the fluid gel structure was able to fully develop, allowing interparticle interactions to occur and interparticulate helices to form, in turn storing more energy (greater G').

For each production method, the fluid gel samples displayed similar G'' measurement pathways. Both shared almost identical values to the G' up until the end of the helix-coil transition at 60 °C and 70 °C, and start of the coil-helix transition at 55 °C and 60 °C for the jacketed pin-stirrer and rheometer methods respectively (Figures 5.4a and 5.12b). Thereafter, a steady increase was observed, which is reflective of the samples' elastic distortion of the entangled/disentangled network during structural rearrangement, in response to the low-amplitude oscillatory deformation perturbation (Morris et al., 2012).

Low-amplitude oscillatory deformation tests were also performed on the 2 wt. % *LA* gellan gum fluid gel samples formulated in the rheometer using a cooling rate of 3 °C/min, for the remaining seven shear rates (0.5, 1, 5, 200, 400, 600 and 1000 s⁻¹) after their formation, during heating and cooling. Very similar structural ordering to that observed for the 50 s⁻¹ gel in Figure 5.12 was found for each sample on both heating and

cooling, with the three distinct conformational regions being present and the T_m 's = ~ 50 °C. Increasing the applied shear rate during fluid gel formation resulted in reduced G' and G'' values. This is consistent with varying the applied shear rate during fluid gel production in Section 5.2.4.1 on the resulting gel viscosity. Thus, it can also be attributed to the cyclisation of disordered charged polymer chains at the molecular surface towards free ions in the surrounding, forming much smoother surfaces that limit the likelihood of any interparticle interactions (Norton et al., 1998) giving decreased viscoelastic behaviour with increasing shear rate.

5.2.4.3. Viscometric material response post fluid gel production

The size of the fluid gel particles is dictated by the dynamic equilibrium between two competing processes (Carvalho & Djabourov, 1997). These are the process by which the small gel nuclei grow, controlled by the cooling rate during fluid gel production and the coalescence and break-up processes, which occur at the initial stages of the process, and are controlled by the shear environment applied. When producing fluid gels using the rheometer, the applied cooling rate is constant (3 °C/min), which suggests that it is only the applied shear that determines the equilibrium particle size. Therefore, increasing the applied shear rate during fluid gel production should indeed result in a size reduction of the obtained particles (Gabriele et al., 2009).

In order to investigate whether these assumed differences in the particle size of the fluid gel, have an effect on the post-production flow behaviour of these systems the following analysis was performed. The viscosity of fluid gel samples (2 wt.%), produced using a range of applied shear rates (0.5 – 1000 s⁻¹) and at a constant cooling rate of 3 °C/min, was measured immediately after the end of their formation process; the data of

which is shown in Figure 5.13. After production, all samples exhibited virtually identical shear thinning behaviour, despite the assumed differences in particle size between them. Very slight fractional differences in the viscosities were observed with increasing shear rate; with a higher shear rate giving rise to smaller values. However, since these were so small, identical shear thinning behaviour was acknowledged. The reason behind this behaviour is that in highly concentrated systems of (nearly spherical) particles, the flow is characterised on the micro scale by the relative flow of particles “squeezing” past each other. The bulk viscosity would thus be a direct function of the deformability (intrinsic elasticity) and packing of the particles, similarly to the behaviour of highly “packed” emulsions (Mason et al., 1996).

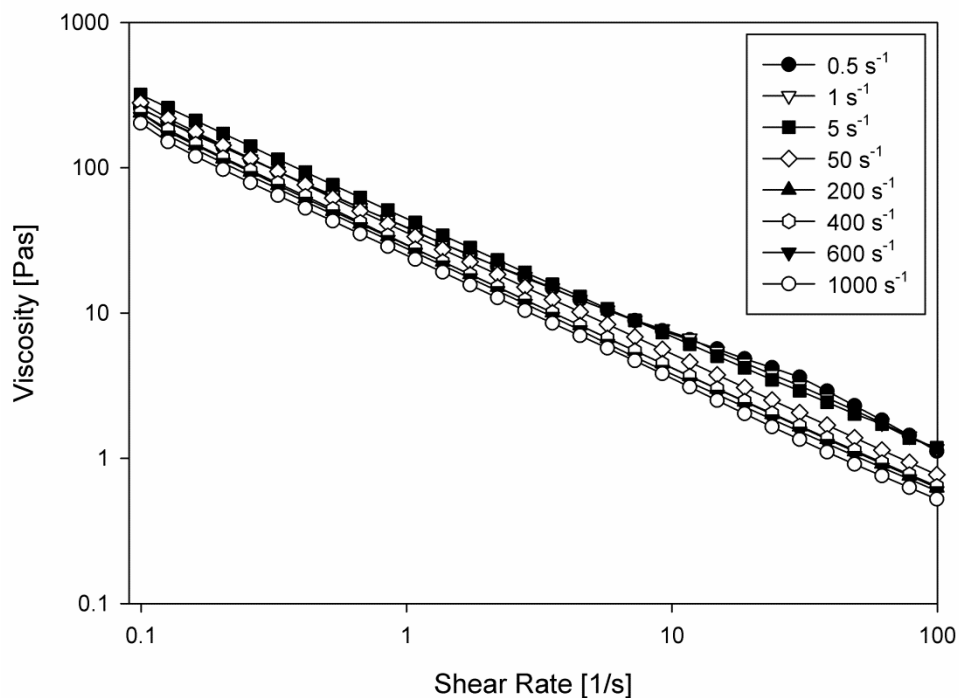


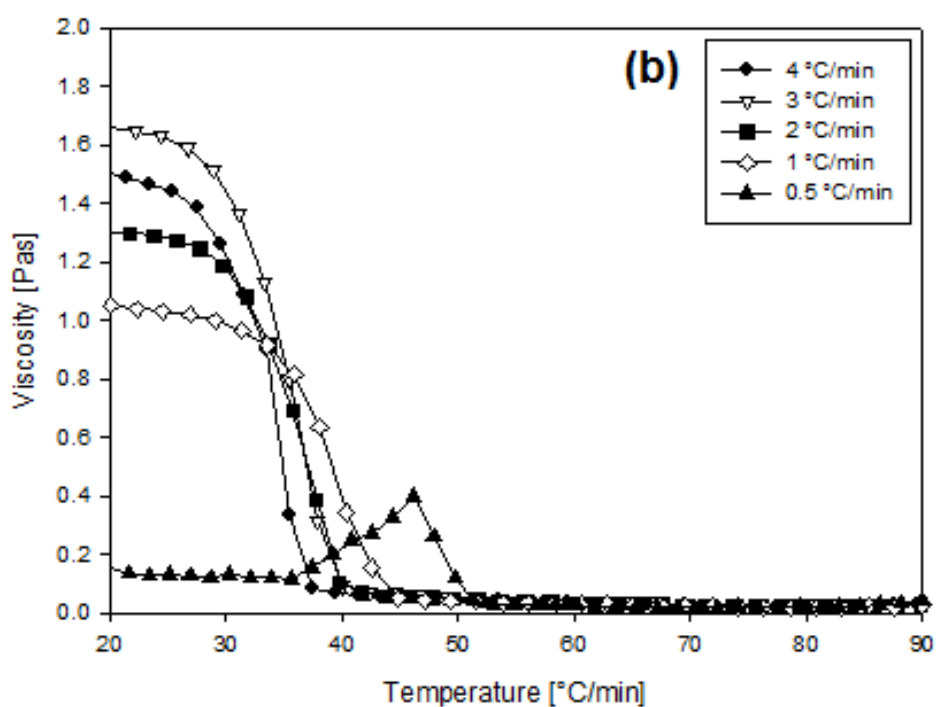
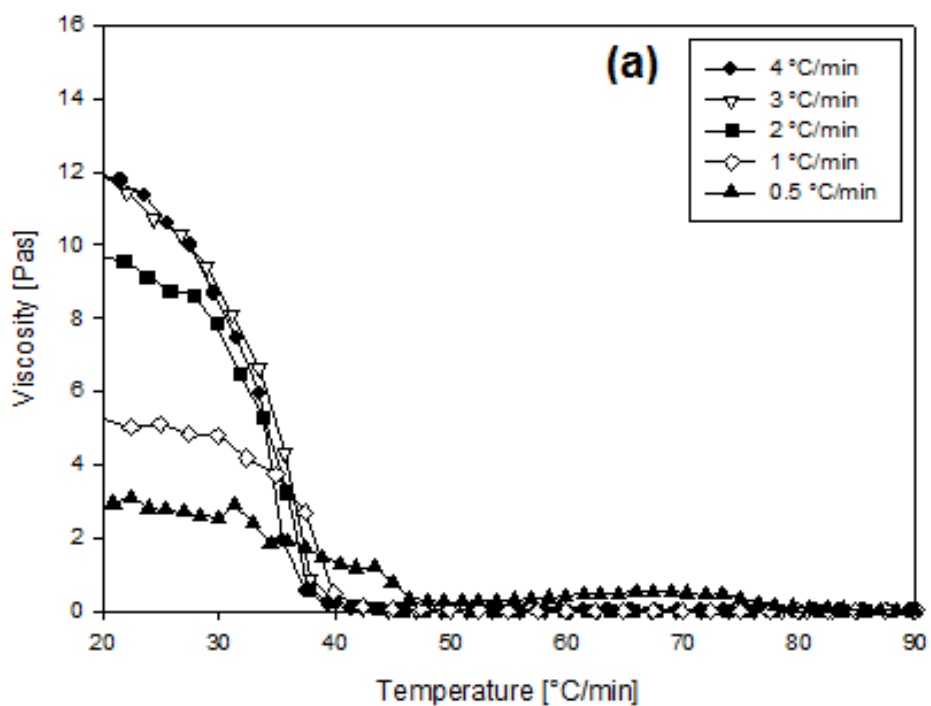
Figure 5.13. Shear thinning behaviour of 2 wt.% low acyl gellan gum fluid gels (produced within a rheometer using a range of applied shear rates ($0.5 - 1000 \text{ s}^{-1}$)), measured immediately after their formation process. All systems were subjected to a constant cooling rate of $3 \text{ }^{\circ}\text{C}/\text{min}$ between $90 - 5 \text{ }^{\circ}\text{C}$ during formation. Each viscosity value is based on a single sample measurement.

For the fluid gels produced using the jacketed pin-stirrer (Section 5.2.1), the applied shear (1500 rpm) and cooling rate ($\sim 30 \text{ }^{\circ}\text{C}/\text{min}$) were kept constant throughout, thus the

effect of applied shear on fluid gel particle size was not monitored. Instead, the post-production flow behaviour was measured by recording the viscosity of the fluid gel samples, 24 hours post-production, as displayed in Figure 5.1. Almost identical shear-thinning flow behaviour is observed between the 2 wt.% *LA* gellan fluid gels formulated using the jacketed pin-stirrer (Figure 5.1) and the fluid gel sample produced using the rheometer at the calculated equivalent shear rate of 50 s^{-1} (Figure 5.13). It could be assumed therefore, that the two fluid gel samples formed using these distinctive production methods, result in respective particle sizes on comparable scales. However, further research using microscopy is required to prove whether this is the case.

5.2.4.4. Effect of cooling rate during fluid gel production

The effect of the applied cooling rate on the production of *LA* gellan gum fluid gels was also investigated. This was assessed by measuring the viscosity of each of the investigated fluid gel systems throughout their production process as a function of temperature and for a range of applied cooling rates ($0.5 - 4 \text{ }^\circ\text{C}/\text{min}$). All fluid gels were produced from the same 2 wt.% *LA* gellan gum “primary” solution, while the applied shear rate during the production process was kept constant initially at 5 s^{-1} , 50 s^{-1} , 200 s^{-1} and 1000 s^{-1} . The resulting viscosity profiles as a function of the applied cooling rate are shown in Figures 5.14a, b, c and d respectively. The data revealed that as the applied cooling rate is reduced, and for all applied shear rates, the viscosity of the systems decreases. Small differences in the viscosities were found between the higher cooling rates of $4 - 2 \text{ }^\circ\text{C}/\text{min}$, with much larger differences being observed thereafter for the slower rates ($1 - 0.5 \text{ }^\circ\text{C}/\text{min}$). Also with decreasing temperature during fluid gel formation, the rapid increases in viscosity observed for each sample (Section 5.2.4.1) occurred much earlier at higher temperatures, with decreasing cooling rate.



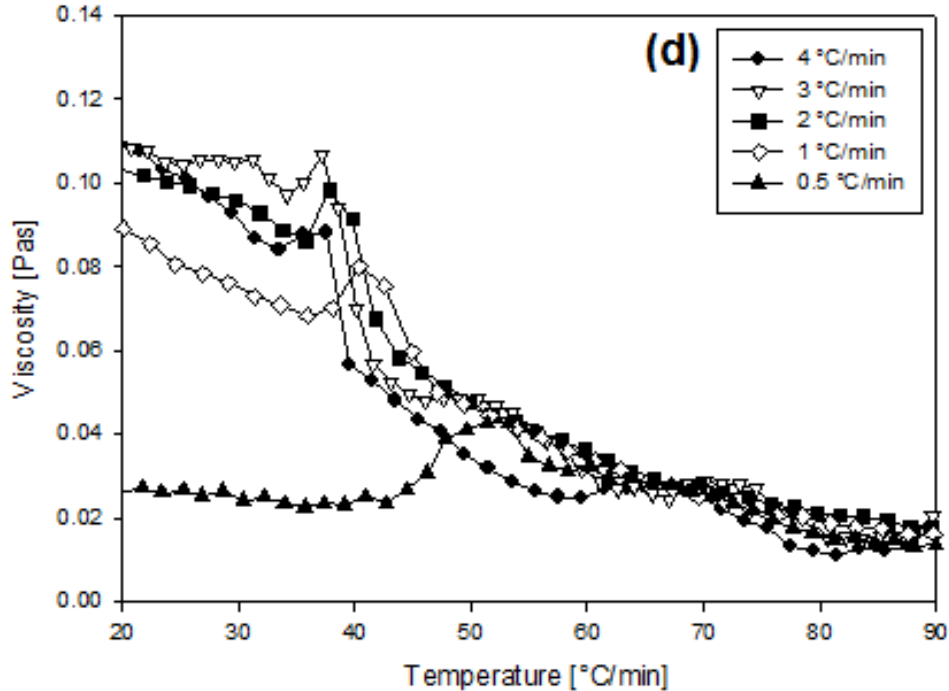
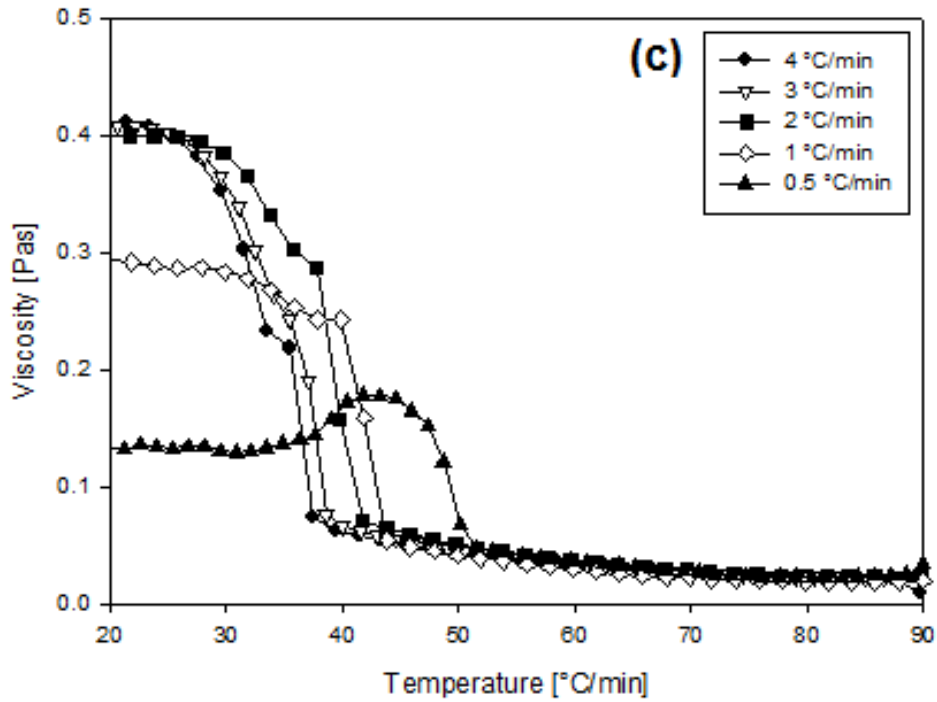


Figure 5.14. Viscosity profiles of 2 wt.% low acyl gellan gum fluid gels, during their production process, as a function of the applied cooling rate (0.5 – 4 °C/min). All systems were subjected to a constant shear rate of (a) 5 s⁻¹, (b) 50 s⁻¹, (c) 200 s⁻¹ and (d) 1000 s⁻¹ between 90 – 5 °C. Each viscosity value is based on a single sample measurement.

Changing the applied cooling rate influences the duration of the fluid gel process, with a reduced cooling rate giving rise to a longer processing time and vice-versa. It is expected that the lower the cooling rate applied during fluid gel formation, the greater the rate at which gelation occurs. For the applied cooling rate of 0.5 °C/min in Figures 5.14a – d when compared to the higher rates, it is observed that the onset of rapid gel particle ordering and growth occurs in the temperature range of 48 – 56 °C; ~ 10 °C earlier than for the higher cooling rates. Within this range the fluid gel particles are growing in size much faster and are more “reactive” in terms of interacting with each other and creating aggregates, than for the equivalent ranges observed for the higher rates. As a result the viscosity increases much more rapidly with decreasing temperature, and over a shorter temperature range. As the particles become very large, they are likely to be broken up by the shear, resulting in the viscosity reduction that follows (Figures 5.14a-d). The molecular damage caused by breaking the large particles, yields heterogeneous fluid gel samples, formed of gel particles and broken up fragments, leading to weak gels with increased viscosity. However, because the gel sample is still being subjected to a constant shear and cooling environment, interparticle interactions diminish and the broken gel fragments are sheared to form a homogeneous sample of small, evenly sized gel particulates with low viscosity behaviour.

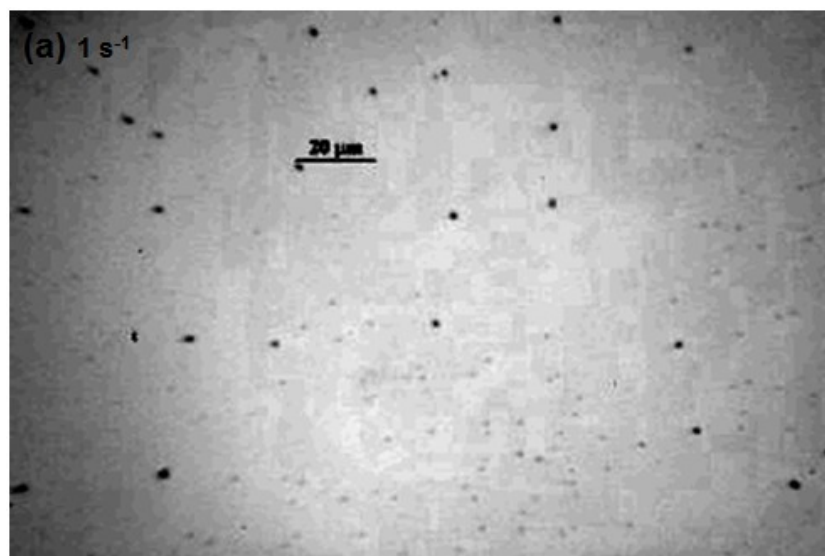
With high cooling rates the gelation process dominates and fluid gels are produced that have high G' characteristics, and thus more solid-like behaviour reflecting larger, more irregularly shaped particles (Cox et al., 2009). This is consistent with what is being observed for the higher cooling rates of 4 – 2 °C/min in Figure 5.14. These large particles are then broken up by the shear, causing structural damage. However, due to the rapid growth in gel particles occurring at lower temperatures (than those at 0.5

°C/min), the particulates are unable to grow to their maximum size before the end of the experimental cooling period to be largely affected by shear damage.

5.2.4.5. Particle size determination

To investigate whether the applied rate of shear during *LA* gellan gum fluid gel production has an influence on fluid gel particle size and shape, micrographs were obtained for the samples (2 wt.%) formulated using shear rates of 1, 5, 50 and 100 s⁻¹, with a cooling rate of 1 °C/min. Samples were taken from the fluid gel systems under investigation in their pure forms, with no further manipulation. The respective micrographs are shown in Figure 5.15.

Each micrograph revealed that irrespective of the applied shear rate, small particles of nearly spherical shape were obtained. It was also apparent for each fluid gel system, that even smaller ‘pin-like’ particles were present too. This supports the previous suggested mechanism (Section 5.2.4.1); that particles are formed from the growth of small gel nuclei, the size of which is determined by the shear environment.



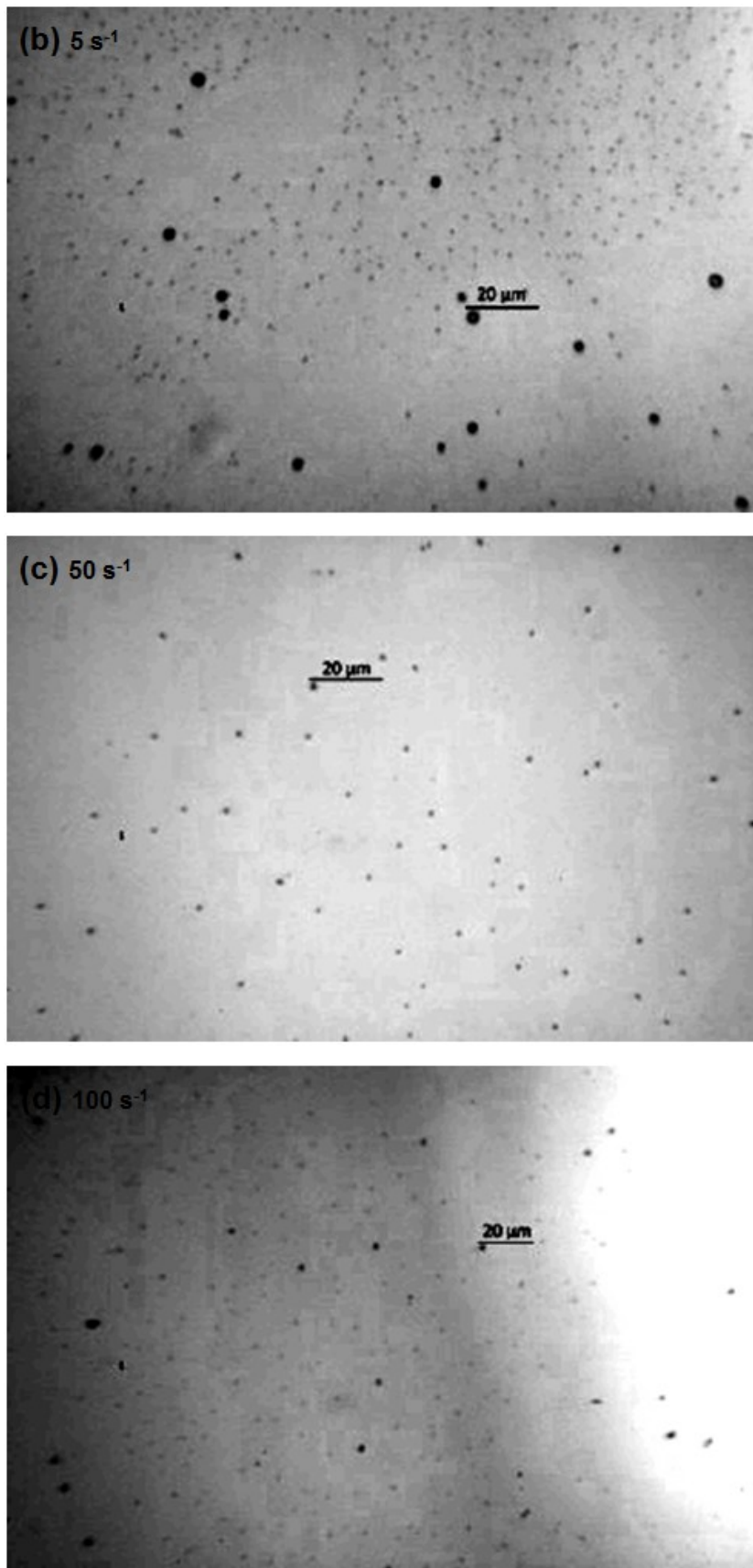


Figure 5.15. Micrographs of 2 wt.% low acyl gellan gum fluid gels produced using a rheometer with an applied cooling rate of 1 °C/min and shear rates of (a) 1, (b) 5, (c) 50, and 100 s⁻¹ (d). Scale = 20 μm.

Fluid gel particles produced using the applied shear rates of 1, 50 and 100 s⁻¹ (Figures 5.15a, c, d) had comparable sizes of 2 µm, suggesting that particle size does not change with increasing shear rate. However, the fluid gel particles produced using the applied shear rate of 5 s⁻¹ (Figure 5.15b) were found to be slightly larger in size, measuring 3.5 µm. These results are in contrast to those previously reported for κ-carrageenan fluid gels produced using the same rheological technique with a 0.5 °C/min cooling rate (Gabriele et al., 2009), where the particle sizes of the produced fluid gels were found to decrease with increasing shear rate. Evidence of irregular-shaped large particles, resembling fragments of a broken up, larger gel structure, was also found for the κ-carrageenan fluid gel system produced at an applied shear rate of 0.5 s⁻¹. For the higher applied shear rates, much smaller, spherical shaped particles were obtained (Gabriele et al., 2009). These experimental findings are in agreement with the literature stating that the size of the fluid gel particles is dictated by the dynamic equilibrium between two competing processes (small gel nuclei growth and coalescence and break-up processes) (Carvalho & Djabourov, 1997). In both this work and that published by Gabriele et al. (2009), the applied cooling rate was constant, suggesting that it is only the applied shear that determines the equilibrium particle size. Increasing the applied shear rate during fluid gel production should therefore, result in a size reduction of the obtained particles (Gabriele et al., 2009).

The reliability of the *LA* gellan fluid gel micrographs collected are thus questioned as to whether they are accurate representations of the true particulate size and shape behaviour at each shear rate. Further attempts were made to obtain clearer micrographs using this technique and CSLM by manipulating the fluid gel samples via dilution and staining using a variety of dyes, including toluidene blue O, which was added to the hot

LA gellan solution prior to fluid gel formation. These efforts however, proved to be unsuccessful.

García et al. (2011) and Rodríguez-Hernández et al. (2003) have been able to successfully obtain micrograph images of *LA* gellan gum fluid and quiescent gels respectively. This they achieved through the covalent labelling of gellan with the fluorescent marker, fluoresceinamine, and observing the samples at room temperature using CSLM. García et al. (2011) observed that 0.25 wt.% gellan fluid gels exhibited a heterogeneous microstructure that was consistent with the occurrence of a dispersion of gel-like polymer clusters with irregular shapes in an aqueous polymer depleted phase. The samples were also void of any anisotropic properties.

For future work it is recommended that a labelling technique of this type is adopted, to decipher whether increasing the applied shear rate during *LA* gellan fluid gel production does indeed result in a size reduction of the obtained particles.

5.2.4.6. *Microstructure ripening*

It is known (Gabriele et al., 2009) that fluid gel systems produced using these methods involves inter-particle interactions during production, and that these persist post-processing, before further developing for significant times after processing is complete. This continuous “strengthening” of the fluid gel structures, is affected by the cooling rates applied during processing, with more extended interactions taking place for those structures produced at higher cooling rates. To understand the time scales over which this “strengthening” process occurs, a microstructure ripening test was performed

on the 2 wt.% LA gellan gum fluid gels formed within the rheometer, using a range of shear rates ($0.5 - 1000 \text{ s}^{-1}$) and an applied cooling rate of $3 \text{ }^\circ\text{C}/\text{min}$ between $90 - 5 \text{ }^\circ\text{C}$.

Figure 5.16 shows the resulting G' data for the fluid gel samples, as a function of increasing shear rate. For each sample, an initial small increase in the G' with time is observed, before continuing to remain at a constant level. In contrast, the G'' data (not shown) for the samples remained fairly constant over time, albeit a 15 Pa decrease at the start, mirroring the initial increases in the G' data.

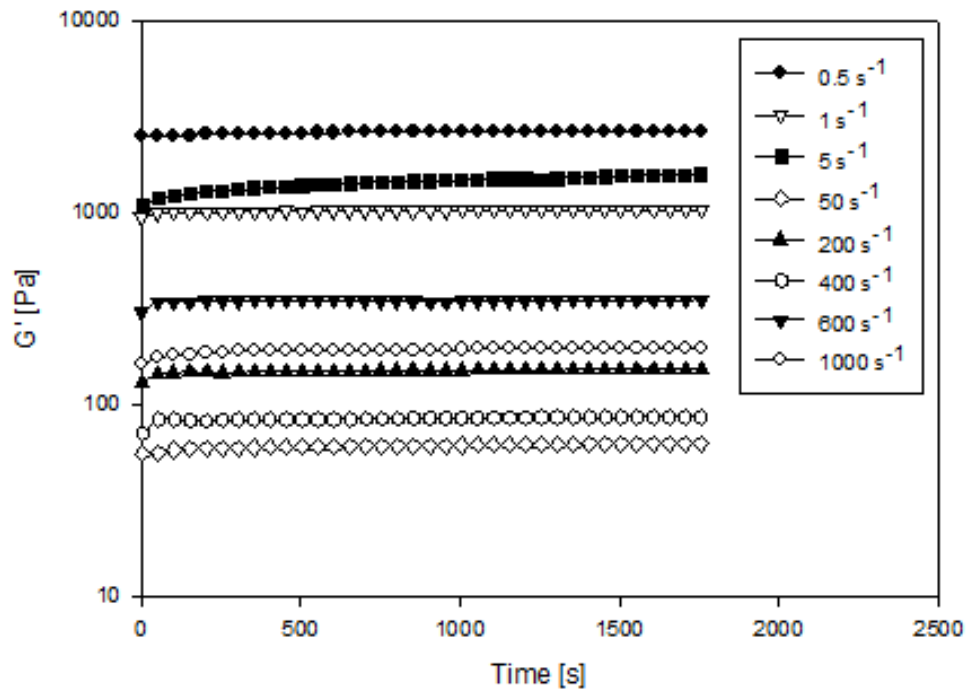


Figure 5.16. Storage (G') modulus for 2 wt.% low acyl gellan fluid gels produced within a rheometer using different shear rates ($0.5 - 1000 \text{ s}^{-1}$) and a cooling rate of $3 \text{ }^\circ\text{C}/\text{min}$ between $90 - 5 \text{ }^\circ\text{C}$, immediately after production. Each modulus value is based on a single sample measurement.

These observations are reflective of the responses of a typical fluid gel to a frequency sweep test of this type. Fluid gels should display characteristics that lie somewhere between a ‘weak gel’ and a ‘strong gel’ in terms of the dependence of the G' and G'' on

frequency, and the phase angle values. The ‘weak gel’ behaviour of fluid gels can be ascribed structurally; closely packed particle interactions allow an elastic network to form at rest, whilst under shear, they are disrupted allowing material flow. The ‘strong gel’ component arises from the strong elasticity of the gel particles, and increases with particle stiffness (Garrec & Norton, 2012). The frequency sweep test data for each of the shear rates shown in Figure 5.16 displayed strong dependencies of the G'' on the phase angle, suggesting weak gel criteria. However, the phase angle values were fairly low, as a result of the G' being significantly higher than the G'' across the frequency range, indicating strong gel characteristics. It was found that the fluid gel samples produced via the lower shear rates had the highest G' at the start of the kinetic experiment. This is since, the low shear rate allows for a greater proportion of inter-particle molecular ordering to occur during formation, with bridges forming between the neighbouring particles being highly likely.

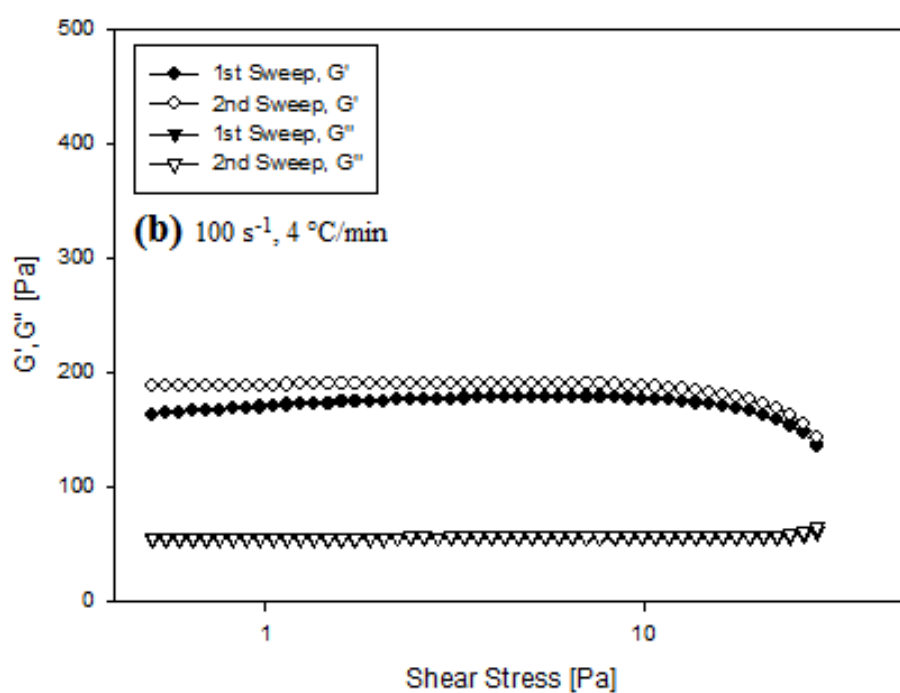
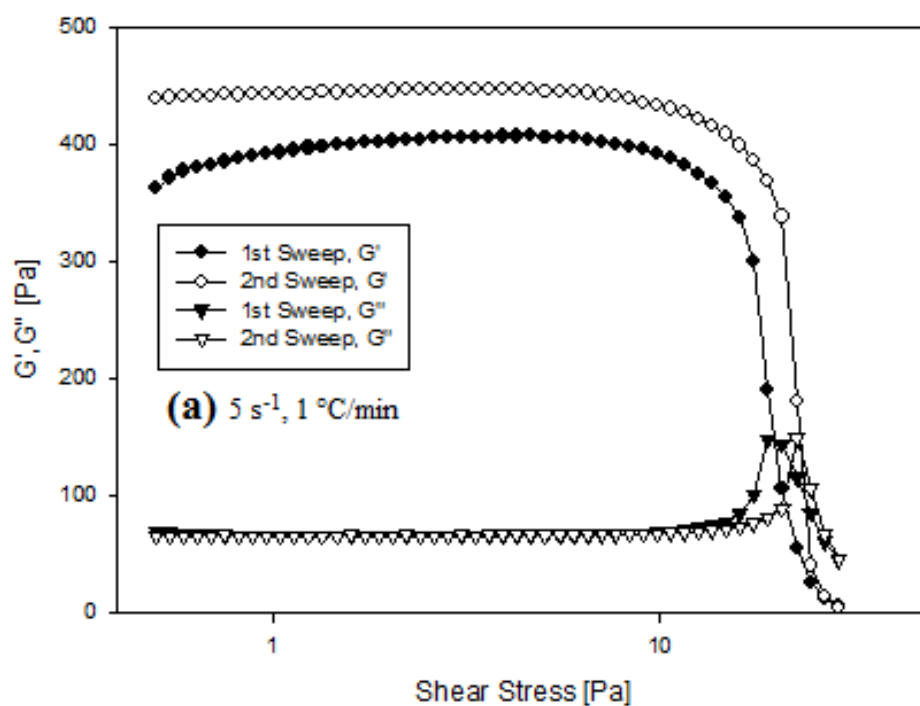
In contrast, the 2 wt.% *LA* gellan fluid gel sample produced using the jacketed pin-stirrer exhibited much higher viscoelastic behaviour (Figure 5.2) than any of the fluid gel samples produced with varying shear rates within the rheometer. The most obvious reason for this, is that the 24 hour ‘ripening’ period given to the 2 wt.% *LA* gellan fluid gel sample produced using the jacketed pin-stirrer, was a sufficient time scale to allow the fluid gel structure to fully develop and strengthen, thus allowing all inter-particle interactions to occur.

5.2.4.7. Structure recovery

Three of the *LA* gellan fluid gel samples produced using varying combinations of controlled shear and cooling regimes within the rheometer were subjected to a strain-

recovery test. The sample combinations were as follows: 2 wt.% *LA* gellan cooled at 1 °C/min with an applied shear rate of 5 s⁻¹, 2 wt.% *LA* gellan cooled at 4 °C/min with an applied shear rate of 100 s⁻¹, and 2 wt.% *LA* gellan cooled at 6 °C/min with an applied shear rate of 100 s⁻¹. Figure 5.17 shows the resulting G' and G'' data for the respective samples (5 s⁻¹, 1 °C/min (5.17a); 100 s⁻¹, 4 °C/min (5.17b); and 100 s⁻¹, 6 °C/min (5.17c)).

For the system in Figure 5.17a, a small increase in the G' is observed during the 1st stress sweep until a shear stress of ~ 1 Pa is applied. This indicates that the structure of the fluid gel is changing due to inter-particle interactions in the system continuing to occur after production, and during the 1st stress sweep experiment itself. Between shear stresses of ~ 1 Pa and ~ 7 Pa, the G' and G'' remain constant. Thereafter, the fluid gel structure then begins to fail and finally collapses. Allowing the system to rest and then performing the 2nd stress sweep, revealed little change in the G'' values indicating that the structure of the fluid gel system had fully recovered to its initial state during the relaxation period. However, with the G' values (despite the initial increase observed in the 1st sweep being absent) a small separation of ~ 30 Pa, was observed between the 1st and 2nd stress sweeps, with the latter being greater than the former. This suggests that the structure of the fluid gel system also recovers to its initial state during the relaxation period, but for some reason ‘over-structures’ to reform a gel that is slightly firmer. This could be attributed to the relaxation time period being longer than what was necessary.



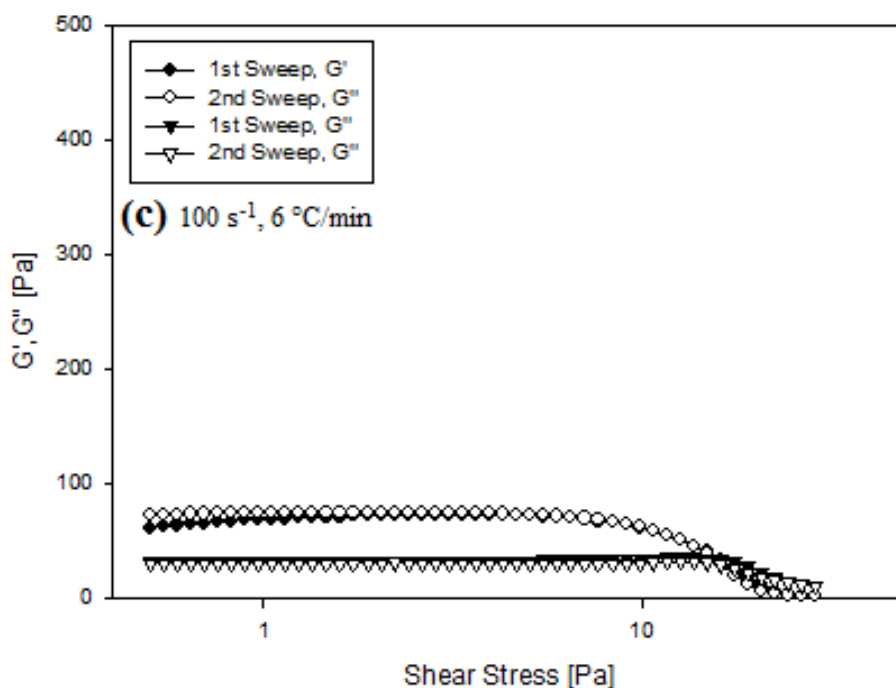


Figure 5.17. Storage (G') and loss (G'') moduli from stress-sweep measurements (1 Hz) for 2 wt.% low acyl gellan gum fluid gels produced within a rheometer using the shear and cooling rates (a) 5 s^{-1} , $1 \text{ }^\circ\text{C}/\text{min}$, (b) 100 s^{-1} , $4 \text{ }^\circ\text{C}/\text{min}$ and (c) 100 s^{-1} , $6 \text{ }^\circ\text{C}/\text{min}$. The 1st sweep was carried out 24 hours after the production of the fluid gels and, after a “resting” stage of 10 min, it was followed by a 2nd sweep. Each of the stress-sweep moduli values are based on a single sample measurement.

For the system in Figure 5.17b, a fractional increase in the G' (smaller than that observed in Figure 5.17a) is displayed during the 1st stress sweep until a shear stress of $\sim 1 \text{ Pa}$ is applied. This again is due to the fluid gel structure changing, as a result of system inter-particle interactions continuing to occur post-production, and during the 1st stress sweep experiment. Between shear stresses of $\sim 1 \text{ Pa}$ and $\sim 10 \text{ Pa}$, the G' and G'' moduli remain constant. Thereafter, the fluid gel structure then begins to fail and finally collapses. Allowing the system to rest and then performing the 2nd stress sweep, revealed little change in the G' and G'' values, and the initial increase in the G' observed in the 1st sweep was absent. Thus, the structure of the fluid gel system fully recovered to its initial state during the relaxation period, with no structural ripening.

Comparing the systems in Figure 5.17b and Figure 5.17c, the applied shear rate during production was kept constant at 100 s^{-1} , but the cooling rate was increased by $2 \text{ }^{\circ}\text{C}/\text{min}$. Very similar structural recovery behaviour was observed in the two figures, albeit the shear stress at which structural failure began to occur in Figure 5.17c was evident slightly earlier at $\sim 8 \text{ Pa}$. The key difference was the formation of a weaker gel with reduced firmness (by $\sim \frac{1}{2}$) (Figure 5.17c) on increasing cooling rate. Incidentally, a similar observation was also noted between Figures 5.17a and 5.17b, when the applied cooling rate was increased from $1 - 4 \text{ }^{\circ}\text{C}/\text{min}$. These observations are contradictory in terms of gel strength when compared with what was discussed previously in Section 5.2.4.4, with an increasing applied cooling rate giving rise to firmer and stronger gels. The structural recovery results, suggest that by increasing the applied cooling rate, the strength of the resulting fluid gels decreases as a consequence of fewer interactions occurring between particles; a shorter processing time and a reduction in the degree of bridging between the formed particles.

5.2.5. Acid exposure of low acyl gellan gum fluid gels

5.2.5.1. Direct acid addition

A variety of acid fluid gel structures can be generated through the direct, dropwise addition of 0.5 % (0.137 mol/dm³) HCl acid to the aqueous *LA* gellan solution during the production process (prior to shearing), inducing a range of pH environments. This process of direct acid addition is a fast method of acidification that is fairly novel for biopolymers of this type.

5.2.5.1.1. Viscometric material response post acid fluid gel production

To assess the viscometric material response post acid fluid gel production, each of the 1 wt.% *LA* gellan gum acid fluid gel samples were subjected to viscosity measurements 24 hours after production. Figure 5.18 shows the viscometric data as a function of pH for 1 wt.% *LA* gellan gum fluid gels produced within the jacketed pin-stirrer (5.18a) and 1 wt.% *LA* gellan gum quiescent gels (5.18b) for comparison. Each displayed very similar responses in viscosity on pH reduction, with the acid gels with acidity from natural pH – pH 3 displaying much higher resistances to flow than those at pH 2. Initial acidification from neutral pH to pH 3.5 causes a large increase in ordering and aggregation to occur between the individual gellan chains immediately upon acidification (Moritaka et al., 1995), resulting in marked increases in gel viscosity. However, on further decrease in pH below the pK_a of the glucuronate residues of gellan, at ~ pH 3.4, over-structuring occurs, causing the gels at pH 2 to be extremely weak and turbid, and showing precipitation of the polymer (Moritaka et al., 1995). As a result an almost sponge-like, weak structure is created rather than a stronger homogeneous one. It is very likely that gel structuring at pH 2 is disrupted by the shear applied during the

acidification process, and that much lower levels of shear-induced disruption would occur for the mixing conditions found in the stomach. Singh (2007) reported that the shear force on the surface of a food particle (~ 0.00043 N) is insignificant in comparison to the crushing or grinding force due to the walls of the stomach (0.2 N).

At pH 2, both the 1 wt.% *LA* gellan gum acid fluid gel and the 1 wt.% *LA* gellan gum quiescent gel displayed non-Newtonian shear-thinning flow behaviour (Figures 5.18a and 5.18b respectively). However, for the respective gels with acidities from natural pH – pH 3, a range of individual viscosity yield stresses appear to exist between the shear stress range of 0.07 – 1 Pa. For each pH, a minimum force exertion (shear stress) was required to induce flow behaviour. As soon as the yield stresses had been exceeded, the liquid samples then proceeded to display shear-thinning behaviour (Cui, 2004). This pseudoplastic flow behaviour is characteristic of the stiff polysaccharide chains present in gels of this type under reduced pH conditions.

Incidentally, the fact that such similar viscosity trends were observed between the 1 wt.% *LA* gellan acid fluid gels and the 1 wt.% *LA* gellan quiescent gels further supports the proposal, that the internal polymeric fluid gel particle network structure is equivalent to that of their quiescently cooled counterparts (Caggioni et al., 2007).

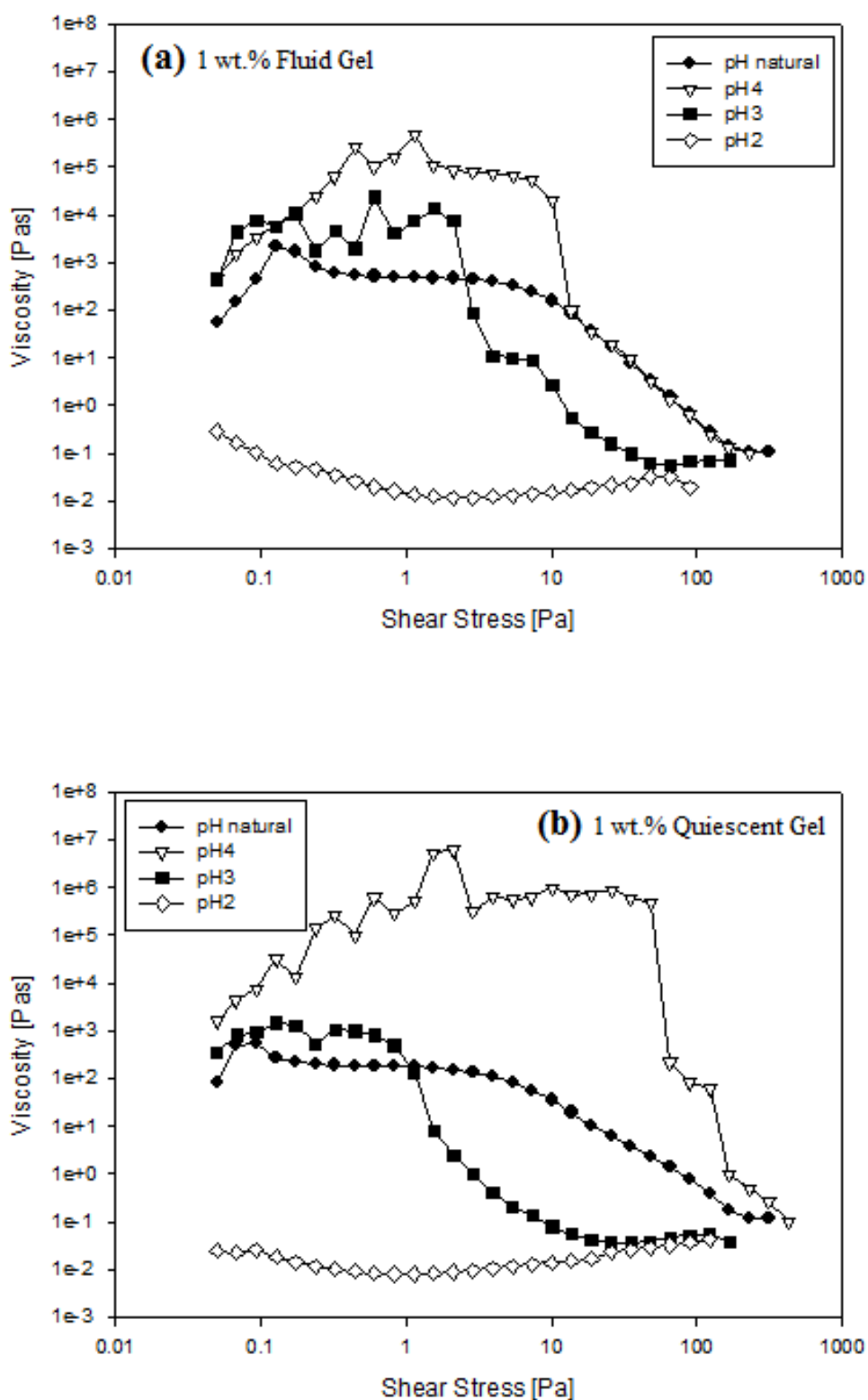


Figure 5.18. Viscometric data as a function of pH for 1 wt.% low acyl gellan gum fluid gels produced within a jacketed pin-stirrer (1500 rpm shaft speed, 100 ml/min pump rate, 15 °C water bath, ~ 30 °C/min cooling rate) (a), and 1 wt.% low acyl gellan quiescent gels (b) for comparison. Each viscosity value is based on a single sample measurement.

5.2.5.1.2. Viscoelastic material response

Morris et al. (2012) reported that biopolymer gels such as gellan form part of a continuum from solutions of individual molecules at one extreme to close-packed solids at the other, as the extent of intermolecular association is increased by varying conditions such as pH. They stated that optimum cross-linking will occur somewhere along the continuum; less association will give a weaker network; and greater association will give larger aggregates with consequent reduction in the effective number of individual junctions, until ultimately the network collapses into a solid precipitate. This interpretation is consistent with the phase separation observed as a decrease in the G' values at 1.00 Hz in Figure 5.19 for the 1 wt.% LA gellan gum fluid gels produced within the jacketed pin-stirrer at pH 2, confirmed by the observation of turbidity at the pH level where their strength began to decrease.

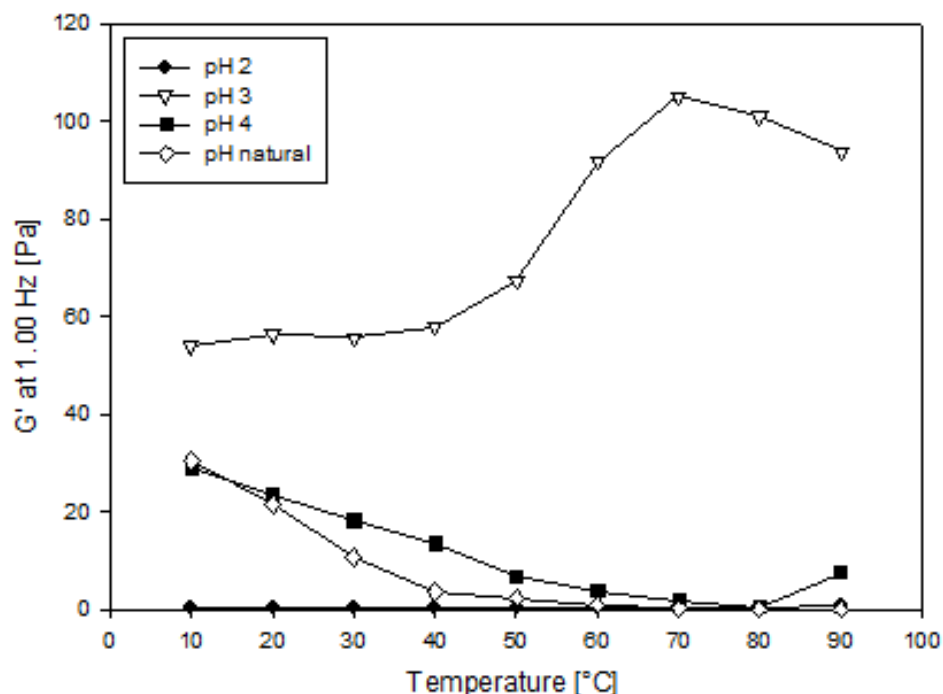


Figure 5.19. Storage (G') moduli at 1.00 Hz as a function of pH, for 1 wt.% low acyl gellan gum fluid gels produced within a jacketed pin-stirrer (1500 rpm shaft speed, 100 ml/min pump rate, 15 °C water bath, ~ 30 °C/min cooling rate), following frequency tables from 0.1 – 10 Hz every 10 °C during a temperature heating ramp. Each modulus value is based on a single sample measurement.

The G' data, which was measured during a temperature ramp (10 – 90 °C) shows (Figure 5.19) that, for the remaining pH values, the elasticity and strength of the gels increases systematically with pH reduction. This demonstrates that the gels become stronger, as a result of greater numbers of cross-links between the polymer chains promoted at the lower pH conditions, and is in good agreement with the flow curve data reported in Figure 5.18a. Albeit in Figure 5.18a, the pH 4 acid fluid gel displays the greatest strength amongst the gels, compared to the pH 3 acid fluid gel in Figure 5.19.

The G' data (Figure 5.19) shows that with decreasing pH gelation occurs sooner. This is observed as the onset of gelation at higher temperatures for the acid fluid gels at lower pH. Although, Figure 5.19 displays the data for the acid fluid gel de-structuring, previous discussions centring the coil-helix transition (Section 5.2.4.2) have proved that there are minimal differences in the gellan fluid gel heating and cooling moduli data, in terms of trend curves, thus the above can be assumed for the heating profile.

The elastic moduli recorded for the acid fluid gel samples at acidities of natural pH and pH 4 are similar with increasing temperature. Melting of the aggregated stable structures occurs, breaking inter-helical bonds etc. (pH 5: 10 – 40 °C; pH 4: 10 – 50 °C), before moving into the conformational helix-coil transition phase (pH 5: 40 – 70 °C; pH 4: 50 – 80 °C), and finally the region where the solution exists in the disordered coil state (pH 5: 70 – 90 °C; pH 4: 80 – 90 °C). The elastic moduli recorded at pH 3 exhibit extended fluid gel deformation events, as a consequence of the speed of the gelation process. Between 10 – 40 °C, a constant elasticity level is observed, which represents a minimum particle size unaffected by cooling or heating below the final gelation set point at 40 °C. During heating between 40 and 70 °C de-fixing of the gelled particle structures proceeds, disordering the hydrocolloid chains within the particles, creating disordered chain segments at the surface of the particle giving them a ‘hairy’ nature (Norton et al.,

1998, 1999; Cox et al., 2009). The completion of the melting occurs between 70 and 90 °C where full conformational disordering and aggregate break up takes place. The absence of a region, where the solution exists in the disordered coil state is explained by the fact that during formation on heating (of the aqueous solutions, prior to shear exposure) under such low pH conditions, ordering and aggregation between the individual gellan polymer chains occurs immediately upon acidification (Moritaka et al., 1995). The effects of pH on gellan gelation have been associated with the lower charge density of chains at lower pH values (Horinaka et al., 2004). They suggested that, since the carboxyl group included in the gellan chain is a weak acid group, and that the degree of dissociation of carboxyl groups in aqueous systems is dominated by the dissociation constant, the lower the pH value, the smaller the fraction of dissociated carboxyl groups, making the gellan a less anionic polyelectrolyte. It is then expected that the less anionic chains aggregate with one another more easily, due to the lower electrostatic repulsion. In addition, the decrease in electrostatic repulsion between the intramolecular segments may result in the suppression of gellan chain expansion (Yamamoto & Cunha, 2007), making association even easier. This overall ease of aggregation caused by decreasing the pH via the direct addition of HCl acid explains the decrease in time to reach the gel point, the more densely linked structure at equilibrium and consequent changes in gel strength, deformability and turbidity.

5.2.5.2. *Post-production acid exposure*

The previous section compared the two methods of fluid gel production via the use of a rheometer and a jacketed pin-stirrer. The former is advantageous in that it can characterise the delicate fluid gel sample, without any risk of damaging it during handling. However, the technique is not particularly typical of industrial processes. The

jacketed pin-stirrer method on the other hand, is more suited for commercial processes, thus this was incorporated for the post-production acid exposure experiments.

5.2.5.2.1. Effect of biopolymer concentration

Post-production exposure of the *LA* gellan gum fluid gels to an acidic environment can be used to assess their response to prolonged acid conditions that are similar to those found in the stomach during and post-meal ingestion. It is widely accepted (Yamamoto & Cunha, 2007; Norton et al., 2011) that the *LA* gellan gum form is acid-sensitive. Research (Norton et al., 2011; Bradbeer et al., 2014) has shown that the *LA* gellan gum gel strength increases on exposure to a HCl acid bath soak. This is a result of the existing gel networks already partially formed within the gels prior to soaking, being reinforced on acid exposure. Ordering and aggregation between individual gellan chains occurs immediately upon acidification (Moritaka et al., 1995).

Each of the *LA* gellan gum fluid gel samples were soaked in 0.5 % (0.137 mol/dm³) HCl acid baths overnight (~ 14 hours). This simulated stomach conditions during digestion and allowed investigation of the effects of prolonged acid exposure on the mechanical properties of the gellan fluid gels after formation. Increases in gel strength were observed qualitatively for the 1 and 2 wt.% *LA* gellan gum fluid gels formulated using the jacketed pin-stirrer unit, post HCl acid bath soak by the change in gel state from a fluid to a solid. Figure 5.20 shows the calculated true stress/true strain curves following compression tests performed on these solid gels, as a function of the number of cycles (or passes) that the gel was processed through the pin-stirrer unit during fluid gel formation. Note that one cycle is equal to one full pass through the pin-stirrer unit. The continuous cycle was formed when the inlet and outlet solution tubes were fed from the final sample container to create a linked system.

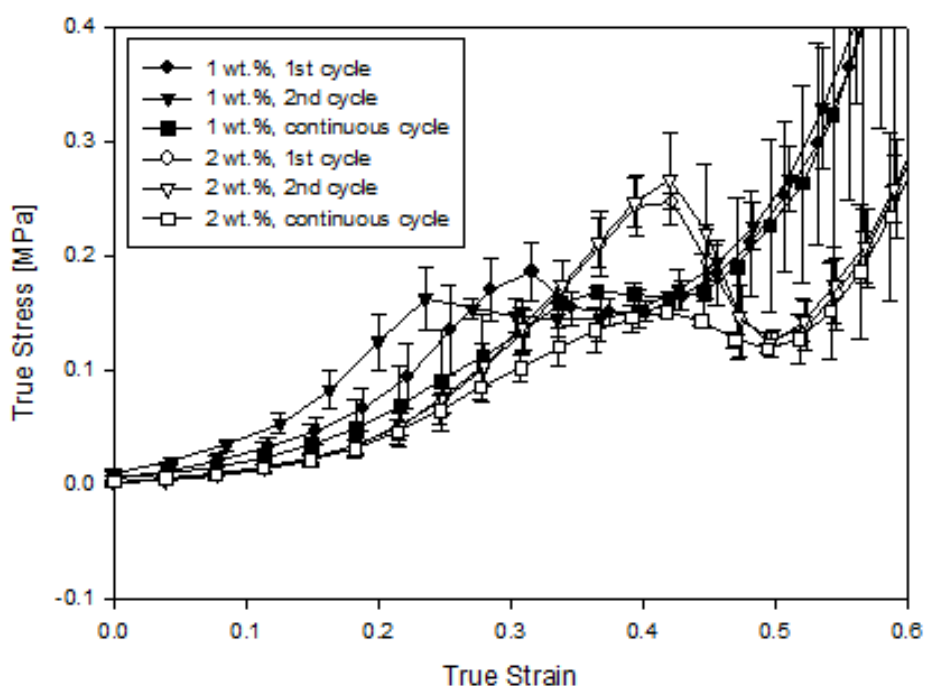


Figure 5.20. True stress/true strain curves for 1 and 2 wt.% low acyl gellan gum fluid gels produced using a jacketed pin-stirrer (1500 rpm shaft speed, 100 ml/min pump rate, 20 °C water bath, ~ 30 °C C/min cooling rate), following exposure to a 0.5 % HCl acid bath soak overnight. All measurements were carried out in triplicate with a compression rate of 1 mm/s. Where error bars cannot be observed, they are smaller than the data points.

Each of the samples displayed purely brittle fracture behaviour, with a rapid decrease in the applied stress once the gels fail at strains between 0.28 – 0.375 (1 wt.%) and 0.425 – 0.43 (2 wt.%), where a clear fracture point is observed. The error bars for all measurements until failure are relatively small, which enforce that the performed compression tests give a good representation of the behaviour of these systems. Error bars on the data recorded after the structures have failed are larger due to the random nature of fracture propagation through the gel matrix.

In terms of gel stiffness and their resistance to fracture post HCl acid bath soak, minimal differences were found between the fluid gel samples (1 and 2 wt.%) collected after the first two cycles. However, for the samples (1 and 2 wt.%) collected during a continuous cycle, a reduction in gel strength and stiffness was observed, and a smaller force was needed to induce fracture (Figures 5.20 and 5.21). An exception to this was

apparent with the 1 wt.% work of fracture data (Figure 5.21), where a small increase in fracture resistance was observed between the second and continuous cycles, but this was treated as an anomalous result due to its small scale.

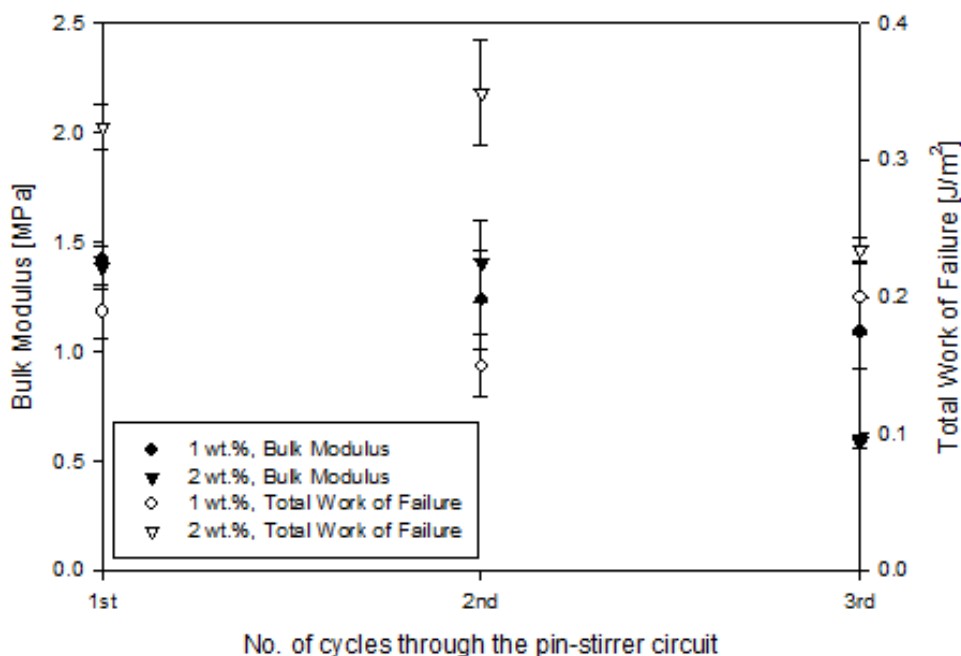


Figure 5.21. Bulk modulus and total work up to fracture data for 1 and 2 wt.% low acyl gellan gum fluid gels produced using a jacketed pin-stirrer (1500 rpm shaft speed, 100 ml/min pump rate, 20 °C water bath, ~ 30 °C/min cooling rate), following exposure to a 0.5 % HCl acid bath soak overnight.

The continuous cycle samples were exposed to the shear force and cooling environment for greater time periods than for the first and second cycle samples. It has been reported that interparticle interactions diminish with continued cooling and shearing of this type during processing, although some interactions will still persist (Cox et al., 2009). Therefore, it would be expected for the fluid gel structures to be weaker and less responsive to the acid exposure, resulting in weaker acid gels. In addition, the cooling rate implemented (~ 30 °C/min) during fluid gel production was high. With high cooling rates the gelation process dominates and fluid gels are produced that have high G' characteristics, and thus more solid-like behaviour indicating larger, more irregularly shaped particles (Cox et al., 2009). These large particles are then likely to be broken up by the shear, causing molecular damage. As a result, heterogeneous fluid gel samples

are produced, consisting of gel particles and broken-up fragments, leading to weak gels with reduced packing fractions. This together with the diminished interparticle interactions within the gel structures reduces the subsequent response to acid and weak acid gel behaviour is observed.

Gellan polymer concentration was shown to influence the fluid gel structural properties, following exposure to acid environment. The 2 wt.% *LA* gellan fluid gel samples were stiffer and showed greater resistances to fracture post-acid exposure, when compared to the 1 wt.% *LA* gellan gum fluid gel samples (Figure 5.21). This was evident, irrespective of the number of processing cycles during production. The concentration dependency can be explained by the principle, that with increasing biopolymer concentration, firmer gels are produced, as a result of the increased extent of interactions occurring between the hydrocolloid chains. For comparison purposes, quiescent *LA* gellan gum gels (1 – 2 wt.%) were also assessed post-production in terms of their response to prolonged HCl acid exposure. Figure 5.22 shows the calculated true stress/true strain curves, as a function of gellan concentration. Each sample displayed purely brittle fracture behaviour, with a rapid decrease in the applied stress when the gels failed at strains between 0.38 – 0.41. The 1 and 2 wt.% quiescent gels were shown to have larger break stresses and strains (Figure 5.22) than any of the 1 – 2 wt.% *LA* gellan fluid gel samples formulated using the jacketed pin-stirrer (Figure 5.20). The same trends were also reflected in terms of gel stiffness and their resistance to fracture post HCl acid bath soak, with the quiescent gels being stiffer and having greater resistances to fracture (Figure 5.23) than their fluid gel counterparts (Figure 5.21). The quiescent gels having greater gel strengths on acid can be explained by the theory that in the absence of shear, the re-ordering during cooling can take place between particles, thus the products require a greater force to allow the particles to move past one another and store more

energy (Garrec & Norton, 2012). In turn, stronger gels are formed that exhibit greater resistance to elastic deformation past the elastic limit.

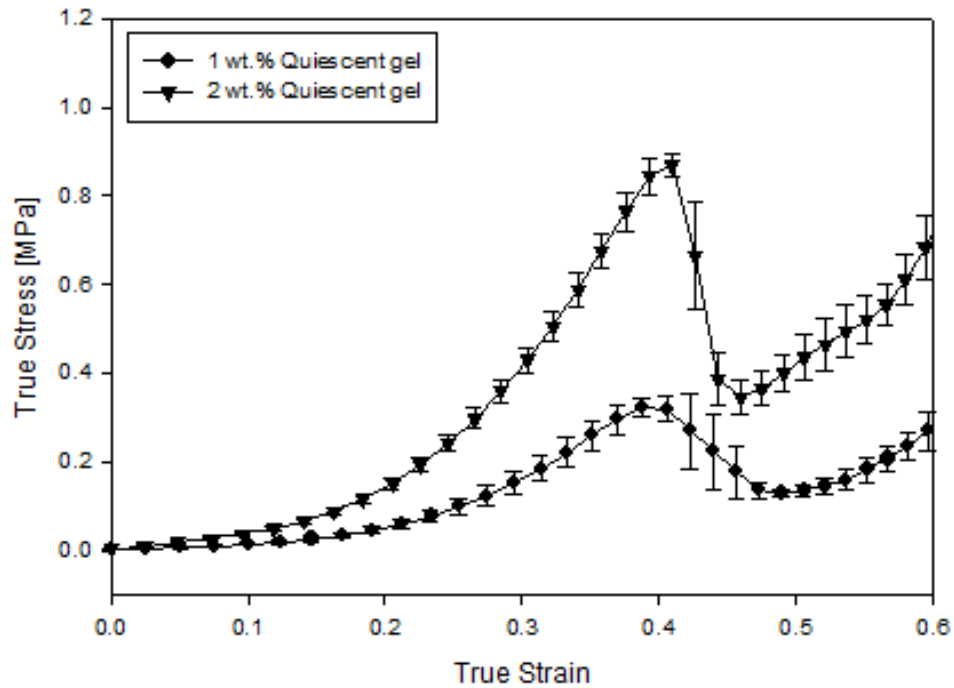


Figure 5.22. True stress/true strain curves for 1 and 2 wt.% low acyl gellan gum quiescent gels, following exposure to a 0.5 % HCl acid bath soak overnight. All measurements were carried out in triplicate with a compression rate of 1 mm/s. Where error bars cannot be observed, they are smaller than the data points.

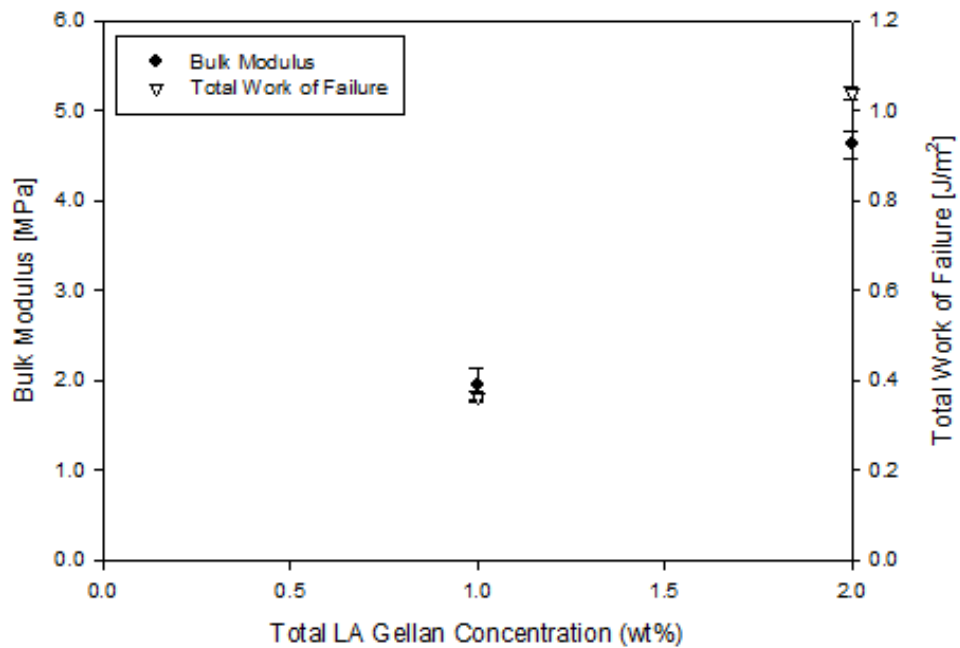


Figure 5.23. Bulk modulus and total work up to fracture data for 1 and 2 wt.% low acyl gellan gum quiescent, following exposure to a 0.5 % HCl acid bath soak overnight.

5.2.5.2.2. Effect of processing conditions

To assess the acid gelation of the 0.25 and 1 wt.% *LA* gellan gum fluid gels formulated using the varying pump rates (50 – 200 ml/min) and pin-stirrer shaft speeds (275 – 1500 rpm); each sample was assessed post-production in terms of their response to a prolonged exposure to a HCl acid environment as previously described. Figure 5.24 shows the calculated true stress/true strain curves, as a function of increasing pump rate.

At each concentration, significant increases in gel strength were observed qualitatively for all of the varying *LA* gellan gum fluid gels, post acid soak by the change in gel state from a fluid to a solid; reinforcing the existing unaggregated gel networks already present.

Texture analysis of the fluid gels revealed that at low concentrations (0.25 wt.%, Figures 5.24a – d), manipulating the processing conditions during production has minimal impact on the resulting acid fluid gels' stiffness and overall strength after subjection to an acid soak. Each of the samples displayed purely brittle fracture behaviour, with a rapid decrease in the applied stress once the gels fail at strains between 0.29 – 0.39 and stresses of $\sim 0.016 - 0.022$ MPa. The error bars for all measurements until failure are relatively small, which reinsurance that the performed compression tests give a good representation of the behaviour of these systems. Error bars on the data recorded after the structures have failed are larger due to the random nature of fracture propagation through the gel matrix.

Gellan polymer concentration was shown to influence the structural properties of the fluid gels, following exposure to an acidic environment. The 1 wt.% *LA* gellan fluid gel samples were stiffer and showed greater resistances to fracture post-acid exposure, when compared to the 0.25 wt.% samples (Figures 5.24a – d). This was evident, irrespective

of the varying processing conditions that the samples were exposed to during production. The concentration dependency can once again be explained by the principle, that with increasing biopolymer concentration, firmer gels are produced, as a result of the increased extent of interactions occurring between the hydrocolloid chains, following the subsequent increase in particle elasticity (Frith et al., 2002) and volume fraction (Norton et al., 1999). A shift in the strain at which the gel samples fracture to lower values, with decreasing gellan concentration from 1 wt.% - 0.25 wt.% was also observed. These shifts are indicative of an increase in gel brittleness, and coincide well with the structure recovery observations in Figure 5.7, where the 0.25 wt.% fluid gel samples were seen to collapse immediately on application of an applied shear.

Texture analysis of the 1 wt.% *LA* gellan fluid gel samples (Figures 5.24a – d) revealed that manipulating the pin-stirrer shaft rotation speeds during production did result in slight variations in their subsequent gel stiffness's and overall strength after subjection to an acid soak. These variations will be discussed individually for the samples formulated using the pump rates of 50, 100, 150 and 200 ml/min in Figures 5.24a, 5.24b, 5.24c, and 5.24d respectively. For the 1 wt.% *LA* gellan fluid gels formulated using a pump rate of 50 ml/min (Figure 5.24a), each of the samples produced using the four pin-stirrer shaft speeds displayed purely brittle fracture behaviour, with a rapid decrease in the applied stress once the gels failed at strains between 0.36 – 0.42. Variations in the failure stress of the samples however, were evident, with the lower shaft speeds (500 and 275 rpm; failure stress: 0.35 and 0.36 MPa) used giving rise to firmer gels than those used at the higher shaft speeds (1500 and 1000 rpm; failure stress: 0.22 and 0.25 MPa).

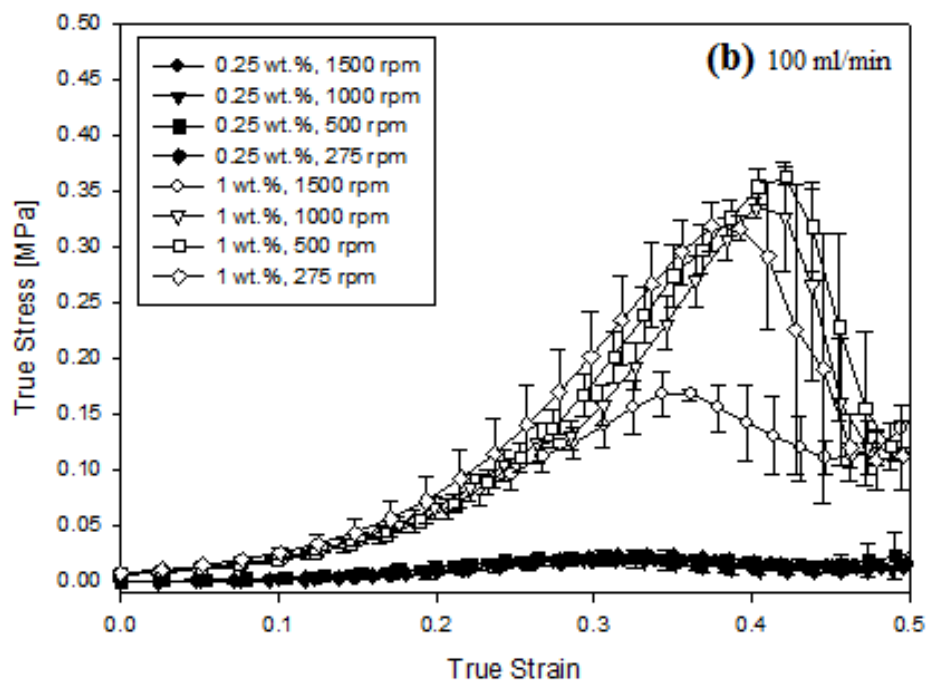
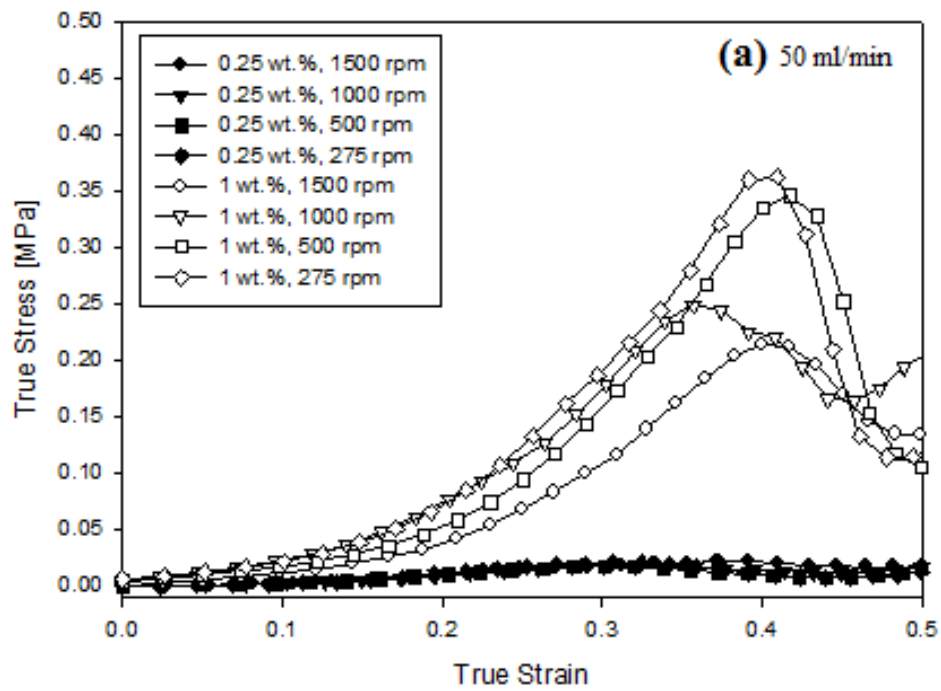
For the 1 wt.% *LA* gellan fluid gels formulated using a pump rate of 100 ml/min (Figure 5.24b), each of the samples displayed purely brittle fracture behaviour, with a

rapid decrease in the applied stress once the gels failed at strains between 0.34 – 0.42. Similar failure stresses were observed for the samples formulated using the shaft speeds of 275 – 1000 rpm at 0.32, 0.34 and 0.36 MPa respectively. However, the sample formulated using a shaft speed of 1500 rpm gave rise to a much weaker gel, fracturing at a stress of 0.17 MPa.

For the 1 wt.% *LA* gellan fluid gels formulated using a pump rate of 150 ml/min (Figure 5.24c), each of the samples displayed purely brittle fracture behaviour, with a rapid decrease in the applied stress once the gels failed at strains between 0.34 – 0.40. In this case, similar failure stresses were observed for the samples formulated using the shaft speeds of 275, 500 and 1500 rpm at 0.30, 0.31 and 0.29 MPa respectively. However, the sample formulated using a shaft speed of 1000 rpm resulted in a firmer gel, fracturing at a stress of 0.36 MPa.

Lastly, for the 1 wt.% *LA* gellan fluid gels formulated using a pump rate of 200 ml/min (Figure 5.24d), each of the samples displayed purely brittle fracture behaviour, with a rapid decrease in the applied stress once the gels failed at strains between 0.36 – 0.39. Here, similar failure stresses were also found for the samples formulated using the shaft speeds of 275, 500 and 1500 rpm at 0.36, 0.32 and 0.33 MPa respectively. However, the sample formulated using a shaft speed of 1000 rpm gave rise to a much firmer gel, fracturing at a stress of 0.42 MPa.

Despite, these small variations in the failure stresses with varying pin-stirrer shaft speed, no clear relation between gel firmness and using specific shaft speed rates was evident.



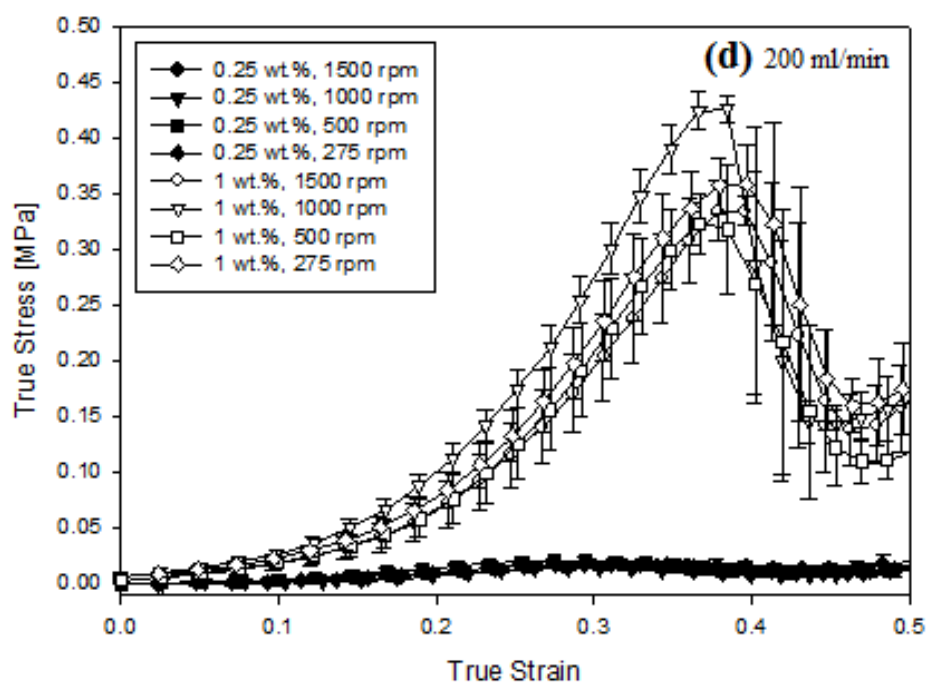
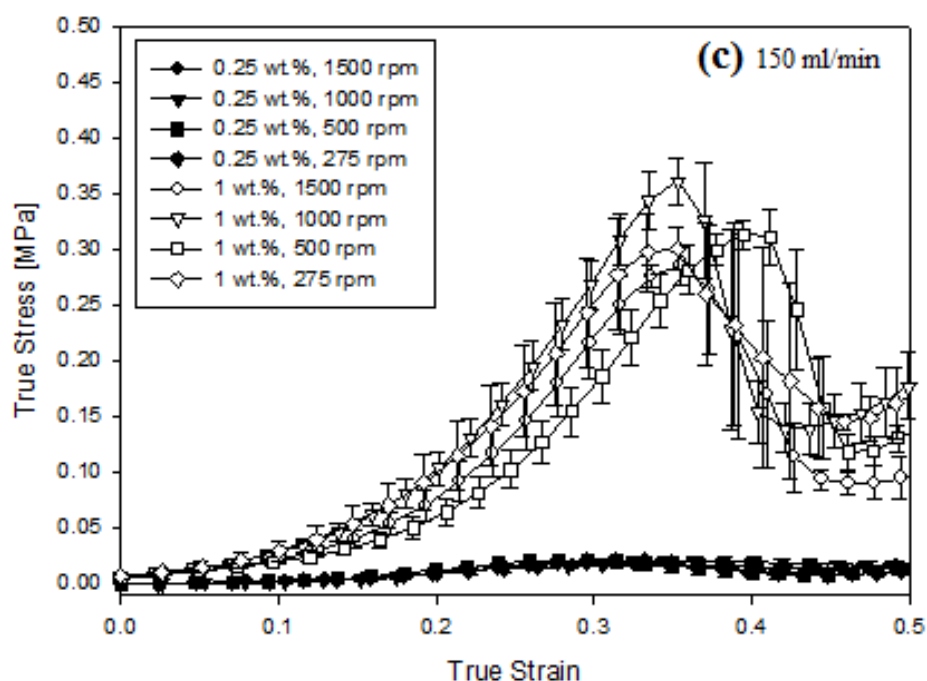


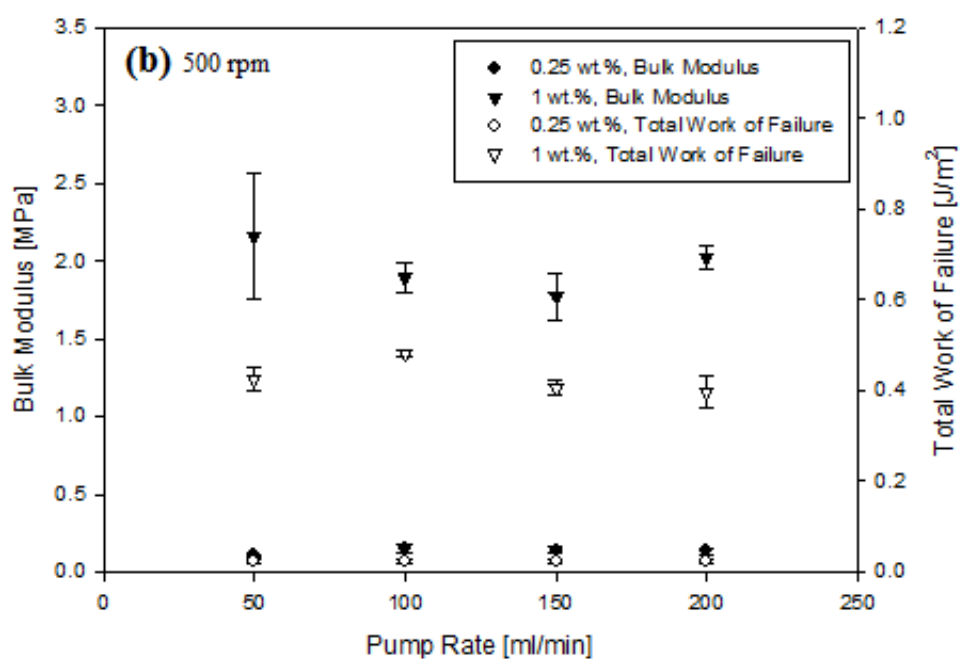
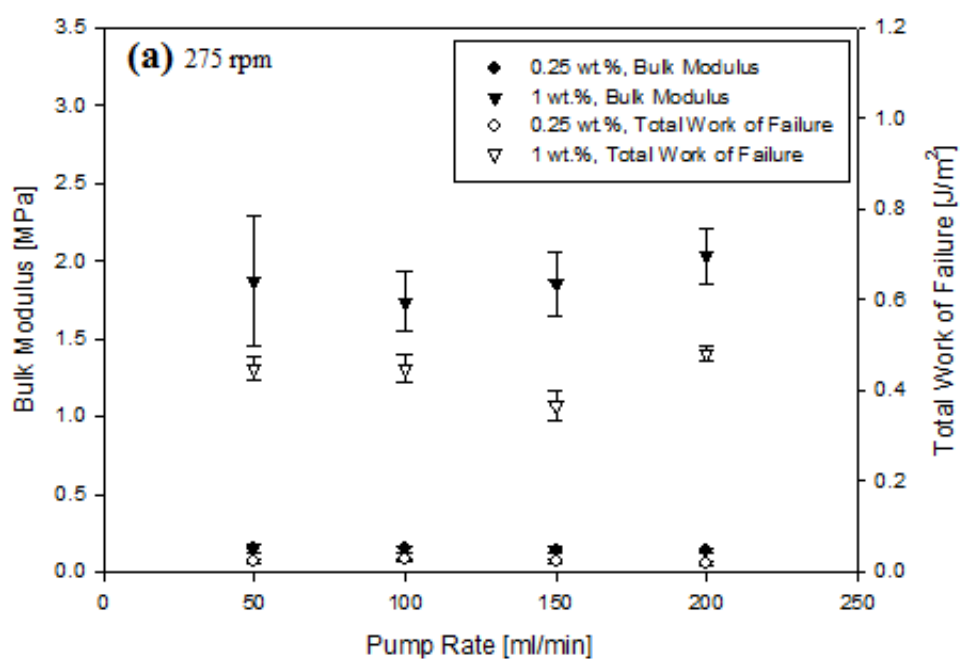
Figure 5.24. True stress/true strain curves for 0.25 and 1 wt.% low acyl gellan gum fluid gels produced within a jacketed pin-stirrer (average cooling rate, °C/min (per pump rate): 15 (50), 40 (100), 60 (150), 75 (200)) using varying shaft speeds (1500 – 275 rpm) and pump rates (a) 50, (b) 100, (c), 150, and 200 (d) ml/min, following exposure to a 0.5 % HCl acid bath soak overnight. All measurements were carried out in triplicate with a compression rate of 1 mm/s. Where error bars cannot be observed, they are smaller than the data points.

In terms of gel stiffness and their resistance to fracture post HCl acid bath soak, generally minimal differences were found between the fluid gel samples at each concentration. No significant trends in the bulk moduli and work of fracture values were reported, as a function of increasing pump rate for each pin-stirrer shaft rotation speed (Figures 5.25a – d). Each value lay within a fairly consistent range, with the occasional variable increase and decrease present. These inconsistencies are a reflection of the observations made in the stress-strain curves for the 1 wt.% *LA* gellan samples (Figures 5.24a – d), where for each pump rate, samples produced using differing shaft speeds exhibited increased firmnesses over others, with no significant trends evident between them. These variations are thought to be a result of standard experimental error during production, rather than an influence from the manipulated processing parameters.

The high textural similarity between these *LA* gellan fluid gel samples, post HCl acid soak could be explained by a critical threshold point of fluid gel homogeneity being reached. During the overnight HCl acid bath soaks the newly formed fluid gel structures are exposed to the acidic environment for long periods of time. *LA* gellan gum gel strength increases on exposure to a HCl acid bath soak (Norton et al., 2011; Bradbeer et al., 2014), as a result of ordering and aggregation between individual gellan chains occurring immediately upon acidification (Moritaka et al., 1995). This reinforces the existing gel networks already partially formed within the gels prior to soaking. Thus, it is suggested that any variations that exist in the *LA* gellan fluid gel structures as a consequence of the processing conditions they are subjected to during production, are subsequently destroyed during the prolonged acid exposure to form equivalent equilibrated acid gel structures. In the other words, each structure interacts with the acid in the same way by achieving maximum protonation of the carboxyl groups, encouraging rapid ordering and aggregation between the hydrocolloids chains, until identical

structures emerge. The rate at which the identical structures are formed are likely to be affected by the initial processing condition used to form the original fluid gels; with those originally formed of less aggregated structures taking longer to restructure. Regardless of the differing rates however, each sample subsequently behaves with a uniform response when assessed by the compression tests during texture analysis. To fully test this theory, the fluid gels produced using the varying processing conditions would need to be soaked in the HCl acid baths for shorter and varied time periods (e.g. for 1, 3 and 5 hours), to identify the time-scales at which these equilibrated structures are formed, and also whether differences between the varying processing conditions are evident prior to their formation.

To summarise, it has been found that *LA* gellan fluid gels formulated using different processing conditions, can subsequently be structured via exposure to an acidic environment to yield equilibrated acid gel structures. This mechanism could be advantageous if a number of processes are required to formulate a specific food product that is then expected to self-structure on exposure to an acidic environment during digestion, with the former processing to have no subsequent influence on the latter.



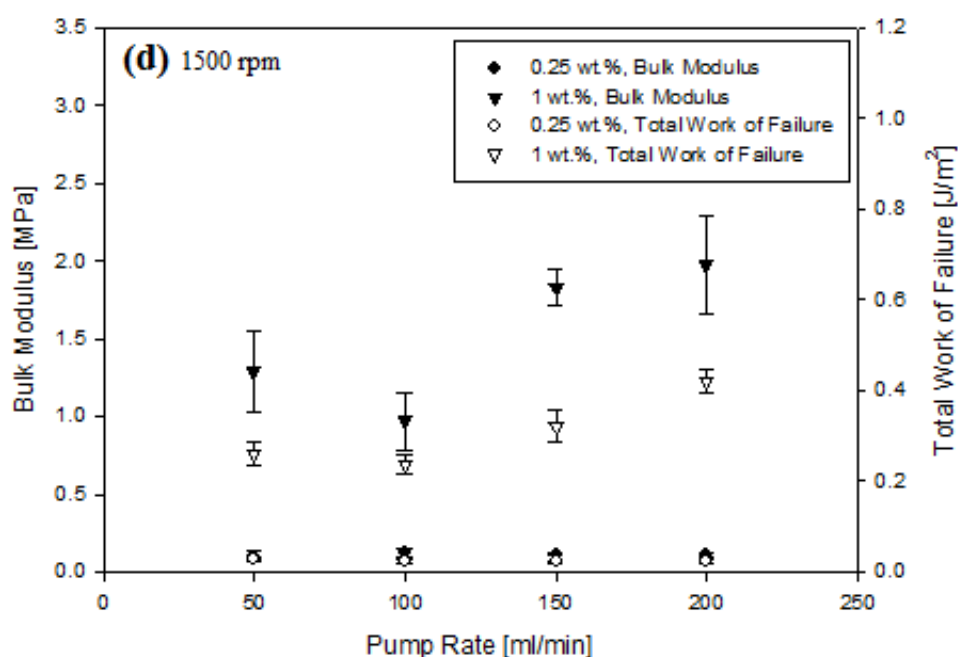
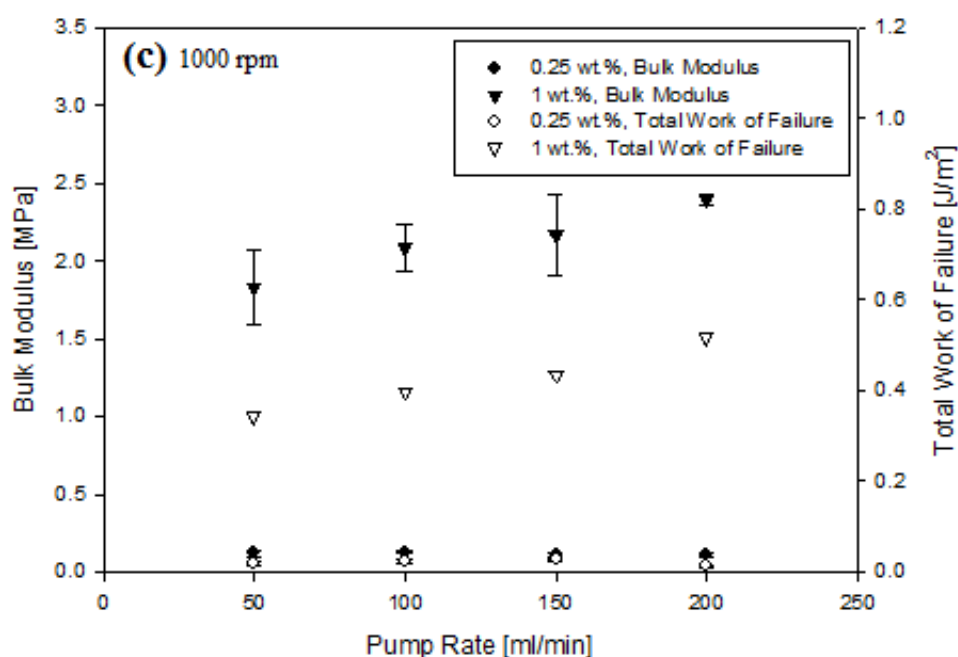


Figure 5.25. Bulk modulus and total work up to fracture data for 0.25 and 1 wt.% low acyl gellan gum fluid gels produced within a jacketed pin-stirrer (average cooling rate, °C/min (per pump rate): 15 (50), 40 (100), 60 (150), 75 (200)) using varying pump rates (50 – 200 ml/min) and shaft speeds (a) 275, (b) 500, (c), 1000, and 1500 (d) rpm, following exposure to a 0.5 % HCl acid bath soak overnight.

5.2.5.2.3. *Effect of pH*

To assess the acid gelation of the *LA* gellan gum acid fluid gels, they also were assessed post-production in terms of their response to prolonged HCl acid exposure. Quiescent *LA* gellan gum gels were also exposed in this way for fluid gel comparison. Figure 5.26 shows the calculated true stress/true strain curves, as a function of pH. Each of the samples displayed purely brittle fracture behaviour, with a rapid decrease in the applied stress once the gels fail at strains between 0.2 – 0.35.

It is accepted that the gelation of gellan can be induced by the reduction in pH, with Grasdalen and Smidsrød (1987) describing HCl acid as “the most potent gel-former”. However, the variation in gel strength with increasing concentration of acid is not monotonic. Initial acidification from neutral pH to pH 3.5 causes a large increase in break stress (Picone & Cunha, 2011), but on further decrease in pH below the pK_a of the glucuronate residues of gellan at pH 3.4 (Haug, 1964), break stress decreases (Norton et al., 2011) and by pH 2 the gels are extremely weak and turbid, and show phase separation of polymer and solvent (Moritaka et al., 1995). This behaviour is particularly evident in Figure 5.26, where the *LA* gellan acid fluid gels at acidities of natural pH and pH 4 were stiffer and more resistant to fracture than those at lower pH levels. In fact, for the samples with acidities of pH 3 and pH 2, the compression tests were unable to be performed, since the gels were too weak to be tested, following their collapse on removal from the visking tubing. For both the 1 wt.% *LA* gellan gum quiescent and acid fluid gels at acidities of pH natural and pH 4, a reduction in the failure stress and a shift in strain to lower values with decreasing pH was observed. The latter shift in strain values is indicative of an increase in gel brittleness, whilst the reduction in break stress can be attributed to the combination of the acid concentration and low gellan concentration within the sample, giving rise to a weak network.

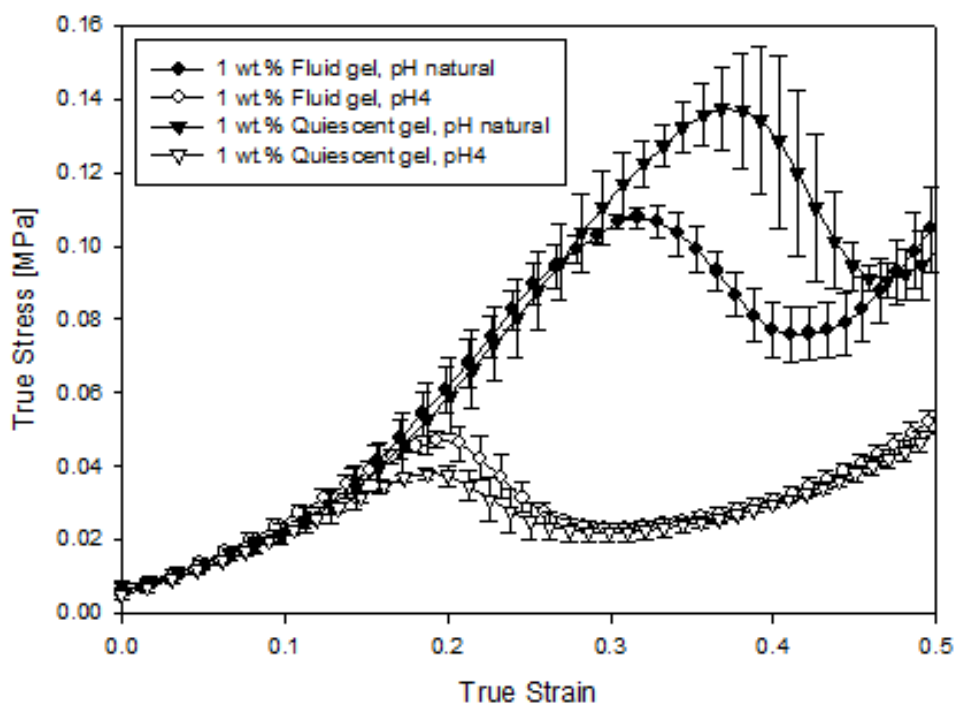


Figure 5.26. True stress/true strain curves as a function of pH for 1 wt.% low acyl gellan gum fluid gels produced within a jacketed pin-stirrer (1500 rpm shaft speed, 100 ml/min pump rate, 15 °C water bath, ~ 30 °C/min cooling rate), and 1 wt.% low acyl gellan gum quiescent gels, following exposure to a 0.5 % HCl acid bath soak overnight. All measurements were carried out in triplicate with a compression rate of 1 mm/s. Where error bars cannot be observed, they are smaller than the data points.

Minimal differences are observed between the total work of failure and bulk modulus data respectively (Figure 5.27) for the *LA* gellan gum quiescent and acid fluid gels at the pH 4 acidity. However, slightly larger differences for each were observed for the samples at their natural pH, with the quiescent gel sample having both the larger break stress and strain. This observation further reinforces the outcomes of the viscoelastic responses with temperature observed for the 2 wt.% *LA* gellan gum fluid gels (at their natural pH) produced under shear using the rheometer, and with the quiescent gels formed on cooling in the absence of shear, in which higher values were reported for the latter (Section 5.2.4.2). Each can be explained by the theory that in the absence of shear, the re-ordering during cooling can take place between particles forming interparticulate helices, thus the products require a greater force to allow the particles to move past one

another and store more energy (Garrec & Norton, 2012). In turn, stronger gels are formed that exhibit greater resistance to elastic deformation past the elastic limit.

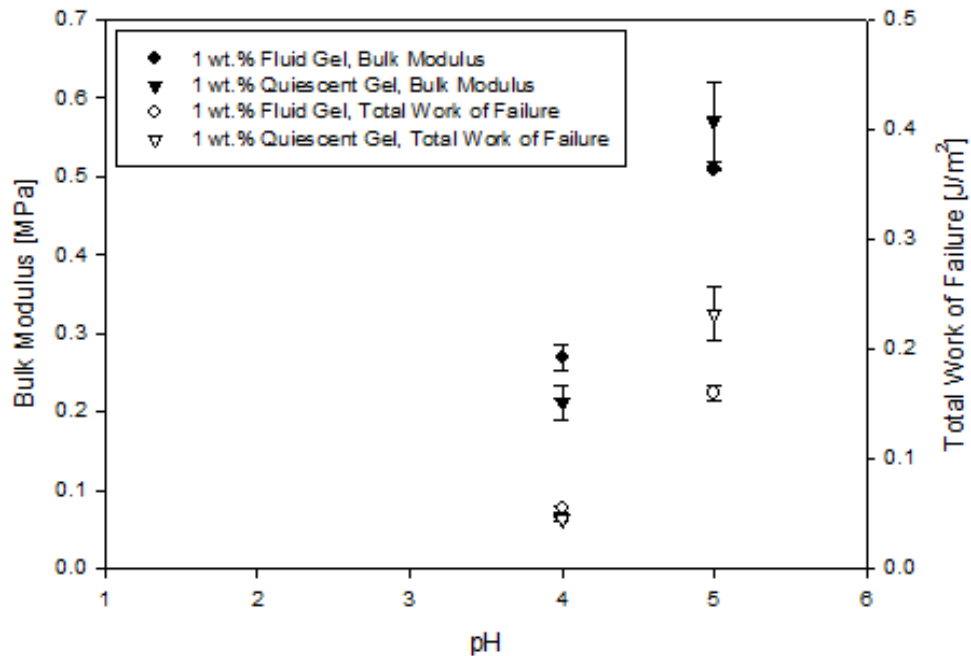


Figure 5.27. Bulk modulus and total work of failure data as a function of pH for 1 wt.% low acyl gellan gum fluid gels produced within a jacketed pin-stirrer (1500 rpm shaft speed, 100 ml/min pump rate, 15 °C water bath, ~ 30 °C/min cooling rate), and 1 wt.% low acyl gellan gum quiescent gels, following exposure to a 0.5 % HCl acid bath soak overnight.

5.3. Conclusions

With the potential use of fluid gels in low fat and reduced calorie foods, as well as within self-structuring satiety based food formulations that take advantage of the natural digestive processes, their formation and properties were explored. This was achieved by investigating the role of shear applied during gelation and HCl acid exposure on *LA* gellan gum fluid gels using two different production methods, to understand the influence of processing conditions on their structure and material response. Viscometry and low-amplitude oscillatory deformation tests were performed on the fluid gel samples after their formation. These gave an insight into their material properties, molecular ordering

and structure development, in addition to the identification of the coil-helix transition temperatures. The acid gelation of the *LA* gellan gum fluid gels was investigated through the direct addition of HCl acid, inducing a range of pH environments and also via post-production in terms of their response to a prolonged exposure to an acidic environment. The findings were promising since they demonstrated that the structuring of *LA* gellan gum fluid gels can be controlled by both the process used for their production and by exposure to an acidic environment (both during and post-production). Fluid gel structural stability was also found to be maintained over time, which provides confidence in their application within food products that require considerable shelf-life storage times.

Lastly, it was found that *LA* gellan fluid gels formulated using different processing conditions, can subsequently be structured via exposure to an acidic environment to yield equilibrated acid gel structures. Thus, acid gelation was shown to override processing parameters. This mechanism could be advantageous if a number of processes are required to formulate a specific stable food product that is then expected to self-structure on exposure to an acidic environment during digestion, with the former processing to have no subsequent influence on the latter.

Chapter 6

LOW ACYL GELLAN GUM AND CO-SOLUTE MIXED GELS

6.1. Introduction

This chapter presents the results of the investigations on low acyl (*LA*) gellan gum quiescent and fluid gel structures incorporating low levels (0 – 50 %) of sugars (glucose, sucrose and fructose) as energy sources. The aim of the work was to work towards providing a solution to consumers experiencing a sense of fullness without satisfaction after the consumption of a self-structuring product. The influence of sugar on the structuring of the gellan gels, the energy (sugar) release mechanism, and the influence of gel structure on the energy release properties is discussed.

6.2. Results & Discussion

6.2.1. Characterisation of low acyl gellan gum and co-solute mixed quiescent gels, and a subsequent measure of their % co-solute release

6.2.1.1. Gel structure

LA gellan gum and co-solute mixed quiescent gels were produced at total polymer concentrations of 2, 3 and 4 wt.%; each containing low levels (0 – 50 %) of the co-solutes glucose, sucrose and fructose respectively. The textural properties of the gels were then assessed by performing compression tests, whose subsequent force/distance data was then converted into true strain (ϵ_H) and true stress data (σ_T) (Section 3.2.1.2) to produce true stress/true strain curves.

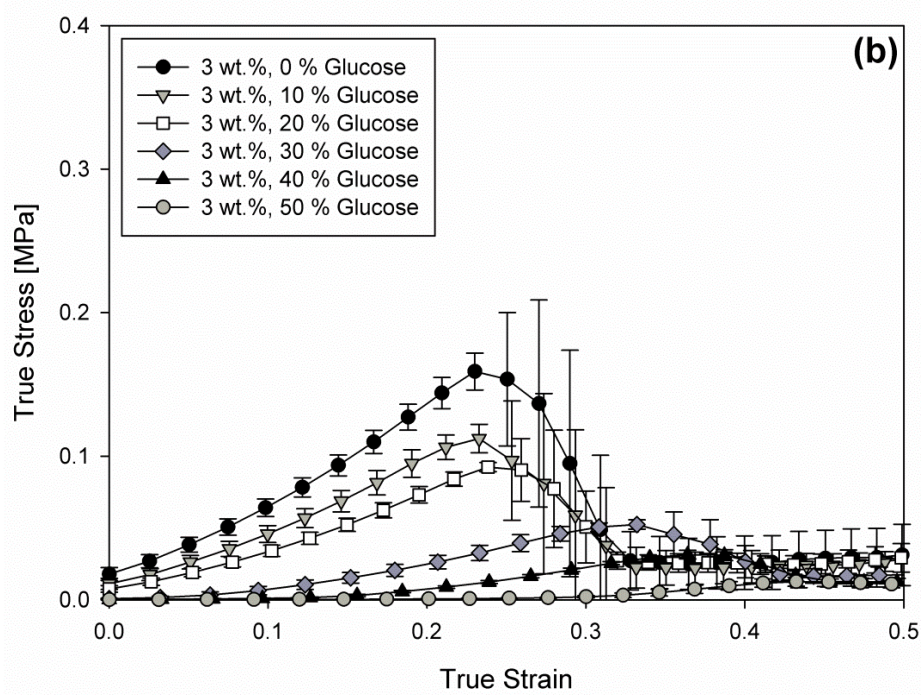
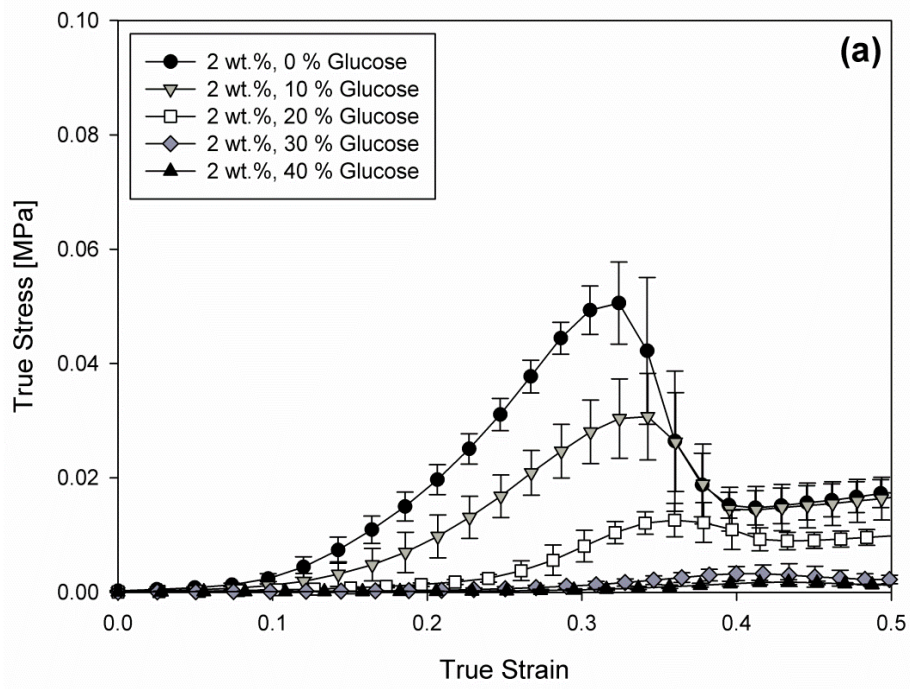
6.2.1.1.1. Glucose

Addition of glucose to the gellan gum aqueous solutions during production has a significant influence on their subsequent textural properties. Figure 6.1 shows the resulting

true stress/true strain curves for 2 wt.% (6.1a), 3 wt.% (6.1b) and 4 wt.% (6.1c) *LA* gellan gum quiescent gels, as a function of increasing percentage glucose substitution. The bulk modulus and work up to fracture values calculated from this data are plotted in Figures 6.2a and 6.2b respectively.

Each of the samples displayed purely brittle fracture behaviour, with a rapid decrease in the applied stress once the gels fail at strains between 0.32 - 0.43 (2 wt.%), 0.23 – 0.43 (3 wt.%) and 0.29 – 0.34 (4 wt.%). The error bars for all measurements until failure are relatively small, which confirm that the performed compression tests give a good representation of the behaviour of these systems. Shifts in the failure strains to higher values were observed for the 2 and 3 wt.% mixed glucose gellan gels with glucose substitution levels of 20 – 50 %. These increases in strain values are indicative of a decrease in gel brittleness and enhanced gellan network elasticity. When using a higher total polymer concentration (4 wt.%, Figure 6.1c) the increases in the failure strains with increasing glucose co-solute level were less obvious. Although the failure strain values for the mixed gellan glucose gels with 0 % glucose and 50 % glucose were found to be similar, with the intermittent samples having slightly reduced failure strains. These observations are likely to be a result of the increasingly dense gellan network structure that is formed with increasing polymer concentration, restricting the mobility of the gellan chains and the glucose molecules within the aqueous gel matrix.

Both Figures 6.1 and 6.2 display concentration dependence, that with increasing biopolymer concentration, firmer gels that are more resistant to fracture are produced as a result of the increased extent of interactions occurring between the hydrocolloid chains.



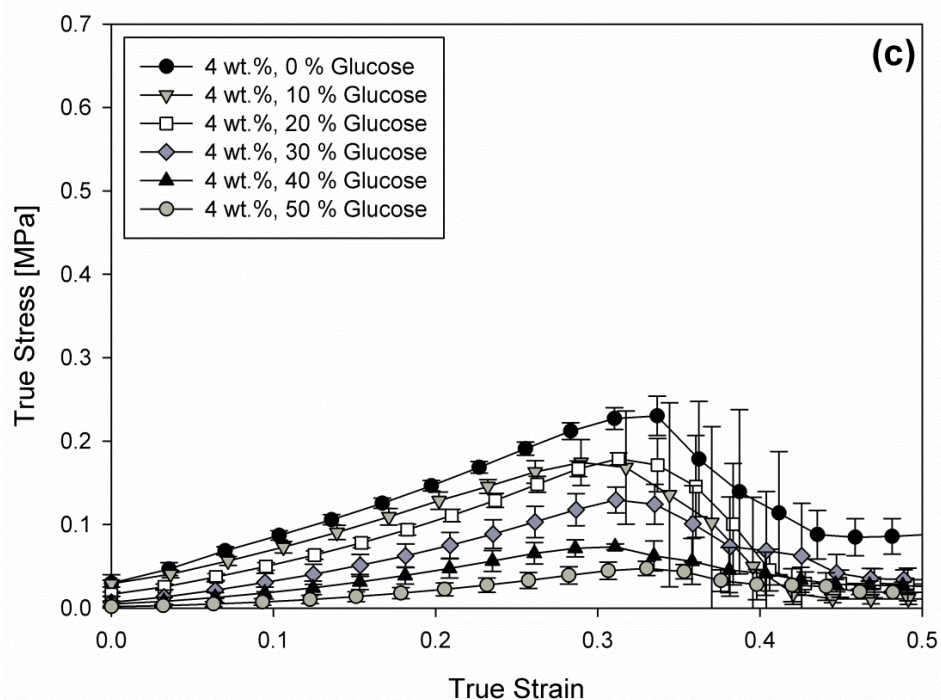


Figure 6.1. True stress/true strain curves for 2 wt.% (a), 3 wt.% (b) and 4 wt.% (c) low acyl gellan gum quiescent gels, as a function of increasing % glucose substitution (0 – 50 %). All measurements were carried out in triplicate with a compression rate of 1 mm/s. Where error bars cannot be observed, they are smaller than the data points.

Increasing the glucose concentration levels within the gellan quiescent gels had a rather different impact on the resulting gel strength and firmness values. Decreased failure stresses, bulk modulus and work up to fracture values were observed at each gellan concentration (Figures 6.1 and 6.2) with increasing percentage glucose level; resulting in significantly weaker gel structures. The 2 wt.% gellan glucose sample with 50 % substituted glucose was in fact, too weak to be tested and collapsed on removal from the storage container prior to compression. These results suggest that the glucose concentration is equally as influential over the gellan gel mechanical properties as the total biopolymer concentration. Interaction between the glucose and gellan concentrations was significant for each of the parameters studied, suggesting that the effect of glucose on the gel mechanical properties depends on the gellan concentration. This effect was most prominent with true failure stress (Figure 6.1).

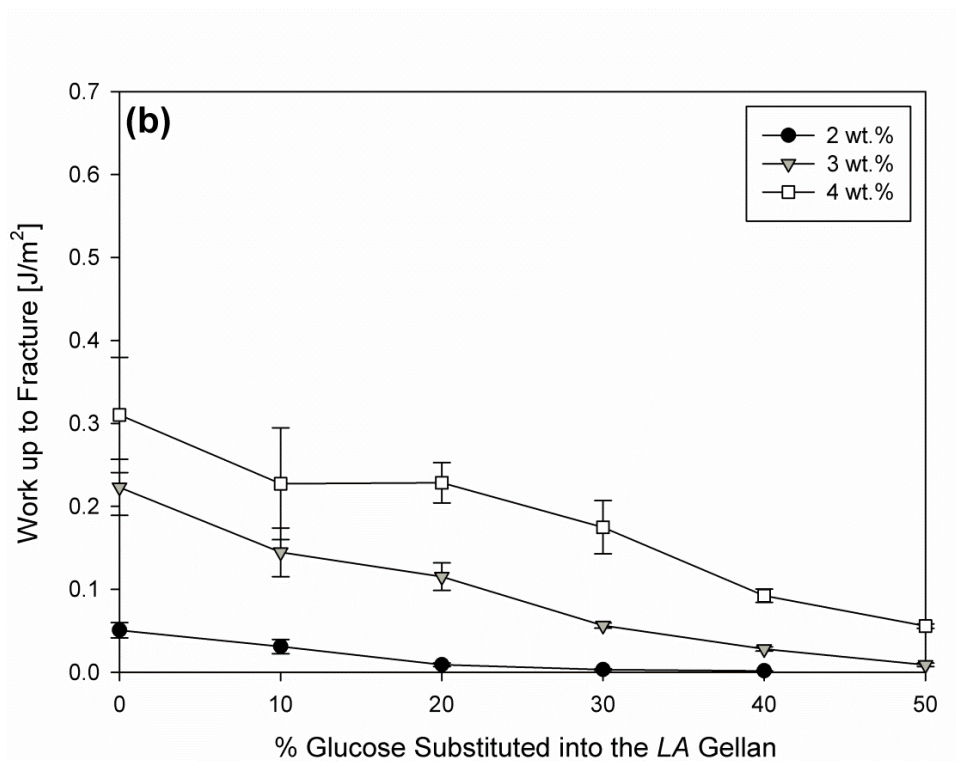
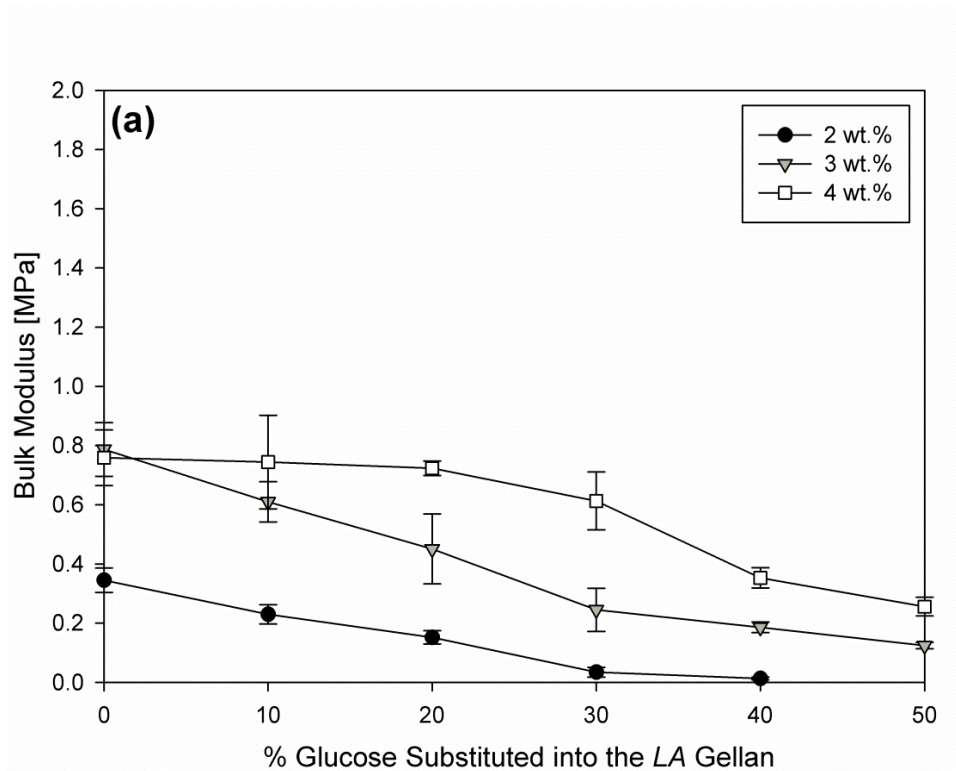


Figure 6.2. Bulk modulus (a) and work up to fracture (b) data for the low acyl gellan gum quiescent gels substituted with 0 – 50 % glucose, as a function of increasing polymer concentration (2 – 4 wt.%).

Although, the effect of gellan concentration was highly significant for all parameters, causing true failure stress (Figure 6.1) and bulk modulus (Figure 6.2a) to increase and true failure strain (Figure 6.1) to decrease (increase of brittleness).

The smooth linear decrease in bulk modulus values (Figure 6.2) implies that a semi-interpenetrating network structure exists. The *LA* gellan polymer chains form a continuous gel matrix with full cross-linking that result in a substantially ordered gellan network, in which small amounts of the glucose are dispersed. The glucose molecules, although not completely excluded from the gellan phase, are predominantly solvated in the aqueous media, forming a solvent of inferior quality with the water molecules that inhibit its extensive polymer aggregation (Sworn & Kasapis, 1998). This assumption is made from observations from Morris et al. (2012) who stated that when there is no indication of discontinuity in properties (as would be expected from phase separation) an interpenetrating network structure is dominant (for mixtures of *HA* and *LA* gellan gum), which can be translated to the mixtures of *LA* gellan and sucrose.

In high sugar (> 60 %) deacylated (*LA*) gellan gels, the presence of the co-solute prevents aggregation and transforms the network into an assembly of sparsely cross-linked (via cations) flexible chains (Papageorgiou & Kasapis, 1995).

The reduction in bulk modulus values with increasing glucose concentration for the mixed glucose gellan gels (Figure 6.2a) is due to a hindrance of aggregation of the gellan chains (Sworn & Kasapis, 1998). This is further evidenced by the increase in the failure strains observed in Figure 6.1, which are indicative of more flexible, less aggregated polymer networks. Sworn and Kasapis (1998) also reported that although using increasingly high levels of co-solute will inevitably contribute to the pliability of the systems, the large number

of relatively small molecules may also physically reduce aggregation of the gellan gum double helices in the same ways argued for agarose and κ -carrageenan gels (Watase et al., 1990; Nishinari et al., 1990). The explanations were based on there being a reduced availability of water molecules for the formation of thermodynamically stable junction zones (Watase et al., 1990).

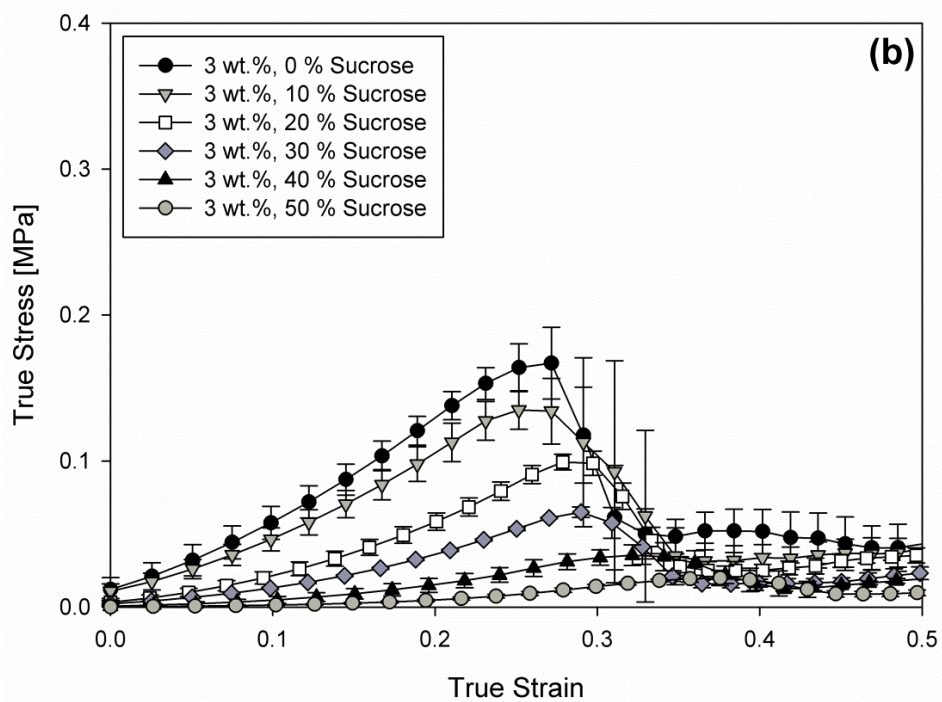
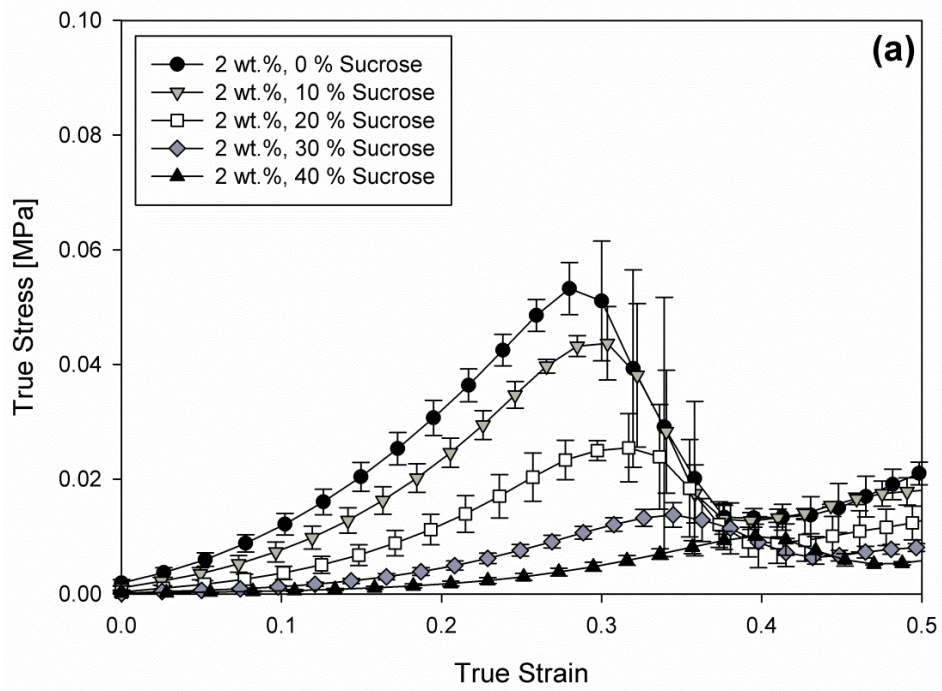
Overall, increasing the glucose concentration within the mixed gellan quiescent gels creates more elastic networks (Figure 6.1), which require higher forces to induce fracture and cause complete disruption. Flory (1941) associated calculated bulk and Young's modulus values with the number of active junction zones in a biopolymer network. This together with the observed decrease in bulk modulus values on increasing glucose concentration (Figure 6.2a) argues for limited aggregation in increasing sugar environments. It is expected that more flexible, entropic gellan chains are created as a result of the reduction in the size and degree of crosslinking in intermolecular aggregates, and these are likely to withstand substantial stretching before breaking (Sworn & Kasapis, 1998).

6.2.1.1.2. Sucrose and Fructose

The addition of sucrose and fructose individually to the gellan gum aqueous solutions also had significant influences on their subsequent textural properties. Many of these physical properties drew close resemblances to those observed for the formed mixed glucose gellan gels, and they were also found to depend on the total polymer concentration. Figures 6.3 and 6.4 show the resulting true stress/true strain curves for the 2 wt.% (6.3a & 6.4a), 3 wt.% (6.3b & 6.4b) and 4 wt.% (6.3c & 6.4c) *LA* gellan gum quiescent gels, as a function of increasing percentage sucrose (Figure 6.3) and fructose (Figure 6.4) substitution. The bulk

modulus and work up to fracture values calculated from this data for the mixed sucrose gellan and mixed fructose gellan gels are plotted in Figures 6.5 and 6.6 respectively.

All of the mixed sucrose and mixed fructose gellan gels displayed purely brittle fracture behaviour, with rapid decreases in their applied stress once they had failed respectively at strains between 0.28 - 0.40 and 0.29 – 0.43 (2 wt.%), 0.27 – 0.37 and 0.21 – 0.34 (3 wt.%) and 0.25 – 0.30 and 0.23 – 0.27 (4 wt.%). As observed with the mixed glucose gellan gels with glucose substitution levels of 20 – 50 %, shifts in the failure strains to higher values were also evident for the equivalent 2 and 3 wt.% mixed sucrose and mixed fructose gellan gels. These increases are again indicative of more flexible, less aggregated polymer networks. Increased failure strains were also less obvious for the 4 wt.% mixed sucrose and mixed fructose gellan gels (Figures 6.3c & 6.4c), with the failure strain values for the gels with 0 % and 50 % co-solute being comparable. No clear relationships were found between the magnitude and shift pattern of the failure strain values and the nature of the co-solute; indicating that the gel elasticity was not significantly altered by the type of sugar. Overall, these observations provided further confirmation that interactions between the co-solute and gellan concentration are significant, and that their influence on the gel mechanical properties are dependent on the gellan concentration.



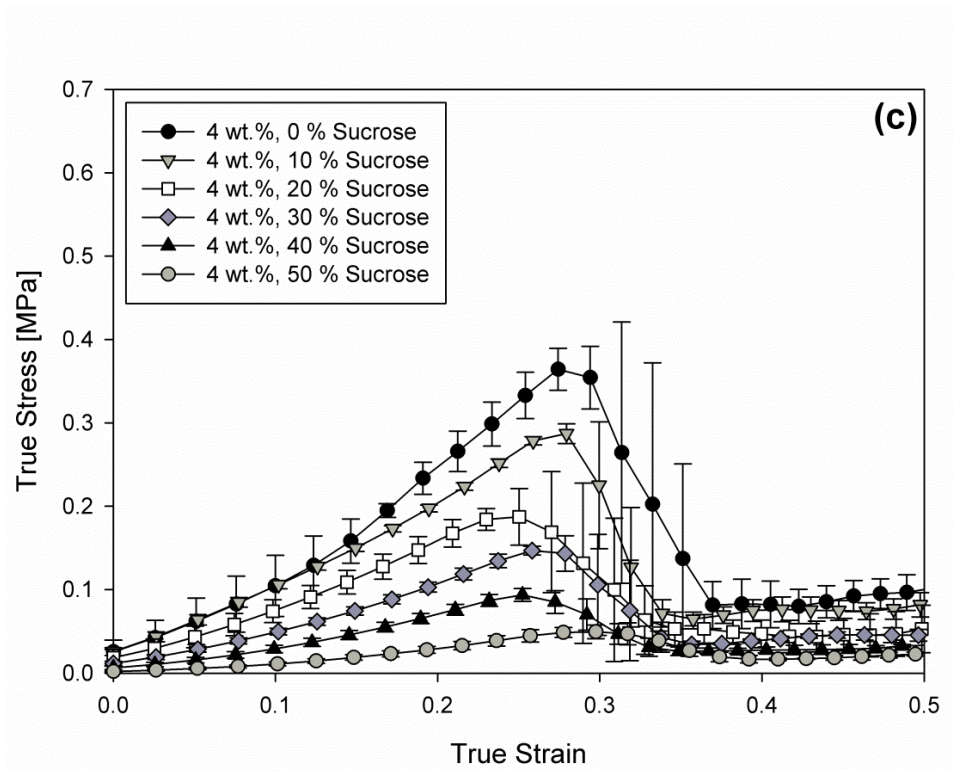
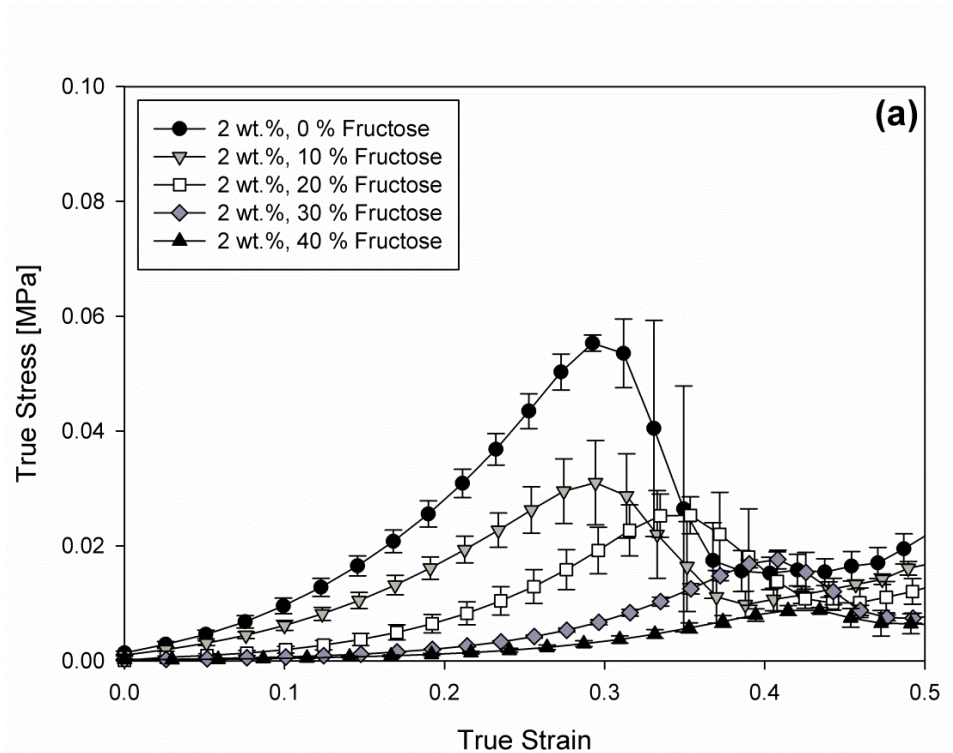


Figure 6.3. True stress/true strain curves for 2 wt.% (a), 3 wt.% (b) and 4 wt.% (c) low acyl gellan gum quiescent gels, as a function of increasing % sucrose substitution (0 – 50 %). All measurements were carried out in triplicate with a compression rate of 1 mm/s. Where error bars cannot be observed, they are smaller than the data points.



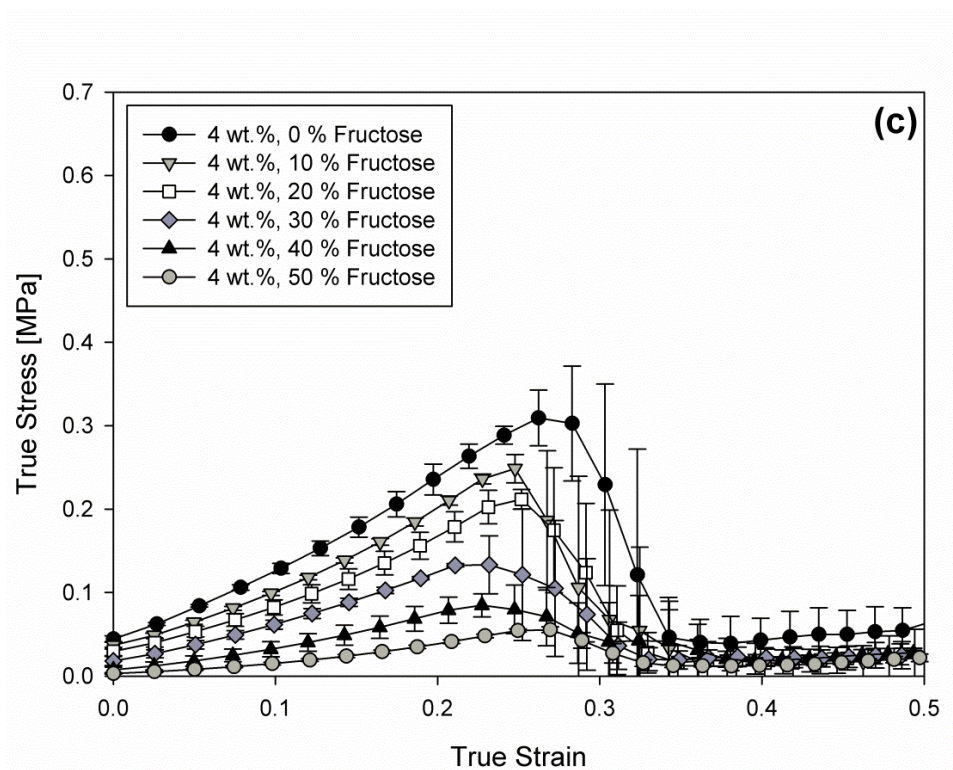
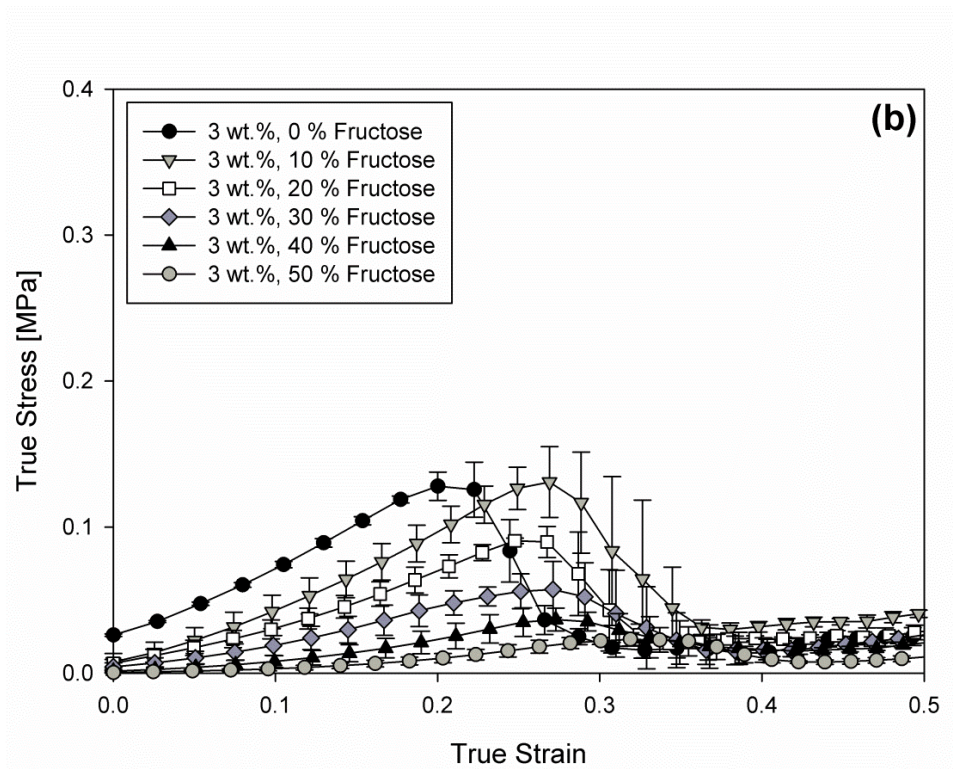


Figure 6.4. True stress/true strain curves for 2 wt.% (a), 3 wt.% (b) and 4 wt.% (c) low acyl gellan gum quiescent gels, as a function of increasing % fructose substitution (0 – 50 %). All measurements were carried out in triplicate with a compression rate of 1 mm/s. Where error bars cannot be observed, they are smaller than the data points.

Both the mixed sucrose and mixed fructose gellan gels displayed concentration dependency, that with increasing biopolymer concentration, firmer gels that were more resistant to fracture were produced (Figures 6.5 & 6.6). Decreased failure stresses, bulk modulus and work up to fracture values were also observed at each gellan concentration (Figures 6.3 – 6.6) with increasing percentage co-solute level; resulting in significantly weaker gel structures. Likewise with the 2 wt.% mixed glucose gellan sample with 50 % substituted glucose, the equivalent mixed sucrose and mixed fructose gellan gels were too weak to be subjected to compression testing. Interactions between the co-solutes and the gellan concentrations were also significant for each of the parameters studied, reaffirming that the effect of the co-solute on the gel mechanical properties depends on the gellan concentration. This effect was once again most prominent with true failure stress (Figures 6.3 & 6.4).

The progressive decrease in failure stress values with increasing co-solute concentration within *LA* gellan gum gels, in the absence of added cations is uncommon. Generally, the addition of co-solutes in the presence of low cation concentrations or in their absence to gellan gum aqueous solutions leads to a strengthening and stabilisation of the resulting gellan networks, and in turn produces much firmer gels (Miyoshi et al., 1998; Miyoshi & Nishinari, 1999b; Morris et al., 2012; Bayarri et al., 2002; Kawai et al., 2008, Kasapis, 2006; Evageliou et al., 2010). This behaviour was also observed for *LA* gellan sucrose gels in the presence of low calcium concentrations (Tang et al., 2001). However when the calcium concentration was increased, compression testing showed that the failure stress decreased with increasing sucrose concentration (Tang et al., 2001). The close similarities between this work and the results presented in this chapter suggest that the commercial gellan gum used to obtain the latter is likely to have high calcium or other divalent cation content. This was supported by Morris et al. (2012) who stated that commercial gellan samples do indeed contain greater

amounts of divalent cations. Although, full compositional analysis of the commercial *LA* gellan gum used in this study needs to be conducted to confirm this. Using commercial gellan with its high divalent cation content gives gels that are close to or at the optimum degree of crosslinking, which in turn causes excessive aggregation when in the presence of added sugar, weakening the network (Gibson & Sanderson, 1997). In addition, the high divalent cation content is also thought to adequately stabilize the negative charges of the gellan double helices, so that the excess cations then hinder helical aggregation (Tang et al, 2001). In this case, the progressive addition of sucrose would hinder the growth of junction zones and lead to considerable decrease in the gellan gel strength.

Based on the observation of smooth linear decreases in the bulk modulus values for the mixed sucrose and mixed fructose gellan gels (Figures 6.5 & 6.6), semi-interpenetrating network structures were also assigned to each system, with the *LA* gellan forming a continuous segmented network with full cross-linking, in which small amounts of the sugar molecules are dispersed. When comparing the bulk modulus and work up to fracture values for each of the three co-solutes, small variations were evident suggesting that the nature of the co-solute also influences the gellan gel network structure. It was observed (Figures 6.2, 6.5 & 6.6) across all of the gellan concentrations, irrespective of the co-solute concentration that the mixed glucose gellan gels were much weaker than the mixed sucrose gellan and mixed fructose gellan gels. The order of strength for the latter two mixed gellan gel types however, varied upon increasing gellan and co-solute concentration. For all of the 2 wt.% *LA* gellan mixed gels and the 3 wt.% *LA* gellan mixed gels with co-solute levels between 10 – 20 %, the order for the three sugars studied was glucose < fructose < sucrose. Increasing the co-solute concentration in the 3 wt.% *LA* gellan mixed gels and for each of the 4 wt.% *LA* gellan mixed gels, this order changed to glucose < sucrose < fructose. Sworn & Kasapis (1998) also reported different sugar order sequences for gellan gum when using different concentrations

of cosolute. With regard to stress at failure at each gellan concentration (Figures 6.1, 6.3 & 6.4) the order for the three sugars studied was glucose < fructose < sucrose. This order was also observed by Evageliou et al. (2010) for the stress at failure and Young's modulus of 0.5 wt.% *LA* gellan gels with co-solute concentrations varying from 0 – 15 %, and by Sworn & Kasapis (1998) for the modulus of 0.5 wt.% *LA* gellan gels with co-solute concentrations up to 10 wt.%. Several different orders for the three sugars studied have been proposed for *LA* gellan gum (Gibson & Sanderson, 1997; Miyoshi & Nishinari, 1999b; Morris et al., 2012; Tait et al., 1972; Tang et al., 2001), many of which depart from the orders displayed in this work. However, most of them are in agreement that either sucrose or fructose substituted *LA* gellan gels give rise to firmer gels than those incorporating glucose. For these reasons, the explanations used to explain their respective orders will be adapted to this work to enable an improved understanding into the results obtained. Tang et al. (2001) argued that sucrose is more effective than fructose at stabilising the orderly packed gellan double helices in aqueous solutions through their readiness towards crystallisation. Sucrose can be readily crystallised in aqueous solutions, whereas fructose cannot due to rapid conversion among pyranose-ketofuranose structures. The hydroxyl groups in the crystal structure of sucrose form intramolecular and intermolecular hydrogen bonds (Brown & Levy, 1963). In concentrated aqueous solutions the sucrose molecules are orderly packed; the glucose units in gellan chains may replace the glucose units of sucrose molecules in this orderly molecular packing (Tang et al., 2001). This would have a stabilising effect on the orderly packed gellan double helix in aqueous solutions (Papageorgiou et al., 1994), resulting in higher gelling temperatures with increasing sucrose concentration, and overall stronger gel networks when compared to fructose. Fructose molecules are randomly packed in aqueous solutions and thus do not exhibit this stabilisation effect to the orderly packing of gellan molecules (Tang et al., 2001).

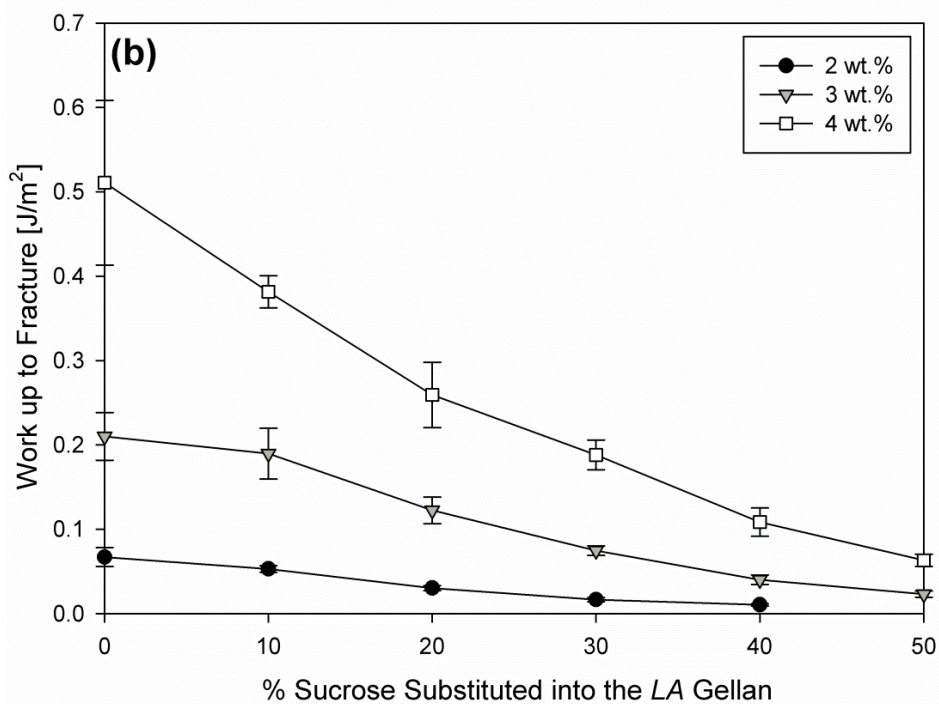
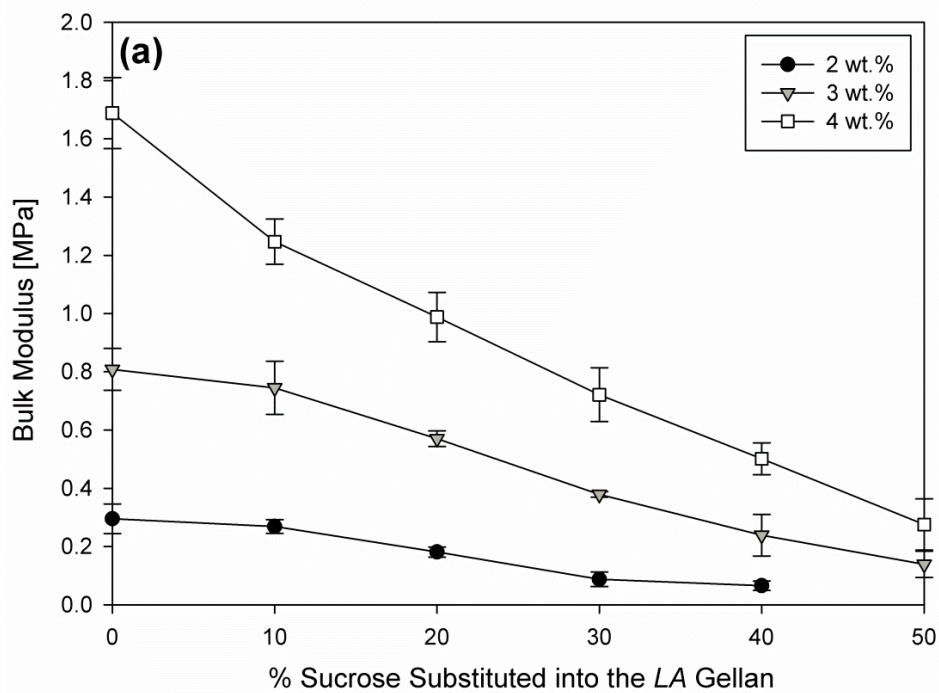


Figure 6.5. Bulk modulus (a) and work up to fracture (b) data for the low acyl gellan gum quiescent gels substituted with 0 – 50 % sucrose, as a function of increasing polymer concentration (2 – 4 wt.%).

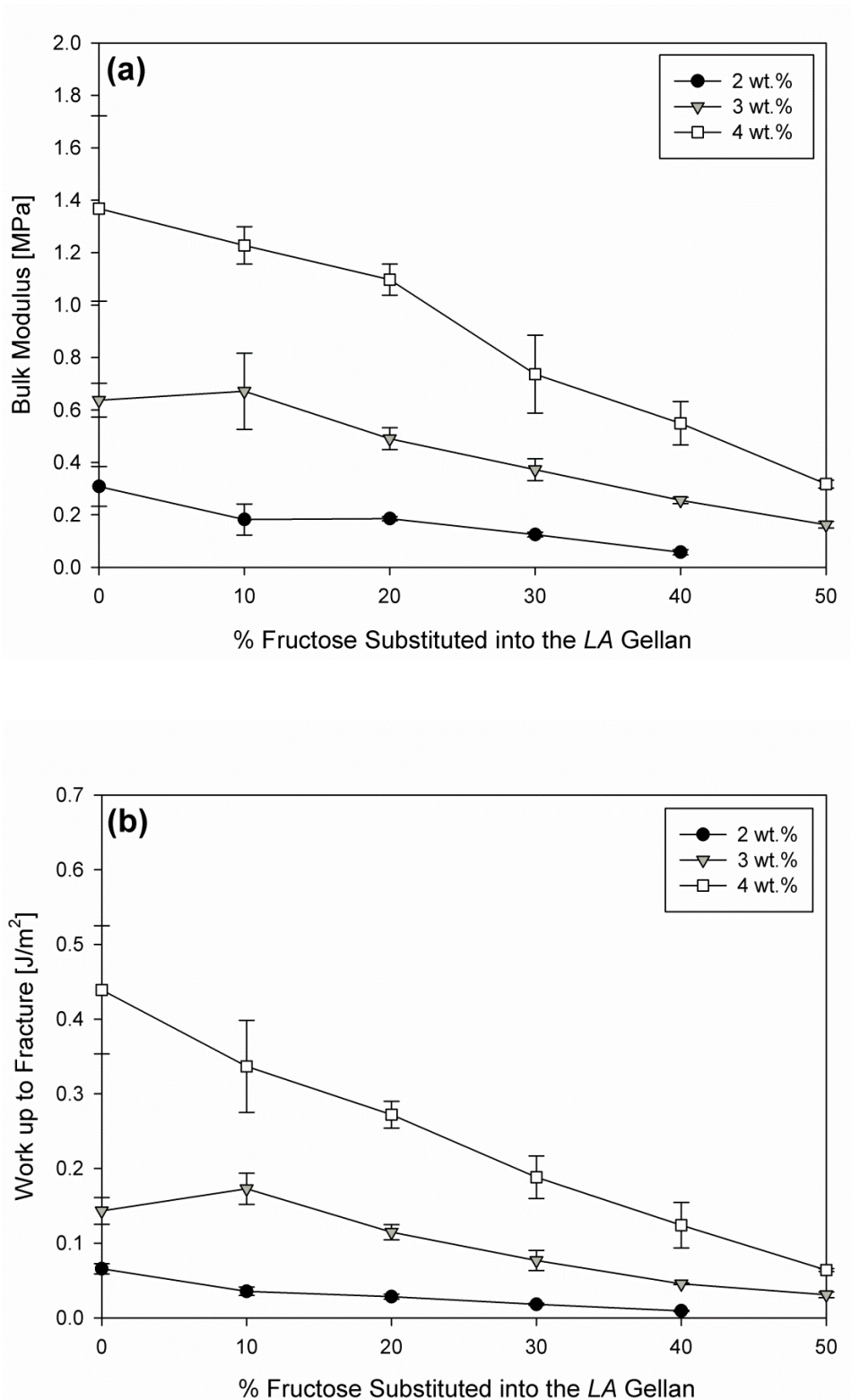


Figure 6.6. Bulk modulus (a) and work up to fracture (b) data for the low acyl gellan gum quiescent gels substituted with 0 – 50 % fructose, as a function of increasing polymer concentration (2 – 4 wt.%).

The solvent quality of the three sugars used in this work in the gellan polymeric mixtures, is dependent on the average number of water molecules in their respective hydration layers that surround the individual sugar molecules (Sworn & Kasapis, 1998). Sucrose being a disaccharide has a larger average number of 6.6 water molecules (Coulate, 1994), than for the smaller monosaccharides fructose and glucose. The monosaccharides have a reduced solvent quality due to their smaller size resulting in weaker gels overall, but their lower hydration numbers enable there to be extra free water available to the gellan gum, contributing to the formation of better developed networks (Sworn & Kasapis, 1998).

Tait et al. (1972) suggested using NMR and dielectric relaxation studies that the effectiveness of sugars is connected to the number of equatorial hydroxyl groups, whose spacing were shown to be compatible with the lattice structure of water. Applying this theory to the three sugars used in the work, the anticipated order would be fructose < glucose < sucrose. Fructose and glucose are of equal molecular weight however a reduced effect is expected with fructose based on the molecular architectural differences between the fructose furanose and glucose pyranose ring structures (Sworn & Kasapis, 1998). It was found (Tait et al., 1972) that most of the hydroxyl groups in the glucose structure were in an equatorial configuration with adjacent oxygen molecules that covered a distance of 0.486 nm; this being the ideal match for a water lattice. This high co-solute water compatibility however, reduces the availability of water molecules for the formation of thermodynamically stable junction zones. The furanose conformation of fructose was found to have fewer equatorial hydroxyl groups (Tait et al., 1972). Thus, the water molecules in mixed fructose gellan systems are structured less efficiently, and instead form hydrogen bonds with the gellan helical chains forming more cohesive networks overall. The respective order of the sugars observed within the results presented in this chapter for the low gellan (2 – 3 wt.%) and low co-solute (10 – 20 %, 3 wt.% only) concentrations clearly depart from the expected order proposed by Tait et al.

(1972), with the glucose systems exhibiting considerably lower gel strengths than expected. This at present cannot be explained by a single factor, but could be related to the use of different forms or sources of the same co-solute, different total polymer concentrations, polymer composition and different co-solute solvation techniques during gel preparation in the respective investigations.

Lastly, following on from the earlier suggestion that the commercial gellan gum used within this work contains a high divalent cation content, which in turn causes excessive aggregation in the presence of added sugar, the subsequent network weakening has been related to varying sugar type. It was suggested that gel strength with varying sugar type decreased with increasing extent of further association, giving the following order of effectiveness: sucrose < glucose < fructose (Gibson & Sanderson, 1997). This departs from the sequence observed for the 3 wt.% mixed gellan gels (30 – 50 % co-solute concentrations only) and the 4 wt.% mixed gellan gels, with the glucose systems once again exhibiting much lower gel strengths than those expected. The differences again were related to the varying experimental conditions in each study.

To summarise, this work relating to gel structure clearly shows that the biopolymer concentration, and the concentration, configuration and conformation of monomeric and dimeric sugars has a significant effect on the properties of the *LA* gellan gum and co-solute mixed gel systems.

6.2.1.2. Viscoelastic material response: Identification of the coil-helix transition

The prepared *LA* gellan gum and co-solute mixed quiescent gel aqueous samples (90 °C) were loaded onto the pre-heated rheometer plate (90 °C) and their viscoelastic material response to frequency table tests during a temperature cooling ramp (every 10 °C) measured. Rheological examination of the viscoelastic material response of the gels is important for understanding the mechanisms of gelation in order to better manipulate textural attributes (Nickerson et al., 2004). These assessments enable the temperature dependence of gellan network formation to be studied at relatively low levels of co-solute (0 – 50 %), and for their respective coil-helix temperatures (T_{ch}) to be determined.

6.2.1.2.1. Glucose

Addition of glucose to the gellan gum aqueous solutions was found to have a notable impact on their subsequent mechanisms of gel formation and viscoelastic material response. These physical properties were also found to depend on the total polymer concentration. Figures 6.7a and 6.7b show the G' and G'' versus temperature measurements for 2 wt.% *LA* gellan gum quiescent gels, as a function of increasing glucose concentration. The data plotted was taken at 1 Hz from the table of frequencies that were performed within the linear viscoelastic region (LVR) for gellan (1 % strain). On cooling, a sharp rise over a narrow temperature range is observed for G' at ~ 50 °C for the sample with 0 % glucose (Figure 6.7a), which reached a maximum point, before continuing to increase with reduced temperature. This was attributed to the coil-helix transition period, where conversion of the polymer from the disordered random coil state to the double-helix form occurs (García et al., 2011; Yamamoto & Cunha, 2007; Chandrasekaran & Radha, 1995). However, conformational ordering does not in itself give a cohesive network. Formation of true gels

requires association of double helices into stable aggregates to form junction zones (Morris et al., 2012). The rapid rise in G' signifies the formation of a three-dimensional ordered structure (Tsoga et al., 1999). The presence of cations can stabilise the gellan network by shielding the electrostatic repulsion of the carboxyl side groups, thereby permitting tight binding and aggregation of helices at lower temperature, or lead to the reduction of coil dimensions at higher temperatures (Morris et al., 1980; Kobayasi et al., 1994).

In the absence of added cations, the formation of stable associations between the flexible thermally moving gellan coils at high temperatures is prevented (Whittaker et al., 1997). Reduction in the configurational freedom of polymeric chains on cooling however, allows the batch salts from the commercial *LA* gellan gum to induce a gelation process (Whittaker et al., 1997). This was observed in Figure 6.7a by the continued increase in G' values after the coil-helix transition period. A single drop in this region is also observed at 30 °C. This is attributed to a breakdown of adhesion between the sample and the flat surface of the cone and plate geometry, as a result of producing brittle gels that have notable degrees of syneresis and slippage (Whittaker et al., 1997).

The coil-helix transition temperatures T_{ch} were determined by extrapolating a tangent line from the steepest part of the rise of G' during the coil-helix transition period to zero, on the G' vs. temperature plot. Note that the plot scales were adjusted in order to visualise the broad transitions clearly, and that this is a very approximate method for calculating T_{ch} . T_{ch} for the gellan sample with 0 % glucose was ~ 56 °C. Increasing the co-solute concentration from 0 – 50 % glucose resulted in very similar viscoelastic gelling mechanistic behaviours for each sample, with the coil-helix transition periods all occurring in the ~ 50 °C temperature region (Figure 6.7a). However, progressive decreases in both the G' magnitude and the

calculated T_{ch} 's of the mixed gellan gels were also evident: $T_{ch} = \sim 55\text{ }^{\circ}\text{C}$ (10 %); $\sim 53.5\text{ }^{\circ}\text{C}$ (20 %); $\sim 50\text{ }^{\circ}\text{C}$ (30 – 40 %); $\sim 45\text{ }^{\circ}\text{C}$ (50 %).

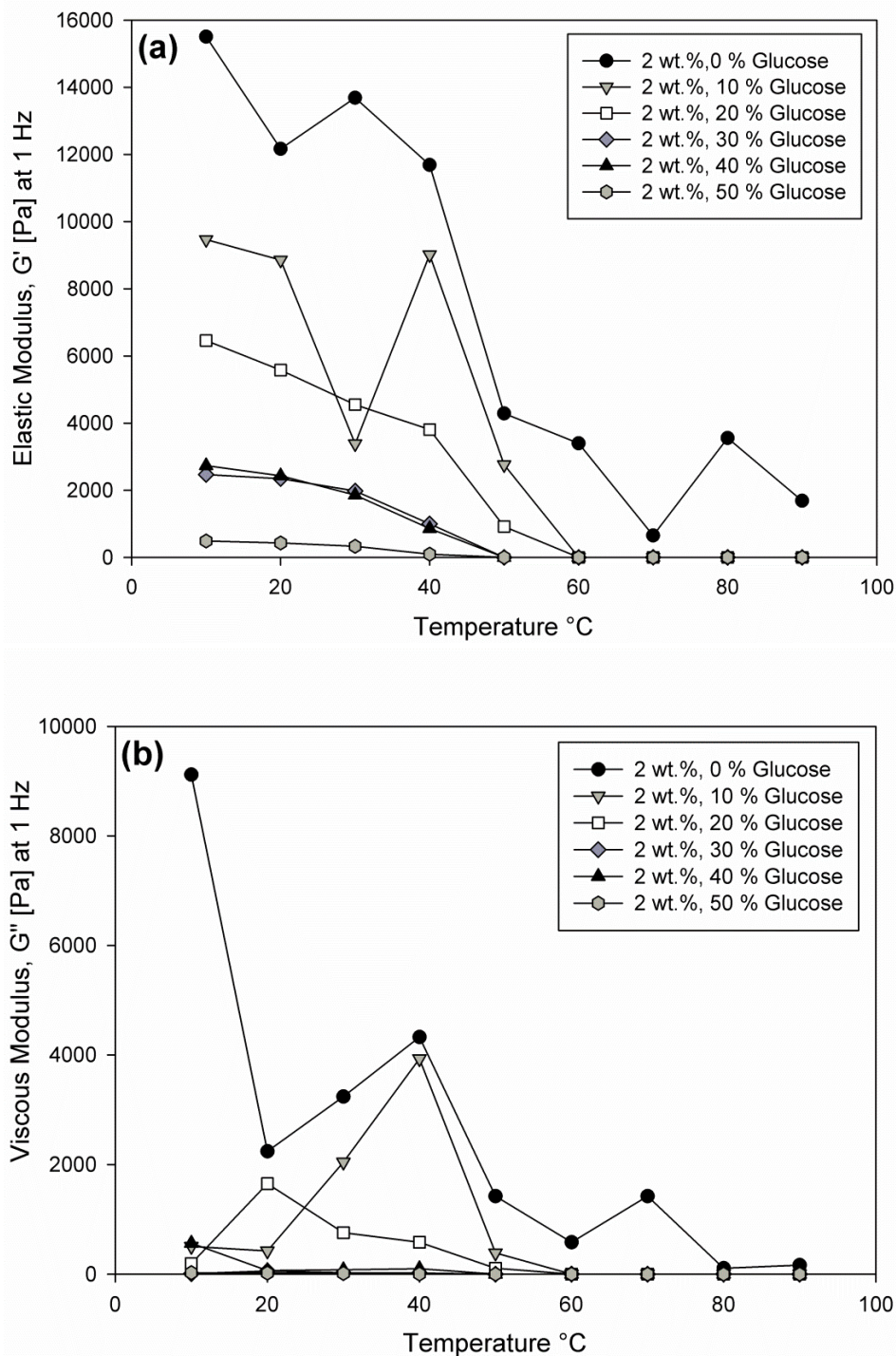


Figure 6.7. Elastic (a) and viscous (b) modulus measurements at 1 Hz versus temperature for 2 wt.% low acyl gellan gum quiescent gels, as a function of increasing % glucose substitution (0 – 50 %) during a temperature cooling ramp (90 – 10 °C), whilst performing frequency tables from 0.1 – 10 Hz at 10 °C intervals. Each of the modulus readings are based on a single sample measurement.

This implied that with increasing glucose concentration the orderly packing of the gellan double helices is hindered and the number of junction zones reduced, resulting in significantly weaker structures with decreased gel strength. The results also indicate a decreased mechanical and thermal stability with increasing glucose concentration, suggesting that glucose addition to the mixed gellan gels has a destabilising effect. Additionally, a single drop in the continued G' increase period following the coil-helix transition period was also observed at ~ 40 °C for the 10 % glucose gellan sample, as for the sample with 0 % glucose (Figure 6.7a). However, with increasing percentage glucose, this drop disappeared and the G' values were observed to increase steadily. This change could suggest that increasing the glucose concentration in the mixed gellan systems leads to gels with decreased brittleness and increased elasticity. Alternatively, these drops could be attributed to noisy data measurements, due to test variability with the rheometer equipment. Repeating these measurements, would confirm indeed whether this is so.

For each of the mixed glucose gellan samples in Figure 6.7, the G' values recorded as a function of frequency of oscillation were higher than those of the G'' across the entire temperature cooling range, thus verifying the dominance of a characteristic gel structure. Although the mixed glucose gellan gel networks are weak, the G' values are constant and remain well above the spectrum of G'' throughout the accessible frequency range (Whittaker et al., 1997). Very similar gelling temperatures and gelling mechanisms were also observed between the G' and G'' measurements for each sample, confirming viscoelastic solid behaviour and evidence that the coil-helix transition and the sol-gel transition occurred concurrently during the cooling process.

Overall, the results in Figure 6.7 displayed the opposite viscoelastic material trends to those expected for mixed gellan glucose gels with low co-solute concentrations. The literature states that low levels of co-solutes have a stabilising effect on *LA* gellan during

cooling, where the T_{ch} and T_{gel} and gel strength (examined by G', G'' measurements) increase as the co-solute level is increased (Nickerson et al., 2004; Miyoshi et al., 1998; Whittaker et al., 1997; Miyoshi & Nishinari, 1999b; Tang et al., 2001). Similar trends have also been reported for other biopolymer-sugar systems with low co-solute concentrations (Oakenfull & Scott, 1986; Papageorgiou & Kasapis, 1995; Papageorgiou et al., 1994). For these trends, the effects of a sugar on the coil-helix transition of a polymer have been attributed (Miyoshi et al., 1998) to one or both of the following factors: (1) the direct hydrogen bonding between hydroxyl groups in the polymer and in the sugar and/or (2) the structural change of water as a solvent. Hence, sugar increases the number of elastically active network chains by forming hydrogen bonds or increases the effective concentration of gellan by immobilising water molecules. Miyoshi et al. (1998) concluded for commercial gellan gum in the sodium form that the effect of sugar (glucose and mannose) did not seem to be a direct result of changes caused by intermolecular binding between the hydroxyl groups in gellan gum and the sugars; stabilising the double helices. Instead, sugars indirectly influenced the interaction between gellan gum and water as a solvent, due to hydration in gellan gum gels in the presence of sugars (Miyoshi et al., 1998). Thus sugar was thought to increase the number of elastically active network chains by forming hydrogen bonds through the water molecules in gellan gum solutions, so that the G' and thermal stability of gellan gum solutions increase with increasing concentration of sugar.

Research has shown that the addition of intermediate levels of co-solutes to *LA* gellan gels (30 – 60 % (Whittaker et al., 1997); 70 – 75 % (Nickerson et al., 2004); 70 – 80 % (Sworn & Kasapis, 1998)) caused progressive weakening of the network structures, where the magnitude of G' declined with increasing co-solute concentration. This pays a close resemblance to the results observed in Figure 6.7 for the *LA* gellan glucose mixed gels. In the intermediate co-solute systems (Nickerson et al., 2004; Whittaker et al., 1997; Sworn &

Kasapis, 1998) the steep rise in G' (Figure 6.7) evident at lower co-solute levels was replaced by a bimodal cooling profile, where G' increased slowly with cooling, followed by a rapid rise, which eventually crossed over G'' to enter a rubbery plateau region. It is thought (Nickerson et al., 2004; Tang et al., 2001) that the bimodal cooling profile is a result of inhibited aggregation by the viscous co-solute system, whereby the high viscosity of the medium hinders migration of the gellan double helices and their ordering to existing junction zones during gelation. This in turn leads to a reduction in the size of the junction zones (and reduced gel strength) in the sugar gels compared to those in aqueous gels (Tang et al., 2001).

In terms of network formation during the bimodal cooling profile, the first steady rise in G' is said (Nickerson et al., 2004) to be associated with the progressive accumulation of aggregates with increasing chain entanglement, whilst the second rise in G' represents the rapid interactions between these aggregates causing them to increase in size and number until a 3D-network is formed. Nickerson et al. (2004) claimed that this type of bimodal profile could also occur within the low co-solute range, but that the sensitivity limits of the rheometer used during their work prevented the collection of supporting evidence. Regardless, the claim is promising in terms of explaining the results in Figure 6.7. Here, initial steady increases in the G' values prior to the observed coil-helix transition periods are apparent for the gellan samples with 0 % and 10 – 20 % glucose at ~ 70 °C and ~ 60 °C respectively, which then merge with the main signals at ~ 50 °C to give T_{ch} 's of ~ 56 °C, ~ 55 °C and ~ 53.5 °C. For the 30 – 40 % mixed glucose gellan samples in Figure 6.7, no low gradient ascents in the G' were observed prior to the coil-helix transition period at ~ 50 °C, but one was apparent for the 50 % mixed gellan glucose sample at ~ 50 °C which then merged with the main signal at 40 °C to give a T_{ch} of ~ 45 °C. Shifts in the onset temperature of this second G' rise to lower temperatures in Figure 6.7, with increasing co-solute concentration have also been reported for the bimodal profiles (Nickerson et al., 2004).

Although the shifts occurred within a much lower temperature range of $\sim 35 - 39$ °C, compared to that of $\sim 50 - 70$ °C in Figure 6.7. Helix-coil transition temperature periods have been reported to occur at ~ 50 °C (Miyoshi et al., 1998) on cooling for mixed co-solute gels in the presence of sufficient sugar however, reassuring the significance of this difference. Overall, the decreases in the onset temperatures of the mixed co-solute gellan gels reflect the decreased hydration and ordering of the gellan chains with increasing co-solute concentration (Evageliou et al., 1998). Increasing the co-solute concentration (within an intermediate range) also causes the gellan chains to become more flexible and to have higher degrees of configurational freedom, which lead to lightly cross-linked entropic dominated networks (Nickerson et al., 2004). The continuous weakening of the gellan network in intermediate (40 – 60 %) mixed co-solute gellan systems with increasing co-solute concentration, has been attributed to the water shortage and enhanced hydrogen bonding between the co-solutes and the remaining water molecules destabilising the rigid aggregated helices in the aqueous gellan gel (Whittaker et al., 1997). These helices then become associated with intermolecular interactions, which in turn increase the maximum network strength considerably, for example from 60 kPa at 30 % sucrose to a magnitude in the order of hundreds for 60 % sucrose (Whittaker et al., 1997). Throughout the proposed intermediate co-solute ranges in the literature (30 – 60 % (Whittaker et al., 1997); 70 – 75 % (Nickerson et al., 2004); 70 – 80 % (Sworn & Kasapis, 1998)), both types of macromolecular arrangement coexist, creating composite systems with a single structuring agent. This composite system is therefore assumed for the mixed glucose gellan samples presented in Figure 6.7.

In addition to the intermediate co-solute gellan bimodal systems displaying a weakening in the gellan network structures with increasing co-solute concentration, excessive cations have also been observed to decrease gellan strength, but these had no effect on the gellan gelling temperatures (Tang et al., 1994, 1995, 1996, 1997a, 1997b). A later study by

the same researchers (Tang et al., 2001) however, noted that the failure to observe changes in the gelling temperatures was due to differing calcium concentrations used, which were shown to give varying gelling temperatures providing evidence they could be reduced with excessive cation concentration. In addition, gelling temperatures and the strength of gels were also found to decrease when both divalent cation and sucrose concentrations were high (Tang et al., 2001). This result may help to explain why weakening in the gellan network structures with increasing co-solute concentration was observed in Figure 6.7, if in fact the commercial gellan used in this work as suggested earlier for the texture analysis results (Section 6.2.1.1.2.), does indeed contain a high proportion of calcium or other divalent cations. However, even if compositional analysis is performed on the commercial gellan to confirm whether this is so, very small numbers of other cations also accompany the predominant cation, which may influence the gel-sol and helix transition behaviours (Miyoshi et al., 1998). This is because the size and the thermal stability of junction zones may be influenced strongly by these cations. Also, even if the gellan sample was monodisperse and completely in one cation form, sugar molecules may interact with the gellan molecules to form different junction zones with various thermal stabilities and sizes (Miyoshi et al., 1998). Thus, it is clear that many different conflicting factors can yield results such as those observed in Figure 6.7 that do not conform to previous reported trends.

It was observed that increasing the biopolymer concentration of the mixed gellan-glucose (0 – 50 %) samples from 2 wt.% to 3 wt.% and 4 wt.% resulted in much firmer gels with increased gel strength, and thus final G' and G'' values following the coil-helix transition period with increased magnitude. Systematic increases in the final values of G' as a function of polymer concentration have also been recorded by Nakamura et al. (1993) when gellan solutions were quenched at temperatures well below that of the conformational transition. Both reflect the increased extent of interactions occurring between the gellan polymer chains.

Increasing the glucose concentration (0 – 50 %) at each polymer concentration however, remained to cause progressive weakening of the network structures with decreasing magnitude of G' and G'' and reduced gelling temperatures. The G' values recorded at each polymer concentration as a function of frequency of oscillation also remained to be higher than those of the G'' across the entire cooling range. Further, very similar gelling temperatures and gelling mechanisms were observed between the G' and G'' measurements for each sample at each polymer concentration, confirming viscoelastic solid behaviour. Although, higher amounts of the polysaccharide resulted in earlier gelation as monitored by the sharp rise in the G' traces over a narrow temperature range, and the gelling temperatures of each solution increased with increasing gellan concentration. These results suggest that the glucose concentration is equally as influential over the mixed gellan gel viscoelastic behaviour as the total biopolymer concentration. Interaction between the glucose and gellan concentrations was significant for each of the parameters studied, suggesting that the effect of glucose on the viscoelastic behaviour depends on the gellan concentration. This effect was most prominent with the magnitude of the G' and G'' values, however the effect of gellan concentration was also significant for the gelation causing it to occur earlier at higher temperatures, with increasing concentration.

6.2.1.2.2. Sucrose and Fructose

The addition of sucrose and fructose individually to the gellan gum aqueous solutions also had significant influences on their subsequent mechanisms of gel formation and viscoelastic material response. Many of these physical properties drew close resemblances to those observed for the mixed glucose gellan gels described previously, and they were also found to depend on the total polymer concentration. Figures 6.8a and 6.9a and 6.8a and 6.9b

show the G' and G'' versus temperature measurements for 2 wt.% *LA* gellan gum quiescent gels, as a function of increasing sucrose (Figure 6.8) and fructose (Figure 6.9) concentration.

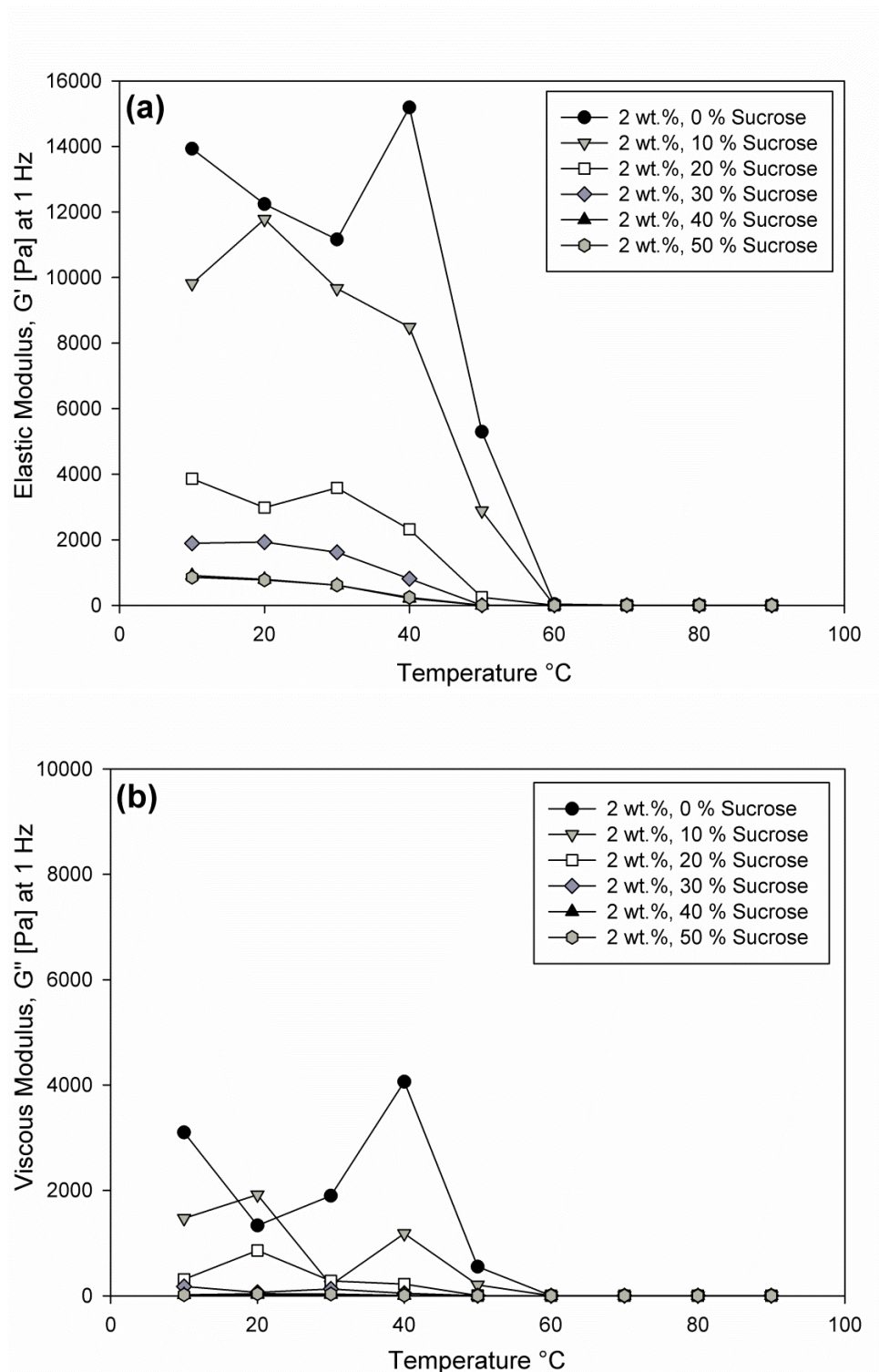


Figure 6.8. Elastic (a) and viscous (b) modulus measurements at 1 Hz versus temperature for 2 wt.% low acyl gellan gum quiescent gels, as a function of increasing % sucrose substitution (0 – 50 %) during a temperature cooling ramp (90 – 10 °C), whilst performing frequency tables from 0.1 – 10 Hz at 10 °C intervals. Each of the modulus readings are based on a single sample measurement.

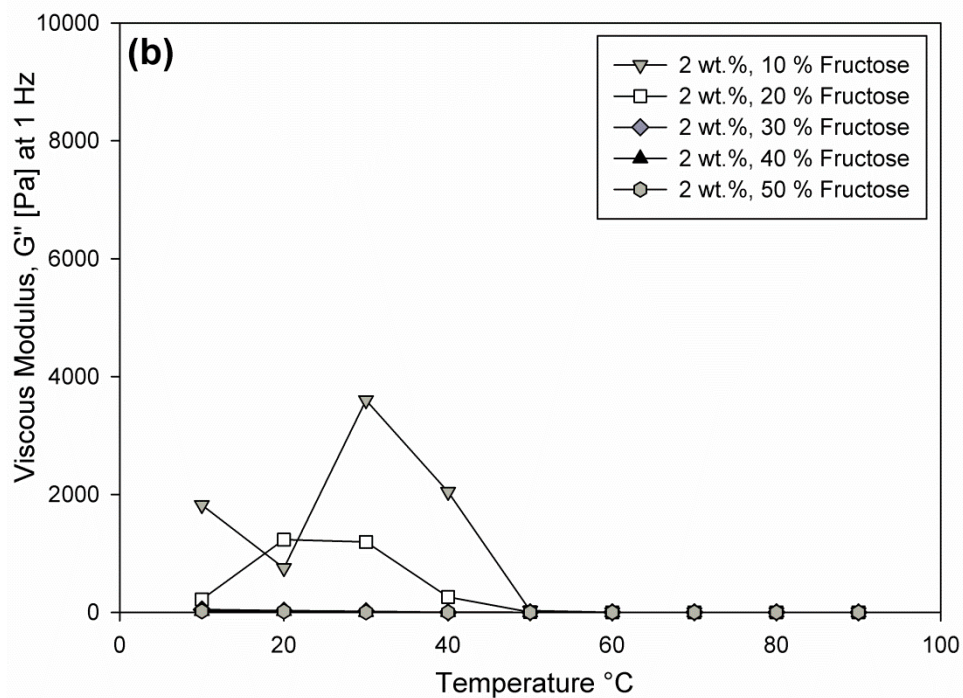
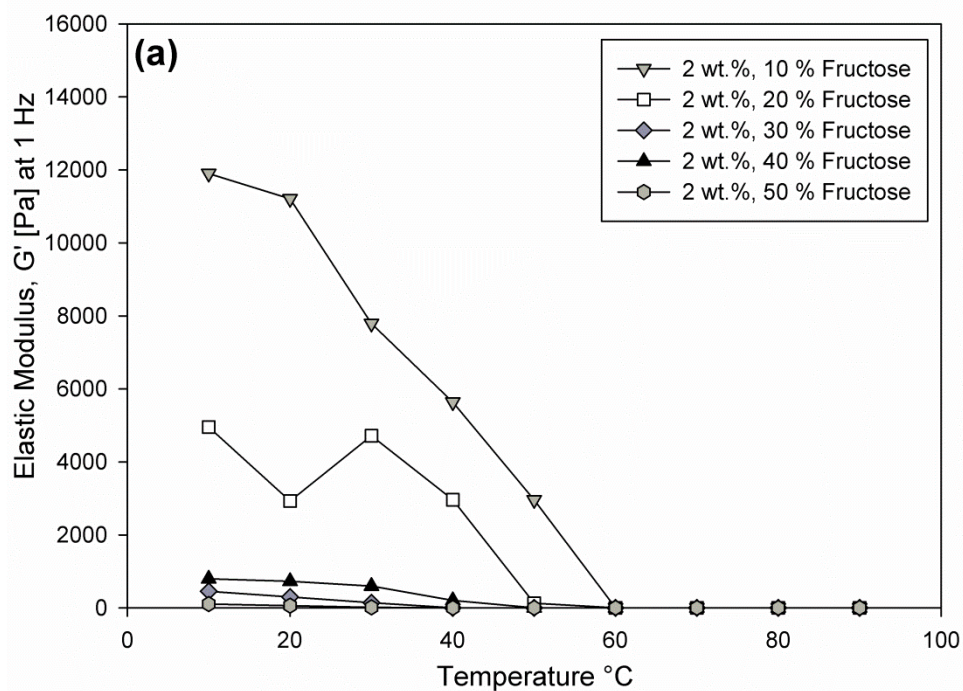


Figure 6.9. Elastic (a) and viscous (b) modulus measurements at 1 Hz versus temperature for 2 wt.% low acyl gellan gum quiescent gels, as a function of increasing % fructose substitution (0 – 50 %) during a temperature cooling ramp (90 – 10 $^{\circ}\text{C}$), whilst performing frequency tables from 0.1 – 10 Hz at 10 $^{\circ}\text{C}$ intervals. Each of the modulus readings are based on a single sample measurement.

All of the mixed sucrose and mixed fructose gellan gels displayed on cooling, the same narrow coil-helix transition period at ~ 50 °C, where the G' was observed to rise sharply up to a maximum, before continuing to increase with reduced temperature, as for the mixed gellan glucose gels. Note that measurements for the 2 wt.% gellan sample with 0 % fructose were omitted (Figure 6.9), due to the limited number of samples (20) specified for each assay kit. It was assumed that the results would yield data similar to those presented for the equivalent 2 wt.% gellan samples with 0 % glucose and 0 % sucrose, respectively (Figures 6.7 and 6.8).

Increasing the co-solute concentration from 10 – 50 % for both sucrose and fructose also resulted in progressive decreases in both the G' magnitude and the calculated T_{ch} 's of the mixed gellan gels. For the mixed sucrose and mixed fructose gels respectively these were: $T_{ch} = \sim 55$ °C and 52.5 °C (10 %); ~ 52 °C and 51 °C (20 %); ~ 50 °C (30 %); ~ 50 °C and 45 °C (40 %); ~ 45 °C and 35 °C (50 %). Bimodal cooling profiles were also apparent in the mixed sucrose and mixed fructose gellan gels (Figures 6.8 and 6.9), where initial steady increases in the G' values prior to the observed coil-helix transition periods were evident for each co-solute at ~ 70 °C for the 0 – 10 % gels and ~ 60 °C for the 20 % gels, which then merged with the main signals at ~ 50 °C to give the T_{ch} 's listed above. No low gradient ascents in the G' were observed for the 30 % samples prior to their coil-helix transition period at ~ 50 °C, but they reappeared for the 40 – 50 % mixed co-solute gellan gels at ~ 50 °C which then merged with the main signals at 40 °C. Likewise with the mixed glucose gellan samples, these shifts in the onset temperatures with increasing co-solute concentration were clear and reflect the decreased hydration and ordering of the gellan chains with increasing co-solute concentration (Evageliou et al., 1998). Overall, this implied that with increasing sucrose and fructose concentration the orderly packing of the gellan double helices is hindered and the number of junction zones reduced, resulting in significantly weaker

structures with decreased gel strength. The results also indicate a decreased mechanical and thermal stability with increasing co-solute concentration, suggesting that co-solute addition to the mixed gellan gels has a destabilising effect.

Single drops in the continued G' increase period following the coil-helix transition period were also observed between $\sim 20 - 40$ °C for the 10 – 30 % mixed gellan sucrose and fructose samples (Figure 6.8a and 6.9a). However with increasing percentage co-solute thereafter, this drop disappeared and the G' values were observed to increase steadily. This was comparable with the gellan glucose mixtures, although no decrease was observed at 30 % glucose (Figure 6.7a). These changes suggest that increasing the sucrose and fructose concentration in the mixed gellan systems also leads to gels with decreased brittleness and increased elasticity, but that the extent is greater than with the glucose mixed gellan systems. Alternatively, these drops could also be attributed to noisy data measurements, due to test variability with the rheometer equipment. Repeating these measurements, would confirm indeed whether this is so.

For each of the mixed sucrose and mixed fructose gellan samples (Figures 6.8 and 6.9), the G' values recorded as a function of frequency of oscillation were also higher than those of the G'' across the entire temperature cooling range, verifying the dominance of characteristic gel structures. Very similar gelling temperatures and gelling mechanisms were also observed between the G' and G'' measurements for each of the samples, confirming viscoelastic solid behaviour and evidence that the T_{ch} and the T_{sg} occurred concurrently during the cooling process.

Increasing the biopolymer concentrations of the mixed sucrose and mixed fructose gellan samples from 2 wt.% to 3 wt.% and 4 wt.% also resulted in much firmer gels with increased gel strength that with increasing co-solute concentration were progressively

weakened, as explained for the mixed glucose gellan samples. The G' values recorded at each polymer concentration as a function of frequency of oscillation also remained higher than those of the G'' across the entire cooling range, and very similar gelling temperatures and gelling mechanisms were observed for the two measurements with each sample. Higher amounts of the polysaccharide did however result in earlier gelation and increased gelling temperatures of the samples with increasing gellan concentration. The relationship between the concentration and the co-solutes was the same as that described for the mixed glucose gellan gels.

Comparing the viscoelastic modulus measurements for the three sugars at the end of the coil-helix transition period for all co-solute concentrations (Figures 6.7 – 6.9), the order of gel strength was sucrose < glucose < fructose. This order is supportive of that proposed by Gibson & Sanderson (1997) for mixed gellan gels formed from commercial gellan containing high divalent cation content, which suggested that gel strength with varying sugar type decreased with increasing extent of further association with the gel networks that are close to or at the optimum degree of crosslinking. Thus, further implying that the commercial gellan used to formulate the mixed gellan co-solute gels in this work also had high divalent cation content.

The calculated T_{ch} 's for the respective 2 wt.% mixed gellan gels with increasing co-solute concentration however, display lower temperature values for the fructose gels and comparable values for the glucose and sucrose gels, favouring the reverse order fructose < glucose \leq sucrose. This order is close to and supportive of that observed for the textural analysis results of the mixed gels at the same biopolymer concentration (Section 6.2.1.1.2), and is strongly argued in the literature. Tang et al. (2001) argued that sucrose is more effective than fructose at stabilising the orderly packed gellan double helices in aqueous solutions through their readiness towards crystallisation. This stabilising effect results in

higher gelling temperatures with increasing sucrose concentration, and overall produces stronger gel networks when compared to fructose (Papageorgiou et al., 1994). The fructose molecules are randomly packed in aqueous solutions and do not exhibit this stabilisation effect, thus adding fructose to gellan solutions has little effect on the gelling temperature (Tang et al., 2001).

Further, Sworn & Kasapis (1998) argued that sucrose formed stronger gellan polymeric mixtures than fructose or glucose based on their solvent quality being dependable on the average number of water molecules in their respective hydration layers that surround the individual sugar molecules. Sucrose being a disaccharide has a larger average number of 6.6 water molecules (Coulate, 1994), than for the smaller monosaccharides fructose and glucose. Thus, the monosaccharides have a reduced solvent quality due to their smaller size resulting in weaker gels overall.

Finally, Tait et al. (1972) argued the same order for the three sugars based on their effectiveness being connected to the number of equatorial hydroxyl groups, whose spacing were shown to be compatible with the lattice structure of water. Fructose and glucose are of equal molecular weight however a reduced effect is expected with fructose based on the molecular architectural differences between the fructose furanose and glucose pyranose ring structures (Sworn & Kasapis, 1998). This is explained in greater detail in Section 6.2.1.1.2, but overall the water molecules in the mixed fructose gellan systems are structured less efficiently.

Based on this strong support, the calculated T_{ch} 's rather than the viscoelastic modulus measurements for the respective 2 wt.% mixed gellan gels with increasing co-solute concentration, were thought to be more representative for the three sugars, giving a true reflection of their gel strength.

6.2.1.3. Measuring the % co-solute release using spectrophotometry

6.2.1.3.1. Glucose

Increasing the concentration of glucose within 2 – 4 wt.% *LA* gellan mixed glucose quiescent gels had a notable effect on the subsequent levels of glucose released from their network structures. Figure 6.10 shows the measurements of percentage glucose release for these gels, substituted with 10 – 50 % glucose following an 18 hour diffusion period, as a function of increasing polymer concentration.

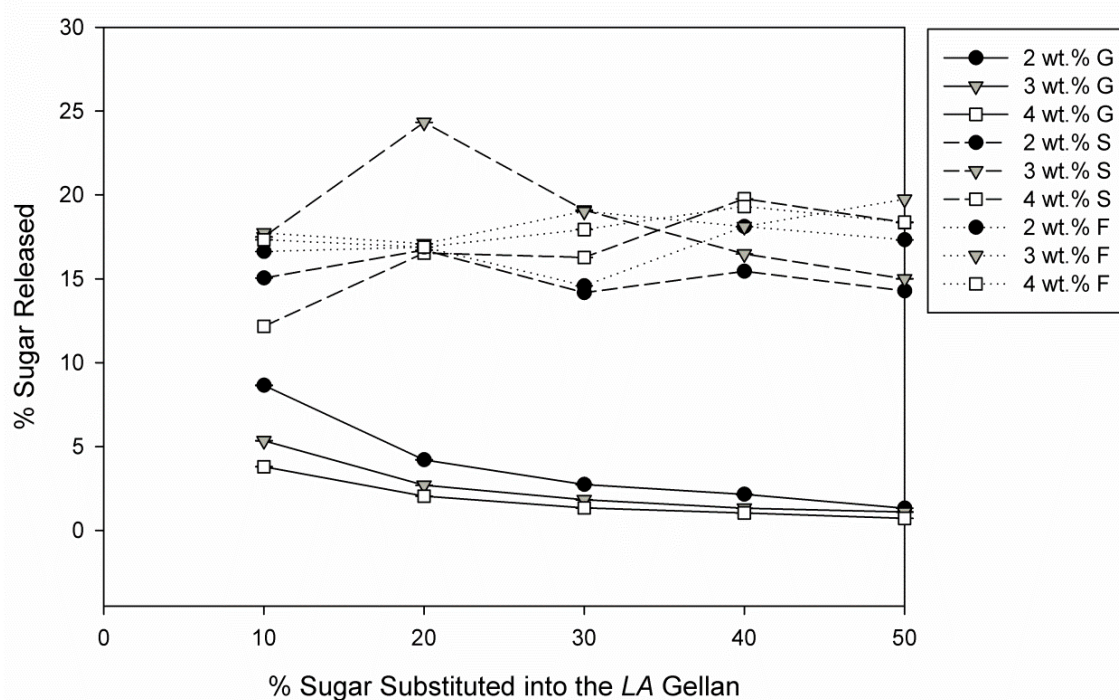


Figure 6.10. Measurement of % sugar (glucose (G), sucrose (S) and fructose (F)) released from low acyl gellan gum quiescent gels substituted with 10 – 50 % sugar following an 18 hour diffusion period, as a function of increasing polymer concentration (2 – 4 wt.%). All measurements were carried out in triplicate. Where error bars cannot be observed, they are smaller than the data points.

A significant decrease in the glucose released is observed between the measurements recorded for the mixed glucose gellan gels with 10 and 20 % glucose, at each biopolymer concentration. Further increasing the glucose concentration, continued to result in a decrease

in the glucose released from the gels, but this occurred much more steadily. This suggests that the mixed co-solute gellan gel network is weaker at lower glucose levels, enabling greater diffusion of the glucose molecules into the double distilled water used to measure the percentage release of the sugar. Thus increasing the glucose concentration leads to stronger mixed co-solute gellan gel networks that are reinforced either directly or indirectly by the glucose molecules, restricting their subsequent mobility and measured release.

Increasing the gellan biopolymer concentration of the mixed glucose gels from 2 wt.% - 3 wt.% - 4 wt.% also resulted in a decrease in the glucose released from their structures, as a consequence of the increasing extent of interactions occurring between the hydrocolloid chains. In other words, the mobility of both the gellan helical chains and the glucose molecules within the continuous gel matrices are restricted, which hinder subsequent glucose diffusion and measured release. These results suggest that the glucose concentration is equally as influential over the mixed co-solute gellan gel strength and its sugar release properties, as the total biopolymer concentration. Interaction between the glucose and the varying gellan concentrations was significant in the measured glucose release from the mixed co-solute gellan gels, suggesting that the effect of glucose on these properties depends on the gellan concentration.

6.2.1.3.2. Sucrose and Fructose

Increasing the concentration of the sucrose and fructose separately within 2 – 4 wt.% *LA* gellan mixed co-solute quiescent gels also had a notable impact on the subsequent levels of co-solute released from their network structures. Figure 6.10 also shows the measurements of percentage sucrose and fructose release for these gels, substituted with 10 –

50 % co-solute following an 18 hour diffusion period, as a function of increasing polymer concentration.

For the 2 wt.% mixed sucrose gellan gels, a consistent sucrose release is observed (Figure 6.10) at ~15 % with increasing sucrose concentration. This shows that increasing the sucrose concentration has no additional effect on the subsequent sucrose release from the mixed gellan co-solute gels, implying that the gel network reaches a structural reinforcement threshold at 10 % added sucrose giving a fixed percentage sucrose release which remains with further added co-solute. Increasing the gellan concentration of the mixed sucrose gels from 2 wt.% - 3 wt.% also resulted in a fairly consistent sucrose release (Figure 6.10) at ~17 % with increasing sucrose concentration, except for an increased measurement at 20 % added sucrose which was considered to be an anomalous result due to experimental error. Further increasing the gellan concentration to 4 wt.% had a rather different influence over the subsequent percentage sucrose release however, with increasing sucrose concentration. A progressive increase in the percentage sucrose release from ~13 – 20 % (Figure 6.10) is observed with increasing sucrose concentration, suggesting that the mixed gellan sucrose gel networks are being progressively weakened. It was shown in Section 6.2.1.1.2 that the addition of increasing levels of sucrose to the gellan gels results in highly flexible, less aggregated polymer networks that have enhanced elasticity. Further, Tait et al. (1972) stated that sucrose's high co-solute water compatibility (based on high levels of equatorial hydroxyl groups whose spacing were highly compatible with water's structural lattice) reduces the availability of water molecules for the formation of thermodynamically stable junction zones. Thus this formation of a solvent in the aqueous media with the water molecules would inhibit the extensive polymer aggregation of the gellan phase, weakening the network (Sworn & Kasapis, 1998). Together, these factors contribute to the overall weakening of the mixed

sucrose gellan systems with increasing sucrose concentration, in turn maximising the sucrose molecule mobility and their subsequent measured release.

It is also noted in Figure 6.10 that the orders of gellan concentration at each co-solute level are the reverse of those observed for glucose, resulting in an increase in sucrose release with increasing concentration. This could be a consequence of the influence sucrose has over the gellan network structure, suggesting that it has a greater impact on the molecular ordering through its inhibition of polymer-chain aggregation, than the gellan concentration increasing the extent of their interactions.

For the 2 – 4 wt.% mixed fructose gellan gels, a consistent fructose release is observed (Figure 6.10) between ~17 – 19 % with increasing fructose concentration, excluding the considered anomalous result observed for the 2 wt.%, 30 % sample. Likewise for the 2 wt.% mixed sucrose gellan gels, this shows that increasing the fructose concentration has no additional effect on the subsequent fructose release from the mixed co-solute gellan gels, implying that the gel network reaches a structural reinforcement threshold at 10 % added fructose giving a fixed percentage fructose release which remains with further added co-solute. Increasing the gellan biopolymer concentration was shown to enhance the percentage fructose release, suggesting that fructose like sucrose also has a greater influence over the gellan network structure, than the gellan concentration.

Comparing the measured percentage sugar releases for the three co-solutes, sucrose and fructose were found to have comparable levels (~ 15 – 20 %) which were considerably higher than those for glucose (~ 1 – 8 %). The much lower release levels for glucose suggest that the mobility of the glucose molecules within the mixed glucose gellan network is being restricted by its structural form to a greater extent than for the other co-solutes in their respective systems, and/or that the glucose molecules are being incorporated within the gellan

network directly through bonding, thereby both restricting their subsequent diffusion from the mixed glucose gellan systems. The first suggestion has already been disproved using texture analysis (Section 6.2.1.1.2) where it was found across all of the gellan concentrations, irrespective of the co-solute concentration that the mixed glucose gellan gels were much weaker than the mixed sucrose gellan and mixed fructose gellan gels, thus implying a greater mobility and greater release of the glucose molecules. It was therefore suggested that the orderly packed glucose units in the gellan structure may replace the glucose units in the aqueous gel solution in a similar manner proposed by Tang et al. (2001) for sucrose (Section 6.2.1.1.2). This would have a stabilising effect on the orderly packed gellan double helix in the aqueous solutions (Papageorgiou et al., 1994), resulting in stronger gel networks with increasing glucose concentration, and subsequent decreasing glucose release as observed in Figure 6.10.

6.2.1.4. Measuring the % co-solute release over time

To explore the variation of percentage co-solute release over time for varying diffusion periods, the 2 wt.% *LA* gellan mixed glucose (10 – 50 %) and 2 wt. % *LA* gellan mixed sucrose (10 – 50 %) systems were selected and exposed to diffusion times of 1h, 5h and 10h. The same technique used to accurately monitor the co-solute release in Section 6.2.1.3 was followed, and comparisons were made using the results collected after their 18h diffusion periods. The mixed fructose gellan samples were omitted from these tests due to their percentage release measurements in Section 6.2.1.3 having great similarity to those of the mixed sucrose gellan systems. Direct comparison between the disaccharide and monosaccharide sugars systems also wanted to be maintained to investigate whether their release rates were different.

6.2.1.4.1. Glucose and Sucrose

Increasing the diffusion period time for the 2 wt.% mixed glucose gellan and mixed sucrose gellan gels had a notable impact on the subsequent levels of co-solute released from their network structures. Figures 6.11 and 6.12 show the measurements of percentage glucose and sucrose release over time for these gels substituted with 10 – 50 % co-solute, as a function of increasing diffusion time (Figures 6.11a & 6.12a) and increasing percentage co-solute concentration (Figures 6.11b & 6.12b). For the mixed glucose gellan gels, it is observed that the percentage glucose released at each co-solute level, decreases at a steady and equal rate with increasing diffusion time (Figure 6.11). Increasing the glucose concentration for the three additional diffusion times also produced the same trends as those observed in Section 6.2.1.3.1 for the 18h diffusion period, and can be explained in the same manner. Although an anomalous result was apparent for the mixed glucose gellan system with 10 % glucose, after a 1h diffusion period; this was accounted for by experimental error.

Overall, these results imply that the influences of glucose over the gellan network structure and the composition of the mixed glucose gellan systems themselves do not change significantly over time.

For the mixed sucrose gellan gels, it is observed that the percentage sucrose released at each co-solute level, increases at a rapid, but proportionate rate with increasing diffusion time (Figure 6.12). For the three additional diffusion times, increasing the sucrose concentration causes the measured percentage sucrose to increase steadily. This is due, as for the 4 wt.% mixed sucrose gellan gels following an 18h diffusion period (Section 6.2.1.3.1), to a progressive weakening of the mixed sucrose gellan networks and can be explained accordingly. Overall, these results suggest that the rate of diffusion for the sucrose molecules over time compared with the glucose molecules is much slower. This is most likely to be attributed to the larger molecular size of the disaccharide, and the greater influence of sucrose over the gellan network structure leading to the progressive weakening of the mixed sucrose gellan systems over time. These results and the fact that the percentage sucrose released after 18 h was found to be significantly higher than that for glucose, further suggest that the glucose is being incorporated within the gellan structure, as discussed in Section 6.2.1.3.2.

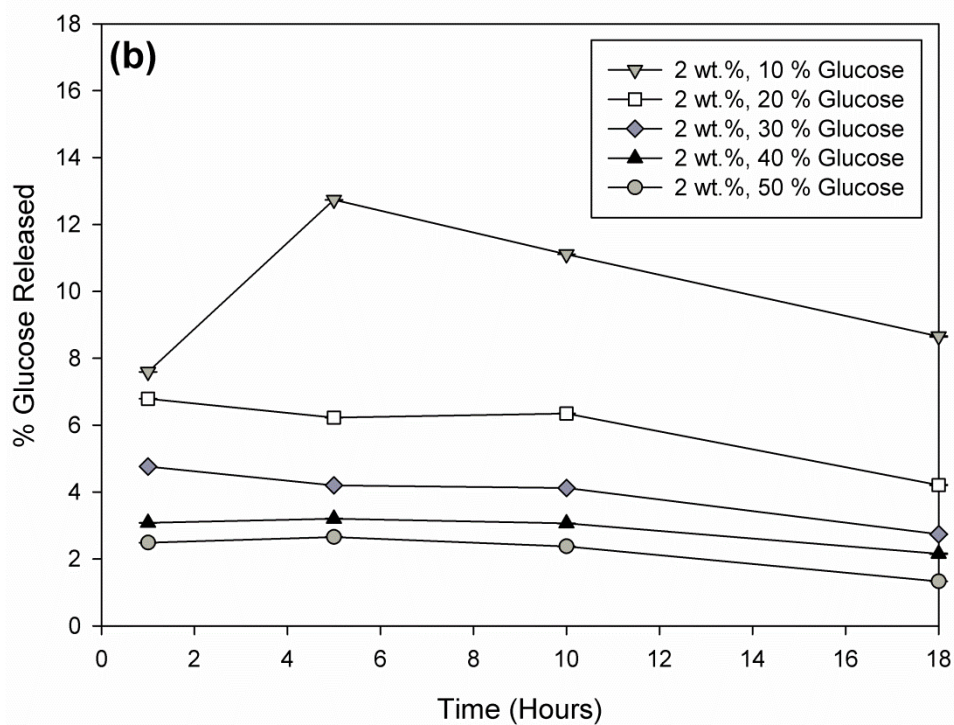
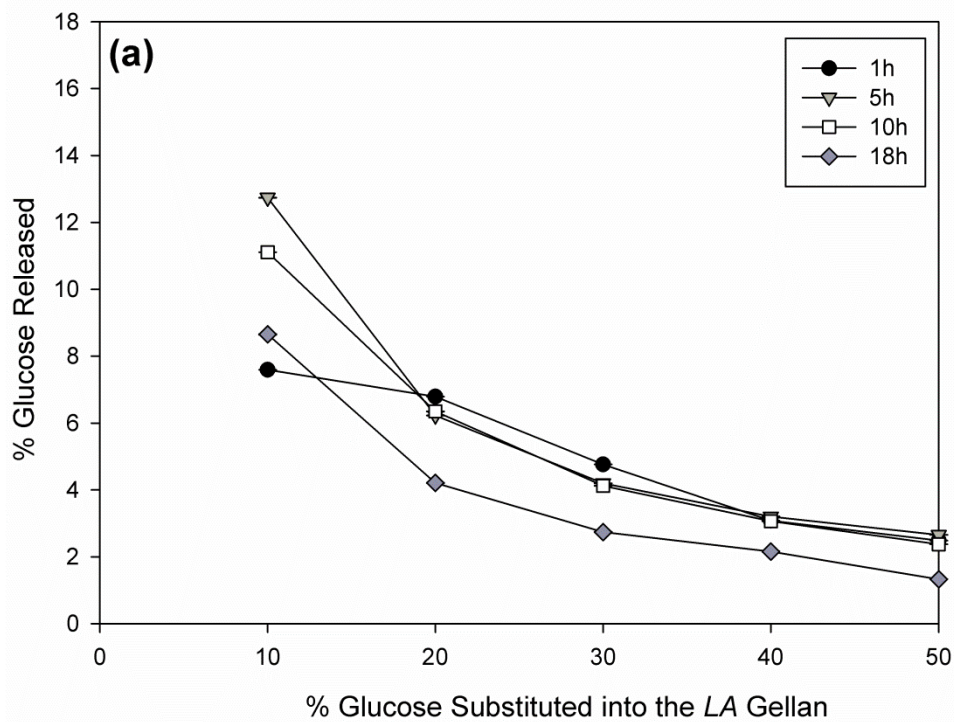


Figure 6.11. Measurement of % glucose released over time (hours) from 2 wt.% low acyl gellan gum quiescent gels substituted with 10 – 50 % glucose, as a function of increasing diffusion time (a) and increasing % glucose substitution (b). All measurements were carried out in triplicate. Where error bars cannot be observed, they are smaller than the data points.

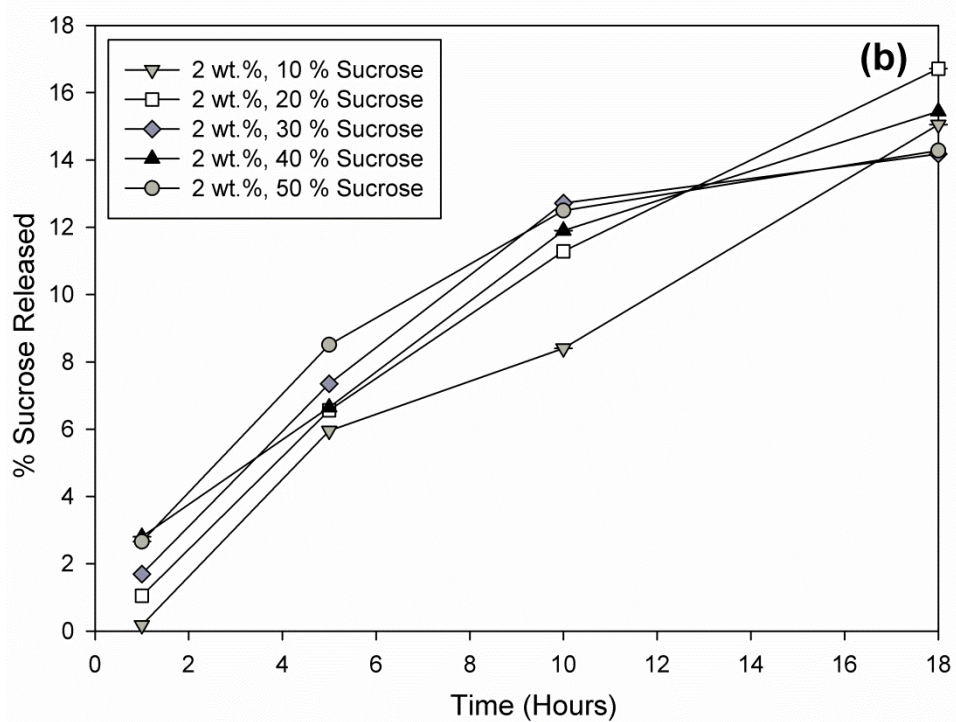
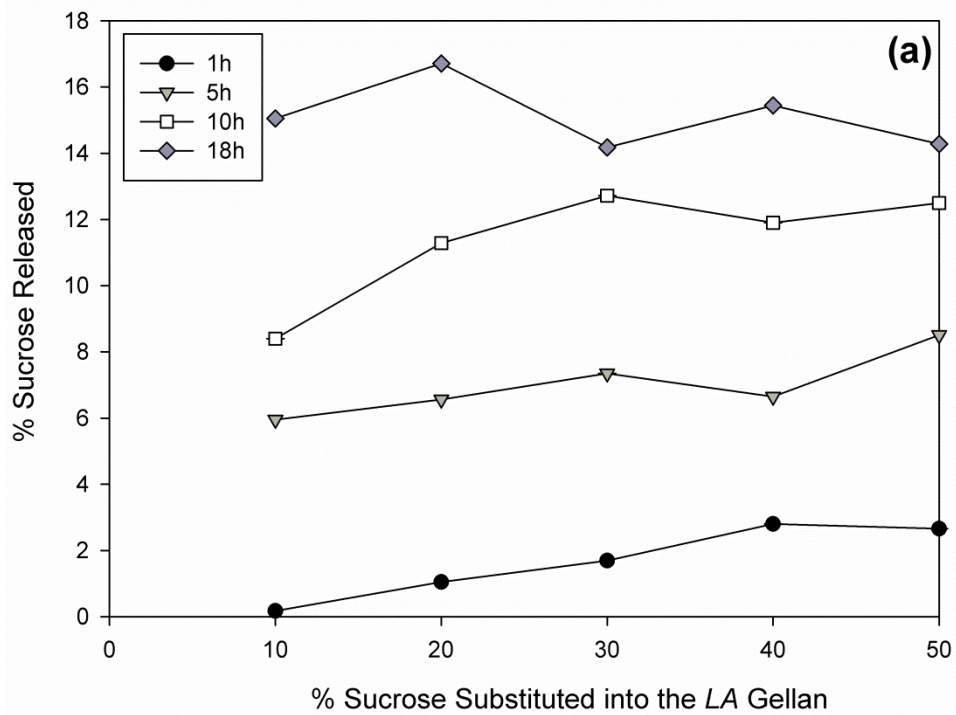


Figure 6.12. Measurement of % sucrose released over time (hours) from 2 wt.% low acyl gellan gum quiescent gels substituted with 10 – 50 % sucrose, as a function of increasing diffusion time (a) and increasing % sucrose substitution (b). All measurements were carried out in triplicate. Where error bars cannot be observed, they are smaller than the data points.

6.2.2. Characterisation of low acyl gellan gum and co-solute mixed fluid gels, and a subsequent measure of their % co-solute release

6.2.2.1. Viscoelastic material response: Identification of the helix-coil transition

To assess the gel formation and molecular ordering behaviour of the 0.5 – 2 wt.% *LA* gellan gum and co-solute mixed fluid gels, the formed samples (described in Section 3.2.8.1) after ~ 24 h refrigerated storage (3 °C) were loaded onto the pre-set rheometer plate (10 °C), and their viscoelastic material response to frequency table tests during a temperature heating ramp measured. These assessments enable the temperature dependence of gellan network deformation to be studied at relatively low levels of co-solute (0 – 50 %), and for their respective T_{hc} 's to be determined.

6.2.2.1.1. Glucose and Sucrose

The addition of glucose and sucrose individually to the gellan gum aqueous solutions prior to fluid gel production had a notable impact on their subsequent mechanisms of gel deformation and viscoelastic material response. Figures 6.13a and 6.14a and 6.13b and 6.14b show the G' and G'' versus temperature measurements for 0.5 wt.% *LA* gellan gum fluid gels, as a function of increasing glucose (Figure 6.13) and sucrose (Figure 6.14) concentration. The data plotted was taken at 1 Hz from the table of frequencies that were performed within the linear viscoelastic region (LVR) for gellan (1 % strain).

On heating, an initial sharp decline between 10 – 20 °C is observed in both G' and G'' for the samples with 0 % glucose (Figure 6.13) and 0 % sucrose (Figure 6.14), which was then followed by a second steeper decline over a narrow temperature range ending at ~ 30 °C, that remained constant with decreasing temperature. The first decline was attributed to

the unfolding of the double helices in their stable aggregates and the disintegration of the network junction zones, whilst the second decline was attributed to the helix-coil transition period (García et al., 2011; Yamamoto & Cunha, 2007; Chandrasekaran & Radha, 1995). In the latter, conversion of the polymer from the double-helix form to the disordered random coil state occurred, and the rapid decline in G' signifies the deformation of the three-dimensional ordered structure (Tsoga et al., 1999). T_{hc} for the gellan samples with 0 % glucose and 0 % sucrose were both ~ 30 °C. Increasing the co-solute concentration from 0 – 50 % for each of the mixed glucose gellan and mixed sucrose gellan gels resulted in very similar viscoelastic melting behaviours, with the helix-coil transition periods all occurring between $\sim 20 - 30$ °C (Figures 6.13 & 6.14). However, progressive decreases in both the G' and G'' magnitudes for the mixed co-solute gellan fluid gels, as with the quiescent gels (Section 6.2.1.2) were also evident. No obvious decreases in the calculated T_{hc} 's for the mixed co-solute gellan fluid gels were evident with increasing co-solute concentration; all had $T_{hc} = \sim 30$ °C. This suggests that the controlled shear and cooling conditions that the mixed co-solute gellan aqueous gels are exposed to during fluid gel production, have stronger influences over the molecular ordering than the respective sugar concentrations, resulting in comparable ordered structures with varying weaknesses that deform at similar temperatures. The result is also in contrast to the progressive decreases observed in the calculated T_{ch} 's with increasing co-solute concentration for the mixed gellan quiescent gels on cooling. Overall, the results for the mixed fluid gel samples on heating reinforce that with increasing co-solute concentration the orderly packing of the gellan double helices, during fluid gel formation is hindered and the number of junction zones reduced, resulting in significantly weaker structures with decreased gel strength. The results also indicate a decreased mechanical and thermal stability with increasing co-solute concentration, suggesting that co-solute addition to the mixed gellan gels has a destabilising effect.

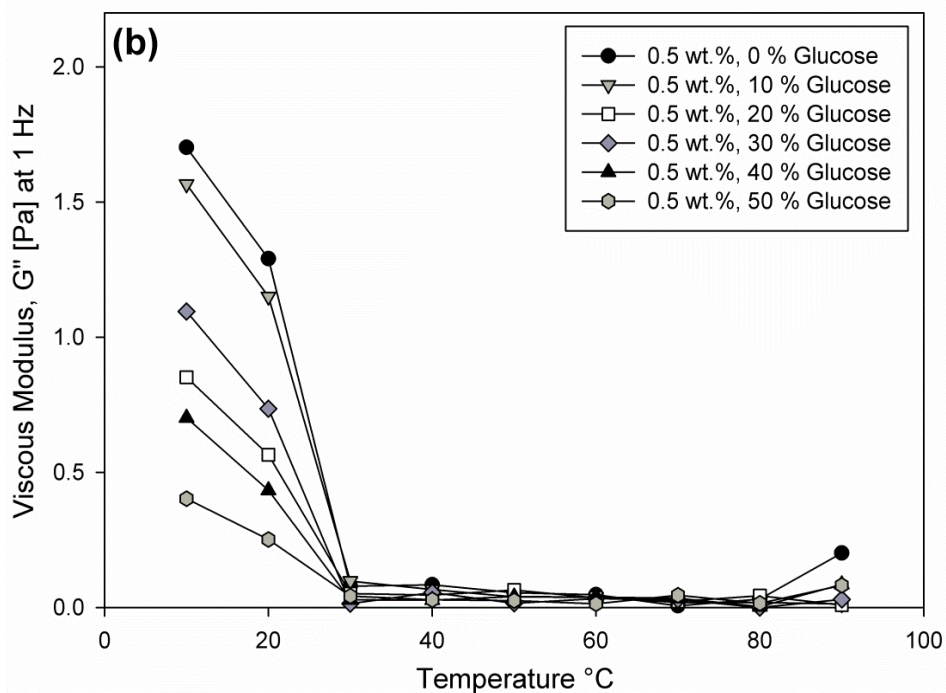
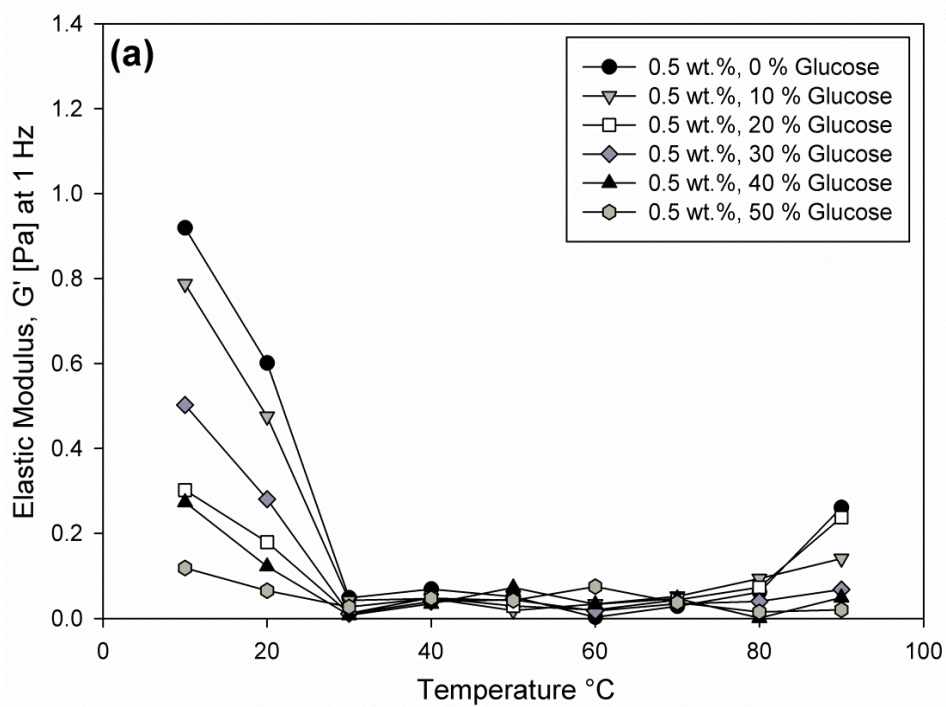


Figure 6.13. Elastic (a) and viscous (b) modulus measurements at 1 Hz versus temperature for 0.5 wt.% low acyl gellan gum fluid gels, as a function of increasing % glucose substitution (0 – 50 %) during a temperature heating ramp (10 – 90 °C), whilst performing frequency tables from 0.1 – 10 Hz at 10 °C intervals. Each of the modulus readings are based on a single sample measurement.

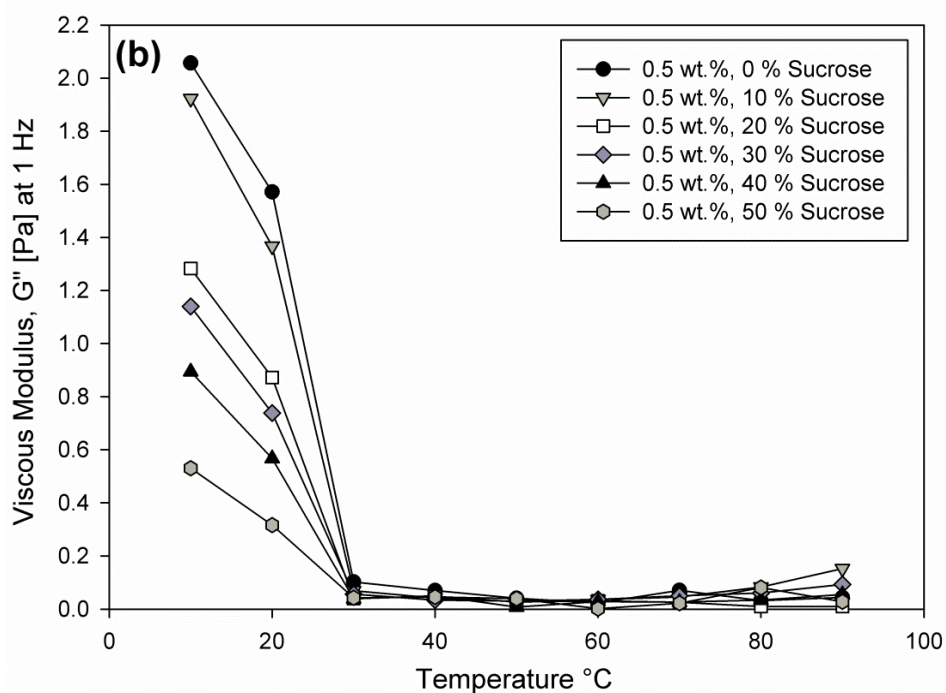
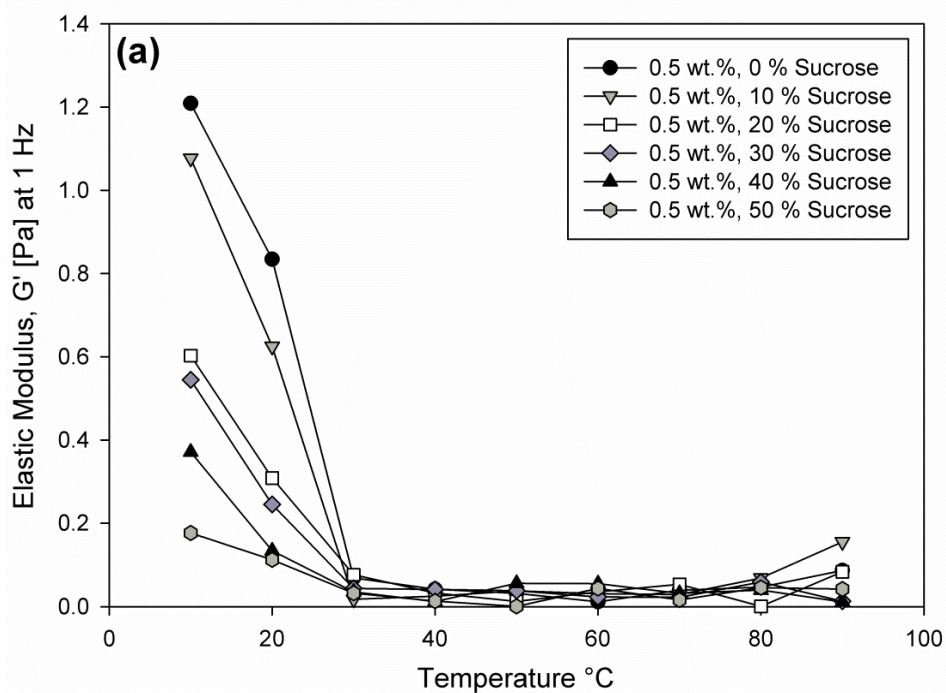


Figure 6.14. Elastic (a) and viscous (b) modulus measurements at 1 Hz versus temperature for 0.5 wt.% low acyl gellan gum fluid gels, as a function of increasing % sucrose substitution (0 – 50 %) during a temperature heating ramp (10 – 90 °C), whilst performing frequency tables from 0.1 – 10 Hz at 10 °C intervals. Each of the modulus readings are based on a single sample measurement.

For each of the mixed co-solute gellan samples (Figure 6.13 & 6.14) the G' values recorded as a function of frequency of oscillation were lower than those of the G'' across the entire temperature heating range, verifying the dominance of characteristic gel structures. Very similar melting temperatures and mechanisms were also observed between the G' and G'' measurements for each sample, confirming viscoelastic solid behaviour and evidence that the T_{hc} and the T_{gs} occurred concurrently during the heating process. It was observed that increasing the biopolymer concentration of each of the mixed co-solute gellan fluid gels from 0.5 wt.% to 1 wt.% and 2 wt.% resulted in much firmer gels with increased gel strength, and thus final G' and G'' values prior to the helix-coil transition period with increased magnitude. Increasing the co-solute concentration at each polymer concentration however, caused progressive weakening of the network structures with decreasing magnitude of G' and G'' . The G' values recorded at each polymer concentration as a function of frequency of oscillation also remained to be higher than those of the G'' across the entire heating range, and very similar gelling temperatures and mechanisms were observed for the two measurements with each sample. Higher amounts of the polysaccharide did however result in earlier gelation and increased gelling temperatures by $\sim 5 - 8$ °C for the samples with increasing gellan concentration. At these higher gellan concentrations (1 & 2 wt.%) progressive decreases in the calculated T_{hc} 's with increasing co-solute concentration became evident, reflecting the decreased hydration and ordering of the gellan chains with increasing co-solute concentration (Evageliou et al., 1998). The relationship between the concentration and the co-solutes was assumed to be the same as that described for the mixed co-solute gellan quiescent gels in Section 6.2.1.2.

Comparing the viscoelastic material responses of the mixed co-solute gellan quiescent gels (Section 6.2.1.2) and the mixed co-solute gellan fluid gels, resemblances in their mechanisms of formation and deformation with increasing co-solute and polymer

concentration were apparent. However, the temperature ranges of ~ 50 °C and ~ 30 °C at which their coil-helix and helix-coil transitions occurred respectively, at each polymer concentration differed. Helix-coil transition temperature periods have been reported however, to occur at ~ 30 °C by Miyoshi et al. (1998) on both cooling and heating during DSC and rheological analysis for 1 wt.% mixed co-solute gellan gels in the absence of sugar. Further increasing the co-solute concentration to ~ 30 % resulted in cooling and heating curves of G' and G'' almost identical to those recorded for 2 wt.% gellan gels in the absence of sugar, with an increase in the T_{ch} to ~ 37 °C (Miyoshi et al., 1998). Thus, the combination of using high polymer concentrations with increasing co-solute concentrations results in increased network transition temperature ranges, reassuring the significance of this difference. In addition to the increased gelling temperature range, the mixed co-solute gellan quiescent gels also had significantly higher viscoelastic (G' and G'') measurements, than those compared to the mixed gellan fluid gels; indicating that the latter are much weaker gels. This observation is supportive of the similar comparisons discussed for the two gel types in Chapter 5.

Comparing the viscoelastic modulus measurements of the mixed co-solute gellan fluid gels for the two sugars prior to the helix-coil transition period for all co-solute concentrations (Figures 6.13 – 6.14), the order of gel strength was glucose < sucrose. This was supportive of the order proposed for each of the mixed gellan quiescent gels in Section 6.2.1.2, and can be explained using the discussed literature (Tang et al., 2001; Sworn & Kasapis, 1998; Coultate, 1994 and Tait et al., 1972) in an identical manner.

6.2.2.2. Measuring the % co-solute release using spectrophotometry

6.2.2.2.1. Glucose and Sucrose

Increasing the concentration of the glucose and sucrose separately within 0.5 – 2 wt.% *LA* gellan mixed co-solute fluid gels had a similar impact on the subsequent levels of co-solute released from their network structures to that observed for the quiescent gels (2 – 4 wt.%) in Section 6.2.1.3. Figures 6.15 and 6.16 show the measurements of percentage glucose and sucrose release for these gels, substituted with 10 – 50 % co-solute following an 18 hour diffusion period, as a function of increasing polymer concentration.

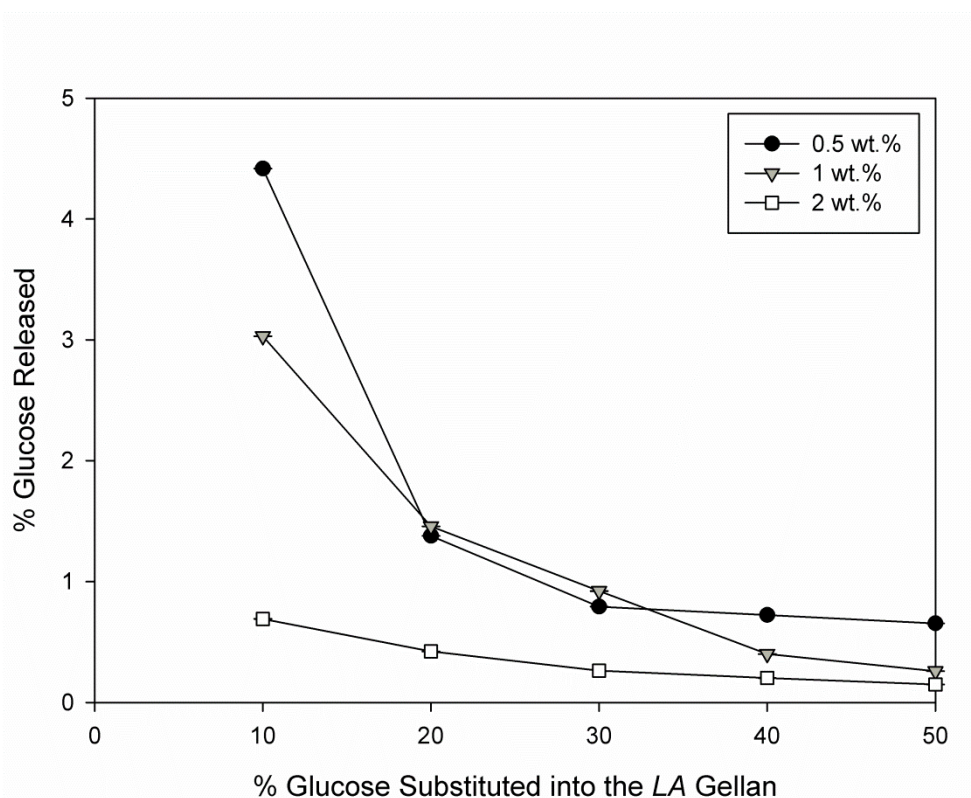


Figure 6.15. Measurement of % glucose released from low acyl gellan gum fluid gels substituted with 10 – 50 % glucose following an 18 hour diffusion period, as a function of increasing polymer concentration (0.5 – 2 wt.%). All measurements were carried out in triplicate. Where error bars cannot be observed, they are smaller than the data points.

For the 0.5 – 2 wt.% mixed glucose gellan fluid gels, increasing both the glucose and gellan polymer concentrations produces very similar trends to those observed in Section

6.2.1.3.1 for the equivalent quiescent gels, and can be explained in the same manner. In comparison, the percentage glucose release values were much greater for the quiescent gels; this suggests that the controlled shear and cooling environments used to formulate the mixed glucose gellan fluid gel structures encourage the incorporation of the glucose within the respective networks to a greater extent. This, in turn, restricts its molecular mobility and subsequent measured release.

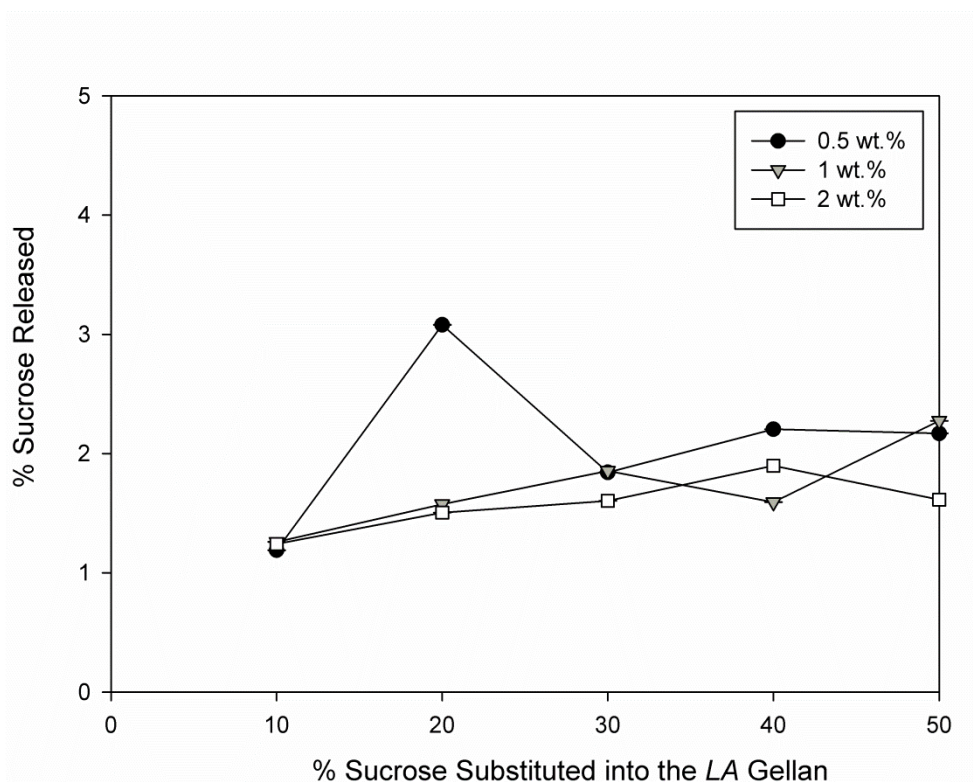


Figure 6.16. Measurement of % sucrose released from low acyl gellan gum fluid gels substituted with 10 – 50 % sucrose following an 18 hour diffusion period, as a function of increasing polymer concentration (0.5 – 2 wt.%). All measurements were carried out in triplicate. Where error bars cannot be observed, they are smaller than the data points.

For the 0.5 – 2 wt.% mixed sucrose gellan fluid gels, increasing the sucrose concentration causes the measured percentage sucrose to increase steadily, as observed for the 4 wt.% mixed sucrose gellan quiescent gels in Section 6.2.1.3.1. This is due to a progressive weakening of the mixed sucrose gellan networks which was discussed earlier for

the quiescent gels. An anomalous result was observed for the 0.5 wt.% mixed sucrose gellan system with 20 % sucrose, but this was insignificant and attributed to experimental error. The percentage sucrose release values were also found to be greater for the quiescent gels, suggesting that the controlled shear and cooling environments used to formulate the mixed sucrose gellan fluid gel structures also encourage the incorporation of the sucrose within the respective networks, as with glucose. However, the extent of this incorporation compared with the glucose molecules is thought to be lower for the sucrose molecules based on their differing size, molecular structure and subsequent solvation effects.

6.3. Conclusions

A challenge in the design of self-structuring foods that respond to the environmental conditions experienced inside the human stomach is the incorporation of materials that will modulate energy delivery and slowly release calories after consumption. Consumers are interested in healthier new products with decreased amount of sugars present. As the sweetness and the texture of these new products should not be significantly altered, a study on the behaviour of various sugars and their mixtures seems necessary. This was achieved by investigating the production and properties of *LA* gellan quiescent and fluid gels, containing low levels of the co-solutes glucose, sucrose and fructose. Rheological analysis enabled an improved understanding into the molecular ordering and structure development of these samples, and identified their coil-helix transition temperatures. Whilst, UV-Vis spectrophotometric and texture analysis methods investigated the co-solute release profiles of the samples and their structural and material responses to varying co-solute and polymer concentrations. Overall the results were promising, demonstrating that the structural and release properties of *LA* gellan mixed co-solute quiescent and fluid gels (with low levels of co-solute, ≤ 50 %) can be controlled by the processes used for their production and the type

of co-solute. It was found that increasing the sugar concentration in *LA* gellan mixed co-solute quiescent gels resulted in a progressive weakening and enhanced plasticity of their structural networks. A decreased mechanical and thermal stability was also noted, suggesting that sugar addition to the mixed gellan quiescent gels had a destabilising effect. However, adding up to 20 % sugar within the systems was shown to produce functional gel structures; a level which greatly exceeds the average percentage sugar contents in existing food and drink products.

Chapter 7

CONCLUSIONS AND FUTURE RECOMMENDATIONS

7.1. Conclusions

The aim of the work presented in this thesis was to investigate and control the acid-induced gelation of a variety of gellan gum gel forms, in addition to exploring their mechanisms of co-solute release. The purpose of this being to provide optimal polymer selection and the initial breadths of research towards the development of a self-structuring satiety based food product. The following sections summarise the main conclusions made for each of the experimental results chapters.

7.1.1. Acid-sensitive low and high acyl mixed gellan gum systems

- **Mixes of *LA* and *HA* gellan variants produce gels with properties intermediate to either variant alone.**

The mixtures displayed a discontinuous change in gel properties such as bulk modulus as the proportions of *LA* and *HA* gellan were varied showing a phase-separated structure. This was further shown using DSC and rheological analysis, which both displayed separate conformational transitions at temperatures coincident with the two variants at natural pH. No evidence for the formation of double helices involving both *HA* and *LA* molecules was found in this study at natural pH.

- **Acid affects the gelation and gel properties of the separate and mixed *LA* and *HA* gellan gels.**

The resulting gel structures became semi-interpenetrating rather than phase-separated. This was shown by the continuous change in gel properties as the proportions of the two variants were changed. Reducing the acidity of the mixed gellan gel solutions to low pH levels also resulted in shifts of the cooling and heating DSC curves to progressively lower temperatures, with an additional reduction in the amount of heat energy lost and gained. It

was suggested that the gels had become more heat resistant at these reduced pH values. At 50 % *HA* gellan with reduced pH, single melting and gelation peaks were observed. These were suggested to be a result of the merging of the two respective gellan variant transitions, implying that the *HA* and *LA* gellan form helices that incorporate strands of both types at pH values below pH 4.

- ***HA* gellan is less affected by acid exposure than the *LA* variant.**

This was highlighted by the reduced change in bulk modulus values with acid at higher *HA* gellan proportions. The *LA* variant produced more brittle (higher work to fracture) gels with lower bulk modulus values. The mixed gels combined these properties to produce gels that had higher bulk modulus under acidic conditions that did not become brittle.

- **Direct acidification during the gelation of the mixed gels results in phase separation of the gel and solvent at pH's less than 3.**

This was shown by the variation in bulk modulus and work to fracture values of the mixed gels, with phase separation of the gel and solvent being evident for all the *HA* and *LA* proportions at pH's less than 3. The highest bulk modulus achieved was at pH 3 with 50 % of each of the gellan variants.

- **The total biopolymer concentration has an effect on the gel strength, but the relative proportion of *LA* to *HA* gellan has a more significant effect.**

These findings were promising as they clearly demonstrated that structuring as well as de-structuring of the mixed gellan acid gels can be controlled by both the process used for their production and by exposure to an acidic environment. Mixed gellan gels could be used as an ingredient in foods to structure the stomach contents via interaction with the acidic

environment of the stomach. Prolonged exposure to acid starts to reduce the bulk modulus of mixed gellan gels with a large *HA* gellan proportion (> 60 %). It should be stressed though that the behaviour of mixed gellan acid gels, as demonstrated by the findings of this study, is not necessarily expected to be exactly reproduced within the stomach environment due to gastric motility and other physiological phenomena. We do however expect the behaviour to be broadly similar.

7.1.2. Low acyl gellan gum fluid gels

- **Control of the material (*LA* gellan gum and HCl acid concentrations) and process (shear and cooling rates during fluid gel production) parameters manipulates the properties and size of individual fluid gel particles and their interactions between them.**

It was shown that both of the fluid and acid fluid gels produced using the two different production methods (pin-stirrer and rheometer) displayed non-Newtonian shear-thinning flow behaviour. Very close similarities between these methods were observed for the fluid gels in the absence of acid, suggesting that the two distinctive processes were capable of producing particle sizes based on similar scales.

- **Quiescent *LA* gellan gum gels are stronger gels than *LA* gellan gum fluid gels.**

It was shown through the viscoelastic and texture analysis compression test data that compared with the fluid gels, the quiescent gels were characteristically stronger gels, due to the formation of interparticulate helices in the absence of shear on cooling.

- **The *LA* gellan fluid gel internal particle polymeric network and the elasticity of individual particles is equivalent to that of their quiescently cooled counterparts.**

Despite the previous concluding remark, the coil-helix transition and mid-point temperature data recorded for both gel types fell within the same range (30 – 70 °C). In addition, close similarities between the flow curve and viscoelastic behaviour recorded for the *LA* gellan fluid and quiescent gels, further proposed that the above statement is correct.

- **Post-production and direct exposure of the *LA* gellan gum fluid gels to an acidic environment results in an increase in gel strength.**

The variation in gel strength with increasing concentration of acid (via direct-addition) however, was not monotonic, with phase separation of the polymer and solvent proceeding for the fluid gel samples with acidities below pH 3. The G' data for the acid fluid gels also showed that decreasing the pH level, leads to a subsequent reduction in the time taken for gelation to occur. These findings were promising as they clearly demonstrated that the structuring of *LA* gellan gum fluid gels can be controlled by both the process used for their production and by exposure to an acidic environment.

7.1.3. Low acyl gellan gum and co-solute mixed gels

- **Increasing the co-solute concentration in *LA* gellan mixed co-solute quiescent gels results in a progressive weakening and enhanced elasticity of their structural networks.**

This was shown by both viscoelastic and texture analysis compression test measurements. It was suggested that with increasing co-solute concentration the orderly packing of the gellan double helices was hindered and the number of junction zones reduced, resulting in significantly weaker structures with decreased gel strength. The results also indicated a decreased mechanical and thermal stability with increasing co-solute concentration, suggesting that co-solute addition to the mixed gellan gels quiescent had a destabilising effect. Increasing the gellan polymer concentration however, produced firmer

gels that were more resistant to fracture. It was suggested that the co-solute concentration was equally as influential over the mixed gellan gel mechanical properties as the total biopolymer concentration, but that the latter controls the former.

- **The nature of the co-solute influences the *LA* gellan mixed quiescent gel network structure.**

Texture analysis showed that across all of the gellan concentrations, irrespective of the co-solute concentration that the mixed gellan glucose gels were much weaker than the mixed gellan sucrose and mixed gellan fructose gels. The order of strength for the latter two mixed gellan gel types however, varied upon increasing gellan and co-solute concentration. Overall, the effectiveness of the three sugars was attributed to a combination of the following factors: (1) the direct hydrogen bonding between hydroxyl groups in the polymer and in the sugar and (2) the structural change of water as a solvent. Thus, the sugars increased the number of elastically active network chains by forming hydrogen bonds or increased the effective concentration of gellan by immobilising water molecules. The viscoelastic measurements further confirmed the above statement. It was shown for the mixed gellan gels with increasing co-solute concentration (0 – 50 %), that the calculated T_{ch} 's rather than the scale of the viscoelastic modulus measurements were more representative for the three sugars, giving a true reflection of their gel strength (fructose < glucose ≤ sucrose). This order was close to and supportive of that observed for the textural analysis results and is strongly argued in the literature.

- **Increasing the concentration of co-solute within the *LA* gellan mixed co-solute quiescent and fluid gels had a notable effect on the subsequent levels of co-solute released from their network structures.**

A significant decrease in the glucose released was observed between the measurements recorded for the mixed gellan glucose gels with 10 and 20 % glucose, at each biopolymer concentration. Further increasing the glucose concentration, continued to result in a decrease in the glucose released from the gels, but this occurred much more steadily. It was suggested that the mixed gellan co-solute gel network was weaker at lower glucose levels, enabling greater diffusion of the glucose molecules into the double distilled water used to measure the percentage release of the sugar. Thus increasing the glucose concentration further led to stronger mixed gellan co-solute gel networks that were reinforced either directly or indirectly by the glucose molecules, restricting their subsequent mobility and measured release. For the 4 wt.% mixed gellan sucrose quiescent gels and each of the mixed gellan sucrose fluid gels, progressive increases in the percentage sucrose release measurements were observed with increasing sucrose concentration, reflecting continued weakening of the networks. This weakening was attributed to two factors: (1) the highly flexible, less aggregated polymer networks that results with increasing levels of sucrose and (2) sucrose's high co-solute water compatibility which reduces the availability of water molecules for the formation of thermodynamically stable junction zones; both of which maximised the sucrose molecular mobility and their subsequent measured release.

- **Sucrose has greater co-solute release potential than glucose in both *LA* gellan mixed glucose and mixed sucrose quiescent and fluid gels.**

It was suggested that the glucose units in the gellan structure replace the orderly packed glucose units in the aqueous mixed gellan glucose solutions, stabilising the orderly packed gellan double helices which result in stronger gel networks with increasing glucose concentration, and subsequent decreasing glucose release. It was also found that the percentage co-solute release values were much greater for the quiescent gels than the fluid gels. Thus, it was suggested that the controlled shear and cooling environments used to formulate the mixed gellan co-solute fluid gel structures encouraged the incorporation of the co-solutes within the respective networks to a greater extent.

- **Increasing the diffusion period time for the 2 wt.% mixed gellan glucose and mixed gellan sucrose gels had a notable impact on the subsequent levels of co-solute released from their network structures.**

For the mixed gellan glucose gels, it was found that the percentage glucose released at each co-solute level, decreased at a steady and equal rate with increasing diffusion time. The results demonstrated that the influences of glucose over the gellan network structure and the composition of the mixed gellan glucose systems themselves did not change significantly over time. For the mixed gellan sucrose gels, it was found that the percentage sucrose released at each co-solute level, increased at a rapid, but proportionate rate with increasing diffusion time. The results demonstrated that the rate of diffusion for the sucrose molecules over time compared with the glucose molecules was much slower. This was attributed to the larger molecular size of the disaccharide, and the greater influence of sucrose over the gellan network structure leading to the progressive weakening of the mixed gellan sucrose systems over time. These findings are promising as they clearly demonstrate that the structural and sugar release properties of *LA* gellan quiescent and fluid gels, containing low levels of co-solutes can be controlled by the processes used for their production and the type of co-solute.

7.2. Future Recommendations

This section aims to suggest areas that warrant further research based on speculation and conclusions made in this study.

- **Visualisation of *LA* and *HA* mixed gellan gum systems using fluoresceinamine.**
- **Subject the *LA* and *HA* mixed gellan gum systems and the *LA* mixed gellan gum co-solute systems to mimicked gastric environmental soaks.**
- **Encapsulation of the *LA* and *HA* mixed gellan gum systems to control gel self-structuring and energy release. Attention to their subsequent destructuring and associated kinetics is also required, so that the need/desire to re-eat can re-exert itself.**
- **Investigate the production and properties of mixed acid-sensitive hydrocolloid fluid gel systems, and incorporate a HCl acid injection delivery system within the equipment set-up to formulate acid mixed hydrocolloids fluid gel systems. The latter would enable controlled acidification and manipulation of the exposed shear conditions to mimic the gastric motility and physiological phenomena occurring in the stomach.**
- **Improved visualisation of *LA* gellan gum fluid gels using fluoresceinamine.**
- **Carry out a detailed compositional analysis of the *LA* commercial gellan gum used during this study.**
- **Investigate the properties of *LA* mixed gellan gum co-solute systems with other sugars and/or other biopolymer systems incorporating glucose, sucrose and fructose, separately and within acidic environments.**
- **Test the concepts of these self-structuring systems in-vivo**

Chapter 8

REFERENCES

References

- Arora, S., Ali, J., Ahuja, A., Khar, R. K., & Baboota, S. (2005). Floating drug delivery systems: A review. *AAPS PharmSciTech*, 6, E372 – E390.
- Baird, J. K., Talashek, T. A., & Chang, H. (1992). Gellan gum: effect of composition on gel properties. In: G. O. Phillips, P. A. Williams, & D. J. Wedlock (Eds.), *Gums and Stabilisers for the Food Industry 6*, (pp. 479 – 487), Oxford, UK: IRL Press.
- Bayarri, S., Costell, E., & Durán, L. (2002). Influence of low sucrose concentrations on the compression resistance of gellan gum gels. *Food Hydrocolloids*, 16, 593 – 597.
- Bradbeer, J. F., et al. (2014). Self-structuring foods based on acid-sensitive low and high acyl mixed gellan systems to impact on satiety. *Food Hydrocolloids*, 35, 522 – 530.
- Brown, C. R. T., Cutler, A. N., & Norton, I. T., (1996). Liquid based composition comprising gelling polysaccharide capable of forming a reversible gel and a method for preparing such composition, EP0355908.
- Brown, G. M., & Levy, H. A. (1963). Sucrose: Precise determination of crystal and molecular structure by neutron diffraction. *Science*, 141, 921 – 923.
- Buyong, N., & Fennema, O. (1988). Amount and size of ice crystals in frozen samples as influenced by hydrocolloids. *Journal of Dairy Science*, 71(10), 2630-2639.
- Caballero, B. (2007). The global epidemic of obesity: An Overview. *Epidemiol. Rev.*, 29, 1 - 5.
- Caggioni, M., Spicer, P. T., Blair, D. L., Lindberg, S. E., & Weitz, D. A. (2007). Rheology and microrheology of a microstructured fluid: the gellan gum case. *Journal of Rheology*, 51, 851 – 865.
- Carneiro, A. A., Baffa, O., & Oliveira, R. B. (1999). Study of stomach motility using the relaxation of magnetic tracers. *Physics in Medicine and Biology*, 44, 1691 – 1697.
- Carvalho, W., & Djabourov, M. (1997). Physical gelation under shear for gelatin gels. *Rheologica Acta*, 36(6), 591 – 609.

- Cassin, G., Appelqvist, I., Normand, R., & Norton, I. T. (2000). Stress-induced compaction of concentrated dispersions of gel particles. *Colloid and Polymer Science*, 278(8), 777 – 782.
- Chandrasekaran, R., Millane, R. P., Arnott, S., & Atkins, E. D. T. (1988). The crystal structure of gellan. *Carbohydrate Research*, 175, 1 – 15.
- Chandrasekaran, R., & Thailambal, V. G. (1990). The influence of calcium ions, acetate and L-glycerate groups on the gellan double-helix. *Carbohydrate Polymers*, 12, 431 – 442.
- Chandrasekaran, R., Radha, A., & Thailambal, V. G. (1992). Roles of potassium ions, acetyl and L-glycerate groups in native gellan double helix: an X-ray study. *Carbohydrate Research*, 224, 1 – 17.
- Chandrasekaran, R., & Radha, A. (1995). Molecular architectures and functional properties of gellan gum and related polysaccharides. *Trends in Food Science and Technology*, 6(5), 143–148.
- Connolly, S., Fenyo, J. C., & Vandavelde, M. C. (1988). Effect of proteinase on the macromolecular distribution of Acacia Senegal gum. *Carbohydrate Polymers*, 8(1), 23 – 32.
- Coultate, T. P. (1984). In: *Food The Chemistry of Its Components* (2nd Ed.). Royal Society of Chemistry, London.
- Cox, P. W., Spyropoulos, F., & Norton, I. T. (2009). Effect of Processing on Biopolymer Interactions. In: Kasapis, Norton, & Ubbink: *Modern Biopolymer Science*, Elsevier Inc., ISBN: 978-0-12-374195-0, p.p. 199 – 224.
- Crescenzi, V., Dentini, M., & Dea, I. C. M. (1987). The influence of side-chains on the dilute-solution properties of three structurally related bacterial anionic polysaccharides. *Carbohydrate Research*, 160, 283 – 302.
- Cui, S. W. (2004). *Chemistry, Physical Properties and Applications*, Routledge, USA.
- Draget, K. I., Skjåk-Bræk, G., & Stokke, B. T. (2006). Similarities and differences between alginic acid gels and ionically crosslinked alginate gels. *Food Hydrocolloids*, 20, 170 - 175.
- Evageliou, V., Kasapis, S., & Hember, M. W. N. (1998). Vitrification of κ -carrageenan in the presence of high levels of glucose syrup. *Polymer*, 39, 3909 – 3917.

- Evageliou, V., Mazioti, M., Mandala, I., & Komaitis, M. (2010). Compression of gellan gels. Part II: Effect of sugars. *Food Hydrocolloids*, *24*, 392 – 397.
- Fernández Farrés, I., Douaire, M., & Norton, I. T. (2013). Rheology and tribological properties of Ca-alginate fluid gels produced by diffusion-controlled method. *Food Hydrocolloids*, *32*(1), 115 – 122.
- Fiszman, S., & Varela, P. (2013). The role of gums in satiety and satiation: a review. *Food Hydrocolloids*, *32*, 147 – 154.
- Flory, P. J. (1941). Molecular size distribution in three dimensional polymers I. Gelation. *Journal of American Chemical Society*, *63*, 3083 – 3100.
- Frith, W. J., Garijo, X., Foster, T. J., Norton, I. T., (2002). Microstructural origins of the rheology of fluid gels. In: P. A. Williams, & G. O. Phillips (Eds.), *Gums and stabilisers for the food industry, Vol. 11* (pp. 95 – 103). Cambridge: Royal Society of Chemistry.
- Gabriele, A., Spyropoulos, F., & Norton, I.T., (2009). Kinetic study of fluid gel formation and viscoelastic response with kappa-carrageenan. *Food Hydrocolloids*, *23*(8), 2054 – 2061.
- Gabriele, A., Spyropoulos, F., & Norton, I.T., (2010). A conceptual model for fluid gel lubrication. *Soft Matter*, *6*, 4205 – 4213.
- Gabriele, A. (2011). *Fluid Gels: Function, Production and Lubrication*. PhD thesis, University of Birmingham, School of Chemical Engineering, Edgbaston, Birmingham, UK.
- García, M. C., Alfaro, M. C., Calero, N., & Muñoz, J. (2011). Influence of gellan gum concentration on the dynamic viscoelasticity and transient flow of fluid gels. *Biochemical Engineering Journal*, *55*, 73 – 81.
- Garrec, D. A., Frasc-Melnik, S., Henry, J. V. L., Spyropoulos, F., & Norton, I. T. (2012). Designing colloidal structures for micro and macro nutrient content and release in foods. Faraday Disc. <http://dx.doi.org/10.1039/C2FD20024D>.
- Garrec, D. A., & Norton, I. T. (2012). Understanding fluid gel formation and properties. *Journal of Food Engineering*, *112*, 175 – 182.
- Gibson, W. (1992). In: A. P. Imeson, (Ed.), *Thickening and Gelling Agents for Foods*, (pp. 227 – 249), Blackie Academic and Professional, London.

- Gibson, W., & Sanderson, G. R. (1997). Gellan gum. In: A. P. Imeson (Ed.), *Thickening and gelling agents for foods* (2nd ed.) (pp. 119 - 143). London: Blackie.
- Goodall, D. M., & Norton, I. T. (1987). Polysaccharide conformations and kinetics. *Accounts of Chemical Research*, 20(2), 59 – 65.
- Graessley, W. W. (1974). The entanglement concept in polymer rheology. *Advances in Polymer Science*, 16, 1 – 179.
- Grant, G. T., Morris, E. R., Rees, D. A., Smith, P. J. C., & Thom, D. (1973). Biological interactions between polysaccharides and divalent cations: the egg-box model. *FEBS Letters*, 32, 195 – 198.
- Grasdalen, H., & Smidsrød, O. (1987). Gelation of gellan gum. *Carbohydrate Polymers*, 7, 371 – 393.
- Guinard, J. X. & Mazzucchelli, R. (1996). The sensory perception of texture and mouthfeel. *Trends in Food Science & Technology*, 7, 213 – 221.
- Gunning, A. P., & Morris, V. J. (1990). Light scattering studies of tetramethyl ammonium gellan. *International Journal of Biological Macromolecules*, 12, 338 – 341.
- Gunning, A. P., Kirby, A. R., Ridout, M. J., Brownsey, G. J., & Morris, V. J. (1996). Investigation of gellan networks and gels by atomic force microscopy. *Macromolecules*, 29, 6791 – 6796.
- Gunning, A. P., Kirby, A. R., Ridout, M. J., Brownsey, G. J., & Morris, V. J. (1997). Correction to paper in preceding reference. *Macromolecules*, 30, 163 – 164.
- Harris, P., & Pointer, S. J. (1986). *Edible gums*. UK Patent GB 2,128,871B.
- Haslam, D. (2007). Obesity: A medical history. *Obesity Reviews*, 8, Supp. 1: 31 – 36.
- Haug, A. (1964). *Composition and properties of alginate*. Report No. 30. Trondheim, Norway: Norwegian Institute of Seaweed Research.
- Hoad, C. L., Rayment, P., Spiller, R. C., Marciani, L., Alonso, B. D., Traynor, C., et al. (2004). In vivo imaging of intragastric gelation and its effect on satiety in humans. *Journal of Nutrition*, 134, 2293 -2300.

- Horinaka, J., Kani, K., Hori, Y., & Maeda, S. (2004). Effect of pH on the conformation of gellan chains in aqueous systems. *Biophysical Chemistry*, *111*(3), 223 – 227.
- Huang, Y., Tang, J., Swanson, B. G., & Rasco, B. A. (2003). Effect of calcium concentration on the textural properties of high and low acyl mixed gellan gels. *Carbohydrate Polymers*, *54*, 516 – 522.
- Huang, Y., Singh, P., Tang, J., & Swanson, B. G. (2004). Gelling temperatures of high acyl gellan as affected by monovalent and divalent cations with dynamic rheological analysis. *Carbohydrate Polymers*, *56*, 27 – 33.
- Ikeda, S., Nitta, Y., Temsiripong, T., Pongsawatmanit, R., & Nishinari, K. (2004). Atomic force microscopy studies on cation-induced network formation of gellan. *Food Hydrocolloids*, *18*, 727 – 735.
- Jansson, P., Lindberg, B., & Sandford, P. A. (1983). Structural studies of gellan gum, an extracellular polysaccharide elaborated by *Pseudomonas elodea*. *Carbohydrate Research*, *124*, 135 – 139.
- Kaletunc, G., Normand, M. D., Nussinovitch, A., & Peleg, M. (1991). Determination of elasticity of gels by successive compression-decompression cycles. *Food Hydrocolloids*, *5*, 237 – 247.
- Kang, K. S., & Veeder, G. T. (1982). Polysaccharide S-60 and bacterial fermentation process for its preparation. US Patent 4,326,053.
- Kasapis, S., Giannouli, P., Hember, M. W. N., Evageliou, V., Poulard, C., Tort-Bourgeois, B. & Sworn, G. (1999). Structural aspects and phase behaviour in deacylated and high acyl gellan gum systems. *Carbohydrate Polymers*, *38*, 145 – 154.
- Kasapis, S. (2006). The morphology of the gellan network in a high-sugar environment. *Food Hydrocolloids*, *20*, 132 – 136.
- Katchalsky, A. (1971). Polyelectrolytes. *Pure and Applied Chemistry*, *26*, 327 – 373.
- Katsuta, K., Nishimura, A., & Miura, M. (1992). Effects of saccharides on stabilities of rice starch gels. *Food Hydrocolloids*, *6*, 387 – 398.

- Kavanagh, G. M., & Ross-Murphy, S. B. (1998). Rheological characterisation of polymer gels. *Progress in Polymer Science*, 23, 533 – 562.
- Kawai, S., Nitta, Y., & Nishinari, K. (2008). Model study for large deformation of physical polymeric gels. *Journal of Chemical Physics*, 128, 134903.
- Kelco Division of Merck and Co., Inc., San Diego, CA (1993). Gellan Gum: Multifunctional Polysaccharide for Gelling and Texturising.
- Kobayashi, Y., Okamoto, A., & Nishinari, K. (1994). Viscoelasticity of hyaluronic acid with different molecular weights. *Biorheology*, 31, 235 – 244.
- Koliandris, A., Lee, A., Ferry, A. L., Hill, S., & Mitchell, J. (2008). Relationship between structure of hydrocolloid gels and solutions and flavour release. *Food Hydrocolloids*, 22, 623 – 630.
- Kong, F., & Singh, R. P. (2008). Disintegration of solid foods in human stomach. *Journal of Food Science*, 73(5), R67 – 80.
- Kuo, M. S., Mort, A. J., & Dell, A. (1986). Identification and location of L-glycerate, an unusual acyl substituent in gellan gum. *Carbohydrate Research*, 156, 173 – 187.
- Malone, M. E., Appelqvist, I. A. M., & Norton, I. T. (2003). Oral behaviour of food hydrocolloids and emulsions. Part 1. Lubrication and deposition considerations. *Food Hydrocolloids*, 17, 763 – 773.
- Manning, C. E. (1992). *Formation and melting of gellan polysaccharide gels*. PhD thesis, Cranfield Institute of Technology, Silsoe College, Silsoe, Bedford, UK.
- Manning, G. S. (1969a). Limiting laws and counterion condensation in polyelectrolyte solutions I. Colligative properties. *Journal of Chemical Physics*, 51, 924 – 933.
- Manning, G. S. (1969b). Limiting laws and counterion condensation in polyelectrolyte solutions II. Self-diffusion of the small ions. *Journal of Chemical Physics*, 51, 934 – 938.
- Manson J. A., & Sperling, L. H. (1976). *Polymer Blends and Composites*. Plenum Press, New York and London.
- Mao, R., Tang, J., & Swanson, B. G. (2000). Texture properties of high and low acyl mixed gellan gels. *Carbohydrate Polymers*, 41, 331 – 338.

- Marciani, L., Young, P., Wright, J., Moore, R., Coleman, N., Gowland, P. A., & Spiller, R. C. (2001a). Antral motility measurements by magnetic resonance imaging. *Neurogastroenterology & Motility*, *13*, 511 – 518.
- Marciani, L., Gowland, P. A., Fillery-Travis, A., Manoj, P., Wright, J., Smith, A., Young, P., Moore, R., & Spiller, R. C. (2001b). Assessment of antral grinding of a model solid meal with echo-planar imaging. *The American Journal of Physiology – Gastrointestinal and Liver Physiology*, *280*, G844 – G849.
- Mason, T. G., Bibette, J., & Weitz, D. A. (1996). Yielding and flow of monodisperse emulsions. *Journal of Colloid and Interface Science*, *179*(2), 439 – 448.
- Matsukawa, S., Tang, Z., & Watanabe, T. (1999). Hydrogen-bonding behaviour of gellan in solution during structural change observed by ¹H NMR and circular dichroism methods. *Progress in Colloid and Polymer Science*, *114*, 15 – 24.
- Matsukawa, S., & Watanabe, T. (2007). Gelation mechanism and network structure of mixed solution of low- and high-acyl gellan studied by dynamic viscoelasticity, CD and NMR measurements. *Food Hydrocolloids*, *21*, 1355 – 1361.
- Mazen, F., Milas, M., & Rinaudo, M. (1999). Conformational transition of native and modified gellan. *International Journal of Biological Macromolecules*, *26*, 109 – 118.
- Milani, J., & Maleki, G. (2012). Hydrocolloids in Food Industry. In: B. Valdez (Ed.), *Food Industrial Processes – Methods and Equipment* (pp. 17 – 38). InTech Europe: Croatia. ISBN: 978-953-307-905-9.
- Milas, M., Shi, X., & Rinaudo, M. (1990). On the physicochemical properties of gellan gum. *Biopolymers*, *30*, 451 – 464.
- Milas, M., & Rinaudo, M. (1996). The gellan sol-gel transition. *Carbohydrate Polymers*, *30*, 177 – 184.
- Miyoshi, E., Takaya, T., & Nishinari, K. (1994). Gel-sol transition in gellan gum solutions. 1. Rheological studies on the effect of salts. *Food Hydrocolloids*, *8*, 505 – 527.

- Miyoshi, E., Takaya, T., & Nishinari, K. (1995). Effects of salts on the gel-sol transition of gellan gum by differential scanning calorimetry and thermal scanning rheology. *Thermochimica Acta*, 267, 269 – 287.
- Miyoshi, E., Takaya, T., & Nishinari, K. (1996a). Rheological and thermal studies of gel-sol transition in gellan gum aqueous solutions. *Carbohydrate Polymers*, 30, 109 – 119.
- Miyoshi, E., Takaya, T., Williams, P. A., & Nishinari, K. (1996b). Effects of sodium chloride and calcium chloride on the interaction between gellan gum and konjac glucomannan. *Journal of Agricultural and Food Chemistry*, 44, 2486 – 2495.
- Miyoshi, E., Takaya, T., & Nishinari, K. (1998). Effects of glucose, mannose and konjac glucomannan on the gel-sol transition in gellan gum aqueous solutions by rheology and DSC. *Polymer Gels and Networks*, 6(3 - 4), 273 – 290.
- Miyoshi, E., & Nishinari, K. (1999a). Rheological and thermal properties near the sol-gel transition of gellan gum aqueous solutions. *Progress in Colloid and Polymer Science*, 114, 68 – 82.
- Miyoshi, E., & Nishinari, K. (1999b). Effect of sugar on the sol-gel transition in gellan gum aqueous solutions. *Progress in Colloid and Polymer Science*, 114, 83 – 91.
- Mohammed, Z. H., Hember, M. W. N., Richardson, R. K., & Morris, E. R. (1998). Co-gelation of agarose and waxy maize starch. *Carbohydrate Polymers*, 36, 37 – 48.
- Mojaverian, P., Ferguson, R. K., Vlasses, P. H., Rocci, M. L. Jr., Oren, A., Fix, J. A., Caldwell, L. J., Gardner, C. (1985). Estimation of gastric residence time of the Heidelberg capsule in humans: effect of varying food composition. *Gastroenterology*, 89(2), 392 – 397.
- Moresi, M., & Bruno, M. (2007). Characterisation of alginate gels using quasi-static and dynamic methods. *Journal of Food Engineering*, 82, 298 - 309.
- Moritaka, H., Fukuba, H., Kumeno, K., Nakahama, N., & Nishinari, K. (1991). Effect of monovalent and divalent cations on the rheological properties of gellan gels. *Food Hydrocolloids*, 4, 495 – 507.

- Moritaka, H., Nishinari, K., Taki, M., & Fukaba, H. (1995). Effect of pH, potassium chloride, and sodium chloride on the thermal and rheological properties of gellan gum gels. *Journal of Agricultural and Food Chemistry*, *43*, 1685 – 1689.
- Morris, E. R., Rees, D. A., Thom, D., & Boyd, J. (1978). Chiroptical and stoichiometric evidence of a specific primary dimerisation process in alginate gelation. *Carbohydrate Research*, *66*, 145 – 154.
- Morris, E. R., Rees, D. A., & Robinson, G. (1980). Cation-specific aggregation of carrageenan helices: domain model of polymer gel structure. *J. Mol. Biol.*, *138*, 349.
- Morris, E. R., Powell, D. A., Gidley, M. J., & Rees, D. A. (1982). Conformations and interactions of pectins I. Polymorphism between gel and solid states of calcium polygalacturonate. *Journal of Molecular Biology*, *155*, 507 – 516.
- Morris, E. R. (1985). Rheology of hydrocolloids. In: G. O. Phillips, D. J. Wedlock, & P. A. Williams (Eds.), *Gums and stabilisers for the food industry 2*, (pp. 57 – 78). Oxford, UK: Pergamon Press.
- Morris, E. R. (1991). Pourable gels: polysaccharides that stabilise emulsions and dispersions by physical trapping. *International Food Ingredients*, No. 1, Jan/Feb, 32 – 37.
- Morris, E. R., Gothard, M. G. E., Hember, M. W. N., Manning, C. E., & Robinson, G. (1996). Conformational and rheological transitions of welan, rhamsan and acylated gellan. *Carbohydrate Polymers*, *30*, 165 – 175.
- Morris, E. R., Richardson, R. K., & Whittaker, L. E. (1999). Rheology and gelation of deacylated gellan polysaccharide with Na⁺ as the sole counterion. *Progress in Colloid and Polymer Science*, *114*, 109 – 115.
- Morris, E. R. (2009). Functional interactions in gelling biopolymer mixtures. In: S. Kasapis, I. T. Norton, & J. B. Ubbink (Eds.), *Modern Biopolymer Science: Bridging the Divide between Fundamental Treatise and Industrial Application*, (pp.167 – 198). London, UK: Academic Press (Elsevier).
- Morris, E. R., Nishinari, K., & Rinaudo, M. (2012). Gelatin of gellan – A review. *Food Hydrocolloids*, *28*, 373 – 411.

- Morris, G., & Harding, S. (2009). Microbial Polysaccharides. In: M. Schaechter (Ed.), *Encyclopedia of Microbiology, 3rd Edition, Volume 1*, (pp. 482 – 494). Oxford, UK: Elsevier Inc.
- Morris, V. J. (1995). Bacterial polysaccharides. In A. M. Stephen (Ed.), *Food polysaccharides and their applications* (pp. 341 – 375). New York: Marcel Dekker.
- Morris, V. J., & Brownsey, G. J. (1995). Physical chemistry of heterogeneous and mixed gels. In: E. Dickinson, & D. Lorient (Eds.), *Food macromolecules and colloids* (pp. 376 – 389). Cambridge, UK: Royal Society of Chemistry, RSC Special Publication No. 156.
- Morris, V. J., Kirby, A. R., & Gunning, A. P. (1999). A fibrous model for gellan gels from atomic force microscopy studies. *Progress in Colloid and Polymer Science, 114*, 102 – 108.
- Morrison, N. A., Sworn, G., Clark, R. C., Chen, Y. L., & Talashek, T. (1999). Gelatin alternatives for the food industry. *Progress in Colloid and Polymer Science, 114*, 127 – 131.
- Morrison, N. A., Sworn, G., Clark, R. C., Talashek, T., & Chen, Y-L. (2002). New textures with high acyl gellan gum. In: G. O. Phillips, P. A. Williams & D. J. Wedlock (Eds.), *Gums and Stabilisers for the Food Industry 11*, (pp. 297 – 305), Oxford, UK: IRL Press.
- Nakajima, K., Ikehara, T., & Nishi, T. (1996). Observation of gellan gum by scanning tunnelling microscopy. *Carbohydrate Polymers, 30*, 77 – 81.
- Nakamura, K., Harada, K., & Tanaka, Y. (1993). Viscoelastic properties of aqueous solutions: The effects of concentration on gelation. *Food Hydrocolloids, 7*, 435 – 447.
- Nickerson, M. T., Paulson, A. T., & Speers, R. A. (2003). Rheological properties of gellan gum solutions: Effect of calcium ions and temperature on pre-gel formation. *Food Hydrocolloids, 17*(5), 577 – 583.
- Nickerson, M. T., Paulson, A. T., & Speers, R. A. (2004). Time-temperature studies of gellan polysaccharide gelation in the presence of low, intermediate and high levels of co-solutes. *Food Hydrocolloids, 18*, 783 – 794.
- Nishinari, K., Koide, S., & Ogino, K. (1985). On the temperature dependence of elasticity of thermoreversible gels. *Journal de Physique (France), 46*, 793 – 797.

- Nishinari, K., Watase, M., Williams, P. A., & Phillips, G. O. (1990). κ -Carrageenan gels: effects of sucrose, glucose, urea and guanidine hydrochloride on the rheological and thermal properties. *Journal of Agricultural and Food Chemistry*, 38, 1188 – 1193.
- Nishinari, K., & Watase, M. (1992). Effect of sugars and polyols on the gel-sol transition of κ -carrageenan gels. *Thermochimica Acta*, 206, 149 – 162.
- Nitta, Y., Ikeda, S., Takaya, T., & Nishinari, K. (2001). Helix-coil transition in gellan gum gels. *Transactions of MRS-J*, 26, 621 – 624.
- Nitta, Y., Kim, B. S., Nishinari, K., Shirakawa, M., Yamatoya, K., Oomoto, T., et al. (2003). Synergistic gel formation of xyloglucan/gellan mixture as studied by rheology, DSC and circular dichroism. *Biomacromolecules*, 4, 1654 – 1660.
- Noda, S., Funami, T., Nakauma, M., Asai, I., Takahashi, R., Al-Assaf, A., Ikeda, S., Nishinari, K., & Phillips, G. O. (2008). Molecular structures of gellan gum imaged with atomic force microscopy in relation to the rheological behaviour in aqueous systems. 1. Gellan gum with various acyl contents in the presence and absence of potassium. *Food Hydrocolloids*, 22, 1148 – 1159.
- Norton, A. B., Cox, P. W., & Spyropoulos, F. (2011). Acid gelation of low acyl gellan gum relevant to self-structuring in the human stomach. *Food Hydrocolloids*, 25, 1105 – 1111.
- Norton, I. T., Goodall, D. M., Morris, E. R., & Rees, D. A. (1983). Equilibrium and dynamic studies of the disorder-order transition of kappa carrageenan. *Journal of the Chemical Society, Faraday Transactions 1: Physical Chemistry in Condensed Phases*, 79(10), 2489 – 2500.
- Norton, I. T., Foster, T. J., & Brown, C. R. T. (1998). The science and technology of fluid gels. In: P. A. Williams & G. O. Phillips (Eds.), *Gums and Stabilisers for the Food Industry*, Vol. 9 (pp.259 – 268). Cambridge: The Royal Society of Chemistry.
- Norton, I. T., Jarvis, D. A., & Foster, T. J. (1999). A molecular model for the formation and properties of fluid gels. *International Journal of Biological Macromolecules*, 26, 255 – 261.
- Norton, I. T., Smith, C. G., Frith, W. J., & Foster, T. J. (2000). The production, properties and utilisation of fluid gels. *Hydrocolloids*, 2, 217 – 227.

- Norton, I. T., & Frith, W. J. (2001). Microstructure design in mixed biopolymer composites. *Food Hydrocolloids*, *15*(4- 6), 543 – 553.
- Norton, I. T., Frith, W. J., & Ablett, S. (2006). Fluid gels, mixed fluid gels and satiety. *Food Hydrocolloids*, *20*, 229 – 239.
- Nussinovitch, A. (2004). From simple to complex hydrocolloid cellular solids. In: P. A. Williams, & G. O. Phillips (Eds.), *Gums and stabilizers for the food industry*, Vol. 12 (pp. 32 – 42). Cambridge: The Royal Society of Chemistry.
- O’Neill, M. A., Selvendran, R. R., & Morris, V. J. (1983). Structure of the acidic extracellular gelling polysaccharide produced by *Pseudomonas elodea*. *Carbohydrate Research*, *124*, 123 – 133.
- Oakenfull, D., & Scott, A. (1986). Stabilisation of gelatin gels by sugars and polyols. *Food Hydrocolloids*, *1*, 163 – 175.
- Ogawa, E., Matsuzawa, H., & Iwahashi, M. (2002). Conformational transition of gellan gum of sodium, lithium, and potassium types in aqueous solutions. *Food Hydrocolloids*, *16*, 1 – 9.
- Ogawa, E., Takahashi, R., Yajima, H., & Nishinari, K. (2006). Effects of molar mass on the coil to helix transition of sodium-type gellan gums in aqueous solutions. *Food Hydrocolloids*, *20*, 378 – 385.
- Ohtsuka, A., & Watanabe, T. (1996). The network structure of gellan gum hydrogels based on the structural parameters by the analysis of the restricted diffusion of water. *Carbohydrate Polymers*, *30*, 135 – 140.
- Paeschke, T., & Aimutis, W. R. (2008). The effect of hydrocolloids on satiety, and weight loss: a review. In: A. Williams and G. O. Phillips (Eds.), *Gums and Stabilisers for the Food Industry*, Vol. 14 (pp. 313 – 325). RSC Special Publication: Cambridge.
- Papageorgiou, M., Kasapis, S., & Richardson, R. K. (1994). Glassy-state phenomena in gellan-sucrose-corn syrup mixtures. *Carbohydrate Polymers*, *25*, 101 – 109.
- Papageorgiou, M., & Kasapis, S. (1995). The effect of added sucrose and corn syrup on the physical properties of gellan-gelatin mixed gels. *Food Hydrocolloids*, *9*, 211 – 220.

- Phillips, G. O., Wedlock, D. J. & Williams, P. A. (Eds), (1990). Application of microcrystalline cellulose. In: *Gums and stabilisers for the food industry, Vol. 5*. Oxford, UK: IRL Press.
- Picone, C. S. F., & Cunha, R. L. (2011). Influence of pH on formation and properties of gellan gels. *Carbohydrate Polymers*, 84, 662 – 668.
- Picout, D. R., & Ross-Murphy, S. B. (2003). Rheology of biopolymer solutions and gels. *The Scientific World*, 3, 105 – 121.
- Pollock, T. J. (1993). Gellan-related polysaccharides and the genus *Sphingomonas*. *Journal of General Microbiology*, 139, 1939 – 1945.
- Rees, D. A., Morris, E. R., Thom, D., & Madden, J. K. (1982). Shapes and interactions of carbohydrate chains. In: G. O. Aspinall (Ed.), *The polysaccharides, Vol. 1* (pp. 195 – 290). New York: Academic Press.
- Rinaudo, M. (2009). Polyelectrolyte properties of a plant and animal polysaccharide. *Structural Chemistry*, 20, 277 – 298.
- Robinson, G., Manning, C. E., Morris, E. R., & Dea, I. C. M. (1988). Side-chain-mainchain interactions in bacterial polysaccharides. In G. O. Phillips, P. A. Williams, & D. J. Wedlock (Eds.), *Gums and stabilisers for the food industry 4* (pp. 173 – 181). Oxford, UK: IRL Press.
- Robinson, G., Manning, C. E., & Morris, E. R. (1991). Conformation and physical properties of the bacterial polysaccharides gellan, welan and rhamnan. In: E. Dickinson (Ed.), *Food polymers, gels and colloids* (pp. 22 – 33). Cambridge, UK: Royal Society of Chemistry.
- Rochas, C., & Rinaudo, M. (1980). Activity coefficients of counterions and conformation in kappa-carrageenan gels. *Biopolymers*, 19, 1675 – 1687.
- Rodríguez-Hernández, A. I., Durand, S., Garnier, C., Tecante, A., & Doublier, J. L. (2003). Rheology-structure properties of gellan systems: evidence of network formation at low gellan concentrations. *Food Hydrocolloids*, 17, 621 – 628.
- Ross-Murphy, S. B. (1984). Rheological methods. In: H. W.-S. Chan (Ed.), *Biophysical methods in food research. Critical reports on applied chemistry*, (pp. 195 – 290). London, UK: SCI.

- Ross-Murphy, S. B. (2008). Lecture course at Department of Polymer Chemistry, Kyoto University, Japan, March 2008.
- Saha, D., & Bhattacharya, S. (2010). Hydrocolloids as thickening and gelling agents in food: a critical review. *J Food Sci Technol*, 47(6), 587 – 597.
- Sahin, H., & Ozdemir, F. (2004). Effect of some hydrocolloids on the rheological properties of different formulated ketchups. *Food Hydrocolloids*, 18(6), 1015 – 1022.
- Sanderson, G. R., & Clark, R. C. (1984). Gellan gum, a new gelling polysaccharide. In: G. O. Phillips, P. A. Williams, & D. J. Wedlock (Eds.), *Gums and stabilisers for the food industry 2*, (pp. 201 – 210). Oxford, UK: Pergamon Press.
- Sanderson, G. R., Bell, V. L., Burgum, D. R., Clark, R. C., & Ortega, D. (1988). Gellan gum in combination with other hydrocolloids. In: G. O. Phillips, P. A. Williams & D. J. Wedlock (Eds.), *Gums and stabilisers for the food industry 4*, (pp. 301 – 308), Oxford, UK: IRL Press.
- Sanderson, G. R., Bell, V. L., Clark, R. C., & Ortega, D. (1988). The texture of gellan gum. In: G. O. Phillips, P. A. Williams & D. J. Wedlock (Eds.), *Gums and stabilisers for the food industry 4*, (pp. 219 – 229), Oxford, UK: IRL Press.
- Sanderson, G. R. (1990). Gellan gum. In: P. Harries (Ed.), *Food gels*, (pp. 201 – 232), New York: Elsevier Science.
- Seisun, D. (2010). Introduction. In: A. P. Imeson, (Ed.), *Food Stabilisers, Thickeners and Gelling Agents*, (pp.1 – 10), John Wiley & Sons Inc., New York.
- Shimizu, M., Brenner, T., Liao, R., & Matsukawa, S. (2012). Diffusion of probe polymer in gellan gum solutions during gelation process studied by gradient NMR. *Food Hydrocolloids*, 26, 28 – 32.
- Singh, S. K. (2007). Fluid Flow and Disintegration of Food in Human Stomach. Biological Systems Engineering, Office of Graduate Studies, University of California, Davis.
- Smidsrød, O., & Haug, A. (1971). Estimation of the relative stiffness of the molecular chain in polyelectrolytes from measurements of viscosity at different ionic strengths. *Biopolymers*, 10, 1213 – 1227.

- Smidsrød, O., Haug, A., & Lian, B. (1972). Properties of poly(1,4-hexuronates) in the gel state. I. Evaluation of a method for the determination of stiffness. *Acta Chemica Scandinavica*, 26, 71 - 78.
- Sworn, G., Sanderson, G. R., & Gibson, W. (1995). Gellan gum fluid gels. *Food Hydrocolloids*, 9, 265 – 271.
- Sworn, G., & Kasapis, S. (1998). Effect of conformation and molecular weight of co-solutes on the mechanical properties of gellan gum gels. *Food Hydrocolloids*, 12, 283 – 290.
- Sworn, G. (1999). Gellan gum. In: A. Imeson, *Thickening and Gelling Agents for Food*, 2nd ed., Aspen Publishers Inc.: Gaithersburg, MD.
- Sworn, G., (2000). Gellan gum. In: G. O. Phillips, P. A. Williams (Eds.), *Handbook of Hydrocolloids*, (pp. 117 – 135), Woodhead Publishing Limited: Cambridge.
- Sworn, G. (2009). Gellan gum. In: G. O. Phillips, P. A. Williams (Eds.), *Handbook of Hydrocolloids*, 2nd ed. (pp. 204 – 227). Woodhead Publishing Limited: Cambridge.
- Tait, M. J., Suggett, A., Franks, F., Ablett, S., & Quickenden, P. A. (1972). Hydration of monosaccharides: A study by dielectric and nuclear magnetic relaxation. *Journal of Solution Chemistry*, 1, 131 – 151.
- Tanaka, Y., Sakurai, M., & Nakamura, K. (1996). Ultrasonic velocities and circular dichroism in aqueous gellan solutions. *Food Hydrocolloids*, 10, 133 – 136.
- Tang, J., Lelievre, J., Tung, M. A., & Zeng, Y. (1994). Polymer and ion concentration effects on gellan gel strength and strain. *Journal of Food Science*, 59 (1), 216 – 220.
- Tang, J., Tung, M. A., & Zeng, Y. (1995). Mechanical properties of gellan gels in relation to divalent cations. *Journal of Food Science*, 60(4), 748 – 752.
- Tang, J., Tung, M. A., & Zeng, Y. (1996). Compression strength and deformation of gellan gels formed with mono- and divalent cations. *Carbohydrate Polymers*, 29, 11 – 16.
- Tang, J., Tung, M. A., & Zeng, Y. (1997a). Gelling temperature of gellan solutions containing calcium ions. *Journal of Food Science*, 62, 276 – 280.
- Tang, J., Tung, M. A., & Zeng, Y. (1997b). Gelling properties of gellan solutions containing monovalent and divalent cations. *Journal of Food Science*, 62, 688 – 692.

- Tang, J., Mao, R., Tung, M. A., & Swanson, B. G. (2001). Gelling temperature, gel clarity and texture of gellan gels containing fructose or sucrose. *Carbohydrate Polymers*, *44*, 197 – 209.
- Te Nijenhuis, K. (1997). Thermoreversible networks: viscoelastic properties and structure of gels. *Advances in Polymer Science*, *130*, 1 – 252.
- Tsigosa, C., Hainer, V., Basdevant, A., Finer, N., Fried, M., Mathus-Vliegen, E., Micic, D., & Maislos, M. (2008). Management of Obesity in Adults: European Clinical Practise Guidelines. *The European Journal of Obesity*, *1* (2), 106 - 126.
- Tsoga, A., Kasapis, S., & Richardson, R. K. (1999). The rubber-to-glass transition in high sugar agarose systems. *Biopolymers*, *49*, 267 – 275.
- Tsoga, A., Richardson, R. K., & Morris, E. R. (2004). Role of co-solutes in gelation of high-methoxy pectin. Part 2 – anomalous behaviour of fructose: calorimetric evidence of site-binding. *Food Hydrocolloids*, *18*, 921 – 932.
- Upstill, C., Atkins, E. D. T., & Atwool, P. T. (1986). Helical conformations of gellan gum. *International Journal of Biological Macromolecules*, *8*, 275 – 288.
- Valli, R. C., & Miskiel, F. J. (2001). Gellan gum. In: S. S. Cho, & M. L. Dreher (Eds.), *Handbook of Dietary Fibre* (pp. 695 – 720). Marcel Dekker Inc.: New York.
- Valli, R. C., & Clark, R. (2010). Gellan gum. In: A. P. Imeson, (Ed.), *Food stabilisers, thickeners and gelling agents* (pp. 145 – 166). Chichester, UK: Wiley-Blackwell.
- Versantvoort, C. H., Van de Kamp, E., & Rompelberg, C. J. M. (2004). RIVM report 320102002/2004. Development and applicability of an *in vitro* digestion model in assessing the bioaccessibility of contaminants from food. Available from: <http://www.rivm.nl/en/>. Natl. Inst. for Public Health and the Environment, Bilthoven, The Netherlands. Accessed March 2008.
- Watase, M., Nishinari, K., Williams, P. A., & Phillips, G. O. (1990). Agarose gels: effects of sucrose, glucose, urea, and guanidine hydrochloride on the rheological and thermal properties. *Journal of Agricultural and Food Chemistry*, *38*, 1181 – 1187.

Watase, M., & Nishinari, K. (1993). Effect of potassium ions on the rheological and thermal properties of gellan gum gels. *Food Hydrocolloids*, 7, 449 – 456.

Whittaker, L. E., Al-Ruqaie, I. M., Kasapis, S., & Richardson, R. K. (1997). Development of composite structures in the gellan polysaccharide/sugar system. *Carbohydrate Polymers*, 33, 39 – 46.

Williams, P. A., & Phillips, G. O. (2009). Introduction to food hydrocolloids. In: *Handbook of Hydrocolloids*, 2nd edition (pp. 1 – 22). Woodhead Publishing Ltd.: New York.

World Health Organization, (May 2012). “Obesity and Overweight” Fact sheet No. 311, (<http://www.who.int/mediacentre/factsheets/fs311/en/index.html>).

Yamamoto, F., & Cunha, R. L. (2007). Acid gelation of gellan: effect of final pH and heat treatment conditions. *Carbohydrate Polymers*, 68, 517 – 527.

Chapter 9

APPENDICES

9.1. Conferences and Publications

The results obtained during this study were presented at a number of national and international conferences as detailed below:

- Bradbeer, J.F., Spyropoulos, F., & Norton, I.T. *Controlling the acid gelation kinetics of mixed gellan biopolymers*. Presented at the **5th DRINC Dissemination Event, Birmingham, October 2010**. The accompanying poster was presented the award of **‘Best PhD Poster’**. The prize awarded included an industrial visit to the **Danone Research Centre Daniel Carasso, Paris, September 2011**.
- Bradbeer, J.F., Spyropoulos, F., & Norton, I.T. *An investigation into the acid gelation kinetics and flow properties of gellan gum fluid gels*. Poster presentation at the **6th DRINC Dissemination Event, Bristol, April 2011**.
- Bradbeer, J.F., Spyropoulos, F., & Norton, I.T. *An investigation into the acid-induced gelation of low acyl gellan gum fluid gels*. Poster presentation at the **Natural Food Biopolymers: Structure and Bioactivity Conference, Institute of Food Research, Norwich, June 2011** and at the **7th DRINC Dissemination Event, Manchester, October 2011**.
- Bradbeer, J.F., Niknafs, N., Spyropoulos, F., & Norton, I.T. *Self-structuring foods based on acid-sensitive biopolymers to impact on satiety*. Presented at the **Food Structures, Digestion and Health (FSDH) Conference 2012, Palmerston North, New Zealand, March 2012**.
- Bradbeer, J.F., Hancocks, R.D., Spyropoulos, F., & Norton, I.T. *An investigation into the acid gelation, flow properties and particle size of low acyl gellan gum fluid gels*. Poster presentation at the **6th International Symposium on Food Rheology and Structure (ISFRS), Zurich, Switzerland, April 2012**.
- Bradbeer, J.F., Hancocks, R.D., Spyropoulos, F., & Norton, I.T. *Kinetic study of fluid gel formation with low acyl gellan gum*. Poster presentation at the **8th DRINC Dissemination Event, Leeds, May 2012**.

- Bradbeer, J.F., Niknafs, N., Spyropoulos, F., & Norton, I.T. *Self-structuring foods based on acid-sensitive biopolymers to impact on satiety*. Presented at the **Biosciences KTN Young Researchers Food Event 2012, Edinburgh, November 2012**.
- Bradbeer, J.F., Hancocks, R.D., Spyropoulos, F., & Norton, I.T. *Gelling temperature, co-solute release and texture of gellan gels containing glucose or sucrose*. Poster presentation at the **9th DRINC Dissemination Event, Bristol, February 2013**.

A selection of the results presented in this thesis have been published in the following paper:

- Bradbeer, J.F., Hancocks, R.D., Spyropoulos, F., & Norton, I.T. (2014). *Self-structuring foods based on acid-sensitive low and high acyl mixed gellan system to impact on satiety*. *Food Hydrocolloids*, 35, 522 – 530. <http://dx.doi.org/10.1016/j.foodhyd.2013.07.014>.

Following the online publication of the paper, a great interest was expressed in the research and the following media articles were written in response:

- “Food science that fools hunger pangs” (19 August 2013), IChemE. http://www.icheme.org/media_centre/news/2013/food-science-that-fools-hunger-pangs.aspx#.UhhXCpLVB1Y.
- “Satiety latest: researchers develop new gelling agent” (5 September 2013), Food Manufacture. <http://www.foodmanufacture.co.uk/Ingredients/Satiety-latest-researchers-develop-new-gelling-agent>

- “Molecular gastronomy gels could tackle obesity” (4 January 2014), The Telegraph.
<http://www.telegraph.co.uk/health/healthnews/10528911/Molecular-gastronomy-gels-could-tackle-obesity.html>
- “Scientists invent edible gel that gives you a feeling of being full and stops snacking” (5 January 2014), The Mail.
<http://www.dailymail.co.uk/health/article-2533980/Scientists-invent-edible-gel-gives-feeling-stops-snacking.html>
- “Smart Food” (January 2014), Inside Food Magazine, Issue 7.
<http://viewer.zmags.com/publication/29e01362#/29e01362/15>

A patent application (British Patent Application Number GB1104447.6) was also filed on 04.05.11 entitled “Comestible Product” in which the author is noted as an inventor.